Radio frequency (RF) assisted disinfestation of red flour beetle (*Tribolium castaneum*) in stored canola seeds (*Brassica napus* L.)

A Thesis Submitted to the

College of Graduate and Postdoctoral Studies in
Partial Fulfillment of the Requirements for the Degree of
Doctor of Philosophy (Ph.D.)

In the
Department of Chemical and Biological Engineering
University of Saskatchewan

By

Daeung Yu

Permission to Use

In presenting this thesis in partial fulfillment of the requirements for a doctorate of philosophy from the University of Saskatchewan, I agree that the Libraries of this University may make it freely available for inspection. I further agree that permission to copy this thesis in any manner in whole or in part, for scholarly purposes may be granted by Dr. Oon-Doo Baik who supervised my thesis work, or in his absence, by the Dean of the College of Engineering. It is understood that any copying, publication, or use of this thesis or parts thereof for financial gain shall not be allowed without my written permission. It is also understood that due recognition shall be given to me and to the University of Saskatchewan in a scholarly use which may be made of the material in my thesis. Requests for permission to copy or to make other use of material in this thesis in whole or part should be addressed to:

Head of the Department of Chemical and Biological Engineering

University of Saskatchewan

3B48 Engineering Building 57 Campus Drive,

Saskatoon, Saskatchewan

Canada S7N 5A9

Abstract

To control the insect pests in stored grains, conventional methods (fumigation, controlled atmosphere, hot and cold air, and ionizing radiation) have been applied, however those methods have major drawbacks (remaining toxic chemicals, inefficient heating, long treatment time, etc). One of the alternative methods for the disinfestation is radio frequency (RF) heating based on electromagnetic radiation. The main advantage of the RF heating over thermal gradient driven conventional heating methods is volumetric and selective heating. It is governed by the characteristics of the electromagnetic energy, and the electrical, thermal, and physical properties of materials.

Dielectric property of bulk canola seed (*Brassica napus* L.) and red flour beetle (*Tribolium castaneum*, Herbst, 1797) were measured at different moisture contents (5%, 7%, 9%, and 11%), temperatures (30 to 80°C) and frequencies (5 to 30 MHz) using a precision LCR (L : inductance, C : capacitance, and R : resistance) meter and a dielectric test fixture. The dielectric properties decreased with increasing frequency regardless of temperature or moisture content (MC), but increased in proportion to increasing temperature or MC. Other properties (specific heat, thermal conductivity and thermal diffusivity) of the bulk canola seeds increased with temperature or MC. On the other hand, density and emissivity decreased with temperature or MC. Properties (specific heat, thermal conductivity and dielectric properties) of the red flour beetle increased in proportional to increasing temperature, which the excepting of a density, which decreased with increasing temperature.

Temperature distribution in the bulk canola seed at various volumes (small – 196.3 cm^3, medium – 1,766 cm^3, and large – 6,503 cm^3) and MCs (5%, 7%, 9%, and 11%) was determined during RF heating (1.5 kW, 27.12 MHz). The temperature of the small and the large volumes (having relatively larger top and bottom surface areas than the electrode) of seeds decreased from the center toward the wall region due to heat losses from the outer boundary of the seed. The contrast, in the case of the medium volume of seed, a relatively higher temperature at the region between the middle and outer boundary was observed due to the edge effect. A 2% agar gel was used to demonstrate the effect of sample volume on the formation of the electric field affecting the RF heating pattern. The temperature distribution of the 2% agar gel was in good agreement with that of the bulk canola seed.

The mortalities of the red flour beetle infesting canola seeds of the small and medium volumes during RF heating were determined at different end temperatures (30 to 80℃) and initial seed MCs (5%, 7%, 9%, and 11%). Complete mortalities of the adult insects were achieved at 80℃ for the small volume of the seeds at all MCs, at 60℃ and 9% and 11% MCs, and at 70℃ and 5% and 7% MCs for the medium volume. Complete mortalities at the other life stage (pupa, larva, egg) of the insect were achieved at 55℃ at all MCs and volumes. Over 95% mortality of the adult insects was achieved at over 60℃ temperature at any MCs and volumes. Germination, major and minor axes, roundness and colour of the seeds and quality of the seed oil were not affected significantly by RF treatment temperature at all MCs. There is potential to realize complete mortality at all life stages of the insect infesting the seed at 60 ℃ by RF heating, regardless of the volume of the seed sample, with proper design to achieve more uniform temperature distribution and shorter RF heating time.

The thermal death kinetics of the adult red flour beetles infesting the stored canola seed at various MCs (5%, 7%, 9%, and 11%) and volumes (small and medium) of seed were characterised based on the dynamic temperature increment of the seed and experimental data of the insect mortalities during RF heating. The first order reaction model was the most satisfactory to describe the thermal death kinetics of the adult red flour beetle. The determined activation energy (100 kJ/mol) for the thermal death of the adult red flour beetles was lower than that for some other insects (codling moth, Indianmeal moth and navel orangeworm) determined from experiments with a heating block system, which indicated that the adult red flour beetle was more susceptible to thermal death of RF heating than the other insects heated using the heating block.

Selective heating of the red flour beetle in two different volumes of bulk canola seed at 5%, 7%, 9% and 11% MC using the RF heating unit was simulated using the finite element method based commercial simulation package (COMSOL Multi-physics). The simulated temperatures of the seed and insects were compared with measured temperatures at the various MCs and all volumes. Non-uniform RF heating of the seed was observed regardless of the MC or volume. The RF selective heating of the insect was most effective for the small volume of seed at 11% MC. The temperature of the insects was a maximum of 14.6℃ higher than the temperature of the seed.

As an application of the developed simulation, the effect of voltage (tested with half and double the estimated voltages from the previous simulation) on RF heating uniformity and selective RF heating was determined by comparison of simulated temperature distributions of the seed at 11% MC and the insects. The RF heating uniformity in the seeds improved and the selective RF heating

of the insects was enhanced with increasing voltage, regardless of the volume of the seed. To improve RF heating uniformity, mixing the seed with a rotating auger during the RF heating was considered. From further simulations, uniform RF heating of the seeds was observed near the outlet by help of mixing effect.

Acknowledgments

I would like to express my deepest gratitude to my supervisor Professor Oon-Doo Baik for his invaluable guidance, encouragement, and unflinching support in various ways during my study. I would also like to appreciate all the members of my Graduate Advisory Committee Professors Lope G. Tabil, Richard Evitts, Robert T. (Bob) Tyler, and Venkatesh Meda for providing me with constructive comments during the course of my research work. I am also thankful to Dr. Vijaya Raghavan for serving as the external examiner and for very constructive comments

I am so lucky to work and discuss about all my research with Dr. Bijay Shrestha. I acknowledge the technical support from Louis Roth, Rlee Prokopishyn, and Blondin Richard. I am very grateful to Mr. Ian Armer (Manager, Grain quality control division, Viterra Inc.) for providing us with the canola seeds and the technical support. I also gratefully acknowledge Saskatchewan Ministry of Agriculture and Western Grains Research Foundation, Saskatchewan, Canada for the financial support through the Agriculture Development Fund.

Finally, sincere and infinite thanks to my dearest Mr. kyoosung Yu, Mrs. Soonhwa Ha, and Mrs. Jieun Yu for their limitless support and encouragement during my study abroad. I am also grateful to all my best friends - SJ family for giving me infinite encouragement.

TABLE OF CONTENTS

LIST OF FIGURES

LIST OF TABLES

GENERAL INTRODUCTION

A canola seed (*Brassica napus* L.) is one of the major oilseeds produced and consumed worldwide. Approximately 67.7 million metric tons of canola seeds were produced in 2015 – 2016 around the world (USDA Foreign Agricultural Service 2015). Major producing countries of the canola seeds are Austria, Canada, China, European Union, India and the United States. Around 90% of the canola seeds produced in Canada is exported to worldwide markets. This accounts for $ 19.3 billion (including 249,000 jobs and $ 12.5 billion in wages) on the Canadian economy (Canola Council of Canada 2014). Insect pest infestation is a major consideration in international trade of the food products that make hurdles to export market (Gao et al. 2010). An annual loss of 8 to 10% of the oilseeds due to insect pest resulting in millions of dollars losses in the Canadian economy has been reported (Canola Watch 2015). One of the most harmful insect pest in the oilseeds worldwide is the red flour beetle (*Tribolium castaneum*, size ca. 3×0.5×0.3 mm) (Canadian Grain Commission 2013; Mills and Pedersen 1990). These insect pests spoil and decompose the oilseeds.

The fumigation with methyl bromide has been widely used and regarded as one of the practical methods to disinfest various insect pests found in grains and oilseeds. However, it was prohibited since Montreal Protocol because of the health hazards caused by excessive insecticide residues and the destructive effect to the ozone layer (Birla et al. 2008; Griffin 1988; Wang et al. 2004). The other nonchemical treatments to control insect pests such as ionizing radiation, hot air, and cold storage have disadvantages. These techniques require a long treatment time and a substantial capital investment, and may leave live insect pests after the treatments. RF heating based on electromagnetic radiation is volumetric and selective heating, and this technique may avoid the problems posed by the aforementioned nonchemical treatments (Tang et al. 2000).

The RF heating based on electromagnetic radiation is one of the alternative treatments for the disinfestation. A fast volumetric and selective heating are the main advantages of the RF heating, and it is one of the ways to overcome thermal gradient driven conventional heating treatments (Tang et al. 2000). The selective heating of insects depends upon the electrical, physical and thermal properties of the grain and the insects themselves. Usually, grains have lower dielectric properties than those of the insect pest, and it leads to a relatively faster heating of the insects

compared to the treated grains (Guo et al. 2010). There is potential for disinfestation of the insect pest using the RF heating without significant quality degradation of the host grain.

Determining the dielectric properties (dielectric constant, dielectric loss factor) of canola seeds and insects with their thermos-physical properties. Thermal conductivity and diffusivity, specific heat, and emissivity is critically important to understand RF heating of the samples. No comprehensive studies are available on an effect of sample volume and shape on a temperature distribution during RF heating of seeds, on a demonstration of the effect of sample volume on a formation of electric fields and a non-uniform RF heating using 2% agar gel, on an applying the RF heating to disinfest insect pest in stored seeds, on a characterizing thermal death kinetics of the adult insects infesting stored seeds, and on a feasibility study based on computer simulation for RF selective heating of the insects infesting in stored seeds.

Therefore, the main objective of this study was to investigate and develop an efficient process of RF assisted disinfestation of red flour beetle in stored canola seeds. In order to achieve the main goal, the following specific objectives were pursued:

1) to measure the dielectric properties and thermo-physical properties of the canola seeds and the insects,

2) to conduct a feasibility study of RF disinfestation based on selective heating,

3) to determine temperature distributions in bulk canola seeds of various volumes and MCs during RF heating,

4) to demonstrate the effect of the sample volume on the formation of the electric field using a 2% agar gel,

5) to determine the mortalities of the red flour beetles infesting the stored canola seeds,

6) to analyze the effect of the MC, the volume, and the final temperature of the infested seeds on the mortality of the test insect,

7) to compare the physicochemical qualities and germination rate of stored seeds before and after RF treatment,

8) to characterize the thermal death kinetics of the adult insects infesting stored seeds,

9) to develop a computer simulation model for the RF heating of the stored seeds infested with the insects,

10) to compare the simulated and the measured temperature profiles of the stored seeds,

11) to investigate the RF selective heating of the insects in stored seeds via simulation,

12) to see the effect of mixing on the improvement of RF-heating uniformity in simulation, and 13) to design a conceptual scaled-up RF disinfestation unit.

Outline of the Thesis

This thesis is journal paper based and is comprised of seven chapters.

The first chapter determined radio frequency dielectric properties of bulk canola seeds under different temperatures, moisture contents, and frequencies for feasibility of RF disinfestation based on selective heating principle (specific objectives 1 and 2). This chapter was published in *International Journal of Food Properties* 18 (2015) 2746-2763.

The second chapter focused on the determination of thermos-physical properties of stored canola seeds with temperature and moisture content (specific objective 1). It was published in *Journal of Food Engineering* 165 (2015) 156-165.

The third chapter observed temperature distribution in the bulk canola seeds of various volumes and MCs during RF heating, demonstrated the effect of the sample volume on the formation of electric field affecting the RF heating pattern using a 2 % agar gel, and analyzed the effect of seeds MC and volumes on the RF heating uniformity (specific objectives 3 and 4). The chapter was published in *Biosystems Engineering* 148 (2016) 55-67.

In the fourth chapter, immediate and delayed mortalities of the red flour beetle infesting the stored canola seeds were determined, the effects of moisture content, the bulk volume, and the final temperature of the infested seeds on the mortality of the insects were analyzed, and physicochemical qualities and germination rate of the seeds were compared before and after RF treatment (specific objectives 5, 6, and 7). This chapter was published in *Biosystems Engineering* 151 (2016) 248-260.

The fifth chapter characterized the thermal death kinetics of the adult red flour beetles infesting stored canola seeds at various moisture contents and volumes of the seeds based on the dynamic temperature increment of the stored canola seeds and the experimental data of insect mortalities during RF heating (specific objective 8). It was accepted in *International Journal of Food Properties*.

In the sixth chapter, a computer simulation model for the RF heating of the stored canola seeds infested with the red flour beetles was developed, the simulated and the measured temperature histories of the stored canola were compared, and the RF selective heating of red flour beetle in

the stored canola seeds was investigated via simulation (specific objectives 9, 10, and 11). The chapter was submitted to *Engineering in Agriculture, Environment and Food*.

The seventh chapter provides a general discussion, application of the developed simulations, and recommendation for future studies (specific objectives 12 and 13).

References

Birla, S. L., S. Wang, J. Tang, and G. Tiwari. 2008. Characterization of radio frequency heating of fresh fruits influenced by dielectric properties. *Journal of Food Engineering* 89 (4): 390-398.

Canola Council of Canada 2014. http://www.canolacouncil.org/markets-stats/industry-overview/. (June, 13, 2016).

Canadian Grain Commission 2013. http://www.grainscanada.gc.ca/storage-entrepose/pip-irp/rfb-trf-eng.htm. (June, 13, 2016).

Canola Watch 2015. http://www.canolawatch.org/2011/05/09/estimating-flea-beetle-damage-in-canola/. (June, 13, 2016).

Gao, M., J. Tang, Y. Wang, J. Powers, and S. Wang. 2010. Almond quality as influenced by radio frequency heat treatments for disinfestation. *Postharvest Biology and Technology* 58: 225–231.

Griffin, J. P. 1988. Montreal Protocol on Substances That Deplete the Ozone Layer. In Int'l L. (Vol. 22, p. 1261).

Guo, W., S. Wang, G. Tiwari, J. A. Johnson, and J. Tang. 2010. Temperature and moisture dependent dielectric properties of legume flour associated with dielectric heating. *LWT-Food science and technology* 43(2): 193-201.

Mills, R., and J. Pedersen. 1990. *A flour mill sanitation manual*. Eagan Press, ST. Paul, MN.

Tang, J., J. N. Ikediala. S. Wang, J. D. Hansen, and R. P. Cavalieri. 2000. High-temperature-short-time thermal quarantine methods. *Postharvest Biology and Technology* 21 (1): 129-145.

USDA Foreign Agricultural Service 2015. Production, Supply and Distribution Online Database, query for Commodity: "Oilseed, Rapeseed"; Data Type: "Production"; Country: "All countries"; Year: "2015", 2016 (June / 13).

Wang, S. and J. Tang. 2004. Radio frequency heating: a potential method for post-harvest pest control in nuts and dry products. *Journal of Zhejiang University Science* 5 (10): 1169-1174.

CHAPTER 1

RADIO FREQUEENCY DIELECTRIC PROPERTIES OF BULK CANOLA SEEDS (*BRASSICA NAPUS* L.) UNDER DIFFERENT TEMPERATURES, MOISTURE CONTENTS, AND FREQUENCIES FOR FEASIBILITY OF RADIO FREQUENCY DISINFESTATION

Published, *International Journal of Food Properties* 18 (2015) 2746-2763.

Contribution of this paper to overall study

Measurement of dielectric properties of bulk canola seeds at various temperatures, moisture contents, and frequencies (specific objective 1); determination of the penetration depth of electromagnetic energy in the seeds; and demonstration of feasibility of RF disinfestation based on selective heating principle were conducted (specific objective 2) in this chapter as little or no work of those has been done. The developed regression models of dielectric properties of the seeds as functions of temperature, moisture content, and frequency were used for the simulation of the temperature changes of the seeds and the red flour beetle during RF disinfestation in Chapter 6. Based on the dielectric properties of the canola seeds and the red flour beetles, the feasibility of the RF selective heating of the red flour beetle in the seeds was analyzed. All the experiments in this chapter were conducted and the journal paper manuscript was drafted by myself.

1.1 Abstract

The parallel capacitances and resistances of the bulk canola seeds were measured to determine the dielectric properties of canola seeds (*Brassica napus* L.) using an RF dielectric fixture at

different levels of temperature (30 - 80℃) and moisture content, MC (5% - 11% w.b.) over the frequency range of 5 to 30 MHz. The dielectric constant (ε') increased from 3.82 to 7.85 with increasing temperature and decreasing frequency regardless of the seed MCs. The dielectric loss factors (ε'') of the bulk seeds increased with increasing temperature and MC and decreased with frequency, and fell between 0.11 and 13.0. The penetration depth of the electromagnetic (EM) power in the bulk seeds varied from 1.30 to 48.0 m depending upon temperature, frequency, and MC. The distinct correlation of sensitivity of dielectric properties with MC was not observed except that of penetration depth. The dielectric properties of the bulk canola seeds were higher than those of other oilseeds at various MCs, it could be affected by relatively higher linolenic acid content among other fatty acids. The large difference of the dielectric loss factors of insect pests from those of canola seeds showed potential of RF disinfestation based on selective heating of insect pests in the canola seeds. The dielectric properties determined can be used for simulating temperature distribution within the bulk canola seeds during RF process.

1.2 Nomenclature

c	speed of light in free space (3×10^8, $m\cdot s^{-1}$)	R_p	resistance
C_p	specific heat ($J\cdot kg^{-1}\cdot℃^{-1}$)	RF	radio frequency
DF	degree of freedom for error	RMSE	root mean square deviation
DTF	dielectric test fixture	SD	standard deviations
E	electric field strength ($V\cdot m^{-1}$)		
EM	electromagnetic	*Greek symbols*	
f	frequency (Hz)	E	surface emissivity of the sample
MC	moisture content	ε'	dielectric constant
P	power dissipation	ε''	dielectric loss factor
P_{avg}	average power density ($W\cdot m^{-3}$)	ρ	density ($kg\cdot m^{-3}$)
P_d	penetration depth		

1.3 Introduction

Approximately 85% of canola produced in Canada is exported to markets around the world with a worth of billions of dollars. $983 million Canadian canola industries transforms canola seeds into meal and oil, which are subsequently used for manufacturing many other products. The contribution of canola to Canadian economy is $15.4 billion each year including more than $8.2 billion in wages, and 228,000 Canadian jobs (Canola Council of Canada 2011).

The average annual losses of oilseed production due to insect pest in the field and during storage range from 8 to 10% causing millions of dollars in damage (Canola Watch 2011). Fumigation with methyl bromide has been widely used to disinfest various insect pests found in the oilseeds and cereal grains as it has been regarded as the most practical method for disinfestation. However, this method is environmental unfriendly and health hazardous and may leave an excessive insecticide residue in the treated products (Birla et al. 2008).

Conventional disinfestation methods of fumigation that use methyl bromide were banned since the Montreal Protocol because of its destructive effect to the ozone layer (Reagan et al. 1987; Wang and Tang 2004). Researchers have applied other conventional treatments such as ionizing radiation, hot air, and controlled atmosphere or cold storage as possible substitutes for the chemical treatments, however all of these methods still have a large room for further improvement.

One of the alternative treatments for disinfestation is radio frequency (RF) heating, one of the several EM-based electrical heating methods. The key advantage of RF heating over the thermal gradient driven conventional heating methods is that it produces a fast volumetric heating. As a result, this method has been thought as a way to overcome the problems with conventional thermal disinfestations techniques (Tang et al. 2000). Jiao et al. (2011) have shown significant reduction in treatment time using RF heating compared to existing heating methods. Because of larger penetration depth of RF waves (meters), higher volume of grains could be disinfested as needed for the grain handling industries. Another important advantage of RF heating is the selective heating of the insect pests, in which the insects in grains would be destroyed at the temperatures lethal to them with a minimal or tolerable thermal degradation of the grain qualities. Although the frequency is the same, the ε'' and ε' for the insect and grain are different as these dielectric properties depend on various material properties such as concentration of ion, moisture content (MC), and density. If the ion concentration and MC of the insect are higher than those of the grain,

RF heating can be very effective for disinfestations. Further, the grains can be dried to a desired level while it is being disinfested.

The objectives of this study were (1) to measure and analyze the dielectric properties of the bulk canola seeds at various temperatures, MCs, and frequencies, (2) to analyze dielectric dependence on fatty acids, (3) to determine the penetration depth of EM energy in the bulk canola seeds, (4) to develop regression models of the dielectric properties, and (5) to demonstrate a feasibility of RF disinfestation based on selective heating.

1.4 Materials and methods

1.4.1 Theory

The permittivity of a dielectric material, ε is defined as (Choi and Konrad 1991) :

$$\varepsilon = \varepsilon' - j\varepsilon^{"} \tag{1.1}$$

where The ε' represents the polarization of a material, or the ability of a material to storing electrical energy or charges within the applied EM field. The $\varepsilon^{"}$ expresses quantity of heat dissipation that results from the conduction loss of charges, and dipolar or ionic losses, in other words the ability of the material to dissipate the electrical energy into heat energy compared to vacuum. Generally, dipole rotation loss (ε_d'') and ionic conduction loss (ε_σ'') summed to the total ε'', $\varepsilon'' = \varepsilon_\sigma'' + \varepsilon_d''$. The penetration depth of an EM wave within dielectric materials is determined by the frequency, and the dielectric properties of the material in free space (Von Hippel 1954). The following equation was used to estimate P_d (Shrestha and Baik 2013a) :

$$P_d = \frac{c}{2\pi f} \frac{1}{\sqrt{2\varepsilon'\left[\sqrt{1+\left(\varepsilon^{"}/\varepsilon'\right)^2}-1\right]}} \tag{1.2}$$

where, c = the speed of light in free space (3×10^8 m/s), ε' = the dielectric constant, $\varepsilon^{"}$ = the dielectric loss factor, and f = the frequency (Hz). The ratio of temperature increment rate of insect to that of canola seed was also estimated following the procedure described by Shrestha and Baik.[10] The average power generated inside a material was calculated as shown in Eq. (1.3) (Choi and Konrad 1991).

$$P_{avg} = 2\pi\varepsilon^0 f E^2 \varepsilon^{"} = \rho C_p \frac{d\,T}{d\,t} \tag{1.3}$$

where P_{avg} = the average power density (W m^{-3}), ε^0 = vacuum permittivity (8.85 × 10^{-12} F m^{-1}), C_p = the specific heat of the material (J kg^{-1}°C^{-1}), ρ = the bulk density of the material (kg m^{-3}), E = the electric field strength (V m^{-1}), f = the frequency (Hz), dT/dt = the rate of temperature increase. The power dissipation ratio (P_{ic}) of insect (P_{avg_i}) to canola seed (P_{avg_c}) at 27.12 MHz was described using Eq (1.4) as follows:

$$P_{ic} = \frac{P_{avg_i}}{P_{avg_c}} = \frac{E_i^2}{E_c^2}\frac{\varepsilon_i^{"}}{\varepsilon_c^{"}} \tag{1.4}$$

where E_i = the electric field strength within insect bodies (V m^{-1}), E_c = the electric field strength within canola seeds (V m^{-1}), $\varepsilon_i^{"}$ = the loss factor of the insect, $\varepsilon_c^{"}$ = the loss factor of the canola seed Electric field strength (E) within materials was estimated with a theoretical model Eq. (1.5), derived from basis of interaction of EM waves (Stratton 2007).

$$E_{guest} = E_{host}\left(\frac{3\varepsilon_{host}}{2\varepsilon_{host}+\varepsilon_{guest}}\right) \tag{1.5}$$

where ε_{host} and ε_{guest} are the permittivity of the host and guest material. Eq. (1.5) was transformed into Eq. (1.6) based on assuming both the canola seed and insect are homogeneous dielectrics, and the spherical shape of insect is surrounded by air.

$$E_{ic} = \frac{E_i}{E_c} = 3\left(\frac{1}{2+\frac{\varepsilon_i}{\varepsilon_c}}\right) \tag{1.6}$$

ε' was a substitute of ε for low loss materials ($\tan\delta = \varepsilon^{"}/\varepsilon' \ll 1$) in Eq. (1.6) with an acceptable error in E_{ic}. The ratio of temperature increment rate of insect to that of canola seed depicted as ΔT_{ic} was derived from Eqs. (1.3) and (1.4) as shown in Eq. (1.7).

$$\Delta T_{ic} = \frac{\left(\frac{\Delta T}{\Delta t}\right)_i}{\left(\frac{\Delta T}{\Delta t}\right)_c} = P_{ic}\frac{\rho_c C_{pc}}{\rho_i C_{pi}} \tag{1.7}$$

where $(\Delta T/\Delta t)_i$ = the rate of temperature increase of insect (°C s^{-1}), $(\Delta T/\Delta t)_c$ = the rate of temperature increase of canola seed (°C s^{-1}), ρ_i = the density of insect (kg m^{-3}), ρ_c = the density of canola seed (kg m^{-3}), C_{pi} = the specific heat of insect (J kg^{-1} °C^{-1}), C_{pc} = the specific heat of canola seed (J kg^{-1} °C^{-1}). Based on the above equations, a selective heating can be maximized depending on the values of E_{ic} and $\varepsilon_i^{"}/\varepsilon_c^{"}$.

1.4.2 Materials

Top quality canola seeds (B. *napus* L.) at initial MC of 9% were supplied by industrial partner Viterra Inc., Regina, SK, Canada. The seed sample could contain any varieties of the canola seed registered at Canadian Food Inspection Agency. The dielectric properties, specific heat, and densities of rusty grain beetle (C. *ferrugineus* S.) as a function of temperature and MC were obtained from Shrestha and Baik (2013b). However, the effect of temperature on densities of rusty grain beetle seemed negligible, and the densities were, therefore, measured by Von Hippel at room temperature (Shrestha and Baik 2013b).

1.4.2.1 Sample preparation

A standard method was used to determine the MC of the bulk canola seeds (ASAE 2004; Brusewitz 1975). To calculate the average initial MC, seeds weighing 10 g were poured into each of five aluminum moisture dishes followed by placing them in a hot air oven–Despatch, Despatch Industries, MN, USA for 24 h at 103℃. The samples of the canola seeds were prepared at different MCs, 5%, 7%, 9%, and 11% wet weight basis (weight of water/sample weight × 100 %) separately. Samples of the canola seeds at 5% and 7% were prepared by drying a known mass of canola seeds at initial MC (9%) to the pre-calculated weight in a hot air oven set up at 40℃. Samples at 11% MC were prepared by spraying a pre-calculated amount of distilled water on known mass of the seeds at initial MC contained in a glass jar. The jar was constantly and manually shook and rotated while spraying with water. The air-tight jars were left at room temperature (23℃) for 3 days with periodic tumbling to achieve an equilibrium MC followed by cold storage (4℃) until used. A digital scale with an accuracy of ± 0.01g (Symmetry, PR4200, Cole–Parmer Instrument Co., IL, USA) was used for all weighing. The samples from the cold storage were left at room temperature for 1 h and the final MC of samples were checked before using them.

1.4.2.2 Specific heat, densities, and porosity of canola seeds

A differential scanning calorimeter (DSC) (Q2000, TA Instruments, Inc., New Castle, Del) was used to measure heat capacity of the materials. A hermetically sealed aluminium pan including about 10 mg ($\pm$0.01 mg) of sample was loaded into the DSC along with an identical blank aluminium pan for reference. Heating rate was kept constant at 5℃ min^{-1}. Heat capacities of canola seeds at MCs of 5%, 7%, 9%, and 11% were measured at 30 to 75℃. All data were obtained from

five replicates. The bulk density of canola seeds was calculated by measuring mass of known volume of bulk canola seeds in a precision steel cylinder of known volume (500 ± 0.5 ml). The mass of bulk canola seeds was measured after levelling out the top surface with a steel cylindrical bar. An average of five replicates was used.

To calculate particle density, a gas pycnometer was used. A certain mass of the seeds was poured into large cell after calibration of the meter. Nitrogen gas flowed into the reference cell until the pressure reached to about 17 psig. Then, nitrogen gas was allowed to flow into the large cell containing the canola seeds. The initial gas pressure decreased to a new lower equilibrium pressure depending on the volume of the canola seed based on the Archimedes principle. A gas equation was applied to calculate the particle volume using initial and final pressures, and the known volume of reference and sample cell. The porosity was calculated by measured bulk and particle densities.

The porosity of canola seeds was calculated as :

$$\left(1 - \frac{\rho_b}{\rho_p}\right) \times 100 \tag{1.8}$$

where ρ_b is bulk density and ρ_p is particle density.

1.4.2.3 Dielectric properties

The capacitance (C_p) and the resistance (R_p) of bulk canola seeds at different MCs, temperatures, and frequencies were measured using a dielectric test fixture (DTF) (16452, Agilent Technologies, Palo Alto, CA), a computer controlled precision LCR device (4208A, Agilent Technologies, Palo Alto, CA), and other peripheral devices as shown in Fig. 1. 1. To increase the sample volume, and thereof to minimize experimental error, all factory supplied spacers (thicknesses of 1.3, 1.5, 2, and 3 mm) were stacked together (Fig. 1. 1) to obtain a maximum volume of 16.4 mL.[14] The ε of known air (low loss) to water and ethanol media (lossy) was measured using both 3 mm and 7.8 mm spacer (normal and modified fixtures) for the calibration of system in measuring the C_p and R_p (Agilent 2001). The largest volume of the liquid fixture otherwise would be 6.8 mL using the 3 mm-spacer.

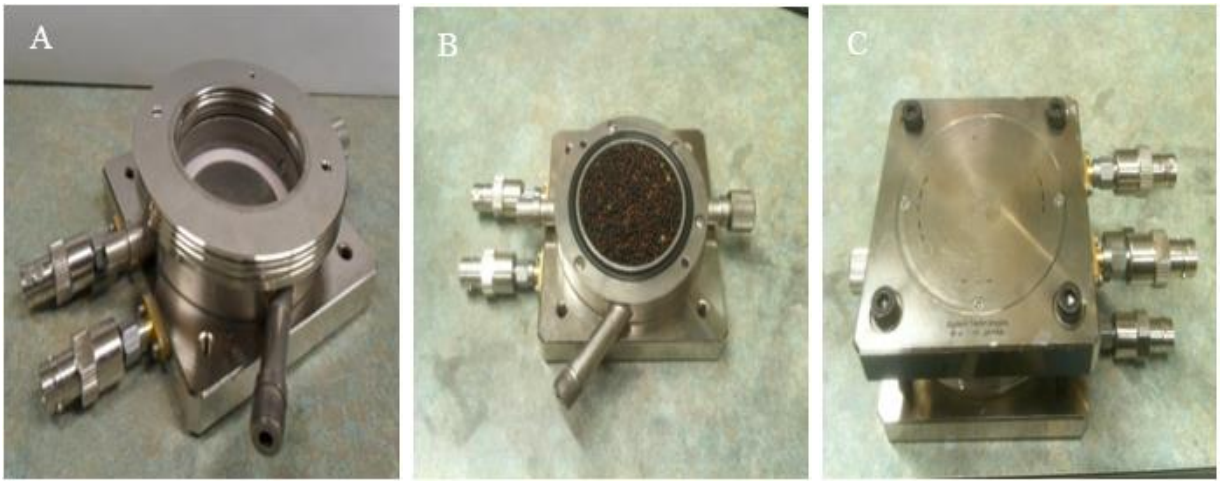

Figure 1. 1. A: bottom half of DTF with new spacer on top, B: the DTF filled with canola seeds, and C: gently closed the DTF using top and bottom halves with canola seed inside.

All parts of the fixture two O-rings, top and bottom halves of the fixture, and spacers, were washed with warm soap water, rinsed using distilled water, and then dried completely before using them. Using the known volume of the fixture, an amount of the canola seeds was calculated from the seed bulk density, and was poured into the fixture so that it is filled completely with several gentle taps to remove pore as much as possible, then closed tightly (Fig. 1. 1). The tightly closed fixture was visually inspected to make sure that the top and the bottom halves of the fixture were leveled along the spacer without leaving any uneven gaps assuring two electrodes parallel to each other.

From the preliminary experiments, it was found that one hour was sufficient to increase the sample temperature from 23℃ to any target temperatures up to 80℃ in the temperature and humidity chamber (Espec, SH-641, Espec Corp., Japan) with an accuracy of ± 0.1℃. The humidity function of the chamber was turned off. The four BNC female connectors of the fixture containing the canola seeds were connected to corresponding male connectors of 1 m 4-terminal BNC cable (16452-61601, Agilent Technologies, Palo Alto, CA) followed by placing it on the chamber shelf. The other ends were connected to the LCR device. To minimize biased error of the LCR device, it was calibrated following the manufacturer's user guide (Agilent 2001). The random error of the system ranged 3% to 28%, depending upon the frequency and temperature (Agilent 2001). The measured C_p and R_p were used to calculate ε' and ε'' of the test bulk seeds using Eqs. (1.9) and (1.10). All data were obtained using the same batch of canola seeds. To minimize the random error,

an average of five replicates was used throughout this work unless otherwise mentioned (Agilent 2001).

$$\varepsilon' = \mathrm{dC_p} \,/\, A\varepsilon_o \tag{1.9}$$

$$\varepsilon'' = d \,/ 2\pi f A \varepsilon_o R_p \tag{1.10}$$

where ε' = dielectric constant, d = distance between two electrodes (m), C_p = parallel capacitance (F), A = electrode area (m^2), ε_o = air permittivity, 8.85 $\times 10^{-12}$ (F / m), ε'' = dielectric loss factor, f = frequency (Hz), and R_p = parallel resistance (Ω).

1.4.2.4 Penetration depth (P_d)

Penetration depth is an important parameter to evaluate heating uniformity within materials, and to design efficient EM heating units. Penetration depth in the bulk canola seeds at different MCs, temperatures, and frequencies were calculated according to Eq. (1.3) (Von Hippel 1954). An average of five replicates was used.

1.4.3 Statistical analysis

The mean values and the standard deviations (SD) of the measured dielectric properties were calculated. The effects of MC, frequency, and temperature on the dielectric properties of the bulk canola seeds were investigated using the factorial design. The modeling was performed using the stepwise regression analysis in SPSS 20.0 (SPSS Inc., Chicago, IL, USA).The regression model derived from experimental data using SPSS Statistics 20.0 (SPSS Inc., Chicago, IL, USA) was used to estimate relative sensitivities of the outputs (calculated values from the regression model) of dielectric properties and penetration depth to temperature at various MCs at 27.12 MHz. It was described as the ratio of the percent variation of output (dielectric properties) to that of input (temperature) with different MCs. The percent variation of output and input was calculated as Eq. (1.11). The dielectric properties at 55℃ and the average temperature (55℃) were used as the reference output and input.

$$\text{The percent variation (\%)} = \frac{\text{Out(In)put} - \text{Reference out(in)put}}{\text{Reference out(In)put}} \times 100 \tag{1.11}$$

1.5 Results and discussion

1.5.1 Density and porosity of canola seeds

Measured bulk and particle densities and calculated porosities as functions of temperature and MC are listed in Tables 1. 1. In general, densities decreased with temperature. Increased particle size of canola seed increased the total volume air voids and decreased mass of canola seed due to the evaporation of moisture resulting in decreasing densities. The bulk and particle densities ranged from 655 to 670 kg·m^{-3} and 1064 to 1137 kg·m^{-3}, respectively. The porosity of canola seeds ranged from 38.286 to 41.626. It decreased with temperature and MC due to decreasing ratio of ρ_b to ρ_p.

Table 1. 1. Specific heats, densities, and porosities of rusty grain beetle (C. *ferrugineus* S.) and canola seeds (B. *napus* L.) at indicated temperatures and MCs (Stratton, 2007).

Moisture content	Canola seed				Rusty
(w. b.)	5%	7%	9%	11%	49%
Temp (℃)	Specific heat (kJ kg^{-1} C^{-1})				
30	1.85	1.94	2.07	2.14	4.10
45	2.30	2.39	2.56	2.63	4.47
60	2.54	2.66	2.85	2.98	4.66
75	2.74	2.89	3.02	3.26	4.73
	Bulk density (× 10^2 kg m^{-3})				
30	6.68	6.66	6.69	6.70	
45	6.63	6.62	6.63	6.63	
60	6.59	6.61	6.57	6.57	5.20 at 25°C
75	6.57	6.61	6.56	6.55	
	Particle density (× 10^2 kg m^{-3})				
30	11.37	11.25	11.11	11.12	
45	11.20	11.10	10.95	10.96	11.7 at 25 °C
60	11.00	10.95	10.80	10.82	
75	10.87	10.81	10.65	10.64	
	Porosity				
30	41.63	40.90	40.14	40.16	
45	40.89	40.34	39.56	39.56	55.56 at 25 °C
60	40.08	39.70	39.15	38.29	
75	39.42	39.23	38.39	38.36	

1.5.2 Dielectric constant (ε') of canola seeds

Fig. 1. 2 shows the ε' of bulk canola seeds as a function of frequency, and temperature for four levels of MCs. The ε' decreased almost linearly with increasing frequency for all MCs. It was attributed to rapidly alternating EM fields at higher frequencies significantly diminishing reorientation of the dipoles, distortion of ionic bonds, and the interfacial polarization mechanism within the test material resulting in less polarization (Shrestha and Baik 2011). This phenomenon was in agreement with the Debye's equation which indicates the decrease of the ε' with increasing

frequency (Debye 1929). Pace et al. (1968) also observed a similar trend, in which a sharp decrease of the ε' was observed with further increase of the frequency after general plateau from 1 kHz to 10 MHz. The ε' increased with increasing temperature at different MCs. It was attributed to increased level of dielectric dispersion because of higher ionic conductivity at higher temperatures (Nelson and Bartley 2002). Ionic conductivity normally increases with increasing temperature (Tang et al. 2002). The ε' increased with MC at different frequencies and temperatures. The added moisture enhanced the ionic, and dipole polarizations in the bulk canola seeds resulting in increasing storage of electrical charges under the applied EM field. As expected, the ε' at 11% MC was higher than that of any other MCs at any given frequencies and temperatures. The values ranged from 3.82 to 7.85.

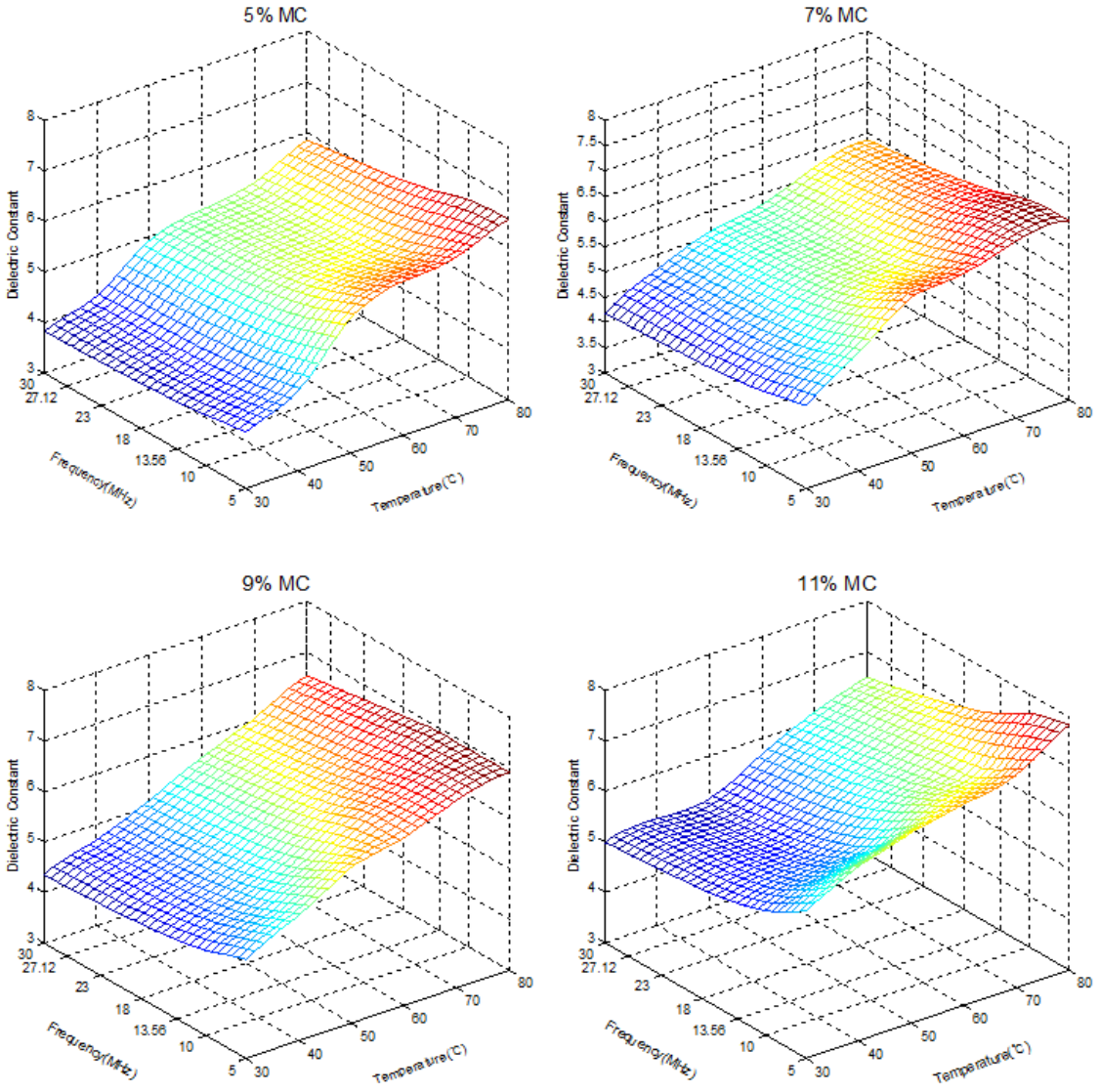

Figure 1. 2. Frequency, temperature and MC dependence of ε' of the bulk canola seeds.

1.5.3 Dielectric loss factor (ε'') of canola seeds

Fig. 1. 3 illustrates the ε'' of the bulk canola seeds as a function of frequency and temperature at four levels of MC. The ε'' decreased with increasing frequency with a dramatic drop to over 50% at 5 MHz to 13.56 MHz regardless of temperature and MC. Diminishing movements of the dipoles and ions due to the rapidly alternating EM fields with increasing frequency resulted in lower ionic conductivity and less conservation of EM energy to heat, consequently decreasing its values. Further increase of frequency to 30 MHz exhibited almost linear decrease of the ε''. The ε'' decreased from 13.03 to 0.112 corresponding to increasing frequency for all MCs, and it almost

linearly increased in proportion to increasing temperature and MC. The increased ε'' at higher temperature was attributed to higher oscillation of the dipoles and movement of the ions resulting from higher thermal agitation of the molecules and ions (Tang et al. 2002; Sipahioglu et al. 2003; Wang et al. 2003; Koskiniemi et al. 2013). The ionic conductivity also mainly affects the ε'' at low frequency range below 200 MHz (Wang et al. 2003; Guan et al. 2004). The ε'' is composed of ionic loss and dipole loss. Ionic loss is caused by migration of ions, and dipole loss by the rotation of water dipoles within alternating electric field. Therefore, the lower viscosity has improved movements of ionic and dipolar enhancing the ε''. The ε'' was enhanced by increasing number of dipoles and free ions in the moisture.

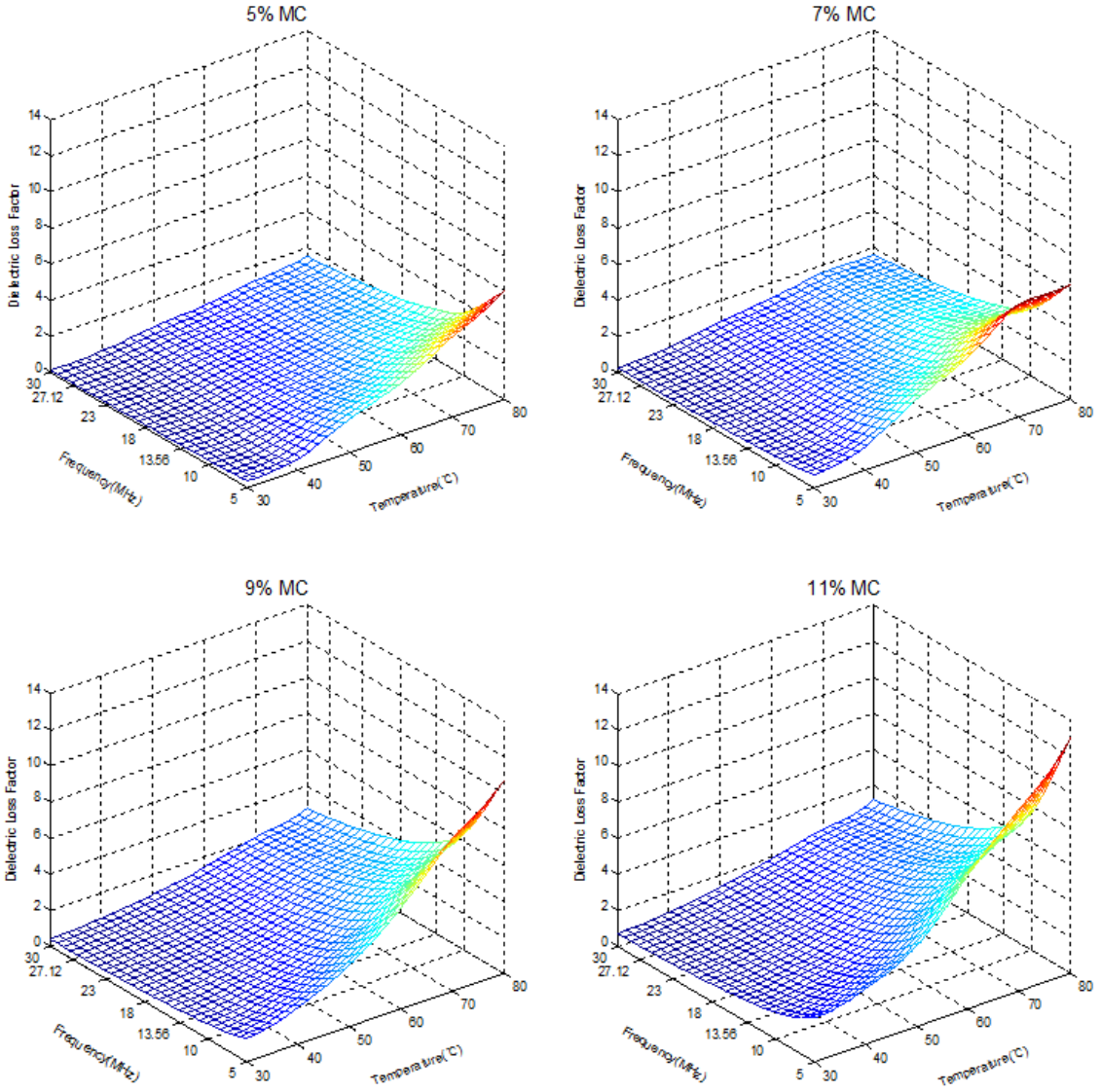

Figure 1. 3. Frequency, temperature and MC dependence of ε" of the bulk canola seeds.

1.5.4 Penetration depth (P_d)

The penetration depths decreased with frequency, temperature and MC as shown in Fig. 1. 4. As explained earlier, the dielectric properties increased with temperature and MC. But, the rapid increase of $\varepsilon^{"}$ comparing to ε' increased the values of $\varepsilon^{"}$ / ε' resulting in decreasing penetration depths. The values for P_d were varied from 1.30 to 48.0 m. A maximum possible electrode gap (less than 1.30 m) and sample size in designing the application chamber can be suggested from the results of P_d for uniform RF treatment for disinfestation of canola seeds.

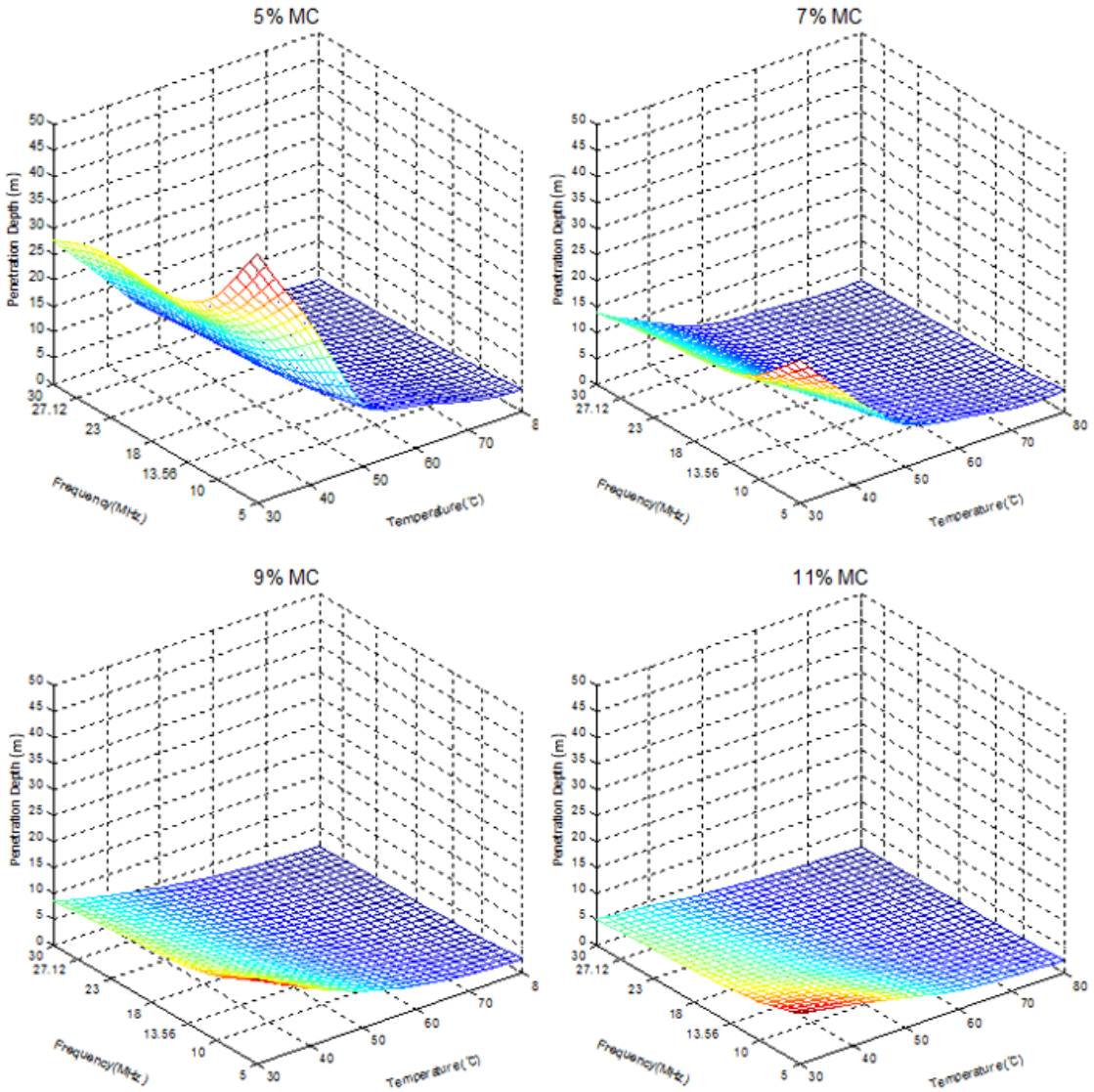

Figure 1. 4. Electromagnetic power penetration depths in the bulk canola seeds as a funtion of temperature, MC, and frequency.

1.5.5 Statistical analysis and models

Regression models for the predictions of the ε' and ε'' are given by Eqs. (1.12) and (1.13). The statistical data, R^2, RMSE, p-value, and DF for errors are presented in Table 1. 2.

$$\varepsilon' = 1.678 - 0.003 \cdot f \cdot \mathrm{MC} - 0.0002 \cdot f \cdot \mathrm{T} + 0.260 \cdot \mathrm{MC} - 0.001 \cdot \mathrm{MC} \cdot \mathrm{T} + 0.051 \cdot \mathrm{T} \quad (1.12)$$

$$\varepsilon'' = -2.720 + 0.112 \cdot f - 0.002 \cdot f \cdot \mathrm{T} - 0.0003 \cdot f \cdot \mathrm{MC} \cdot \mathrm{T} + 0.012 \cdot \mathrm{MC} \cdot \mathrm{T} + 0.001 \cdot \mathrm{T}^2 \quad (1.13)$$

where, $\varepsilon' = \text{dielectric constant}$, $\varepsilon'' = \text{dielectric loss factor}$, T = temperature (℃), MC = moisture content (%), f = frequency (MHz). Based on p-value of each component, the ε' of the bulk canola seeds seems to be affected more by MC and temperature, while MC and frequency seem to most affect the ε''. Although the p-values of MC and temperature are greater than 0.05 they were included in the regression models considering their theoretical and reported effects (Shrestha and Baik 2013a). The higher values of R^2, lower values of RMSE, and p-values < 0.0001 of the models confirmed that these equations could be used to predict the dielectric properties of bulk canola seed. These developed regression models also will be applied to dynamic simulation of selective heating.

Table 1. 2. Statistical parameters for the regressions models of the dielectric properties of canola seeds in Eq. (1.12) and (1.13).

	Eq. (1.12)	Eq. (1.13)
R^2	0.951	0.894
[a] RMSE	0.189	0.683
p-value	<0.0001	<0.0001
[b] DF	167	167
	p-value of each component	
MC	<0.0001	<0.167
Temperature	<0.0001	<0.401
Frequency	<0.041	<0.0001

[a] RMSE : root mean square deviation

[b] DF : degree of freedom

1.5.6 Sensitivity analysis

Fig. 1. 5 indicates sensitivity of dielectric properties and penetration depth as a function of temperature at various MCs at 27.12 MHz in percentage. The distinct correlation of the sensitivity of dielectric properties with MC was not observed except that of penetration depth. The relatively more sensitive dielectric constants of canola seeds were observed at 9% MC with increasing temperature and at 5% MC with decreasing temperature from reference temperature (55℃) compared to those at the other MCs. The sensitivities of ε' of canola seeds at 9% and 5% MC were

around 1.7 and 1.5 times higher than that at 7% and 11% MC and at increased and decreased temperatures (± 45.5%). The relatively more sensitive dielectric loss factors of canola seeds at 5% MC were observed. The sensitivities of ε'' of canola seed at 5% MC were approximately 2.0 and 1.5 times higher than that at 7% and 11% MC and at increased and decreased temperature (± 45.5%). The variation of penetration depth was much higher in low MC of sample (5%) than in high MC of sample (11%). The variation difference was around 290% between sample of 5% MC and 11% MC at 30℃ decreased by -45.5% from the reference temperature. This means penetration depth in lower MC is more sensitive to temperature variation. The higher sensitivity of penetration depth to temperature change suggests that more attention should be given in determining the size of an industrial RF disinfestation chamber for low moisture content canola seeds.

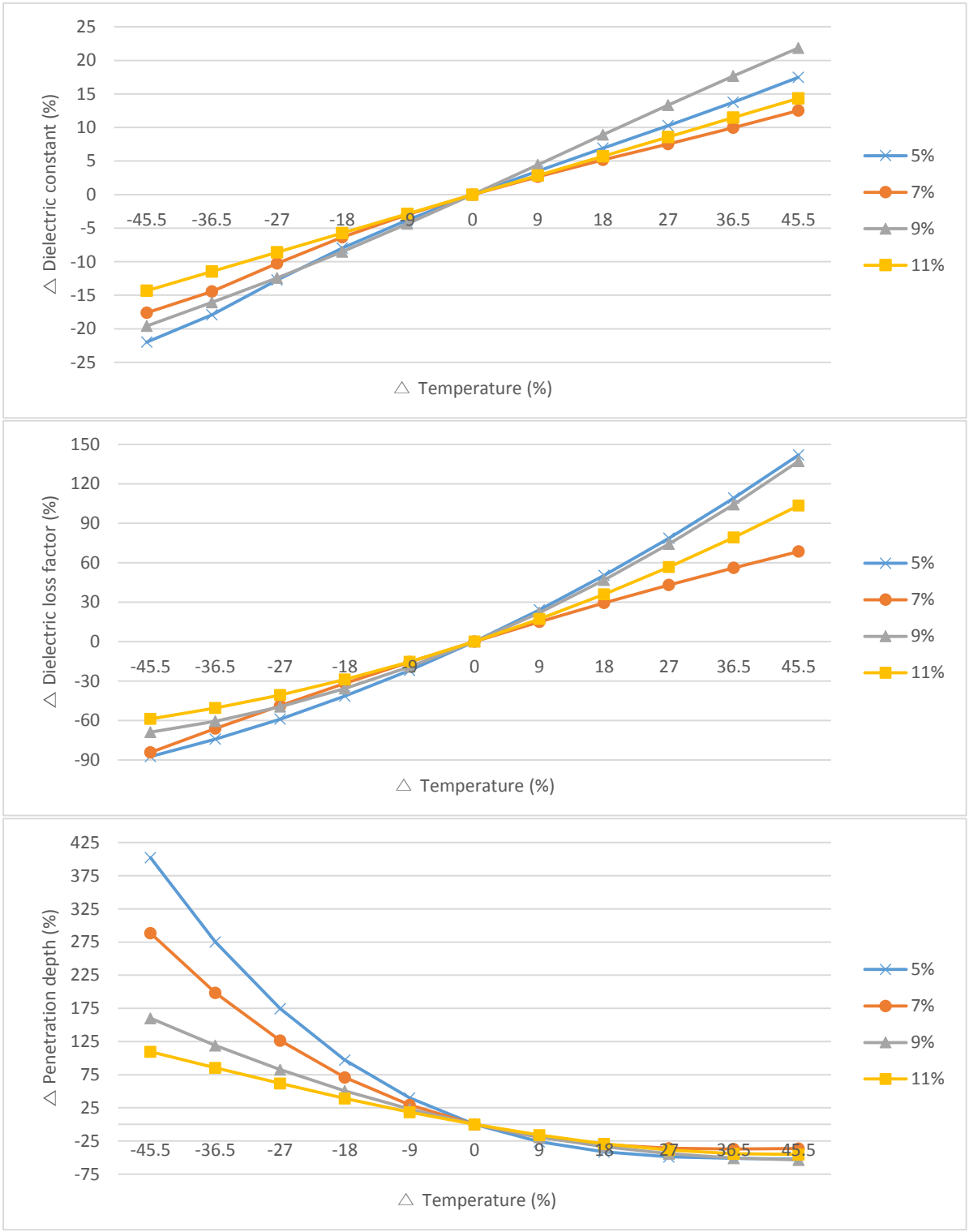

Figure 1. 5. Sensitivity analysis of dielectric properties of the canola seeds and electromagnetic power penetration depth in the bulk canola seeds as a funtion of temperature and MC at 27.12 MHz.

1.5.7 Effect of linolenic acid

The canola seed consists of moisture, ash (minerals), oil, protein, and glucosinolate (Conrad 1982). Oil is the largest component by mass, and it contains caprylic, capric, palmitic, stearic, oleic, linoleic, and linolenic acids (Haq et al. 2009). The ε' of these acids at 1 MHz at 75°C were found from Lizhi et al. (2008) and presented in a bar-chart (Fig. 1. 6). Linolenic and caprylic acids showed the highest values of the ε', 2.493 ± 0.001 and 2.491 ± 0.001 among the fatty acids. Most oilseeds have similar percentage of caprylic acid. The percentages of linolenic acid in soybean (5.36%) and canola oils (7.51%) were much higher compared to those of other oilseeds (0.055%–0.31%) as indicated in Table 1. 3 (Lizhi et al. 2008). The ε' of fatty acid increases with degree of unsaturation or the number increasing of double bonds of unsaturated molecules (Pace et al. 1968; Lizhi et al. 2008; Rudan-Tasic and Klofutar 1999). The linolenic acid has three double bonds of unsaturated molecules more than other fatty acid resulting in the higher ε'. This could be one of the reasons of the higher ε' of the canola oil relative to other oilseeds. It should be noted that other ingredients of canola seed potentially affect ε' along with the linolenic acid although we suspect the effect might be limited. Table 1. 3 shows the dielectric properties of canola seeds are higher than other oilseeds in accordance with the same reason at different MCs, 23–30°C, and 10 MHz (Canola Council of Canada 2011; ASAE 2012; Sacilik et al. 2006; Sacilik et al. 2007; USDA 2011).

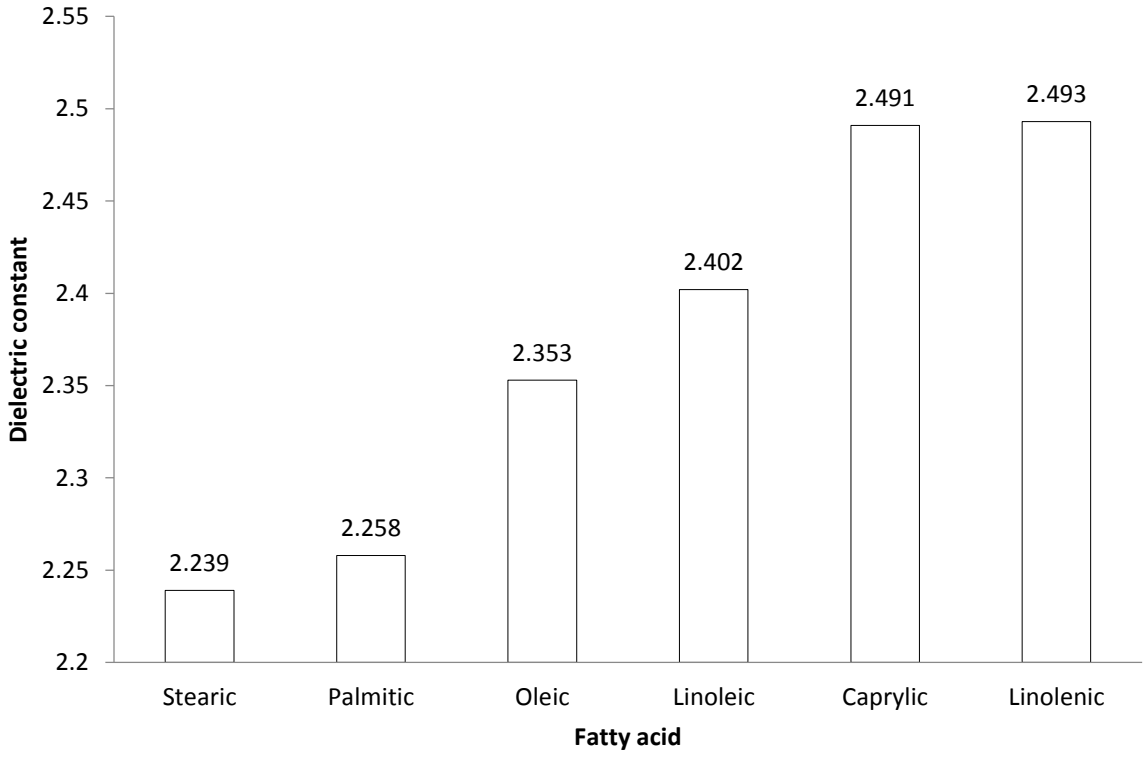

Figure 1. 6. The dielectric constants of fatty acids in the canola seed oil at 1 MHz at 75ºC (data taken from Lizhi et al. 2008).

Table 1. 3. Dielectric constants and loss factors of various oilseeds as a function of linolenic acid content and MC at 10 MHz (data taken from Lizhi et al. 2008).

	Peanut		Safflower		Soy Bean		Canola seed	
				Total oil content (%)				
	49.70		38.45		18.51		45.20	
				Linolenic acid content (%)				
Moisture content (%)	0.055		0.31		5.36		7.51	
				Temperature (℃)				
	24℃		23℃		24℃		30℃	
	ε'	ε''	ε'	ε''	ε'	ε''	ε'	ε''
3.7	-	-	-	-	-	-	-	-
4.7	2.30	0.12	-	-	-	-	-	-
5	-	-	-	-	-	-	4.00	0.27
5.33	-	-	1.42	0.02	-	-	-	-
7	-	-	-	-	-	-	4.45	0.49
8.12	-	-	1.52	0.02	-	-	-	-
8.5	-	-	-	-	3.20	0.24	-	-
9	-	-	-	-	-	-	4.69	0.83
10.91	-	-	1.72	0.04	-	-	-	-
11	-	-	-	-	-	-	5.45	1.50
13.7	-	-	1.79	0.09	-	-	-	-
16.48	-	-	1.91	0.14	-	-	-	-

' - ' indicates data unavailable

1.5.8 Comparison of dielectric properties of bulk canola seeds to those of other oilseeds

The dielectric properties of various oilseeds were obtained from the published works to compare with the measured dielectric properties of bulk canola seeds, which are indicated in Table 1. 3 (ASAE 2012; Sacilik et al. 2007; Worthington and Holley 1967). As shown in Table 1. 3, the range of total oil content was 38.4% to 49.7% except for soy bean (6.8%). The dielectric properties of the bulk canola seeds had the highest values of the dielectric properties (ε' = 5.46, and ε'' = 1.50) among peanut, safflower, and soy bean seed. The dielectric properties of canola seed and soy bean

which have relatively high linolenic acid content were around two or three times higher than those of other oilseeds. As mentioned above, the linolenic acid content of the oilseed could be one of the important factors affecting the dielectric properties at the specific frequency (~10 MHz) and temperature (23–30℃) ranges studied.

1.5.9 Selective heating

The dielectric properties, specific heat, and densities of rusty grain beetles (*Crytolestes ferrugineus* S.) as a function of temperature and MC were obtained from Shrestha and Baik (2013b). As shown in Fig. 1. 7, the electric field strength (*E*) within the insects was weaker than that within the canola seeds by around 0.46–0.73 times. Nevertheless, power dissipation (*P*) in the insects was higher comparing to that within the canola seeds by approximately 1.7–17.3 times (Fig. 1. 8). The dielectric loss factor of the insects was higher than that of the canola seeds by around 6.8 – 43.9 times (Fig. 1. 9). As described by Eq. (1.7), temperature increment in an insect – canola seed mixture (ΔT_{ic}) is affected by power dissipation (P_{ic}), bulk densities (ρ) of the canola seed and insect, and specific heats (C_p) of these (Fig. 1. 10). The ratio of the bulk density (ρ) and specific heat (C_p) of the canola seed to those of the insect calculated using data from Table 1. 1 was less than 1 (approximately 0.65 - 0.86). Therefore, power dissipation (P_{ic}) was the primary affecting factor for ΔT_{ic}. The calculated temperature increment rate of the insect bodies was higher than that of canola seeds by nearly 1.4 to 10.1 times. This suggests that the insects can be heated selectively within the canola seeds. Especially, insects in low moisture content canola seeds can be heated more selectively. It should be, however, noted that this calculation did not consider any conductive heat transfer (cooling) from hotter insect bodies to colder canola seeds. In real situations, the difference between temperature increment rates of insect bodies and canola seed mixture could be smaller. The real selective heating efficiency can be determined empirically or theoretically based on numerical simulations.

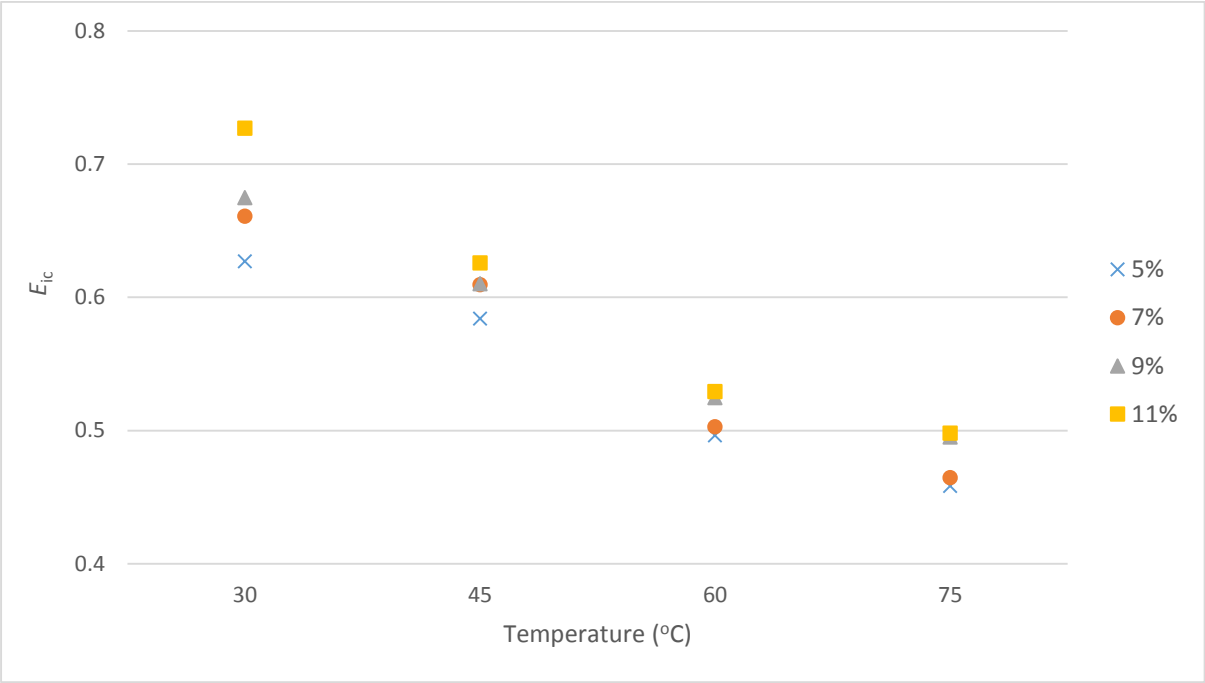

Figure 1. 7. Ratio of approximated electric field strength of rusty grain beetle (C. *ferrugineus* S.) to canola seed (B. *napus* L.) as a function of MC and temperature at 27.12 MHz.

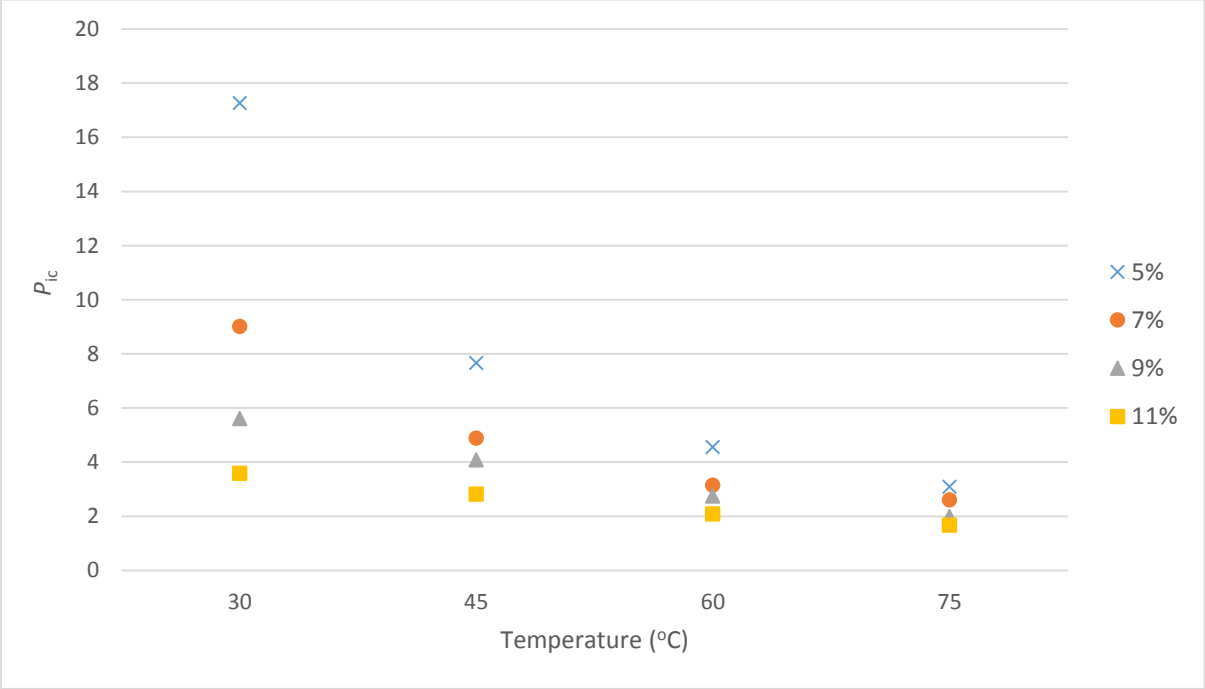

Figure 1. 8. *Rusty grain* beetle (C. *ferrugineus* S.) to canola seed (B. *napus* L.) power dissipation factor for canola seed as a function of MC and temperature at 27.12 MHz.

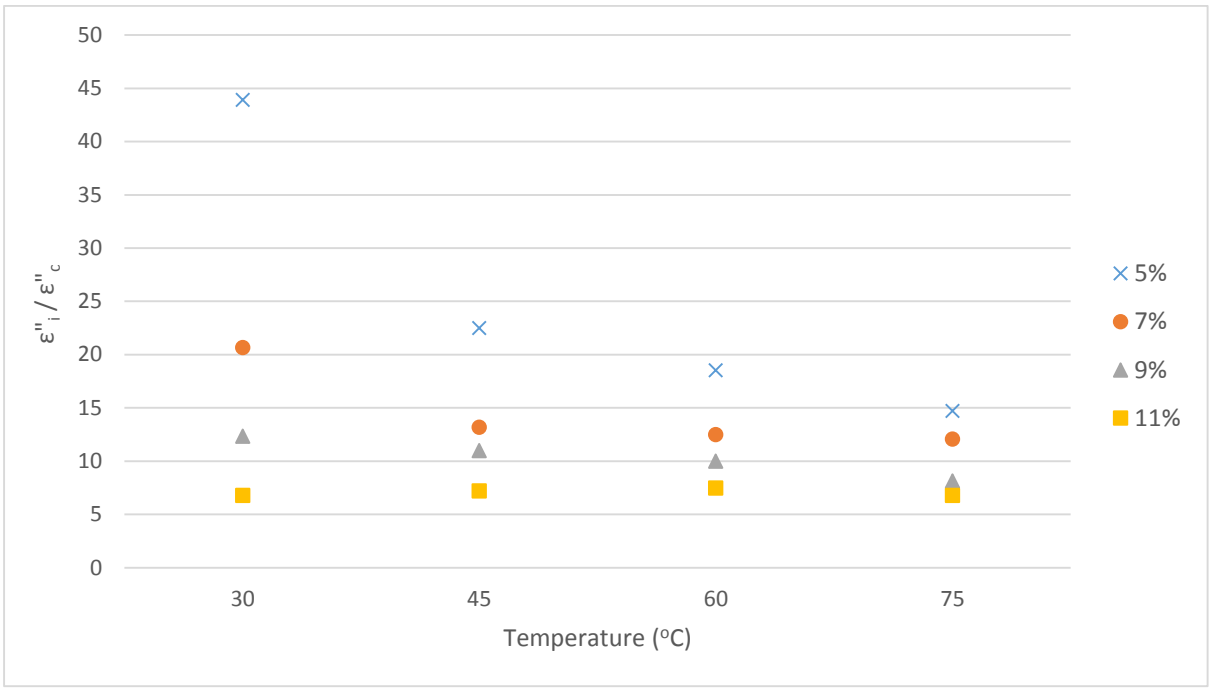

Figure 1. 9. The ratio of dielectric loss factor for canola seed (B. *napus* L.) and rusty grain beetle (C. *ferrugineus* S.) as a function of MC and temperature at 27.12 MHz.

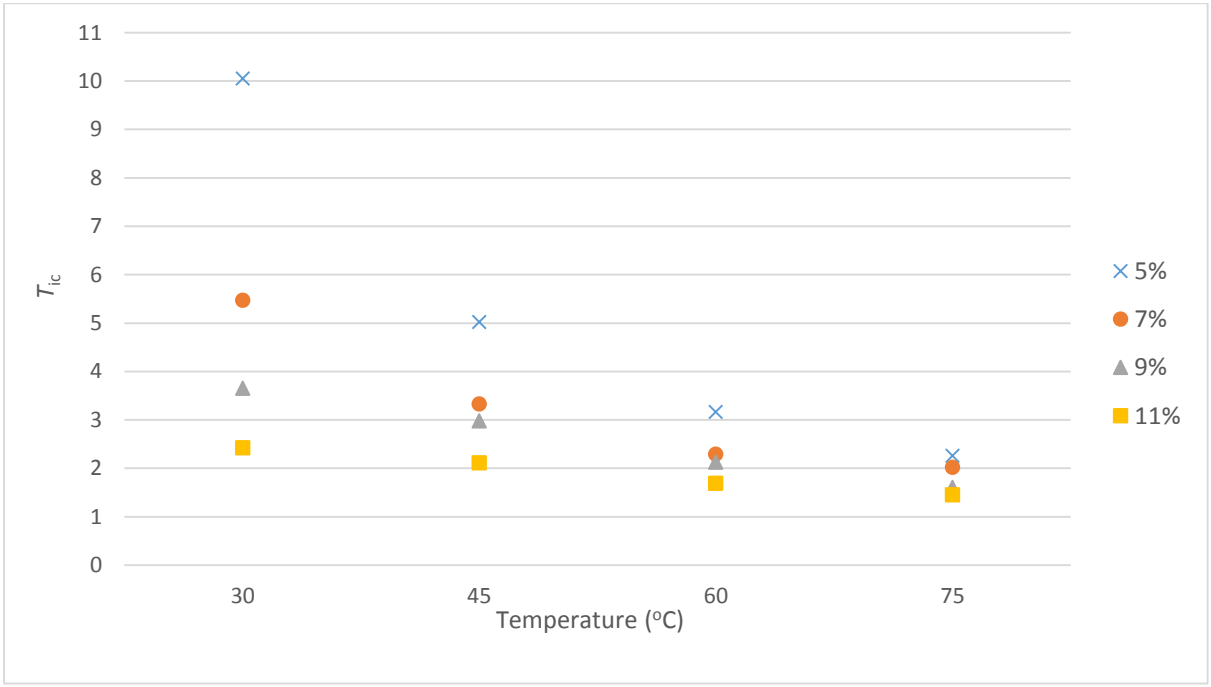

Figure 1. 10. The ratio of temperature increment rate of rusty grain beetle (C. *ferrugineus* S.) to that of canola seed (B. *napus* L.) as a function of MC and temperature at 27.12 MHz.

1.6 Conclusion

1) The dielectric constant (ε') and loss factor (ε'') decreased linearly with increasing frequency, and increased with increasing temperature and MC.

2) Penetration depth within the bulk canola seeds decreased with increasing MC, frequency, and temperature. The variation of penetration depth in drier samples was more sensitive to temperature change compared to that of wetter samples. More attention should be given to design industrial scale RF units with drier canola seeds considering the sensible variation of penetration depth in low MC of canola seeds.

3) A large difference between the dielectric loss factors of insect bodies and canola seeds makes selective heating of the insects among canola seeds feasible. The higher rate of temperature increment of the insect pest compared to that of the canola seed demonstrated a feasibility of RF disinfestation based on selective heating of insect pests at 27.12 MHz.

4) The regression models developed in this study could be used for estimating and simulating the dielectric properties of the bulk canola seeds further to evaluate feasibility of RF disinfestation based on selective heating.

1.7 References

Agilent, H. P. 2001. 4285A Precision LCR meter–operation manual.

ASAE. 2012. D293.4 : Dielectric Properties of Grain and Seed.

ASAE Standard. 2004. S358.2 : Moisture Measurement - Forages. American Society of Agricultural and Biological Enginners, St. *Joseph, US*.

Birla, S., S. Wang, J. Tang, and G. Tiwari. 2008. Characterization of radio frequency heating of fresh fruits influenced by dielectric properties. *Journal of Food Engineering* 89(4): 390-398.

Brusewitz, G. 1975. Density of rewetted high moisture grains. *Transactions of the ASAE*.

Canola Council of Canada 2011. http://www.canolacouncil.org/markets-stats/industry-overview/. (May, 7, 2014).

Canola Watch 2011. http://www.canolawatch.org/2011/05/09/estimating-flea-beetle-damage-in-canola/. (May, 7, 2014).

Choi, C., and A. Konrad. 1991. Finite element modeling of the RF heating process. *Magnetics, IEEE Transactions on* 27(5): 4227-4230.

Conrad, J. H. 1982. United States-Canadian Tables of Feed Composition.

Debye, P. 1929. *Polar molecules* (No. EPFL-BOOK-106114). Dover.

Guan, D., M. Cheng, Y. Wang, and J. Tang. 2004. Dielectric Properties of Mashed Potatoes Relevant to Microwave and Radio-frequency Pasteurization and Sterilization Processes. *Journal of Food Science* 69(1): FEP30-FEP37.

Haq, I., M. Saeed, I. Ahmed, M. Ashraf, and N. Ejaz. 2009. Chemical analysis and characterization of (Brassica napus) Canola oil seed. In *Complex Medical Engineering, 2009. CME. ICME International Conference on* : 1-4.

Jiao, S., J. Johnson, J. Tang, G. Tiwari, and S. Wang. 2011. Dielectric properties of cowpea weevil, black-eyed peas and mung beans with respect to the development of radio frequency heat treatments. *Biosystems Engineering* 108(3): 280-291.

Koskiniemi, C. B., V. D. Truong, R. F. McFeeters, and J. Simunovic. 2013. Effects of Acid, Salt, and Soaking Time on the Dielectric Properties of Acidified Vegetables. *International Journal of Food Properties 16*(4): 917-927.

Lizhi, H., K. Toyoda, and I. Ihara. 2008. Dielectric properties of edible oils and fatty acids as a function of frequency, temperature, moisture and composition. *Journal of food engineering 88*(2): 151-158.

Nelson, S. O., and P. G. Bartley. 2002. Frequency and temperature dependence of the dielectric properties of food materials. *Transactions of the ASAE 45*(4): 1223-1227.

Pace, W. E., W. B. Westphal, and S. A. Goldblith. 1968. Dielectric properties of commercial cooking oils. *Journal of Food Science* 33(1): 30-36.

Reagan, R. 1987. Montreal protocol on substances that deplete the ozone layer: Message from the president of the United States transmitting the Montreal Protocol on substances that deplete the Ozone layer. Done on September 16, 1987, to the Vienna Conventio n for the Protection of the Ozone Layer. Washington, DC: US Government Printing Office, pp. 11.

Rudan-Tasic, D., and C. Klofutar. 1999. Characteristics of vegetable oils of some Slovene manufacturers. *Acta Chim Slov 46*(4): 511-521.

Sacilik, K., C. Tarimci, and A. Colak. 2006. Dielectric properties of flaxseeds as affected by moisture content and bulk density in the radio frequency range. *Biosystems engineering* 93(2): 153-160.

Sacilik, K., C. Tarimci, and A. Colak. 2007. Moisture content and bulk density dependence of dielectric properties of safflower seed in the radio frequency range. *Journal of Food Engineering* 78(4): 1111-1116.

Shrestha, B. L., and O. D. Baik. 2011. Permittivity of Mixtures of Saponaria vaccaria and Ethanol–Water Solution for RF Heating Assisted Extraction of Saponins. Instrumentation and Measurement, *IEEE Transactions on* 60(8): 2861-2871.

Shrestha, B. L., and O. D. Baik. 2013a. Dielectric behaviour of whole-grain wheat with temperature at 27.12 MHz: a novel use of a liquid dielectric test fixture for grains. *International Journal of Food Properties* 18(1): 100-112.

Shrestha, B. L., and O. D. Baik. 2013b. Radio frequency selective heating of stored-grain insects at 27.12 MHz: A feasibility study. *Biosystems Engineering* 114(3): 195-204.

Sipahioglu, O., S. A. Barringer, I. Taub, and A. Prakash. 2003. Modeling the dielectric properties of ham as a function of temperature and composition. *Journal of Food Science* 68(3): 904-909.

Stratton, J. A. 2007. Electromagnetic theory. (Vol. 33). John Wiley & Son.

Tang, J., H. Feng, and M. Lau. 2002. Microwave heating in food processing. *Advances in bioprocessing engineering*: 1-43.

Tang, J., J. Ikediala, S. Wang, J. D. Hansen, and R. Cavalieri. 2000. High-temperature-short-time thermal quarantine methods. *Postharvest Biology and Technology* 21(1): 129-145.

USDA 2011. USDA National Nutrient Database for Standard Reference. http://ndb.nal.usda.gov/ndb/nutrients/report/nutrientsfrm?max=25&offset=0&totCount=0&nutrient1=204&nutrient2=&nutrient3=&subset=0&fg=&sort=f&measureby=m. (May, 7, 2014).

Von Hippel, A. R. 1954. Dielectric properties and waves. NY, John Wiley.

Wang, S., and J. Tang. 2004. Radio frequency heating: a potential method for post-harvest pest control in nuts and dry products. *Journal of Zhejiang University Science* 5(10): 1169-1174.

Wang, S., J. Tang, R. Cavalieri, and D. Davis. 2003. Differential heating of insects in dried nuts and fruits associated with radio frequency and microwave treatments. *Transactions-American Society of Agricultural Engineers* 46(4): 1175-1184.

Worthington, R.E., and K. T. Holley. 1967. The linolenic acid content of peanut oil. *Journal of the American Oil Chemists' Society* 44(8): 515-516.

CHAPTER 2

THERMAL CONDUCTIVITY, SPECIFIC HEAT, THERMAL DIFFUSIVITY, AND EMISSIVITY OF STORED CANOLA SEEDS (*BRASSICA NAPUS* L.) WITH THEIR TEMPERATURE AND MOISTURE CONTENT

Published, *Journal of Food Engineering* 165 (2015) 156-165.

Contribution of this paper to overall study

Knowledge of the thermal and physical properties of the canola seeds is essential to study heat transfer during RF heating of the canola seeds. The thermo-physical properties of bulk canola seeds at various temperatures and moisture contents were measured (specific objective 1) in this chapter as there is no comprehensive researches on the thermal-physical properties of the seeds as functions of their temperature and moisture content. The developed regression models of the properties were used in the simulation of the temperature distributions in the seeds and selective heating of the red flour beetle during RF heating in Chapter 6. All the experiments in this chapter were conducted and the journal paper manuscript was drafted by myself.

2.1 Abstract

Density (ρ), specific heat (C_p), thermal conductivity (k), diffusivity (α), and emissivity (ε) of canola seeds (*Brassica napus* L.) are important engineering parameters in the design of storage, heating, and cooling systems. The properties were determined at moisture contents (MC) ranging from 5 to 11% (M/M) wet basis (w.b.) and temperatures from 40 to 90°C. Bulk (ρ_b) and particle (ρ_p) densities of stored canola seeds decreased with temperature and ranged from 654.0 to 664.8 kg·m^{-3} and 1047 to 1131 kg·m^{-3}, respectively. The C_p of stored canola seeds increased with

temperature and MC, and ranged from 2180 to 3498 $J \cdot kg^{-1} \cdot ℃^{-1}$. The k of stored canola seeds at ρ_b and ρ_p increased with temperature and MC and ranged from 0.06 to 0.13 $W \cdot m^{-1} \cdot ℃^{-1}$ and 0.15 to 0.25 $W \cdot m^{-1} \cdot ℃^{-1}$, respectively. The α of stored canola seeds at ρ_b and ρ_p were calculated from the measured k, C_p, and ρ, and ranged from 0.40×10^{-8} to 5.7×10^{-8} $\cdot m^2 \cdot s^{-1}$, and 6.1×10^{-8} to 8.0×10^{-8} $\cdot m^2 \cdot s^{-1}$. The α of stored canola seeds at ρ_b increased with temperature and MC. The α of stored canola seeds at ρ_p exhibited descending-ascending trends with increasing MC at different temperatures except at 40℃. The ε of stored canola seeds decreased with MC and temperature and ranged from 0.93 to 0.99. Based on the experimental data, regression models for all the properties were developed.

2.2 Nomenclature

C_p	specific heat ($J \cdot kg^{-1} \cdot ℃^{-1}$)	U_{obj}	calculated camera output voltage for a blackbody of temperature (V)
DF	degree of freedom	U_{ref}	theoretical camera output voltage for blackbody of temperature (V)
DSC	differential scanning calorimetry	U_{source}	thermal camera output signal (V)
E	thermal radiation ($W \cdot m^{-2}$)	U_{total}	measured camera output voltage for the actual case (V)
h	height (m)	W	radiation power from blackbody ($W \cdot m^{-2}$)
I	electric current (A)	W_{atm}	radiation emitted by the atmosphere ($W \cdot m^{-2}$)
k	thermal conductivity ($W \cdot m^{-1} \cdot ℃^{-1}$)	w.b.	wet basis (%)
k_b	thermal conductivity at bulk density ($W \cdot m^{-1} \cdot ℃^{-1}$)	W_{obj}	radiation emitted by object ($W \cdot m^{-2}$)
k_p	thermal conductivity at particle density ($W \cdot m^{-1} \cdot ℃^{-1}$)	W_{ref}	radiation from the surroundings reflected by the material surface ($W \cdot m^{-2}$)
M	mass (kg)	W_{source}	radiation power from a source ($W \cdot m^{-2}$)

MC	moisture content (% = M/M, wet basis)		
MDSC	modulated differential scanning calorimeter	*Greek symbols*	
q	heat transfer rate (W)	α	thermal diffusivity ($m^2 \cdot s^{-1}$)
R	electric resistance (Ω)	α_b	thermal diffusivity at bulk density ($m^2 \cdot s^{-1}$)
r	radial axis (m)	α_p	thermal diffusivity at particle density ($m^2 \cdot s^{-1}$)
r_s	sample radius (m)	ε	emissivity
R^2	coefficient of determination	θ	transmittance of the atmosphere
RMSE	root mean square error	ρ	density ($kg \cdot m^{-3}$)
SD	standard deviation	ρ_b	bulk density ($kg \cdot m^{-3}$)
T	absolute temperature (K)	ρ_p	particle density ($kg \cdot m^{-3}$)
T	temperature (℃)	σ	stefan-boltzman constant ($5.670373 \times 10^{-8} \cdot W \cdot m^{-2} \cdot K^{-4}$)
t	measuring time (s)	ω_{cp}	variations in the measurements of c_p
T_0	initial sample temperature (℃)	ω_k	variations in the measurements of k
ΔT	temperature increase (℃)	ω_ρ	variations in the measurements of ρ
U_{atm}	theoretical camera output voltage for a blackbody of temperature (V)		

2.3 Introduction

Canada is a major producer of canola along with other countries such as European Union, the United States, Australia, China, and India. The Foreign Agricultural Service (FAS) reported 58.4 million tons of canola seed were produced in the 2010-2011 season around the world (FAS 2011).

Approximately 90% of canola produced in Canada is exported to markets around the world with a worth of billions of dollars. The contribution of canola to Canadian economy is $19.3 billion each year including more than $12.5 billion in wages, and 249,000 Canadian jobs (Canola Council of Canada 2014). Rapeseed was modified to canola to improve seed quality using traditional plant breeding methods. There are significant differences in agronomic characteristics and yield between rapeseed and canola (Canola Council of Canada 2014).

Heat transfer in a material is governed mainly by its thermal properties, such as thermal conductivity (k), specific heat (C_p), and thermal diffusivity (α). If radiation heat exchange is significant, the emissivity (ε) of the material surface should be included. Therefore, knowledge of these properties is essential to study and design thermal processes, like heating and cooling, handling, storage, and drying of the canola seeds.

Thermal properties, k, C_p, and α of canola (*cultivar NX4-105 RR*) at different temperatures (-20 to 30°C), moisture contents (6 to 16%), and storage times (0, 30, and 60 days) have been reported (Jian et al. 2012, 2013). The research was targeted to study the effect of temperature on thermal properties of canola seeds for storage, but not for the heating and drying.

Thermal properties at higher temperature range needs to be studied for heating or drying processes, but no comprehensive researches have been reported.

Recently, many novel techniques for measurements of k of materials have been developed. Sparrow et al. (2012) developed two novel methods for measurement of k. One of the methods is for high-conductivity media (all metals) and the other is for low conductivity (as air). Among many techniques, two different methods (non-steady-state and steady-state) have been used frequently to determine k of biological materials (Mohesnin 1980; Nesvadba 1982). A line heat source method, based on transient heat transfer (non-steady-state), has been widely used to measure k of biological materials due to its convenience, fast measurement, relatively small sample size, and etc. (Yang et al. 2002).

The thermal radiation exchange is significant when this is temperature gradient between surroundings and object surface temperatures. Thus, the emissivity of canola seeds should be known as functions of temperature and moisture content. However, no related studies have been reported. Particle and bulk densities and porosity are also important properties not only for heat and mass transfer analysis of drying and heating but also for the determination of storage and

packing volume, resistance through beds, shrinkage of food, etc. (Giri and Prasad 2006; Hatamipour and Mowla 2003; Senadeera et al. 2000).

Hence, our research focuses on the determination of thermophysical properties of stored canola seeds with temperature and moisture content for drying and heating. The specific objectives of this study were (1) to measure and analyze k, C_p, α, ε, ρ_b and ρ_p of stored canola seeds under various temperatures (40 to 90℃) and MCs (5 to 11%), and (2) to develop regression models to predict these properties from readily measurable physical quantities, namely temperature and MC.

2.4 Materials and methods

2.4.1 Sample treatment

Top quality canola seeds (B. *napus* L.) at initial MC of 9% (w.b.) were supplied by our industrial partner Viterra Inc., Regina, SK, Canada. The seeds were transported in polypropylene bags and were stored in a cold storage at 4^{o}C before using them.

A standard method (ASABE 2010; Brusewitz 1975) was used to determine the MC of the bulk canola seeds. To calculate the average initial MC, seeds weighing 10 g were poured into each of five aluminum moisture dishes followed by placing them in a hot air oven for 24 h at 103℃.

The samples of the canola seeds of different MCs, 5%, 7%, 9%, and 11% wet weight basis were prepared separately. Samples at 5% and 7% were prepared by drying a known mass of canola seeds at initial MC to the pre-calculated weight in a hot air oven (Despatch, Despatch Industries, Lakeville, MN, USA) set up at 40℃ followed by storing them at cold storage (4℃) until its further used. Samples at 11% were prepared by spraying a pre-calculated amount of distilled water on known mass of the seeds at initial MC contained in a glass jar. The jar was constantly shook and rotated while spraying with water. The air-tight jars were left at room temperature (23℃) for 3 days with periodic tumbling to achieve an equilibrium MC followed by cold storage (4℃) until its further use. A digital scale with an accuracy of ± 0.01g (Symmetry, PR4200, Cole-Parmer Instrument Co., Niles, IL, USA) was used for all weighing. The samples at different MCs from the storage were left at room temperature for 1 h and the final MC of samples were checked before using them for experiments.

2.4.2 Measurement methods

2.4.2.1 Densities (ρ) and porosity

The ρ_b and ρ_p of stored canola seeds were determined by measuring mass of known volume using a precision steel cylinder and a gas pycnometer as functions of temperature at MC of 5, 7, 9, and 11%, respectively. To calculate ρ_p, a certain mass of the seeds was poured into large cell after calibration and conditioning of the pycnometer. Nitrogen gas was passed into the reference cell until the pressure reached to about 17 psig. Then, nitrogen gas was allowed to flow into the large cell containing the test seeds. Based on the Archimedes principle, the initial gas pressure decreased to a new lower equilibrium pressure depending on the volume of the sample. A gas equation was used to calculate the particle volume using initial and final pressures, and the known volumes of reference and sample cells.

To calculate ρ_b, the mass of canola seeds was measured in the precision steel cylinder (500 ± 0.5 mL) after gently dropping the cylinder three times to the ground and levelling out the top surface with a steel cylindrical bar. The ρ_b was calculated using measured mass of canola seeds and known volume of a precision steel cylinder. An average of five replicates was used for both measurements.

The porosity of stored canola seeds was calculated as :

$$\left(1 - \frac{\rho_b}{\rho_p}\right) \times 100 \tag{2.1}$$

where ρ_b is bulk density and ρ_p is particle density.

2.4.2.2 Thermal conductivity (k)

The *k* of sample is calculated using the rate of temperature increment. The *k* probe or a bare wire is used as a heat source to increase sample core temperature for this method. In principle, a wire generates heat at a rate, *q* in W :

$$q = I^2 R \tag{2.2}$$

where *I* is the electric current (A), and *R* is the electric resistance (Ω). The end effects and the mass of the wire are negligible in case of isotropic, homogeneous, and infinitely long cylindrical sample. Heat conduction in a sample is given by the following equation :

$$\frac{\partial T}{\partial t} = \alpha\left(\frac{\partial^2 T}{\partial r^2} + \frac{1}{r}\frac{\partial T}{\partial r}\right) \quad (2.3)$$

where T is the sample temperature (°C), t is the heating time (s), α is the thermal diffusivity ($m^2 \cdot s^{-1}$), and r is the radial axis (m) of the sample. The solution for temperature T is given by Hooper and Lepper (1950):

$$T - T_0 = \frac{q}{2\pi k}\left[A - \ln(rn) + \frac{(rn)^2}{2} - \frac{(rn)^4}{8} + \ldots\right] \quad (2.4)$$

where T_0 is the initial sample temperature, A is a constant, and $n = 1 / 2\sqrt{\alpha t}$. For very small values of n and r, Eq. (2.5) can be approximated to :

$$T - T_0 = \frac{q}{2\pi k}[A - \ln(rn)] \quad (2.5)$$

or

$$T - T_0 = \frac{q}{2\pi k}A - \frac{q}{2\pi k}\ln\left(\frac{r}{2\sqrt{\alpha}}\right) + \frac{q}{4\pi k}\ln(t) \quad (2.6)$$

which shows a linear relationship between $(T - T_0)$ and $\ln(t)$ with the slope $S = q/4\pi k$. The slope S from linear regression on the experimental data and q from Eq. (2.3), the thermal conductivity can be calculated as :

$$k = \frac{I^2 R}{4\pi S} \quad (2.7)$$

Thermal conductivities of stored canola seeds were measured using a KD2 thermal properties analyzer (Decagon Devices, Inc., Pullman, WA) at ρ_b and ρ_p as functions of temperature and MC (Fig. 2. 1). A 153 mm long brass cylinder (inner diameter, id = 25.3 mm, and outer diameter, od = 50.4 mm) was used as sample holders. To measure the thermal conductivity at bulk density (k_b), the cylinder was loaded with a known mass (M) of seeds. The loaded cylinder was softly tapped on the ground five times before measuring the sample height (h) using caliper (± 0.001 mm). The ρ_b was calculated from M, h, and id. To measure the thermal conductivity at particle density (k_p), canola seeds of a known mass were poured and compressed into a specific volume within the cylinder using a piston and a hydraulic press to achieve a desired particle density. The specific volume was pre-calculated with the known mass and the particle density of canola. A line was marked on the piston handle to even up with the top of the cylinder surface once the volume of canola seeds was equal to the pre-determined volume. Compressed sample in the cylinder was bored to make a hole (ca. 1.27 mm) so that the thermal conductivity probe could be snugly inserted into the sample. The cylinder was sealed at the top with a stopper followed by placing it in a

temperature and humidity chamber (SH-641, Espec Corp., Osaka, Japan) with an accuracy of ± 0.1℃. The sample was heated for an hour for thermal equilibrium at desired temperatures. The heating time was obtained from our preliminary test (Shrestha and Baik 2010). All data were obtained from five replicates.

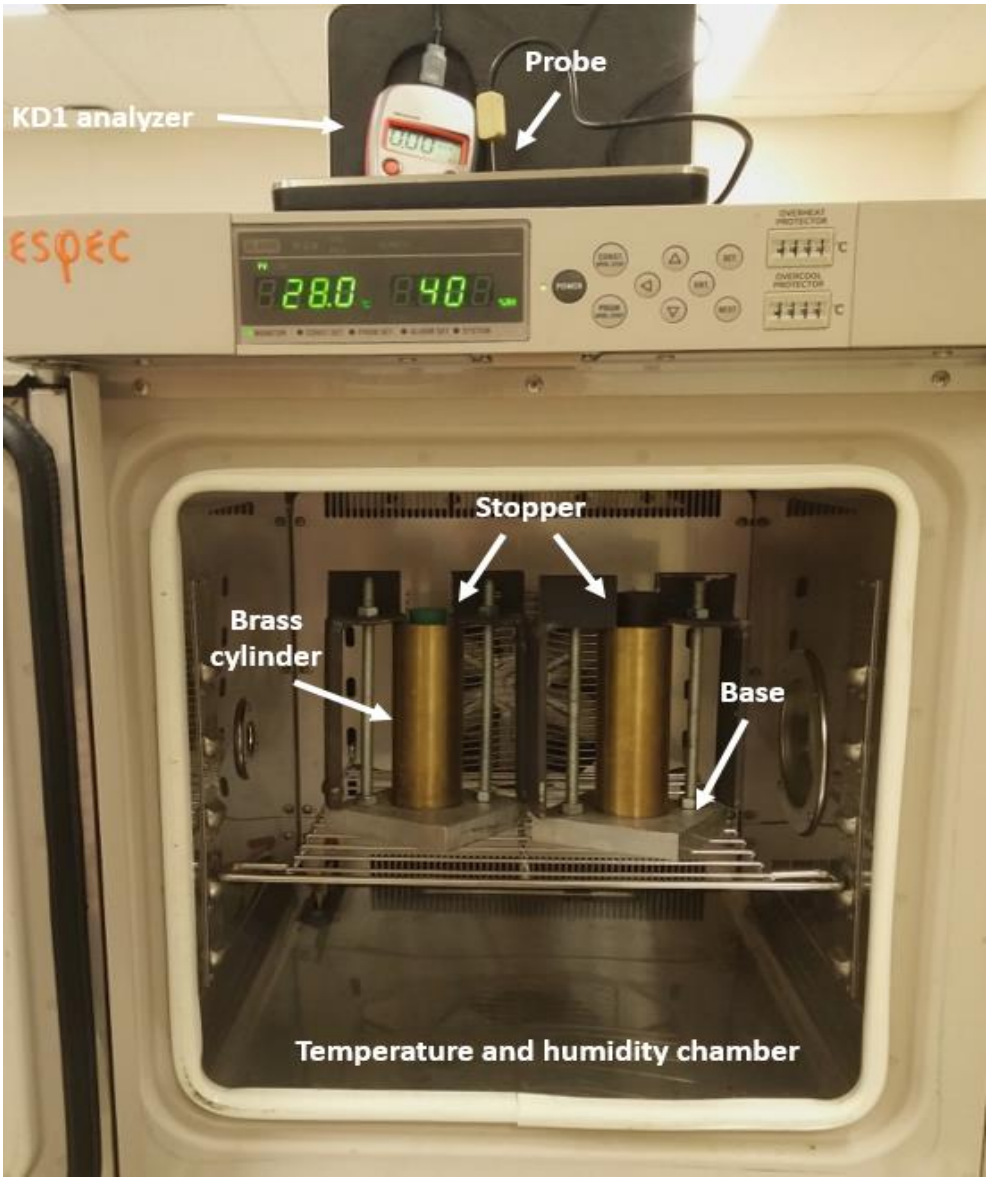

Figure 2. 1. Schematic of measurement of the thermal conductivity of the stored canola seeds

To calibrate a sensor of KD2, the *k* of 0.5% agar-water mixture (Campbell et al. 1991; Ochsner et at. 2003) was determined using the sensor of KD2 at room temperature. The calibration factor was calculated by the ratio of determined *k* of 0.5% agar-water mixture to its standard *k* value. The

KD2 probe, which contains a heating wire and a temperature sensor, was inserted into the sample at a desired temperature, and then it was turned on to measure *k* value.

2.4.2.3 Thermal diffusivity (α)

α was calculated using measured thermal conductivity, density, and specific heat of the canola seeds as :

$$\alpha = \frac{k}{\rho c_p} \tag{2.8}$$

where α is thermal diffusivity ($m^2 \cdot s^{-1}$), k is thermal conductivity ($W \cdot m^{-1} \cdot ℃^{-1}$), ρ is density ($kg \cdot m^{-3}$), and C_p is specific heat ($J \cdot kg^{-1} \cdot ℃^{-1}$).

Due to the uncertainties of other parameters, the probable uncertainty of the calculated α was estimated using uncertainties of k, C_p, and ρ (ω_k, ω_{cp}, and ω_ρ) as (Huggins 1983):

$$\omega_\alpha = \left\{ \left[\frac{\partial[\alpha(k,c_p,\rho)]}{\partial k} \omega_k \right]^2 + \left[\frac{\partial[\alpha(k,c_p,\rho)]}{\partial c_p} \omega_{c_p} \right]^2 + \left[\frac{\partial[\alpha(k,c_p,\rho)]}{\partial \rho} \omega_\rho \right]^2 \right\}^{1/2} \tag{2.9}$$

Substituting Eq. (2.8) into Eq. (2.9) yields:

$$\omega_\alpha = \left\{ \left[\frac{1}{\rho c_p} \omega_k \right]^2 + \left[\frac{k}{\rho {c_p}^2} \omega_{c_p} \right]^2 + \left[\frac{k}{\rho^2 c_p} \omega_\rho \right]^2 \right\}^{1/2} \tag{2.10}$$

where ω_k, ω_{cp}, and ω_ρ are the variations in the measurements of k, C_p, and ρ, and are calculated from repeated measurements at certain confidence limit.

2.4.2.4 Specific heat (C_p)

Many different methods such as adiabatic chamber (Mohsenin 1980), guarded plate (Mohsenin 1980), and differential scanning calorimeter (Tang et al. 1991; Yang et al. 2002) have been used to measure C_p of materials. Among the methods, differential scanning calorimetry (DSC) is a rapid and accurate method for measuring specific heat (Yang et al. 2002). In this method, an empty reference pan and a sample pan are placed on different heaters. The two pans are heated at the exactly same rate by the computer. To accomplish it, the heater for the sample pan needs to generate more heat than the other. The consumed heat from the sample heater is measured by DSC. Heat capacity per unit mass gives C_p:

$$C_p = \frac{q}{M\Delta T} \tag{2.11}$$

where C_p is specific heat ($J \cdot kg^{-1} \cdot ℃^{-1}$), q is heat (J), M is mass (kg), and ΔT is temperature increase (℃).

Recently, modulated DSC (MDSC) has been used for better resolution and increasing sensitivity of complex thermal events. It can separate total heat flow into its heat capacity related (reversing-thermodynamic) and kinetic components (nonreversing-chemical reaction). Conventional DSC measures the difference in heat flow between an inert reference and a sample subjected to the same pressure, temperature, and time. However, in MDSC, a sinusoidal modulation (oscillation) is overlapped with the conventional linear heating.

A modulated differential scanning calorimeter (MDSC) (Q2000, TA Instruments, Inc., New Castle, Del) was used to measure the heat capacity of the test seeds. A standard sapphire was used for calibration of MDSC at the temperature of interest. The A calibration constant was calculated by a ratio of the measured heat capacity of the sapphire to its standard heat capacity. A hermetically sealed aluminium pan containing 10 mg ($\pm$ 0.01 mg) of sample was loaded into the MDSC along with an identical blank aluminium pan for reference. The constant heating rate of $5 ℃ \cdot min^{-1}$ obtained from our preliminary test was used. Heat capacities of stored canola seeds at MCs of 5%, 7%, 9%, and 11% were measured at 40 to 90℃. Data were obtained in quintuplicate considering potential variations with small sample size.

2.4.2.5 Emissivity (ε)

All materials emit thermal radiation above absolute zero. The total amount of thermal radiation is described by the Stefan-Boltzman law as :

$$E = \varepsilon \sigma T^4 \tag{2.12}$$

where E is emitted thermal radiation ($W \cdot m^{-2}$), ε is the emissivity of the material, σ is the Stefan-Boltzman constant ($5.670373 \times 10^{-8} \cdot W \cdot m^{-2} \cdot K^{-4}$), and T is the absolute temperature (K). The above equation can be used to determine the temperature of the emitting material, which is the basic concept of thermal imaging. It can equally be used to estimate ε. In this study, a thermal image camera (FLIR Systems 2009) was used for estimating ε of stored canola seeds. The thermal image camera perceives radiation not only from the object itself, but also from the surroundings reflected to the object surface. A relative humidity of atmosphere, distance between material and camera, temperature of atmosphere, and reflected surrounding temperature were supplied to the thermal image camera to compensate for the effects of different radiation sources.

A thermal camera output signal U_{source} is described as :

$$U_{source} = CW_{source} \tag{2.13}$$

where U_{source} is the thermal camera output signal, C is a constant, and W_{source} is a radiation power from a source ($W \cdot m^{-2}$). The source should be a graybody with an emittance (ε), the radiation would be εW_{source} consequently. The C constant was assigned based on the response of the camera pixels in the camera calibration by manufacturer (personal communication with Murray 2015). The total received radiation power (W_{total}) can be expressed as the sum of radiations from the source object, reflected from ambient to the object, and from atmosphere (FLIR Systems 2009) :

$$W_{total} = \varepsilon\theta W_{source} + (1-\varepsilon)\theta W_{ref} + (1-\theta)W_{atm} \tag{2.14}$$

where ε is the emissivity of the source, θ is the transmittance of the atmosphere automatically detected by the camera (assumed as 1 due to the atmosphere is almost 100% transmissive), W_{source} is the radiation emitted by the source ($W \cdot m^{-2}$), W_{ref} is the radiation from the surroundings reflected to the source surface ($W \cdot m^{-2}$), and W_{atm} is the radiation emitted by the atmosphere ($W \cdot m^{-2}$). Multiplying Eq. (2.15) by the constant (C) of Eq. (2.14) results in :

$$U_{total} = \varepsilon\theta U_{source} + (1-\varepsilon)\theta U_{ref} + (1-\theta)U_{atm} \tag{2.15}$$

where U_{total} is measured camera output voltage for the actual case, ε is the emissivity of the source, θ is the transmittance of the atmosphere, U_{source} is calculated camera output voltage for a blackbody at source temperature, U_{ref} is theoretical camera output voltage for a blackbody at surrounding temperature, and U_{atm} is theoretical camera output voltage for a blackbody at atmosphere temperature. And, solve Eq (16) for ε :

$$\varepsilon = \frac{U_{total} - \theta U_{ref} - (1-\theta)U_{atm}}{\theta U_{Tsource} - \theta U_{ref}} \tag{2.16}$$

Fig. 2. 2 depicts the ε measuring system of stored canola seeds. FLIR Thermo Vision A20 (FLIR Systems Inc., Boston, MA, USA) working at wavelengths of ranging from 0.75 to 3 μm was used to measure the ε of stored canola seeds at various temperatures and MCs. This reflector method was referred to the manufacturer's user's manual (FLIR Systems 2009). Bulanon et al. (2008) also used this method to estimate the ε of citrus for demonstrating the temperature difference between fruit and canopy.

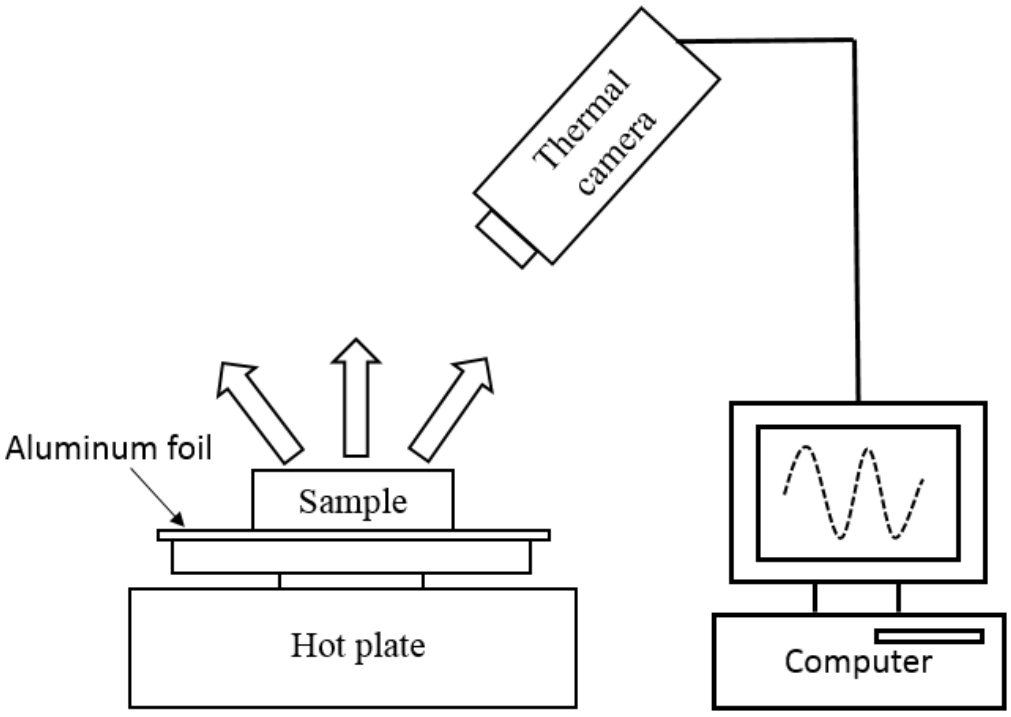

Figure 2. 2. Schematic of the thermal camera assisted emissivity measurement system

The temperature of the surroundings reflected via the seeds to compensate for the radiation reflected into the seeds, the distance between the seed surface and the thermo vision camera, the relative humidity of atmosphere, and the temperature of the atmosphere were taken into account. The distance was measured using a standard ruler, and the relative humidity and the temperature of the atmosphere were measured using an electronic thermo-humidity meter with accuracies of ± 1℃ and ± 3% RH. To measure the temperature of the surroundings reflected, a piece of cardboard covered with the crumpled aluminum foil as a reflector was placed in front of the small steel container containing canola seeds. Setting the ε to be 1.0 (FLIR Systems 2009), the temperature of the surroundings reflected was measured through the thermo vision camera. A piece of plain electrical tape with a known high ε was attached to the seed surface. Then the container was heated uniformly on the hot plate (RCT basic, IKA®, Staufen, Germany) to a desired temperature of the tape at least 20℃ above room temperature. The emissivity of the plain electrical tape was assumed 0.97 according to the user's manual (FLIR Systems 2009). The two spots were designated on the surface regions of tape and canola seeds, respectively in a thermal image. The ε of the tape was set

as 0.97, and the ε of the seeds was continuously changed until its temperature was matched to the temperature of the tape. The ε at this particular instant was the ε of the seeds at the desired temperature.

2.4.2.5 Statistical analysis

The five replicates of the measured k, C_p, ε, ρ_b and ρ_p of the test seeds were used to calculate the averages and the standard deviations (SD). The stepwise regression analysis in SPSS 20.0 (SPSS Inc., Chicago, IL, USA) was used to investigate the effects of MC and temperature on each of property. 3D graphs were plotted using the regression models based on the experimental data by Matlab R2013a (The MathWorks, Inc., Natick, MA).

2.5 Results and discussions

2.5.1 Bulk (ρ_b) and particle (ρ_p) densities and porosity

ρ_b, ρ_p, and porosity of stored canola seeds were plotted as functions of temperature and MC in Fig. 2. 3. All bars indicated in the thesis mean standard deviations. In general, densities decreased with temperature. Increased particle size of the canola seeds with temperature also increased the total volume of air voids resulting in the decreased bulk densities. The ρ_b and ρ_p ranged from 654.0 to 664.8 kg·m^{-3} and 1052 to 1131 kg·m^{-3}, respectively. Similar bulk density range was reported for the canola seeds of a different variety (cultivar NX4-105 RR), which was 602.7 to 654.0 kg·m^{-3} depending on temperatures (-20 to 30℃) and MCs (6 to 16%) (Jian et al. 2012). The minimum and maximum difference between ρ_b and ρ_p were 390.8 kg·m^{-3} and 468.2 kg·m^{-3} over the ranges of temperature and MC. The canola seed continued to expand its volume with temperature resulting in increasing the particle volume. The increased volume was also noticeable by naked eyes. The reduction in ρ_p of the stored canola seed with increasing temperature was mainly due to the increased particle volume which was the inaccessible volume by nitrogen and potentially losing mass from the evaporation of moisture (or absorption of the nitrogen by excess vapor pressure from moisture). Statistical result showed that the temperature and initial MC of canola seeds significantly affected the decrease of particle density. Regression models developed from experimental data with the statistical information are given in Table 2. 1.

The porosity of stored canola seeds was from 37.8 to 41.4. It decreased with temperature and MC due to the increased ratio of ρ_b to ρ_p.

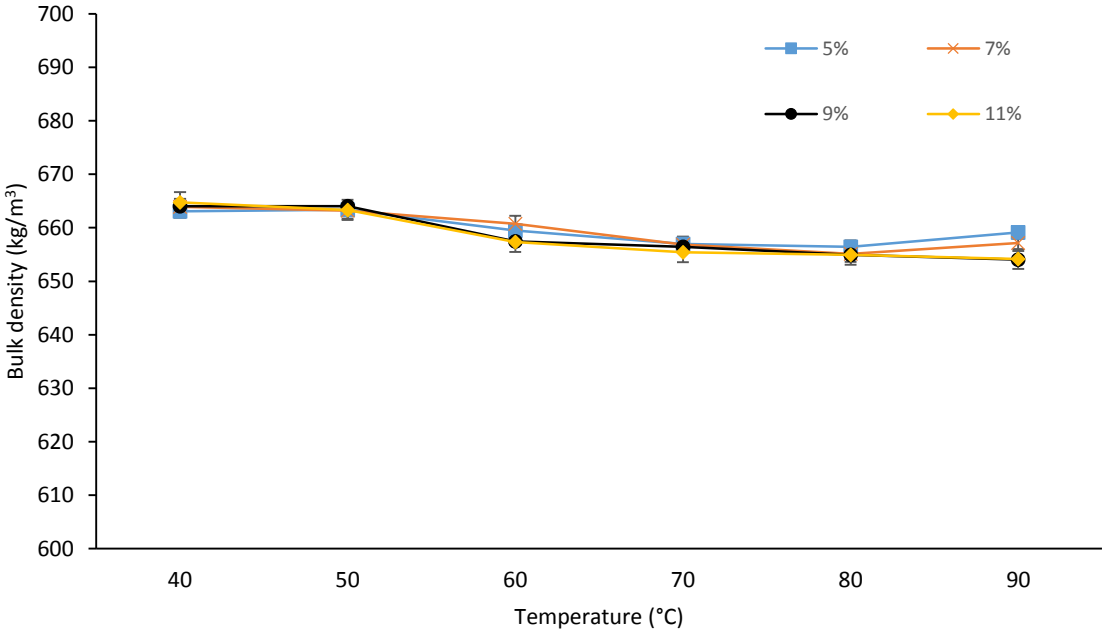

(a)

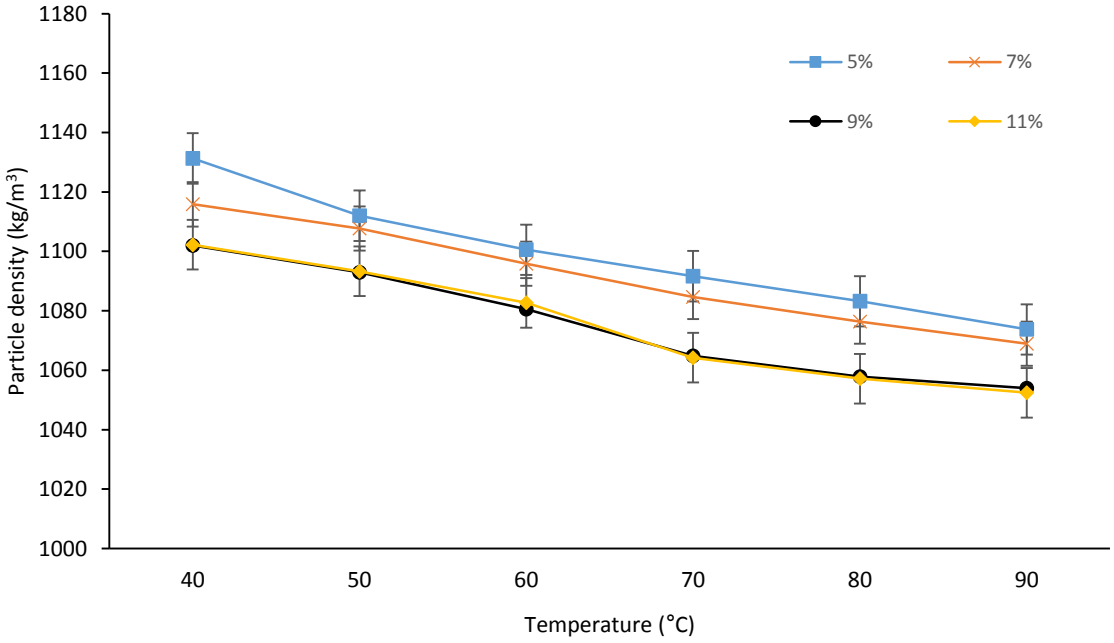

(b)

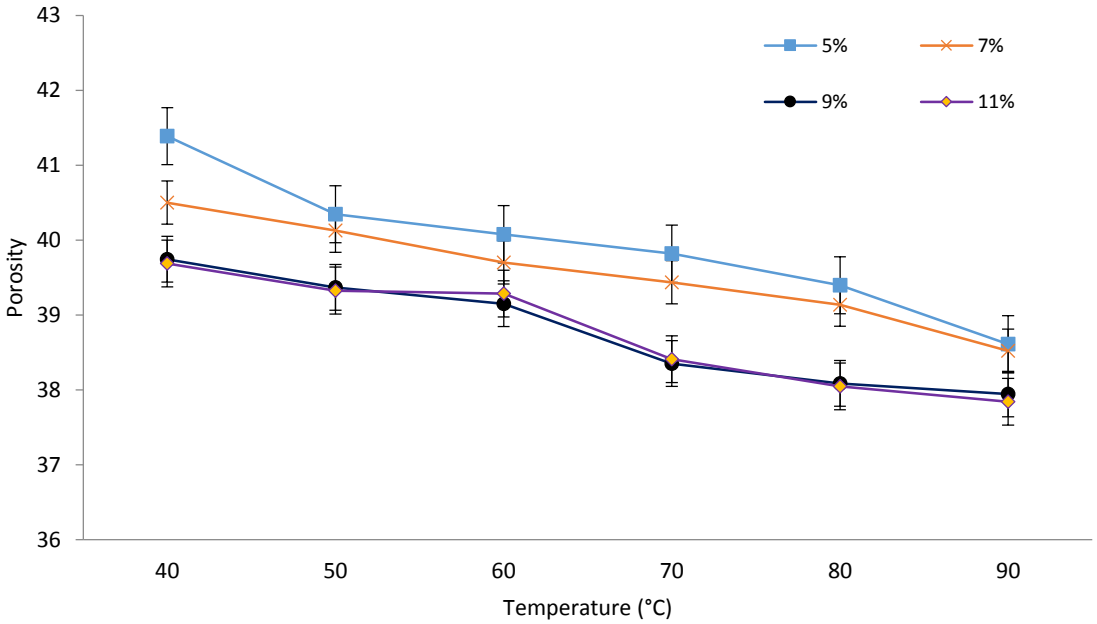

(c)

Figure 2. 3. The ρ_b (a) and the ρ_p (b) and porosities (c) of stored canola seeds as functions of temperature and MC.

Table 2. 1. Regression equations of densities of stored canola seeds and statistical information.

Regression Model	F value	P value	DF [c]	RMSE [d]	R^2
$\rho_b = 681.5 - 0.451 \cdot (T^a) + 2.806 \cdot 10^{-5} \cdot (T^3) - 9.8 \cdot 10^{-6} \cdot (MC^b \cdot T^3)$	237.9	1×10^{-6}	119	1.40	0.86
$\rho_p = 1141 - 2.981 \cdot 10^{-3} \cdot (MC \cdot T^2) + 1.001 \cdot 10^{-5} \cdot (MC \cdot T^3) + 1.11 \cdot 10^{-6} \cdot (MC^2 \cdot T^3)$	200.1	1×10^{-6}	119	9.08	0.84

[a] T = temperature (℃)

[b] MC = moisture content (%, w. b.)

[c] DF = degree of freedom

[d] RMSE = root mean square error

2.5.2 Thermal conductivity (*k*)

Figs. 2. 4 and 2. 5 present the *k* of stored canola seeds at ρ_b and ρ_p with temperature and MC. The *k* of stored canola seeds increased with temperature and MC, because of large number of ions and dipoles present at higher MC, and these entities exhibit higher lattice vibrations at high temperatures facilitating heat transfer (Sweat 1986). These results are in accordance with other researches. Dutta et al. (1988) described that thermal conductivity of rewetted whole grain increased linearly with temperature and MC in the ranges of 10 to 39℃ and 11.5% to 27.2% w.b., respectively. Thermal conductivity of sweet potato also increased with MC and temperature in the ranges of 0.45% to 0.75% w.b. and 20.5 to 60℃ (Farinu and Baik 2007).

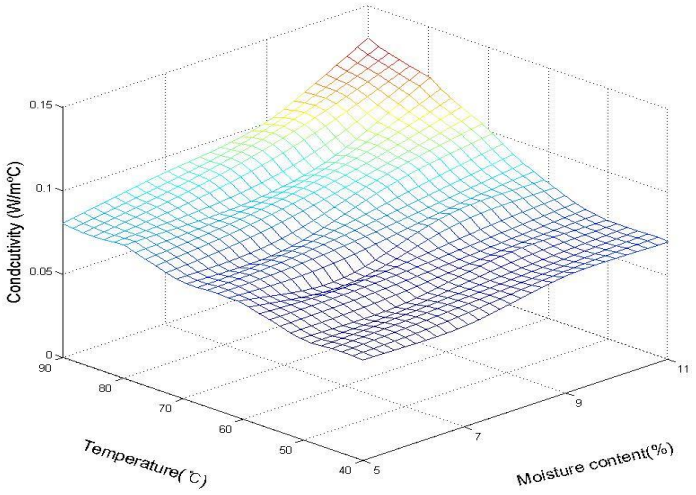

Figure 2. 4. Thermal conductivities of stored canola seeds at bulk density as functions of temperature and MC.

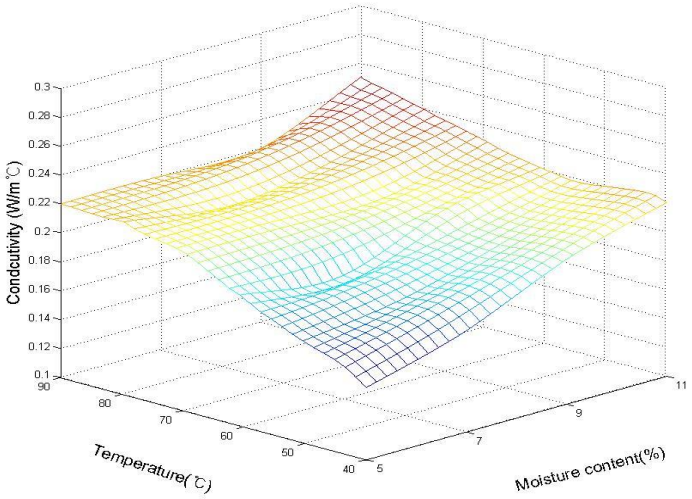

Figure 2. 5. Thermal conductivities of stored canola seeds at particle density as functions of temperature and MC.

It should be noted that k_b and k_p mean thermal conductivities of canola seeds with and without void space between the seeds in this thesis. At all times, the k_p was higher than the k_b. This was attributed to the fact that the canola seeds in the compacted form transferred heat better due to less air voids in the matrix. The k of stored canola seeds at the ρ_b and ρ_p ranged from 0.06 to 0.13 $W \cdot m^{-1} \cdot ℃^{-1}$ and 0.15 to 0.25 $W \cdot m^{-1} \cdot ℃^{-1}$. The relationship between the k, and temperature and MC was modeled significant terms were only used for developing regression equations. The statistical information for the regression models are given in Table 2. 2. Measured and predicted thermal conductivities at the ρ_b and the ρ_p at different temperatures and MCs were compared in Tables 2. 3 and 2. 4.

Table 2. 2. Regression equations of thermal conductivities of stored canola seeds and statistical information.

Regression Model	F value	P value	DF	RMSE	R^2
$k_b = 0.061 + 8.084 \cdot 10^{-10} \cdot (MC^2 \cdot T^3)$	257.2	0	23	0.005	0.92
$k_p = 0.158 + 9.495 \cdot 10^{-5} \cdot (MC \cdot T)$	52.08	0	23	0.013	0.70

MC = moisture content (%)

T = temperature (℃)

Table 2. 3. Thermal conductivities of stored canola seeds at bulk density (k_b) at different temperatures and moisture contents.

Thermal conductivity ($W \cdot m^{-1} \cdot ℃^{-1}$)															
	MC (%, w.b.)														
Temperature (℃)	5%				7%				9%				11%		
	Measured		Predicted	Difference (%) [b]	Measured		Predicted	Difference (%)	Measured		Predicted	Difference (%)	Measured		Predicted	Difference (%)
	Mean	SD [a]			Mean	SD			Mean	SD			Mean	SD		
40	0.06	± 0.000	0.06	3.8	0.06	± 0.000	0.06	5.9	0.07	± 0.010	0.07	6.9	0.07	± 0.000	0.07	3.9
50	0.06	± 0.000	0.06	5.9	0.06	± 0.000	0.07	9.9	0.07	± 0.010	0.07	1.2	0.07	± 0.000	0.07	4.6
60	0.07	± 0.000	0.07	6.6	0.06	± 0.000	0.07	16	0.08	± 0.000	0.08	6.1	0.08	± 0.000	0.08	2.7
70	0.07	± 0.000	0.07	3.0	0.07	± 0.000	0.08	6.6	0.09	± 0.000	0.08	7.3	0.10	± 0.010	0.10	5.5
80	0.08	± 0.010	0.07	10.8	0.08	± 0.000	0.08	1.6	0.09	± 0.000	0.10	5.0	0.12	± 0.010	0.11	7.4
90	0.08	± 0.010	0.08	5.3	0.09	± 0.010	0.10	0.1	0.10	± 0.006	0.11	8.7	0.13	± 0.010	0.13	1.8

[a] SD = standard deviation.

[b] Difference = $\left|k_{measured} - k_{predcted}\right| / k_{measured} \times 100$.

Table 2. 4. Thermal conductivities of stored canola seeds at particle density (k_p) at different temperatures and moisture contents.

Thermal Conductivity ($W \cdot m^{-1} \cdot ℃^{-1}$)															
	MC (%, w.b.)														
Temperature (℃)	5%				7%				9%				11%		
	Measured		Predicted	Difference (%)	Measured		Predicted	Difference (%)	Measured		Predicted	Difference (%)	Measured		Predicted	Difference (%)
	Mean	SD			Mean	SD			Mean	SD			Mean	SD		
40	0.15	± 0.010	0.18	18	0.17	± 0.000	0.19	8.6	0.20	± 0.020	0.19	3.9	0.22	± 0.000	0.20	9.2
50	0.17	± 0.010	0.18	6.9	0.18	± 0.000	0.19	6.2	0.20	± 0.020	0.20	0.4	0.22	± 0.000	0.21	4.4
60	0.19	± 0.010	0.19	1.9	0.18	± 0.000	0.20	9.9	0.21	± 0.020	0.21	0.4	0.22	± 0.000	0.22	0.3
70	0.21	± 0.010	0.19	8.9	0.21	± 0.020	0.21	2.6	0.21	± 0.020	0.22	3.7	0.23	± 0.000	0.23	0.5
80	0.22	± 0.010	0.20	11	0.21	± 0.020	0.21	0.6	0.22	± 0.020	0.23	2.9	0.24	± 0.000	0.24	0.7
90	0.22	± 0.010	0.20	8.8	0.22	± 0.020	0.22	1.0	0.22	± 0.020	0.24	6.8	0.25	± 0.010	0.25	0.8

2.5.3 Specific heat (C_p)

Measured C_p of the stored canola seeds are illustrated at different temperatures and MCs in Fig. 2. 6. It increased with temperature and MC. Similar results were observed from other researches (Jian et al 2013; Kocabiyik and Tezer 2007; Muir and Viravanichai 1972; Sweat 1986). The specific heat of samples is related to heat energy to supply to heat up the samples to a desired temperature. However, during drying the C_p might not be changed dramatically as temperature increases while moisture decreases. The C_p ranged from 2180 to 3498 $J \cdot kg^{-1} \cdot °C^{-1}$. The regression model and its statistical information are given in Table 2. 5. Experimental and predicted data with their percent differences, at different temperatures and MCs are shown in Table 2. 6. The percent difference between the measured and predicted data ranged from 0.03 to 1.6%. Moysey et al. (1977) calculated the specific heat of rapeseed (*Brassica campestris*) which ranged from 1.21 to 2.05 $kJ \cdot kg^{-1} \cdot K^{-1}$ at MC of 5.5 to 19.6% and a temperature range of -25.6 to 19.4°C.

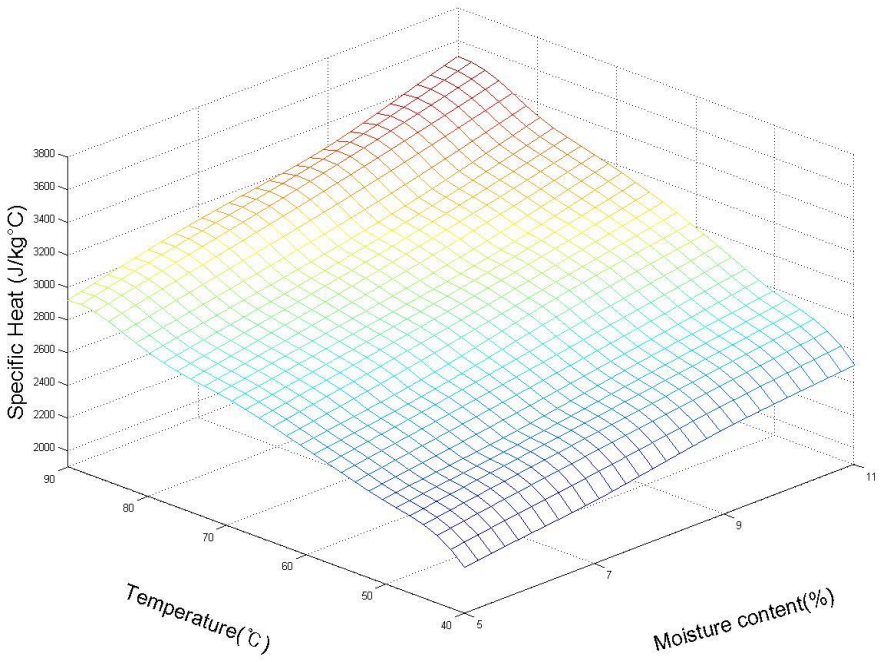

Figure 2. 6. Specific heats of stored canola seeds as functions of temperature and MC.

Table 2. 5. Regression equation for specific heat of stored canola seeds and statistical information.

Regression Model	F value	P value	DF	RMSE	R^2
$C_p = 1115.742 + 24.977 \cdot (MC) + 27.066 \cdot (T) + 0.0487 \cdot (MC^2 \cdot T) - 0.1083 \cdot (T^2)$	1254.0	1×10^{-6}	23	22.76	0.99

MC = moisture content (%)

T = temperature (℃)

Table 2. 6. Specific heat of stored canola seeds at different temperatures and moisture contents.

Specific Heat ($J \cdot kg^{-1} \cdot ℃^{-1}$)															
	MC (%, w.b.)														
Temperature (℃)	5%				7%				9%				11%		
	Measured		Predicted	Difference (%)	Measured		Predicted	Difference (%)	Measured		Predicted	Difference (%)	Measured		Predicted	Difference (%)
	Mean	SD			Mean	SD			Mean	SD			Mean	SD		
40	2180	± 91.49	2199	0.85	2282	±192.6	2295	0.59	2419	± 284.2	2408	0.48	2505	± 131.9	2535	1.2
50	2407	± 125.1	2384	1.0	2507	± 205.3	2492	0.60	2647	± 291.2	2620	1.0	2766	± 142.6	2767	0.06
60	2549	± 141.8	2548	0.07	2669	± 186.3	2668	0.03	2855	± 272.7	2811	1.6	2984	± 155.5	2978	0.20
70	2680	± 160.3	2690	0.36	2816	± 174.6	2821	0.19	2962	± 268.6	2981	0.63	3168	± 228.1	3166	0.05
80	2786	± 187.3	2810	0.85	2931	± 196.7	2953	0.77	3097	± 313.7	3128	1.0	3317	± 341.6	3334	0.51
90	2918	± 242.8	2909	0.31	3102	± 236.9	3064	1.2	3248	± 335.7	3254	0.17	3498	± 437.3	3479	0.54

2.5.4 Thermal diffusivity (α)

Thermal diffusivities of stored canola seeds at the ρ_b and ρ_p were calculated with the mean values of k_b, k_p, ρ_b, ρ_p, and C_p using Eq. (2.8). The thermal diffusivities at the ρ_b and ρ_p are plotted in Figs. 2. 7 and 2. 8 as functions of temperature and MC. The thermal diffusivity at bulk density (α_b) increased with temperature and MC. This was attributed to the fact that the increment rate of k_b with temperature and MC were higher than that of C_p and ρ_b. Other researcher have determined the similar pattern of results (Dutta 1988; Farinu and Baik 2007; Sweat 1986; Yang 2002). The minimum and maximum calculated α_b were 3.4×10^{-8} $m^2 \cdot s^{-1}$ and 5.7×10^{-8} $m^2 \cdot s^{-1}$. Fig. 2. 8 (b) presents descending-ascending trends of thermal diffusivity at particle density (α_p) with increasing MC at different temperatures except 40℃. α is a function of thermal conductivity, specific heat, and density which are dependent on temperature and MC. The descending trend of α_p with MC was due to the fact that the increment rate of C_p with MC were higher than that of k_p. The ascending trend can be explained by the fact that the increment rate of k_p with MC were higher than that of C_p. These descending and ascending trends of α_p with temperature and MC have been reported previously (Dutta et al. 1988; Izadifar and Baik 2007; Shrestha and Baik 2010; Sweat 1986).

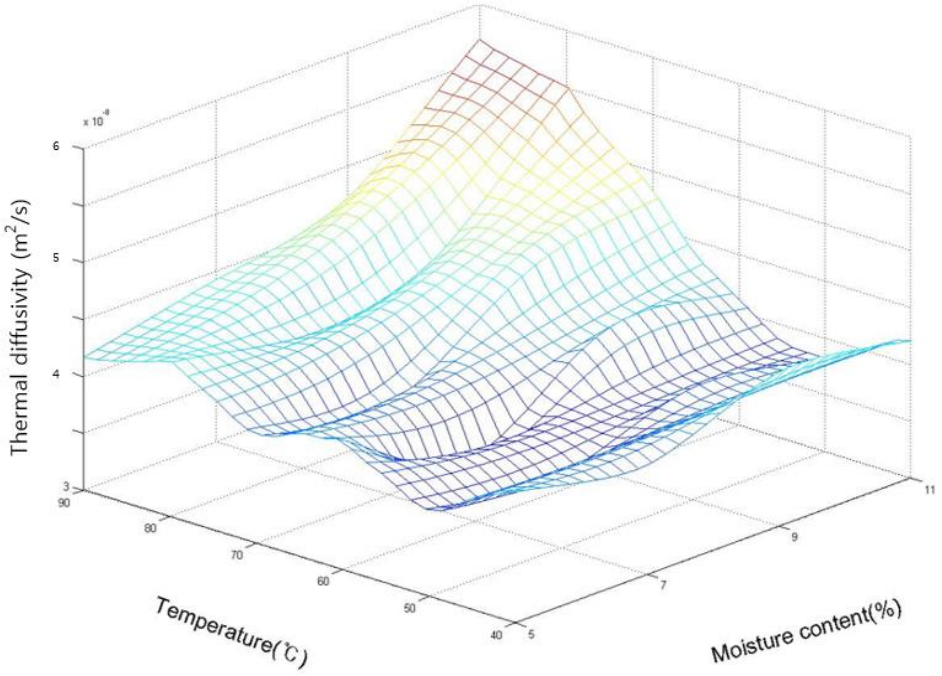

Figure 2. 7. Thermal diffusivities of stored canola seeds at bulk density as functions of temperature and MC.

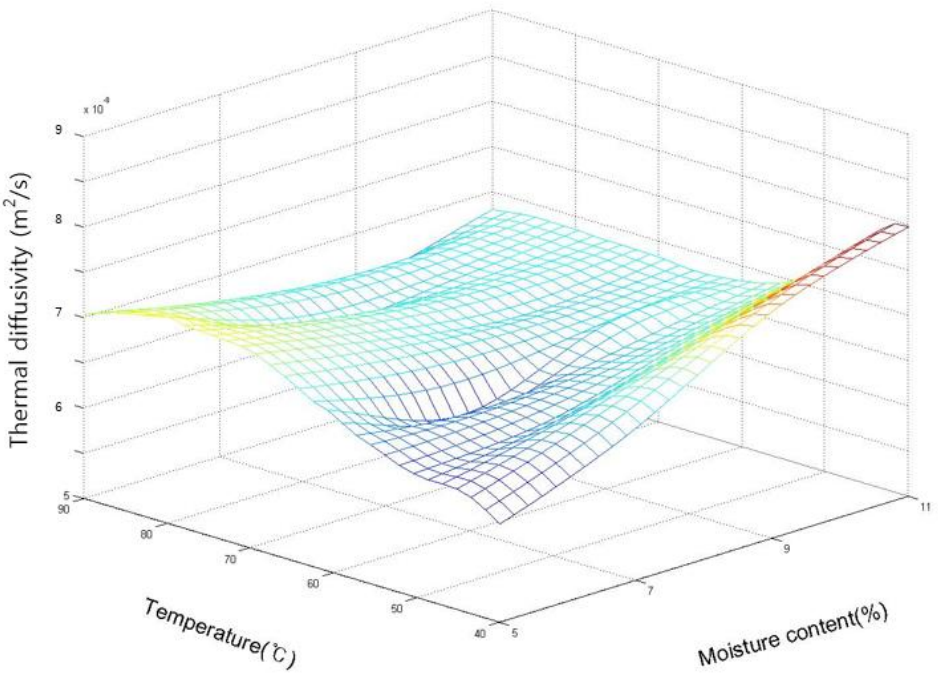

(a)

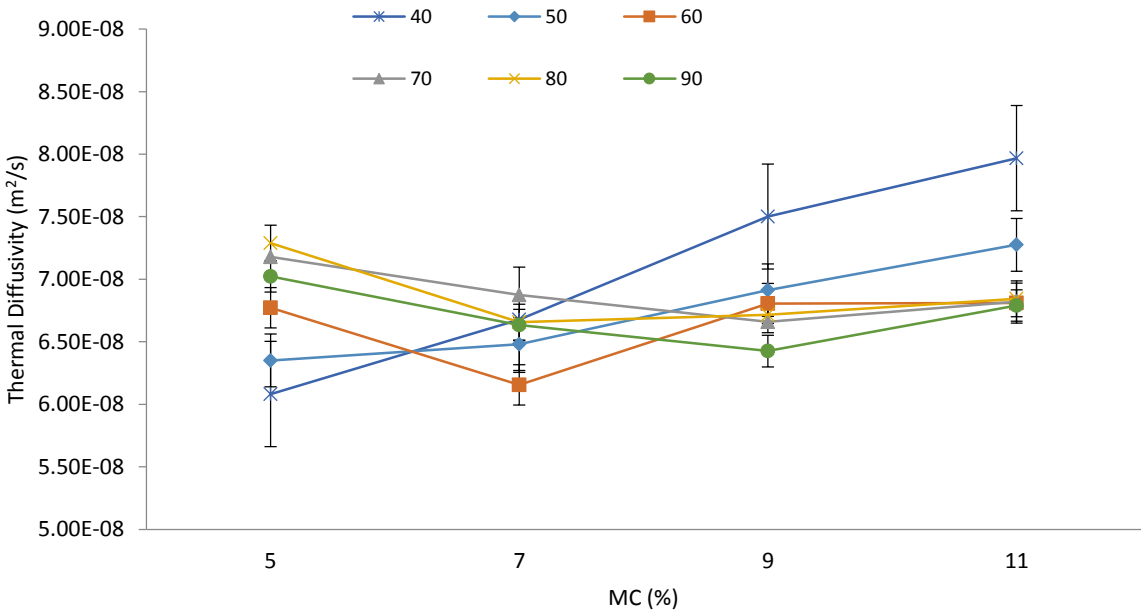

(b)

Figure 2. 8. Thermal diffusivities of stored canola seeds at particle density as functions of temperature and MC in 3D (a) and 2D (b).

At MC of 11% and 40℃, the highest α_p of stored canola seeds was observed, but there was no huge difference between maximum and minimum thermal diffusivities in this study. The values of α_p ranged from 6.1×10^{-8} to 8.0×10^{-8} $m^2 \cdot s^{-1}$.

To develop a regression model, the calculated α from the three measured properties were used in linear regression of SPSS Statistics 20.0 (SPSS Inc., Chicago, IL, USA). The statistical results and the regression equation are given in Table 2. 7. The calculated α, predicted α, and the percent difference at ρ_b and ρ_p at different temperatures and MCs are listed in Tables 2. 8 and 2. 9. The differences between calculated and predicted values of α_b and α_p ranged from 0.72 to 18% and 0.02 to 8.6%, and the R^2 values of α_b and α_p were 0.75 and 0.84, respectively.

Table 2. 7. Regression equations of thermal diffusivities of stored canola seeds at bulk and particle densities and statistical information.

Regression Model	F value	P value	DF	RMSE	R^2
$\alpha_b = [3.865 + 1.917 \cdot 10^{-9} \cdot (MC^3 \cdot T^3)] \cdot 10^{-8}$	66.62	1×10^{-6}	23	0.1×10^{-8}	0.75
$\alpha_p = [-2.165 + 1.197 \cdot (MC) + 0.181 \cdot (T) - 2.452 \cdot 10^{-2} \cdot (MC \cdot T) + 1.304 \cdot 10^{-4} \cdot (MC^3) - 6.524 \cdot 10^{-6} \cdot (T^3) + 6.914 \cdot 10^{-7} \cdot (MC \cdot T^3) + 3.0 \cdot 10^{-9} \cdot (MC^3 \cdot T^3)] \cdot 10^{-8}$	11.94	1×10^{-6}	23	0.2×10^{-9}	0.84

MC = moisture content (%)

T = temperature (℃)

Table 2. 8. Thermal diffusivities of stored canola seeds at bulk density at different temperatures and moisture contents.

Thermal Diffusivity at Bulk Density ($m^2 \cdot s^{-1}$) × 10^{-8}												
Temperature (℃)	MC (%, w.b.)											
	5%			7%			9%			11%		
	Calculated	Predicted	Difference (%)	Calculated	Predicted	Difference (%)	Calculated	Predicted	Difference (%)	Calculated	Predicted	Difference (%)
40	4.2	3.9	6.5	4.0	3.9	1.4	4.4	4.0	9.3	4.2	4.0	4.2
50	3.8	3.9	3.7	3.6	4.0	9.4	4.0	4.0	1.4	3.8	4.2	9.7
60	4.2	3.9	5.9	3.4	4.0	18	4.3	4.2	2.2	4.1	4.4	8.3
70	4.0	4.0	0.72	3.8	4.1	8.1	4.6	4.3	6.2	4.8	4.7	1.6
80	4.4	4.0	8.8	4.2	4.2	0.85	4.4	4.6	3.2	5.5	5.2	6.4
90	4.2	4.0	2.9	4.4	4.3	1.6	4.7	4.9	3.8	5.7	5.7	0.78

Table 2. 9. Thermal diffusivities of stored canola seeds at particle density at different temperatures and moisture contents.

Thermal Diffusivity at Particle Density ($m^2 \cdot s^{-1}$) × 10^{-8}												
Temperature (℃)	MC (%, w.b.)											
	5%			7%			9%			11%		
	Calculated	Predicted	Difference (%)	Calculated	Predicted	Difference (%)	Calculated	Predicted	Difference (%)	Calculated	Predicted	Difference (%)
40	6.1	6.0	1.3	6.7	6.6	1.2	7.5	7.2	3.5	8.0	8.0	0.15
50	6.4	6.4	1.2	6.5	6.7	2.6	6.9	7.0	0.68	7.3	7.4	1.4
60	6.8	6.8	0.10	6.2	6.7	8.6	6.8	6.7	1.0	6.8	7.0	2.1
70	7.2	7.0	2.4	6.9	6.7	2.6	6.7	6.6	1.2	6.8	6.7	1.6
80	7.3	7.1	2.1	6.7	6.7	0.36	6.7	6.5	3.2	6.8	6.7	2.3
90	7.0	7.1	1.7	6.6	6.6	0.02	6.4	6.5	1.4	6.8	6.9	1.6

The probable uncertainty of the calculated α was determined based on uncertainties of k, C_p, and ρ (ω_k, ω_{cp}, and ω_ρ) at 95% confidence limit (twice the standard deviation) using Eq. (2.12). The uncertainty of α_b to k_b, C_p, and ρ_b ranged from 0 to 0.11, 0.34×10^{-8} to 1.4×10^{-8}, and 0.12×10^{-10} to 1.3×10^{-10}. The uncertainty of α_p to k_p, C_p, and ρ_b ranged from 0 to 0.12, 0.51×10^{-8} to 1.8×10^{-8}, and 0.16×10^{-9} to 2.7×10^{-9}. The sensitivity of α was most affected by k followed by C_p and ρ. The effect of k on the variation of α can be confirmed by comparing Figs. 2. 4 and 2. 5, and Figs. 2. 7 and 2. 8.

2.5.5 Emissivity (ε)

Fig. 2. 9 shows ε of stored canola seeds as a function of temperature and MC. ε decreased with temperature and MC. Due to temperature increase and MC decrease during drying, the emissivity of canola seed would be stable. For non-metals, ε tends to be high and decreased with temperature (FLIR Systems 2009). The ε ranged from 0.93 to 0.99. The ε of stored canola seeds is higher than other metallic materials (copper : 0.07, iron : 0.6 ~ 0.7, and stainless steel : 0.45) that means canola seeds can absorb or emit more thermal radiation from its surroundings (Bramson 1968). In case of large temperature difference between the inner wall of a drying chamber and the canola seeds surface, the ε of canola seeds must be known to simulate heat and mass transfer processes for a better accuracy. The regression equation and statistical information are provided in Table 2. 10. The predicted ε are plotted along with the calculated ε in Fig. 2. 9 for comparison. The R^2 value was 0.951 and the minimum and maximum percent difference were 0.009% and 0.659%. Thus, ε of stored canola seeds can be reasonably calculated using the regression model over the temperature and MC ranges of 40 to 90℃ and 5 to 11% w. b., respectively.

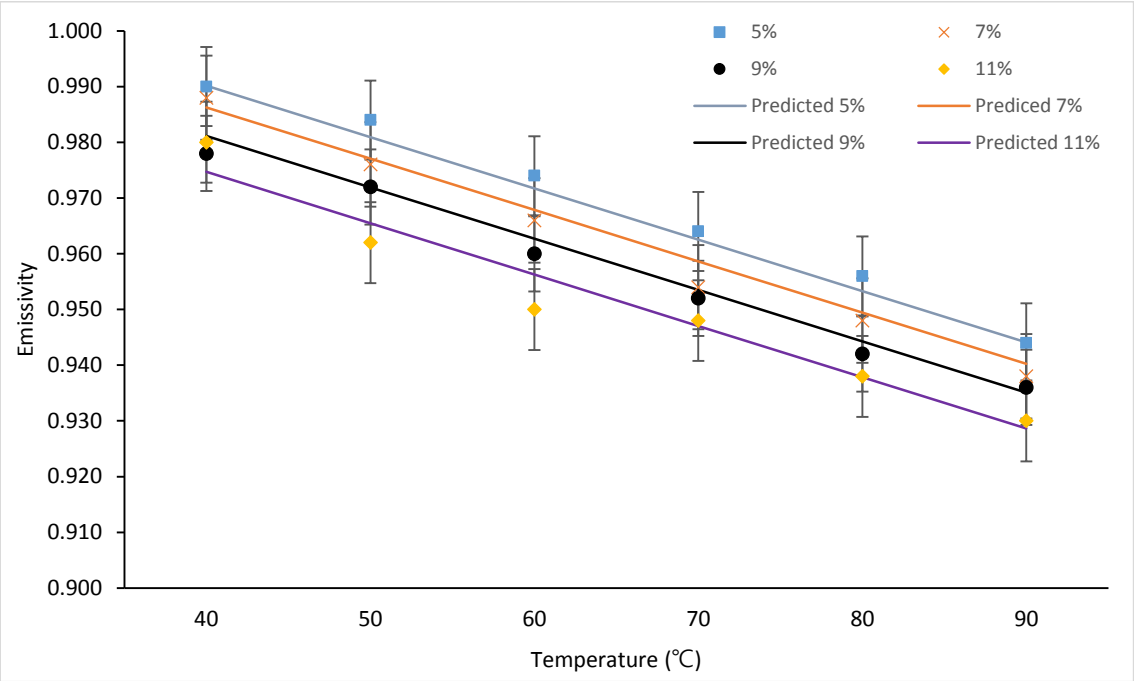

Figure 2. 9. Measured (scattered dots) and predicted values (solid lines) of emissivities of stored canola seeds as functions of temperature and MC.

Table 2. 10. Regression equation of emissivity of stored canola seeds and statistical information.

Regression Model	F value	P value	DF	RMSE	R^2
$\varepsilon = 1.031 - 0.921 \cdot 10^{-3} \cdot (T) - 0.161 \cdot 10^{-3} \cdot (MC^2)$	203.1	1×10^{-6}	23	0.004	0.95

MC = moisture content (%)

T = temperature (℃)

2.6 Conclusion

This study pursued the effects of temperature and MC on the thermal properties of stored canola seeds at heating and drying temperature range. Densities of stored canola seeds decreased with temperature. The porosity of stored canola seeds decreased with temperature and MC due to the increased ratio of ρ_b to ρ_p. The k increased with temperature regardless of MC. The k values predicted using the regression models were differed from the experimental data from 0.14 to 18.0%. The C_p of the stored canola seeds increased linearly with temperature and MC. In general, the canola seeds have the greater C_p at higher temperature and MC. The calculated α of stored canola

seeds from the measured values of k, C_p, ρ_b, and ρ_p of stored canola seeds increased with MC and temperature. A descending-ascending trend of thermal diffusivity was observed at particle density (α_p) with increasing MC at different temperatures except 40°C. The ε of the canola seeds with MC and temperature can be used for calculating radiation energy exchanges between surrounding and canola seeds.

Hence, these properties will be helpful in design and simulation of various processes that involves heat transfer. However, considering limited ranges of temperature and MC in this study, further work with wider ranges of temperature and MC might be useful.

2.7 References

ASABE. 2010. Official Methods of Analysis - S358 (2). American Society of Agricultural and Biological Engineers, MI, USA.

Bramson, M. A. 1968. Infrared radiation, Plenum press, N.Y.

Brusewitz, G. 1975. Density of rewetted high moisture grains. *Transactions of the ASAE*.

Bulanon, D. M., T. F. Burks, T. F., and V. Alchanatis. 2008. Study on temporal variation in citrus canopy using thermal imaging for citrus fruit detection. *Biosystems Engineering* 101(2): 161-171.

Campbell, G. S., C. Calissendorff, and J. H. Williams. 1991. Probe for measuring soil specific heat using a heat-pulse method. *Soil Science Society of America Journal* 55(1): 291-293.

Canola Council of Canada. 2014. http://www.canolacouncil.org/markets-stats/industry-overview/. (January, 23, 2015).

Canola Council of Canada. 2014. http://www.canolacouncil.org/crop-production/canola-grower's-manual-contents/chapter-2-canola-varieties/canola-varieties/. (January, 23, 2015).

Daudin, J. D., and M. V. L. Swain. 1990. Heat and mass transfer in chilling and storage of meat. *Journal of Food Engineering* 12(2): 95-115.

Davey, L. M., and Q. T. Pham. 1997. Predicting the dynamic product heat load and weight loss during beef chilling using a multi-region finite difference approach. *International Journal of Refrigeration* 20(7): 470-482.

Dinčov, D. D., K. A. Parrott, and K. A. Pericleous. 2004. Heat and mass transfer in two-phase porous materials under intensive microwave heating. *Journal of Food Engineering* 65(3): 403-412.

Dutta, S. K., V. K. Nema, and R. K. Bhardwaj. 1988. Thermal properties of gram. *Journal of Agricultural Engineering Research* 39(4): 269-275.

Farinu, A., and O. D. Baik. 2007. Thermal properties of sweet potato with its moisture content and temperature. *International Journal of Food Properties* 10 (4): 703-719.

FLIR Systems. 2009. "ThermoVision SDK: User's Manual", Revision: a372, August, 2009. publication No. T559014.

FAS. 2011. http://www.fas.usda.gov/oilseeds/circular/2011/March/oilseeds.pdf. (January, 23, 2015).

Giri, S. K., and S. Prasad. 2006. Modeling shrinkage and density changes during microwave-vacuum drying of button mushroom. *International Journal of Food Properties* 9(3): 409-419.

Hatamipour, M. S., D. Mowla. 2003. Correlations for shrinkage, density and diffusivity for drying of maize and green peas in a fluidized bed with energy carrier. *Journal of Food Engineering* 59(2): 221-227.

Hooper, F. C., and F. R. Lepper. 1950. Transient heat flow apparatus for the determination of thermal conductivities. National Emergency Training Center.

Huggins, L. F. 1983. Analysis and interpretation. *Instrumentation and Measurement for Environmental Sciences* (Mitchell BW, ed.): 15-02.

Ikebudu, J. A., S. Sokhansanj, R. T. Tyler, B. J. Milne, and N. S. Thakor. 2000. Grain conditioning for dehulling of canola. *Canadian Agricultural Engineering* 42(1): 27-32.

Izadifar, M., and O. D. Baik. 2007. Determination of thermal properties of the rhizome of Podophyllum peltatum for drying and ethanol extraction. *Biosystems engineering* 97(3): 357-370.

Jian, F., D. S. Jayas, and N. D. G. White. 2012. Thermal conductivity, bulk density, and germination of a canola variety with high oil content under different temperatures, moisture contents, and storage periods. *Transactions of the ASABE* 55(5): 1837-1843

Jian, F., D. S. Jayas, and N. D. G. White. 2013. Specific heat, thermal diffusivity, and bulk density of genetically modified canola with high oil content at different moisture contents, temperatures, and storage times. *Transactions of the ASABE* 56(3): 1077-1083.

Kocabiyik, H., and D. Tezer. 2007. Determination of thermal properties of rapeseed. *J. Tekirdag Agric.* Faculty 4(1): 65-70.

Mohsenin, N. N. 1980. Thermal properties of foods and agricultural materials. New York. USA.

Moysey, E. B., J. T. Shaw, and W. P. Lampman. 1977. The effect of temperature and moisture on the thermal properties of rapeseed. *Transactions of the ASAE*.

Muir, W. E., and S. Viravanichai. 1972. Specific heat of wheat. *Journal of Agricultural Engineering Research* 17(4): 338-342.

Murray, J. 2015. Personal Communication. Department of Camera System, FLIR Systems Inc., Boston, MA, USA.

Nelson, S. O. 1965. Dielectric properties of grain and seed in the 1 to 50-mc range. *Transactions of the ASAE* 8(1): 38–48.

Nesvadba, P. 1982. Methods for the measurement of thermal conductivity and diffusivity of foodstuffs. *Journal of Food Engineering* 1(2): 93-113.

Ochsner, T. E., R. Horton, and T. Ren. 2003. Use of the dual-probe heat-pulse technique to monitor soil water content in the vadose zone. *Vadose Zone Journal* 2(4): 572-579.

Senadeera, W., B. Bhandari, G. Young, and B. Wijesinghe. 2000. Physical properties and fluidization behaviour of fresh green bean particulates during fluidized bed drying. *Food and bioproducts processing* 78(1): 43-47.

Shrestha, B. L., and O. D. Baik. 2010. Thermal conductivity, specific heat, and thermal diffusivity of saponaria vaccaria seed particles. *Transactions of the ASABE* 53(5): 1717-1725.

Sparrow, E. M., J. M. Gorman, A. Trawick, and J. P. Abraham. 2012. Novel techniques for measurement of thermal conductivity of both highly and lowly conducting solid media. *International Journal of Heat and Mass Transfer* 55(15): 4037-4042.

Sweat, V. E. 1986. Thermal properties of foods. *Engineering properties of foods* : 49.

Tang, J., S. Sokhansanj, S. Yannacopoulos, and S. O. Kasap. 1991. Specific heat capacity of lentil seeds by differential scanning calorimetry. *Transactions of the ASAE*.

Timbers, G. E. 1975. Properties of rapeseed. 1. Thermal conductivity and specific heat. *Canadian Agricultural Engineering*.

Yang, W., S. Sokhansanj, J. Tang, and P. Winter. 2002. Determination of thermal conductivity, specific heat and thermal diffusivity of borage seeds. *Biosystems engineering* 82: 169-176.

CHAPTER 3

TEMPERATURE DISTRIBUTION IN A PACKED-BED OF CANOLA SEEDS (*BRASSICA NAPUS* L.) WITH VARIOUS MOISTURE CONTENTS AND BULK VOLUMES DURING RADIO FREQUENCY (RF) HEATING

Published, *Biosystems Engineering* 148 (2016) 55-67.

Contribution of this paper to overall study

No comprehensive research has been reported on the effect of the volume and shape of bulk canola seeds on their temperature distribution during RF heating. Furthermore, the effect of the bulk sample volume on formation of the electric field has not been demonstrated using an agar gel. The formation of electric field mainly affects temperature distributions in the seeds during RF heating. Therefore, temperature distributions in the seeds at various volumes and MCs during RF heating were determined (specific objective 3), and the effect of the sample volume on the formation of electric field was demonstrated using 2% agar gel (specific objective 4) in this chapter. The effect of seeds MC and volumes on RF heating uniformity was analyzed using uniformity index. The determined temperature distributions of the seeds as functions of the sample volume and MC and the analyzed effect of the sample volume on the formation of electric field were used for the determination of the thermal death kinetics of the red flour beetles in Chapter 5, the development of the mathematical model of the RF heating in Chapter 6 and the further simulations in Chapter 7, and the design of the conceptual scaled-up RF disinfestation process in Chapter 7. All the experiments in this chapter were conducted and the journal paper manuscript was drafted by myself.

3.1 Abstract

This research investigated temperature distribution in a packed-bed of canola seeds (*Brassica napus* L.) at various moisture contents (5%, 7%, 9%, and 11% wet weight basis) and bulk volumes (small – 196.3 cm^3, medium – 1766 cm^3, and large - 6503 cm^3) during RF heating (1.5 kW, 27.12 MHz). The samples were contained in RF-transparent cylindrical sample holders. To reach a specific temperature, the required RF exposure time decreased with seed moisture content (MC). The hottest spots (80℃) were detected at the geometric centers of the bulk canola seeds of the small and large volumes. In the RF heating of the medium volume samples, the hottest spot (80℃) did move towards the edge from the geometric center with MC due to edge effect. The relatively higher temperatures were observed between middle and outer regions in the medium volume canola seeds unlike the heating of the small and large volumes. The temperature profiles of 2% agar gels at different sizes determined by thermal imaging supported the observations with the bulk canola seeds. Based on the temperature uniformity index values evaluated, more uniform RF heating was observed with the medium bulk volume in spite of the edge effect.

3.2 Nomenclature

C_p	specific heat of material (J kg^{-1}℃$^{-1}$)	ΔT	temperature rise in material (℃)
D	diameter (mm)	Δt	time duration (s)
E	electric field strength (V m^{-1})	UIV	uniformity index value
EM	electromagnetic	W	width (mm)
F	frequency (Hz)		
H	height (mm)	*Greek symbols*	
L	length (mm)	ε''	dielectric loss factor
MC	moisture content (%, wet basis)	$\boldsymbol{\theta}$	temperature uniformity
PEI	polyetherimide	μ	mean of temperature (℃)
Q	volumetric heat generation (W m^{-3})	ρ	bulk density of material (Kg m^{-3})
RF	radio frequency	σ	standard deviation of temperature (℃)

3.3 Introduction

Canola (*Brassica Sp*.) is one of the major grain crops grown worldwide. The canola was produced approximately 67.7 million metric tons in 2015–2016 around the world (USDA Foreign Agricultural Service 2015). The oil and meal processed from the canola have been used for human consumption and animal feed.

The average losses of oilseed damage by insect pest range 8-10% annually causing millions of dollars in the economy (Canola Watch 2015). To control the insect pest, other conventional methods (controlled atmosphere, hot and cold air, and ionizing radiation) were applied as possible substitutes, however these methods still have major drawbacks (inefficient heating, long treatment time, and etc) (Heather and Hallman 2008; Wang and Tang 2004).

One of the alternative method for the disinfestation is the radio frequency (RF) heating which relies on the interactions between electromagnetic (EM) energy and the materials containing polar molecules and ions. It is governed by the characteristics of the electromagnetic energy, and the electrical, thermal, and physical properties of the materials. The main advantages of RF heating over thermal gradient driven conventional heating methods are: RF heating is fast, and it heats the whole materials simultaneously (bulk or volumetric heating). However, RF heating usually ends up with non-uniform heating of substances, but this drawback can be minimized with appropriate sample handling mechanisms.

Mitcham et al. (2004) determined the temperature variations of in-shell walnuts contained in a cylindrical sample holder during RF heating (12 kW, 27 MHz). Birla et al. (2008b) also observed non-uniform RF heating (12 kW, 27.12 MHz) with fresh apples when they investigated RF heating patterns influenced by the dielectric properties of the fresh apples. Hou et al. (2014) also reported non-uniform temperature distributions in bulk chestnuts when RF heated without assistance of any auxiliary equipment (hot air system, mixing, and conveyor) for disinfestation.

The temperature uniformity (θ) by RF heating is not only affected by the thermal, physical, and electrical properties of the sample, but **i**t is also affected by the size, shape, and the position of the sample in the RF applicator. Romano and Marra (2008) simulated the effect of different shapes of samples (cube, cylinder and sphere) on the temperature distribution in meat using a RF heater (100 to 400 W, 27.12 MHz). They found that the meat in cubical shapes had less temperature variations compared to other shapes. The effect of vertical and horizontal positions of model fruits on their

temperature distribution during RF heating was reported by Birla et al. (2008a). Tiwari et al. (2011a) also simulated the RF power (12 kW, 27.12 MHz) uniformity in wheat flour samples with three different shaped containers (cuboid, ellipsoid, and cylinder). They reported that the center parts of the ellipsoid had higher power densities, whereas the other shapes had higher power densities at the edges. No comprehensive researches have been reported on the effect of sample volume and shape of bulk canola seeds on their temperature distribution during RF heating.

The gel samples of different shapes and sizes have also been RF heated to study the temperature distribution in chemically and structurally homogenous objects. In these cases, the temperature distributions are mainly dependent of electric field distribution inside the objects. The electric field formation in 2% agar gel cylinders during pulsed microwave heating was studied by Yang and Gunasekaran (2001). Birla et al. (2008a) investigated RF heating uniformity of model fruits prepared from 1% gellan gels. Birla et al. (2008b) compared the simulated temperature distributions of the stratified spherical model fruits (made of gellan and whey protein gels) with the experimental thermal images for model validation. The effect of sample volume on formation of electric field affecting non-uniform RF heating has not yet been demonstrated using 2% agar gel.

The uniformity index value (UIV) is one of the important indexes to study and design the effective postharvest heating processes. Wang et al. (2008) used the UIV to characterize the temperature distribution in small size crops (wheat, soybean, lentil, and walnut). They suggested that RF treatments for small size crops to control pest could be developed with better heating uniformity than that of large size crops. They also claimed that the UIV could be used as a practical operational parameter for industrial scale continuous RF processes. Wang et al. (2014) evaluated the effectiveness of polyurethane foam on RF heating uniformity with macadamia nuts using the UIV, which were defined as the ratio of the increment of standard deviation of the temperature to that of the average temperature. Jiao et al. (2015) added polyetherimide cylindrical blocks at the bottom and the top of the cylindrical plastic sample container to achieve more uniform heating with RF. The temperature uniformity index (TUI) was used to investigate the effectiveness of the uniformity improvement method for RF heating of peanut butter. They found that polyetherimide cylindrical blocks with diameter of 8 cm resulted the best RF heating uniformity among different diameters of the block.

The objectives of this study were (1) to determine the temperature distribution in the bulk canola seeds of various volumes and MCs during RF heating, (2) to demonstrate the effect of the sample volume on the formation of electric field affecting the RF heating pattern using a 2% agar gel, and (3) to analyze the effects of seeds MC and volumes on the θ.

3.4 Materials and methods

3.4.1 Sample treatment

Top quality canola seeds (B. *napus* L.) at initial moisture content (MC) of 7% wet weight basis were supplied by our industrial partner, Viterra Inc., Regina, SK, Canada. The canola seeds were sealed in polypropylene bags and were stored in a cold storage at 4°C before using them.

The MC of the bulk canola seeds was determined following the standard method (ASAE 2002). Canola seeds (10 g) were poured into an aluminum moisture dish, and then it was placed in a hot air oven (Despatch, Despatch Industries, MN, USA) for 24 h at 103°C. The average MC was calculated from five replicates.

The bulk canola seeds of different MCs (5%, 7%, 9%, and 11%) were prepared separately. Canola samples at MC of 5% were prepared by drying a known mass of canola seeds at initial MC (7%) to the pre-calculated weight in the hot air oven set at 40°C. Canola samples at 9 % and 11 % were prepared by spraying pre-calculated amounts of distilled water on the known masses of the seeds at initial MC contained in a glass jar. The glass jars were continuously shook and rotated while spraying. The air-tight glass jars were left at room temperature (24°C) for 3 days with periodic shaking to achieve a moisture equilibrium. All the samples were stored in a cold storage until used. Canola samples from the storage were left at room temperature for 6 h before using them for experiments. Then, the MC of the samples were measured. A digital scale with an accuracy of ± 0.01 g (Symmetry, PR4200, Cole-Parmer Instrument Co., Niles, IL, USA) was used for all weighing.

The 2% agar gel samples were prepared by dissolving 30 g of agar powder (Agar Powder, Now Foods, Bloomingdale, IL) in distilled water (1500 mL) in a pyrex glass beaker (2000 mL). The agar - distilled water solution was heated on a hot plate (RCT basic, IKA®, Staufen, Germany) until the agar powder was perfectly dissolved. It was then poured into small (*D*: 50 mm × *H*: 100 mm), medium (*D*: 150 mm × *H*: 100 mm), and large (*L*: 255 mm × *W*: 255 mm × *H*: 100 mm)

sample holders made of RF transparent polycarbonate. The gel was allowed to cool at room temperature (23℃) for solidification. The gel thus prepared was covered with a plastic film wrap to prevent moisture loss. It was stored in a cold storage for 16 h to achieve thermal equilibrium for subsequent RF heating (Yang and Gunasekaran 2004).

3.4.2 RF heating system

A 1.5 kW, 27.12 MHz lab-scale RF system (Strayfield Fastran, Berkshire, England) was used for heating of bulk canola seeds (Fig. 3. 1). The surface area of the thin parallel electrode plates was *L*: 250 mm × *W*: 250 mm. The bulk canola seeds in the sample holder were placed in between the center of the two electrodes. The gaps between the upper electrode and top of the holder were set at 1, 15, and 30 mm respectively for small, medium, and large holders to prevent electric arcing. The upper plate was adjusted to a required height by turning the crank on the top of the enclosure. Fiber optic temperature sensors and an associated data logging device with an accuracy of ± 0.8 ℃ (T1^{TM} Fiber Optic Temperature Sensor and ReFlex^{TM} Signal Conditioner, Neoptix, Québec City, Québec, Canada) were used to monitor sample temperatures (T). These readings were transferred automatically through the I O^{-1} device (NI USB 6008, TX) to the data acquisition program (oven.vi) developed on Labview (2010 v. 10) platform. The readings were displayed, and recorded at a predefined interval of time as well.

(a) (b)

Figure 3. 1. The back (a) and the inside (b) views of the RF heating unit; I : optic fiber thermometer device, II : temperature controller, III : I O^{-1} device, IV : data acquisition software, V : electrodes, VI : canola seed samples, VII : T1^{TM} fibre optic temperature sensors.

3.4.3 Temperature distribution

The temperature distributions in the bulk canola seeds were determined at nine locations for the small holder and at twelve locations for the medium and large holders (Fig. 3. 2). Sample holders were made of RF transparent polycarbonate to minimize the effect of the holder on the temperature distributions. The exact locations of the fibre optic temperature sensors are given in Table 3. 1. Temperatures at all locations were measured from 26℃ (initial temperature) to 80℃ (final target temperature) without holding time. This temperature range was chosen considering that 100% mortalities of other similar insect pest were achieved at the temperature range (Armstrong et al. 2009; Shrestha et al. 2013). In our another research, 100% mortalities of the red flour beetle were achieved by RF heating up to final temperatures of 60℃ to 80℃ depending on the volume of the bulk canola seeds (Yu et al. 2016). The assigned final target temperature was higher than those in other researches on thermal death kinetics (Wang et al. 2002; Johnson et al. 2004). Other researchers heated the insects at certain target temperatures with holding times (46℃, 48℃, 50℃, and 52℃ for 50 min, 15 min, 5 min, and 2 min, and 50℃ and 52℃ for 8 min and 1.3 min,

respectively) using an heating block system (non-dielectric heating). Whereas, we continuously increased the temperature of the infested canola seeds up to the assigned final target temperature (80℃) by RF heating without holding and cooling times. These temperature vs time data were also used for our other studies on the mortality of the red flour beetles infesting the canola seeds and its transient thermal death kinetics.

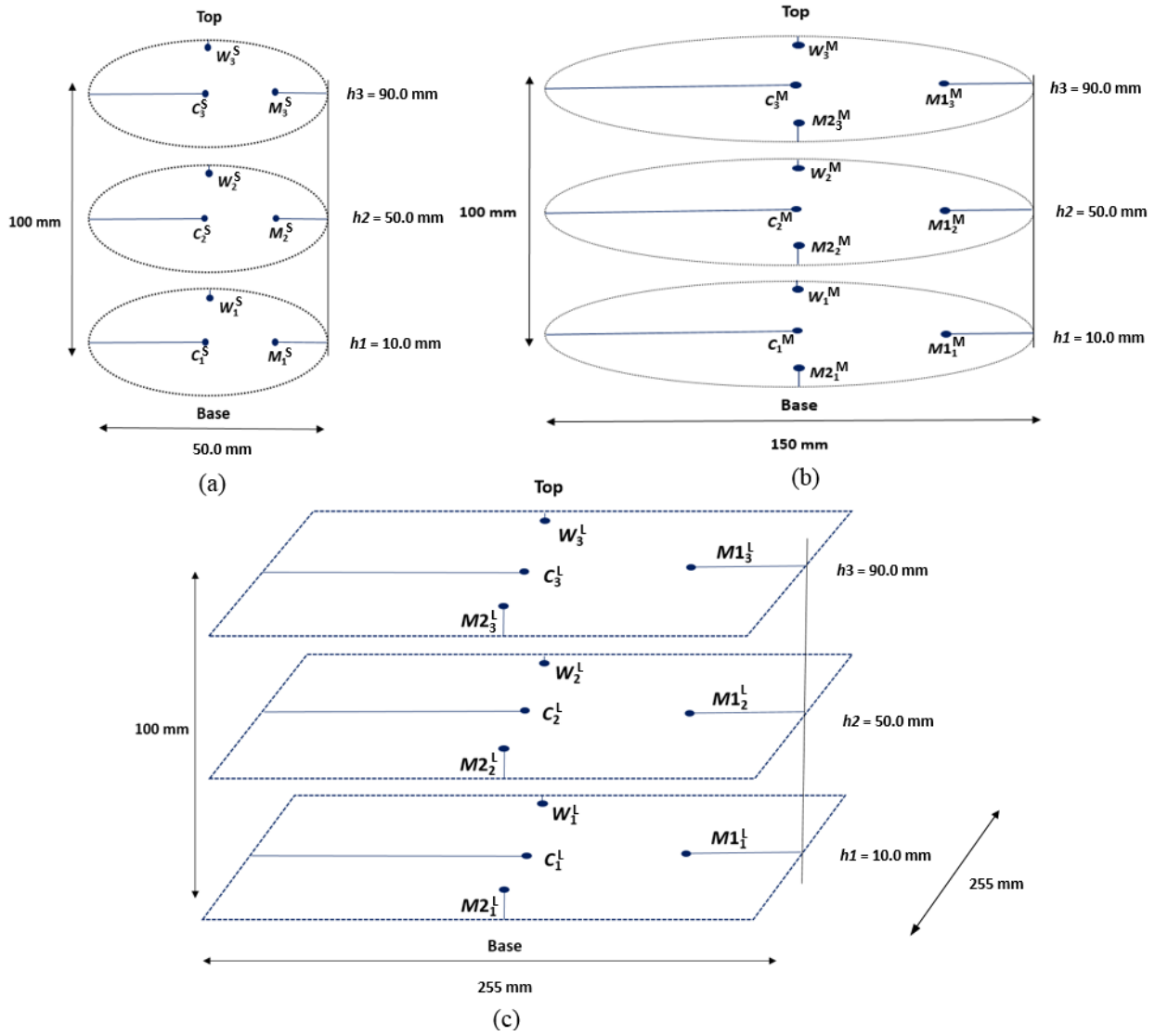

Figure 3. 2. Placement of the temperature sensors and the dimensions of small (a), medium (b), and large (c) volumes: $W^S = W^M = W^L = 1$, $M^S = 12.5$, $M2^M = 18.8$, $M1^M = 37.5$, $M2^L = 32.0$, $M1^L = 64.0$, $C^S = 25.0$, $C^M = 75.0$, and $C^L = 128$ mm away from the inner wall of the each holder at the heights of $h1 = 10$, $h2 = 50$, and $h3 = 90$ mm from its base.

Table 3. 1. Placement of the temperature sensors in the sample holder.

Holder size	Location of sensors (mm)						
	From the wall of the sample holder				From the holder-base		
Small	C^S	M^S		W^S	$h1$	$h2$	$h3$
	25.0	12.5		1.00			
Medium	C^M	$M1^M$	$M2^M$	W^M			
	75.0	32.5	16.0	1.00	10.0	50.0	90.0
Large	C^L	$M1^L$	$M2^L$	W^L			
	128	63.8	31.9	1.00			

$W^S = W^M = W^L = 1$, $M^S = 12.5$, $M2^M = 18.8$, $M1^M = 37.5$, $M2^L = 32.0$, $M1^L = 64.0$, $C^S = 25.0$, $C^M = 75.0$, and $C^L = 128$ mm away from the inner wall of the each holder at the heights of $h1 = 10$, $h2 = 50$, and $h3 = 90$ mm from its base

Temperatures at all locations were determined when the temperature of the hottest spot reached up to 80℃. Three temperature sensors (channels) for the small volume of the seeds and four temperature sensors for the medium and the large volumes of the seeds were used for each layer (top, middle, and bottom) of the seeds. Three different batches of the canola seeds in total were used for each volume of the seeds and then all temperature data were combined together to present temperature distribution. The temperature sensors were calibrated before each measurement and apparently the canola seeds of the same quality and quantity were used for each batch under the same RF heating condition. There still might be experimental errors associated with different batches regardless our efforts to minimize it. The averages and the standard deviations of triplicates for all volumes were reported.

3.4.4 Thermal image of 2% agar gel

The heat generation inside a material by RF energy can be described as Eq. (3.1) (Choi and Konrad 1991).

$$Q = 55.63 \times 10^{-12} f E^2 \varepsilon'' = \rho C_p \frac{\Delta T}{\Delta t} \tag{3.1}$$

From Eq. (3.1), the rate of increase of temperature of the material can be expressed as shown in Eq. (3.2).

$$\frac{\Delta T}{\Delta t} = \frac{55.63 \times 10^{-12} f E^2 \varepsilon''}{\rho C_p} \tag{3.2}$$

where Q is the volumetric heat generation (W m^{-3}), f is the frequency (Hz), E is the electric field strength (V m^{-1}), ε'' is the dielectric loss factor, ρ is the bulk density of the material (kg m^{-3}), C_p is the specific heat of the material (J kg^{-1} ℃$^{-1}$), ΔT is the temperature rise in the material (℃), Δt is the time duration (s). Therefore, the RF heating pattern in the sample is affected by a combination of the electric field strength and other parameters (density, specific heat, and dielectric loss factor) from properties of the sample. Compared to the canola seeds, using the 2 % agar gel as a homogeneous material is more suitable to minimize the effect of non-uniform chemical composition (dielectric properties and specific heat) and physical structure (density and volume) on characterizing the electric field formation which directly affects the RF heating pattern. It is important to note that temperature distribution or electric field strength distribution in the agar gel is not the same as that in the bulk canola seeds. This test can only show the effect of volume of

bulk sample on electric field strength distribution or temperature distribution in the sample. Thermal images were taken at different heights (10, 50, and 90 mm from base) of the 2% agar gel using an infrared thermal camera (Therma-CAM^{TM} Researcher ver. 2.8 SR-1, accuracy ± 2 ℃, FLIR Systems, Portland, OR, USA) immediately after RF heating. The gelation threshold temperature (60℃) of the gel was experimentally determined to avoid the gel from melting down. Therefore the gel was not heated beyond the threshold. The fibre optic temperature sensors were placed at the identical locations for both bulk canola seeds and the gel for ease of comparison.

3.4.5 θ of canola seeds

The temperature uniformities of the bulk canola seeds in both horizontal and vertical directions by RF heating were estimated. The variation of the mean and standard deviation of sample temperature were expressed as shown in Eqs (3.3) and (3.4). (Neter et al. 1996)

$$\Delta\mu = \mu_t - \mu_0 \tag{3.3}$$

$$\Delta\sigma = \sqrt{\sigma_t^2 - \sigma_0^2} \tag{3.4}$$

where μ and σ represent the mean and standard deviation of temperatures, and Δ is the increment. The suffixes 0 and t denote the temperatures at initial and after t seconds of RF heating. The μ_0 and σ_0 were assumed at 26℃ and 0 for convenience, respectively. There was the error between uniformities determined using actual μ_0 and σ_0 and using the assumed μ_0 and σ_0, but we did not consider it as the θ difference was small from preliminary calculation (averagely 0.98% and 1.80% for horizontal and vertical directions). The θ difference ranged from 0.02 to 4.65% and 0.03 to 4.40% for horizontal and vertical directions. Then, the θ can be obtained by combining Eqs. (3.3) and (3.4), and is shown in Eq (3.5) (Gao et al. 2010)

$$\theta = \frac{\Delta\sigma}{\Delta\mu} \tag{3.5}$$

A well-designed RF heating system has usually a small value of θ with slower increment of standard deviation of temperature when the mean temperature rises.

3.4.5 Statistical analysis

Bivariate correlation analysis in SPSS 20.0 (SPSS Inc., Chicago, IL, USA) was used to investigate the effect of seeds MC and volumes on the θ.

3.5 Results and discussion

3.5.1 Temperature distribution in the bulk canola seeds

Figures 3. 3, 3. 4, and 3. 5 show temperature distributions in bulk canola seeds at different MCs and volumes during RF heating. The RF exposure time decreased with seed MC to reach the same core temperature of 80℃. It is due to the enhanced conductivity of ions and dipoles in the bulk canola seeds, which in turn, increased the dielectric loss factor of the material resulting in higher RF power dissipation in the material (Shrestha et al. 2013). In general, the sample temperatures decreased from the center towards the wall region due to the heat losses from the outer boundary of the sample. Figures 3. 4 and 3. 5 illustrate temperature distributions in bulk canola seeds of medium and large volumes respectively. In case of medium volume (Fig. 3. 4), relatively higher temperatures of the bulk canola seeds at the region between the middle and outer boundary were observed compared to those for small and large volumes. The highest temperatures were observed for the bulk canola seeds at 9% and 11% MCs at $M2^{M}$ - $h2$ among other conditions. It was attributed to the edge effect. Tiwari et al. (2011b) found a similar phenomenon when they subjected the wheat flour to RF heating (12 kW, 27.12 MHz). They also verified the experimental results through their computer simulations. The edge effect occurred due to an increasing electric field concentration at the edges and the corners of the container. The net electric field at the outer regions of a sample is larger than that in the inner regions due to the deflected electric fields described in Fig. 3. 6 (Roussy and Pearce 1995; Tiwari et al. 2011b). Figures 3. 3 and 3. 4 described the increasing intensity of the edge heating with increasing volume. It might be affected by increasing surface of the edges and corners. Interestingly, the edge effect was not observed in the large volume of the canola seeds. It implied that the electric field is more uniform at the corners and edges of the sample which has relatively larger surface area than the electrode. The hottest spots (80℃) of the sample of small and large volumes were at the geometric centers (C^{S} and C^{L}). Shrestha et al. (2013) found similar results when they treated bulk wheat samples at different MCs in a cylindrical sample holder (D = 50 mm, H = 100 mm) with RF radiation (1.5 kW, 27.12 MHz). In case with the medium holder, the hottest spot (80℃) was shifted towards the edge of the holder from the geometric center as the seeds at higher MCs were used. It seemed the RF exposure time was not enough to migrate the evaporated moisture from the hotter region near the wall to the inner colder

region of the sample. As indicated in Table 3. 2, the maximum temperature differences between the hottest and the coldest spots in the bulk canola seeds of small, medium, and large volumes were 42.4℃, 38.1℃, and 37.8℃ at the 11%, 11%, and 7% MC respectively. The hottest temperature was at 80℃ and the coldest temperatures were at 37.7℃, 41.9℃, and 42.2℃ for small, medium, and large volumes respectively. The highest average temperatures of the sample in small, medium, and large volumes were 62.3℃, 64.9℃, and 62.9℃ at the 7%, 7%, and 5% MC respectively. Tiwari et al. (2011b) reported that the average temperature and temperature difference of the wheat flour in a plastic container (300 × 220 × 60 mm^3) were 48.25℃ and 22.5℃ respectively after 3 min RF heating (12 kW, 27.12 MHz) with an electrode gap of 155 mm and an air gap of 95 mm. In another work, Wang et al. (2010) reported the average surface temperatures of chickpea, green pea, and lentil were 64.5℃, 61.3℃, and 56.8℃ when they exposed the legumes to RF irradiation (6 kW, 27 MHz). These results also suggested that there is a temperature variation during the RF heating, and the non-uniform heating occurs irrespective of the MCs and volumes of the samples.

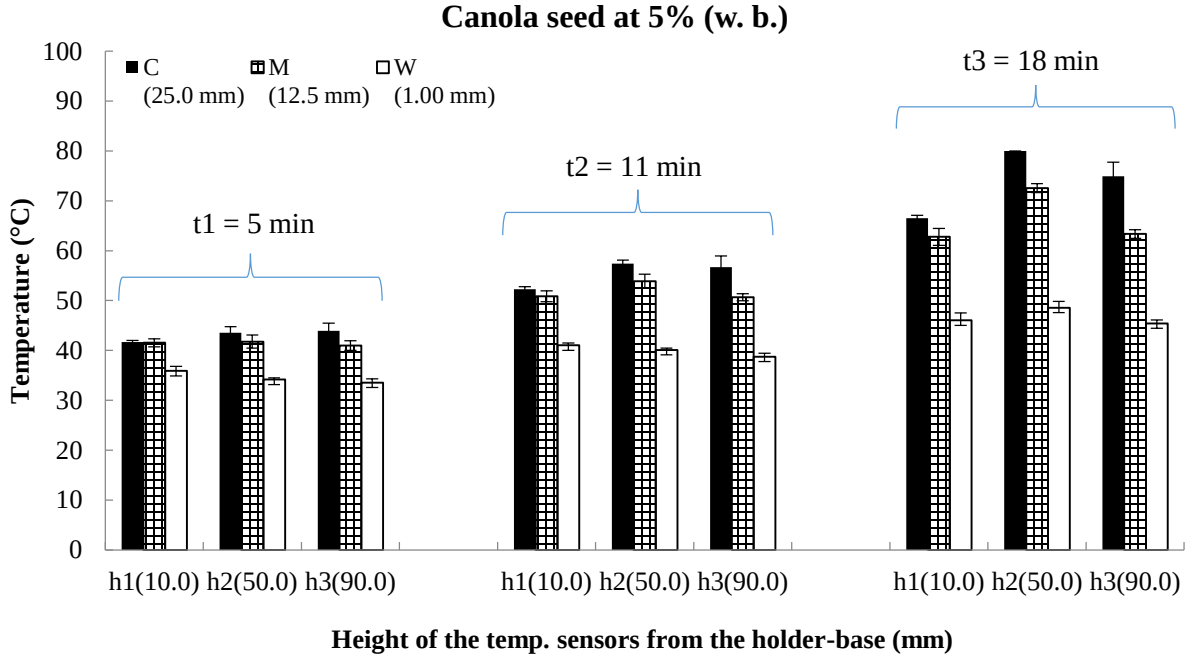

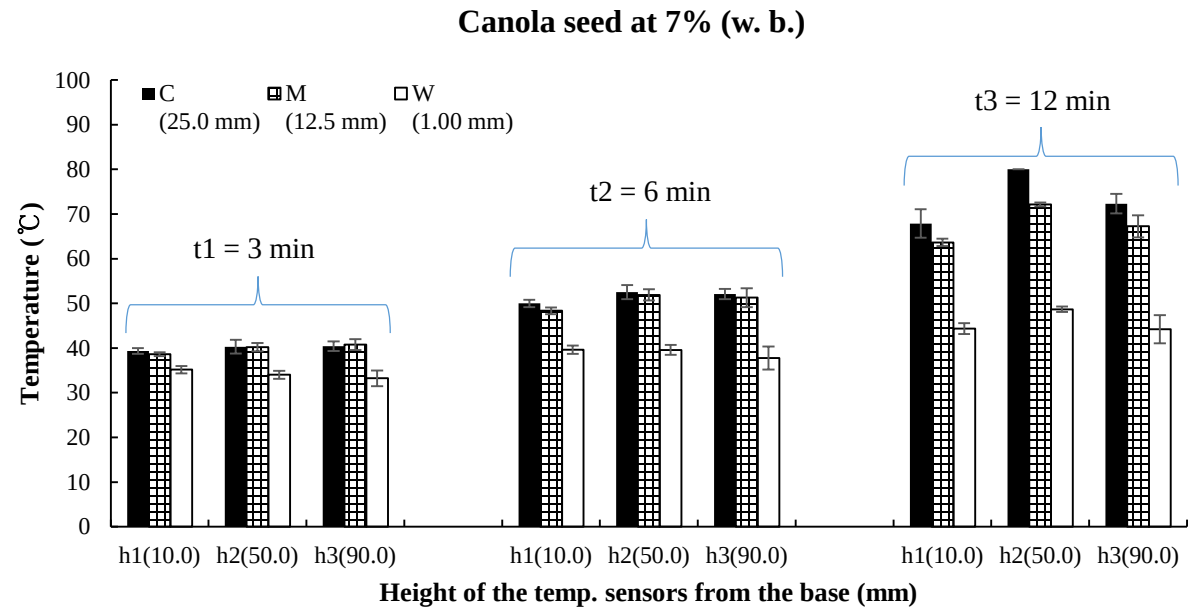
Canola seed at 7% (w. b.)
C (25.0 mm)
M (12.5 mm)
W (1.00 mm)
t1 = 3 min
t2 = 6 min
t3 = 12 min
Temperature (℃)
100
90
80
70
60
50
40
30
20
10
0
h1(10.0) h2(50.0) h3(90.0)
h1(10.0) h2(50.0) h3(90.0)
h1(10.0) h2(50.0) h3(90.0)
Height of the temp. sensors from the base (mm)

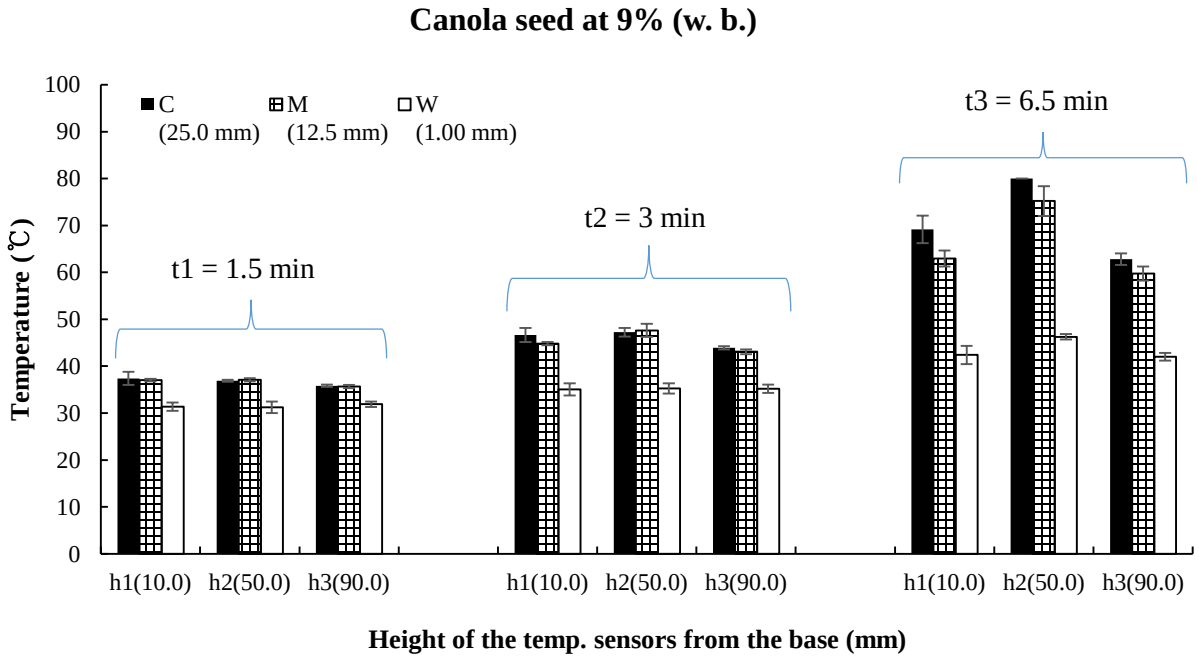
Canola seed at 9% (w. b.)
C (25.0 mm)
M (12.5 mm)
W (1.00 mm)
t1 = 1.5 min
t2 = 3 min
t3 = 6.5 min
Temperature (℃)
100
90
80
70
60
50
40
30
20
10
0
h1(10.0) h2(50.0) h3(90.0)
h1(10.0) h2(50.0) h3(90.0)
h1(10.0) h2(50.0) h3(90.0)
Height of the temp. sensors from the base (mm)

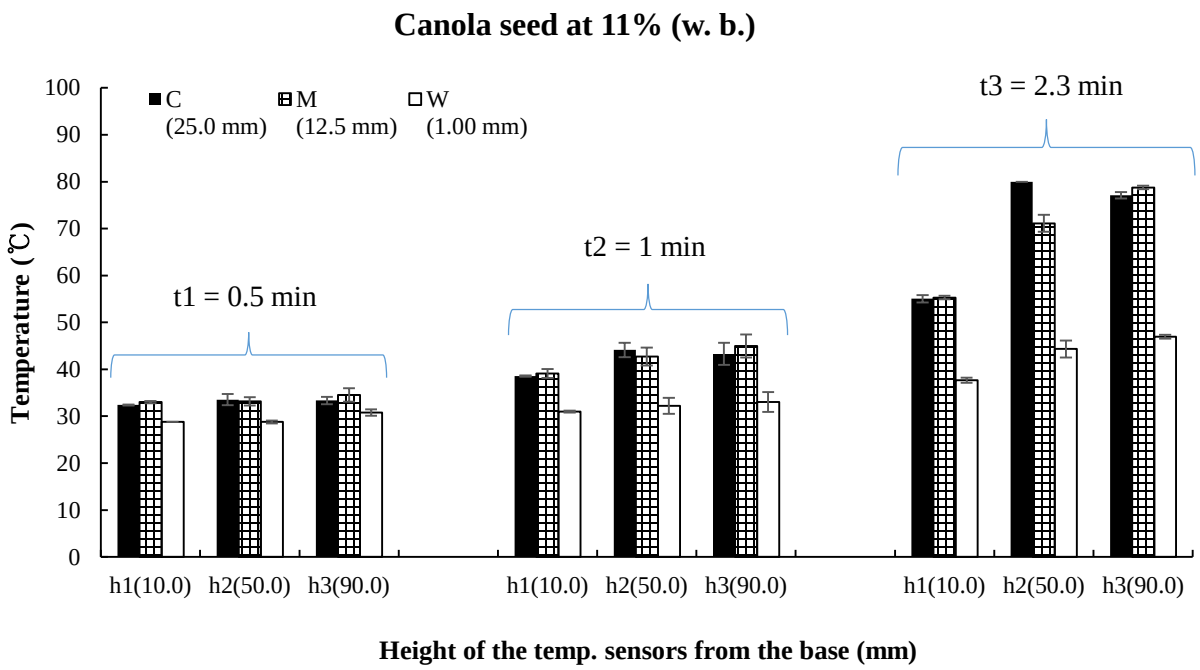

Figure 3. 3. Temperature distributions in the bulk canola seeds of small volume; where t is the RF exposure time, and C (center), M (middle), and W (wall) represent the locations of the temperature sensor at center, in-between C and W, and nearby wall, respectively (n = 3).

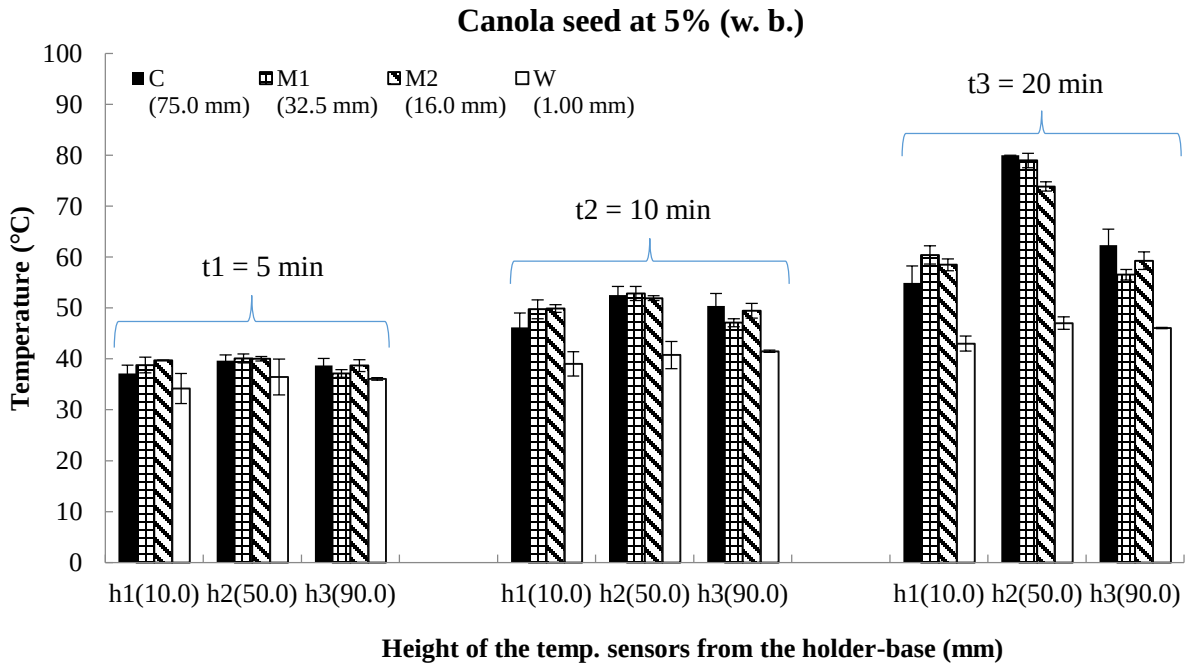

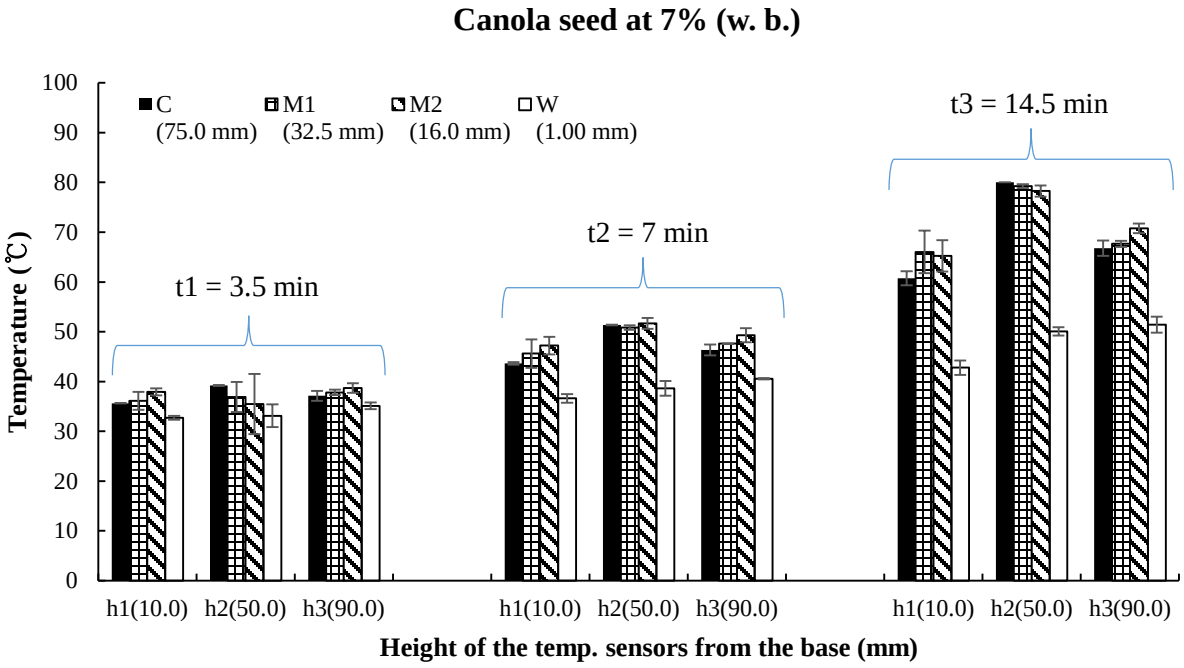
Canola seed at 7% (w. b.)
C (75.0 mm)
M1 (32.5 mm)
M2 (16.0 mm)
W (1.00 mm)
t1 = 3.5 min
t2 = 7 min
t3 = 14.5 min
Temperature (℃)
100
90
80
70
60
50
40
30
20
10
0
h1(10.0) h2(50.0) h3(90.0) h1(10.0) h2(50.0) h3(90.0) h1(10.0) h2(50.0) h3(90.0)
Height of the temp. sensors from the base (mm)

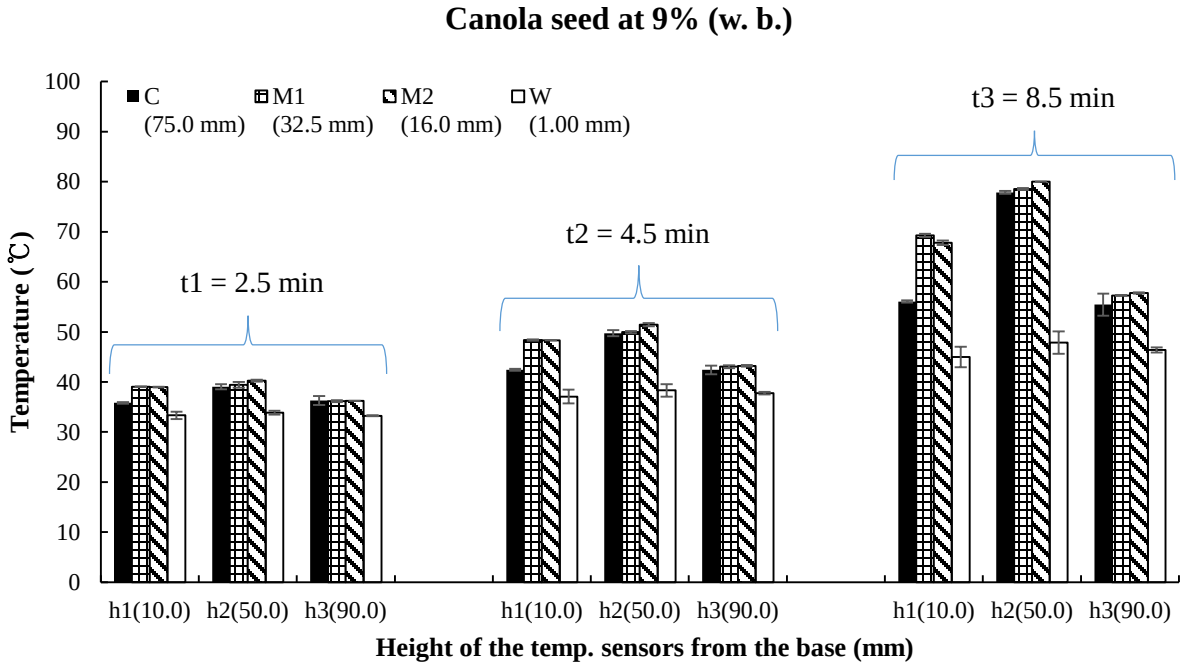
Canola seed at 9% (w. b.)
C (75.0 mm)
M1 (32.5 mm)
M2 (16.0 mm)
W (1.00 mm)
t1 = 2.5 min
t2 = 4.5 min
t3 = 8.5 min
Temperature (℃)
100
90
80
70
60
50
40
30
20
10
0
h1(10.0) h2(50.0) h3(90.0) h1(10.0) h2(50.0) h3(90.0) h1(10.0) h2(50.0) h3(90.0)
Height of the temp. sensors from the base (mm)

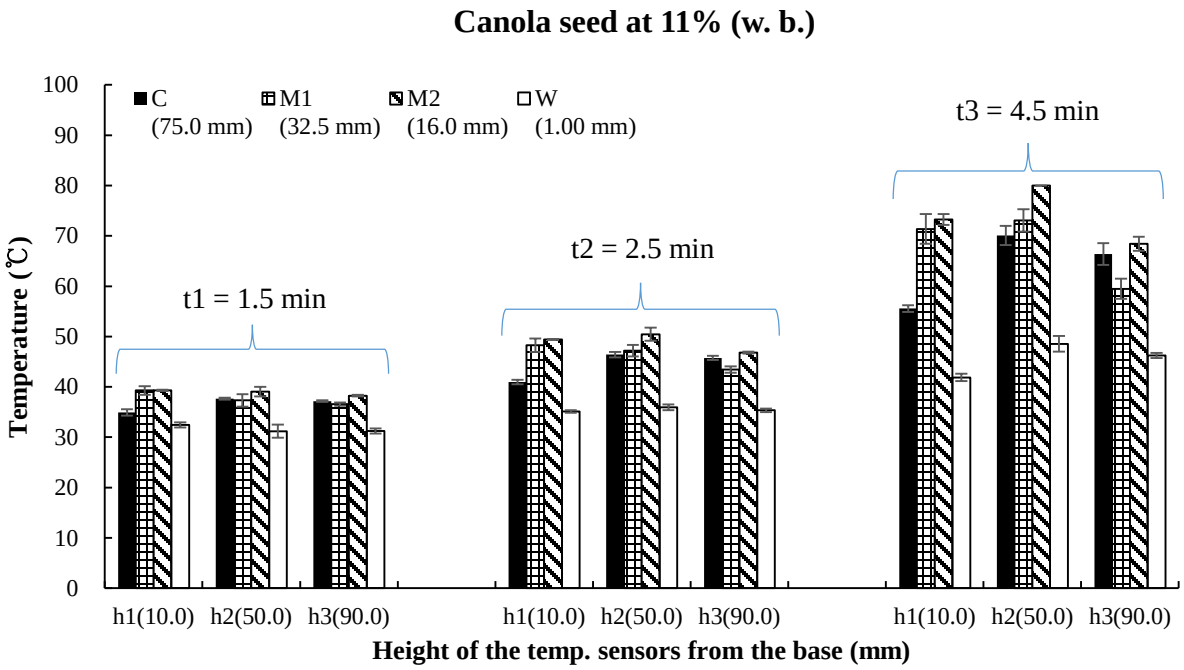

Figure 3. 4. Temperature distribution in the bulk canola seeds of medium volume; where t is the RF exposure time, and C (center), M1 (middle 1), M2 (middle 2), and W (wall) represent the locations of the temperature sensor at center, in-between C and M2, in-between M1 and W, and nearby wall respectively (n = 3).

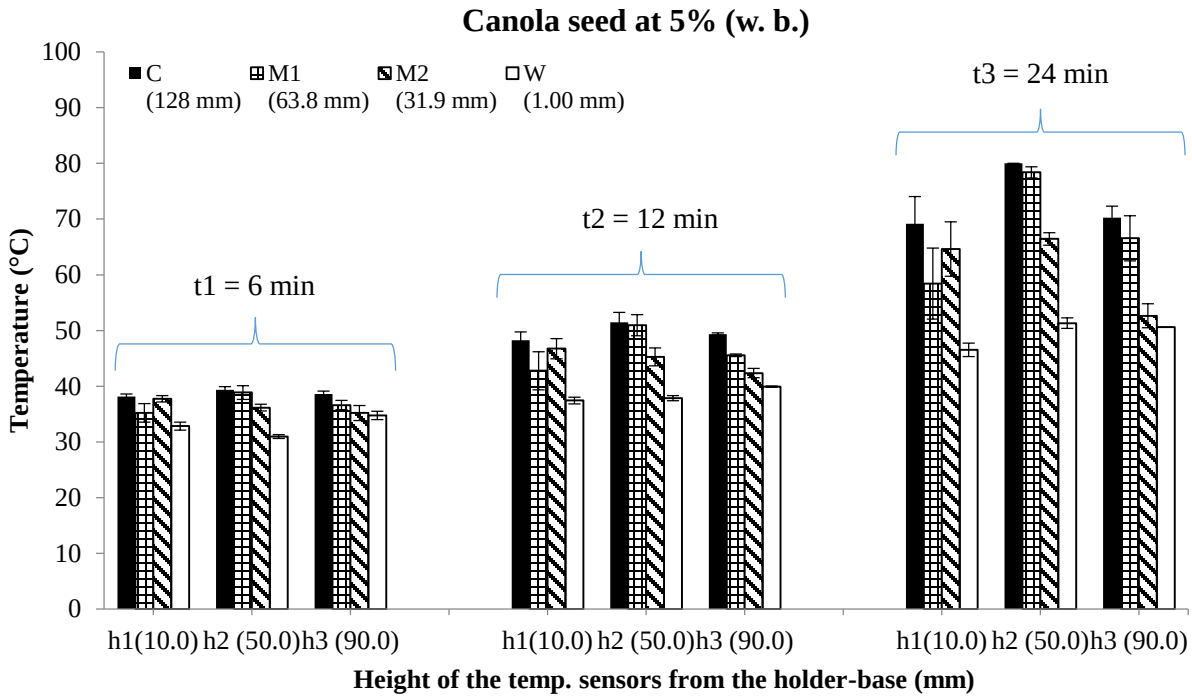
Canola seed at 5% (w. b.)
C (128 mm)
M1 (63.8 mm)
M2 (31.9 mm)
W (1.00 mm)
t1 = 6 min
t2 = 12 min
t3 = 24 min
Temperature (°C)
h1(10.0) h2 (50.0) h3 (90.0)
Height of the temp. sensors from the holder-base (mm)

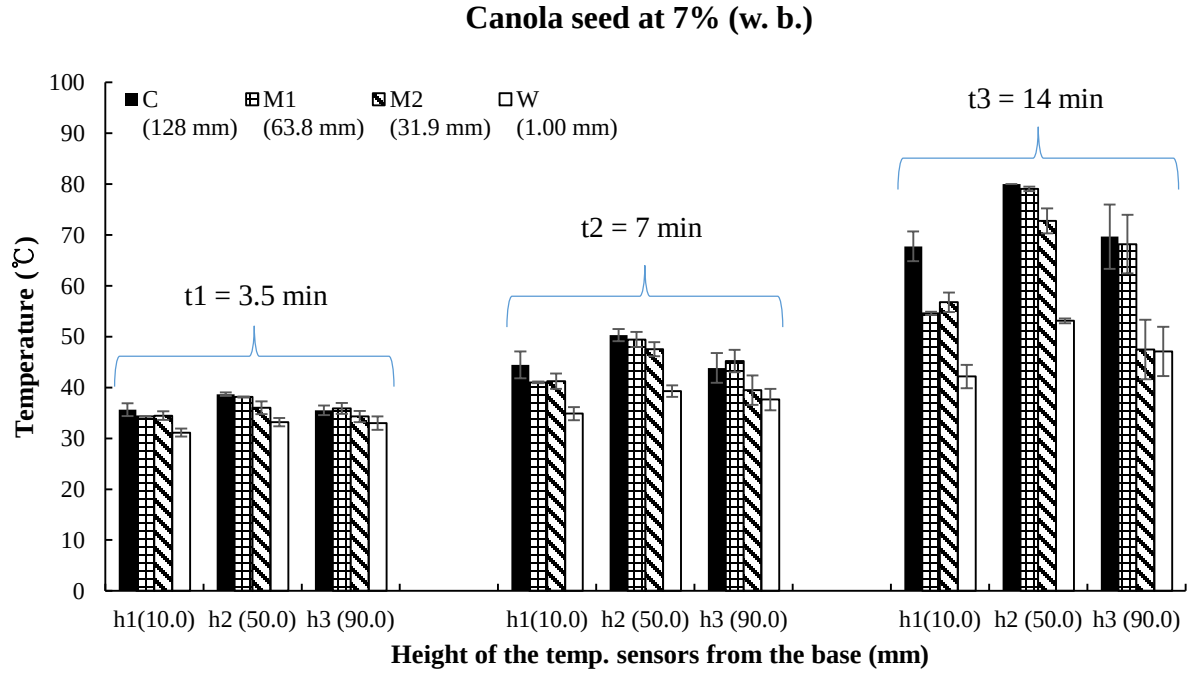
Canola seed at 7% (w. b.)
C (128 mm)
M1 (63.8 mm)
M2 (31.9 mm)
W (1.00 mm)
t1 = 3.5 min
t2 = 7 min
t3 = 14 min
Temperature (℃)
h1(10.0) h2 (50.0) h3 (90.0)
Height of the temp. sensors from the base (mm)

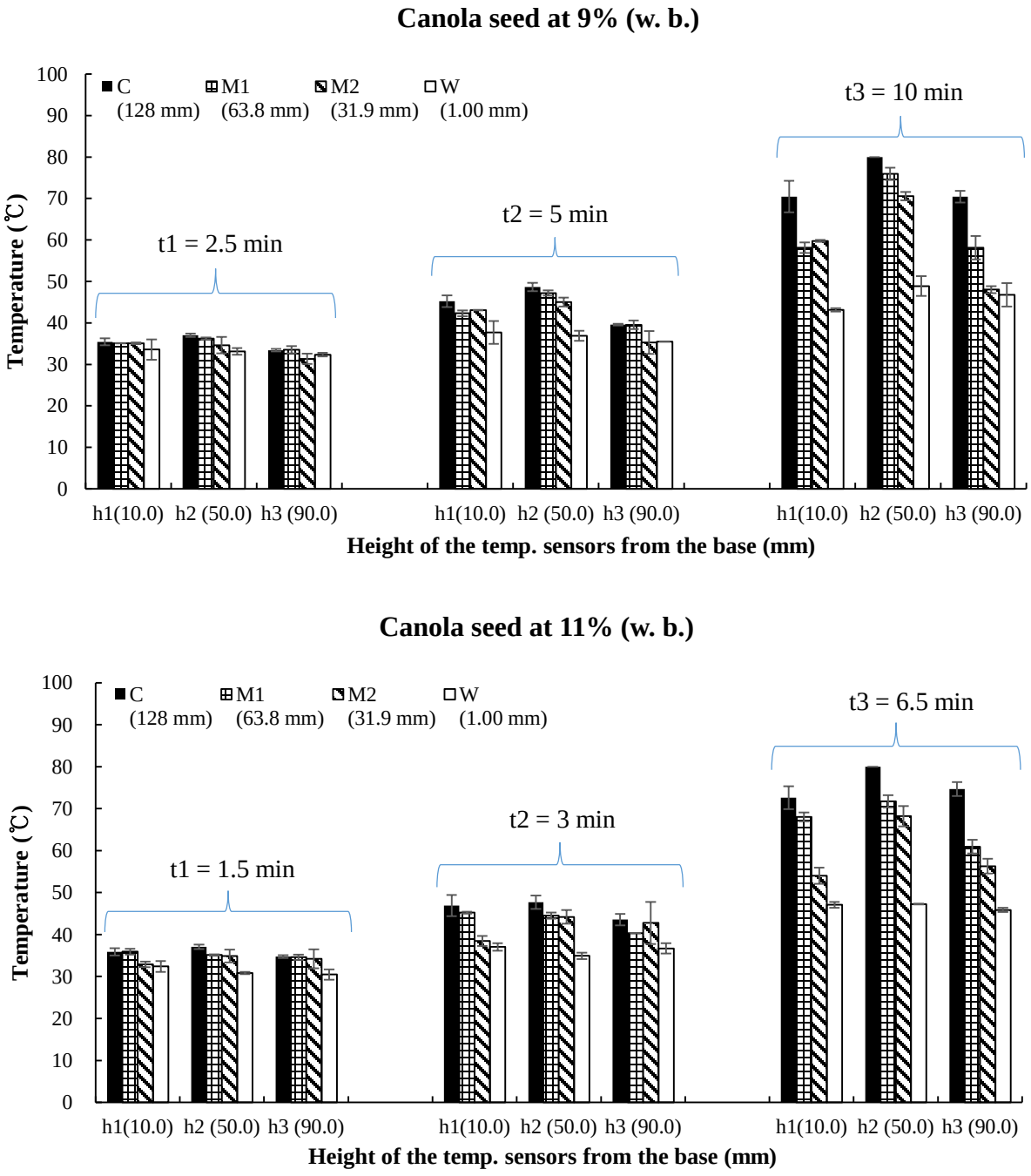

Figure 3. 5. Temperature distribution in the bulk canola seeds of large volume; where t is the RF exposure time, and C (center), M1 (middle 1), M2 (middle 2), and W (wall) represent the locations of the temperature sensor at center, in-between C and M2, in-between M1, and nearby wall respectively (n = 3).

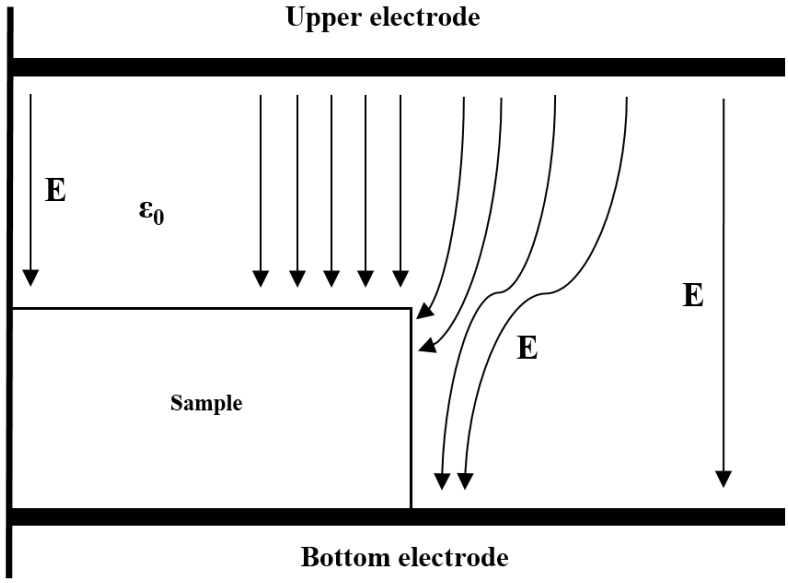

Figure 3. 6. Schematic of the edge heating within two parallel electrodes under the RF electric field (*E*) (Roussy and Pearce 1995).

Table 3. 2. Temperature distributions within the bulk canola seeds during RF heating at different moisture contents in different sizes of holder when the temperature of hottest spot reached up to 80°C.

Size of holder	MC (%)	Height (mm)	RF exposure (min)	Sensor location (mm)				$\triangle T^{a}$	$\triangle T^{b}_{avg}$
				C^{S} (25.0)	M^{S} (12.5)	W^{S} (1.00)			
Small	5	*h*1 (10.0)	18	66.5 ± 0.55	62.8 ± 1.70	46.1 ± 1.49		34.6	62.2 ± 12.2
		*h*2 (50.0)		80.0 ± 0.00	72.6 ± 0.91	48.6 ± 1.30			
		*h*3 (90.0)		74.9 ± 2.83	63.4 ± 0.87	45.4 ± 0.68			
	7	*h*1 (10.0)	12	67.9 ± 3.17	63.7 ± 0.83	44.4 ± 1.20		35.8	62.3 ± 12.5
		*h*2 (50.0)		80.0 ± 0.00	72.2 ± 0.44	48.7 ± 0.63			
		*h*3 (90.0)		72.3 ± 2.17	67.3 ± 2.47	44.2 ± 3.16			
	9	*h*1 (10.0)	6.5	69.2 ± 2.94	62.9 ± 1.69	42.4 ± 1.95		38.0	60.1 ± 13.1
		*h*2 (50.0)		80.0 ± 0.00	75.2 ± 3.18	46.3 ± 0.59			
		*h*3 (90.0)		62.8 ± 1.22	59.8 ± 1.49	42.0 ± 0.82			
	11	*h*1 (10.0)	2.3	55.0 ± 0.77	55.3 ± 0.36	37.7 ± 0.54		42.4	60.7 ± 15.4
		*h*2 (50.0)		80.0 ± 0.00	71.1 ± 1.81	44.3 ± 1.79			
		*h*3 (90.0)		77.1 ± 0.67	78.8 ± 0.40	46.9 ± 0.42			
				C^{M} (75.0)	$M1^{M}$ (37.5)	$M2^{M}$ (18.8)	W^{M} (1.00)		
Medium	5	*h*1 (10.0)	20	54.9 ± 3.37	60.4 ± 1.81	58.5 ± 1.15	43.0 ± 1.49	37.0	60.1 ± 11.7
		*h*2 (50.0)		80.0 ± 0.00	79.0 ± 1.41	73.9 ± 0.93	47.0 ± 1.20		
		*h*3 (90.0)		62.3 ± 3.18	56.5 ± 1.03	59.3 ± 1.73	46.1 ± 0.13		
	7	*h*1 (10.0)	14.5	60.7 ± 1.43	66.0 ± 4.29	65.2 ± 3.17	42.8 ± 1.44	37.2	64.9 ± 11.4
		*h*2 (50.0)		80.0 ± 0.00	79.3 ± 0.38	78.3 ± 1.13	50.1 ± 0.84		
		*h*3 (90.0)		66.8 ± 1.54	67.7 ± 0.60	70.8 ± 0.94	51.4 ± 1.62		
	9	*h*1 (10.0)	8.5	56.1 ± 0.25	69.3 ± 0.32	67.8 ± 0.44	45.0 ± 2.04	35.0	61.6 ± 12.2
		*h*2 (50.0)		77.9 ± 0.30	78.5 ± 0.21	80.0 ± 0.00	47.8 ± 2.23		
		*h*3 (90.0)		55.4 ± 2.21	57.3 ± 0.03	57.8 ± 0.13	46.4 ± 0.52		
	11	*h*1 (10.0)	4.5	55.6 ± 0.68	71.4 ± 2.94	73.2 ± 1.07	41.9 ± 0.73	38.1	62.9 ± 11.8
		*h*2 (50.0)		70.1 ± 1.91	73.1 ± 2.24	80.0 ± 0.00	48.6 ± 1.54		
		*h*3 (90.0)		66.4 ± 2.13	59.8 ± 2.00	68.4 ± 1.39	46.3 ± 0.52		
				C^{L} (128)	$M1^{L}$ (64)	$M2^{L}$ (32)	W^{L} (1.00)		
Large	5	*h*1 (10.0)	24	69.2 ± 4.87	58.4 ± 6.38	64.6 ± 4.86	46.5 ± 1.20	33.5	62.9 ± 10.5
		*h*2 (50.0)		80.0 ± 0.00	78.4 ± 1.00	66.5 ± 1.13	51.3 ± 0.94		
		*h*3 (90.0)		70.3 ± 2.04	66.6 ± 4.05	52.6 ± 2.15	50.6 ± 0.00		
	7	*h*1 (10.0)	14	67.8 ± 2.92	54.6 ± 0.32	56.8 ± 1.90	42.2 ± 2.28	37.8	61.6 ± 12.4
		*h*2 (50.0)		80.0 ± 0.00	79.1 ± 0.43	72.8 ± 2.44	53.1 ± 0.47		
		*h*3 (90.0)		69.7 ± 6.31	68.2 ± 5.74	47.5 ± 5.87	47.1 ± 4.85		
	9	*h*1 (10.0)	10	70.5 ± 3.80	58.1 ± 1.27	59.8 ± 0.21	43.1 ± 0.42	33.3	60.9 ± 11.9
		*h*2 (50.0)		80.0 ± 0.00	76.0 ± 1.48	70.6 ± 1.00	48.9 ± 2.38		
		*h*3 (90.0)		70.4 ± 1.41	58.2 ± 2.83	48.0 ± 0.84	46.8 ± 2.83		
	11	*h*1 (10.0)	6.5	72.6 ± 2.73	68.0 ± 1.08	54.0 ± 1.94	47.1 ± 0.68	34.1	62.2 ± 11.4
		*h*2 (50.0)		80.0 ± 0.00	71.7 ± 1.43	68.2 ± 2.42	47.3 ± 0.10		
		*h*3 (90.0)		74.7 ± 1.65	60.9 ± 1.63	56.3 ± 1.78	45.9 ± 0.49		

$W^{S} = W^{M} = W^{L} = 1$, $M^{S} = 12.5$, $M2^{M} = 18.8$, $M1^{M} = 37.5$, $M2^{L} = 32.0$, $M1^{L} = 64.0$, $C^{S} = 25.0$, $C^{M} = 75.0$, and $C^{L} = 128$ mm away from the inner wall of the each holder at the heights of *h1* = 10, *h2* = 50, and *h3* = 90 mm from its base.

a : maximum temperature difference within the bulk canola seeds at the specified MC.

b : average temperature of the bulk canola seeds at the specified MC.

*n = 3

3.5.2 Temperature profile of the 2% agar gel

Figures 3. 7, 3. 8, and 3. 9 show the temperature profiles of the 2% agar gels of the small, medium, and large volumes at horizontal (*h*1, *h*2, and *h*3) surfaces and vertical surfaces after RF heating. The temperatures shown in the images were slightly lower than the actual temperatures of the samples due to time lapse (approximately 10 second) in the preparation of image taking process. The temperature distributions in the bulk canola seeds were compared with those of the gel to determine whether the temperature discrepancies within the bulk canola seeds were occurred due to the RF system and the volume of the sample or it was because of the inhomogeneity present in the particulate samples. As shown in Fig. 3. 7, the hottest spot of the gel of the small volume was observed near the geometrical center similar to bulk canola seeds (C^{S}-*h*2). Fig. 3. 7(d) showed that the gel of the small volume was heated volumetrically, and the decrease of temperature from the center to the boundary region was likely due to the external heat losses. Fig. 3. 8 described the edge effect of the gel of medium volume. Near the edge and at the corners ($M2^{M}$) of the gel were heated faster than other regions. The reason could be the same as in the case of bulk canola seeds. Hot spot regions of the gel (medium volume) were similar with those of the bulk canola seeds ($M1^{M}$ and $M2^{M}$) at higher MCs (9% and 11%). Interestingly, the edge effect was not observed for the gel of large volume as shown in Fig. 3. 9. This result was similar with that of bulk canola seeds. It proved that the electric field near the edge and the corner regions were bent toward the sample resulting in an increasing electric field concentration therein irrespective of the material in hand. The hottest region of the gel (large volume) was at its geometrical center similar to the bulk canola seeds (C^{L}-*h*2). Overall, the temperature profiles of the gels were in good agreement with those of the bulk canola seeds.

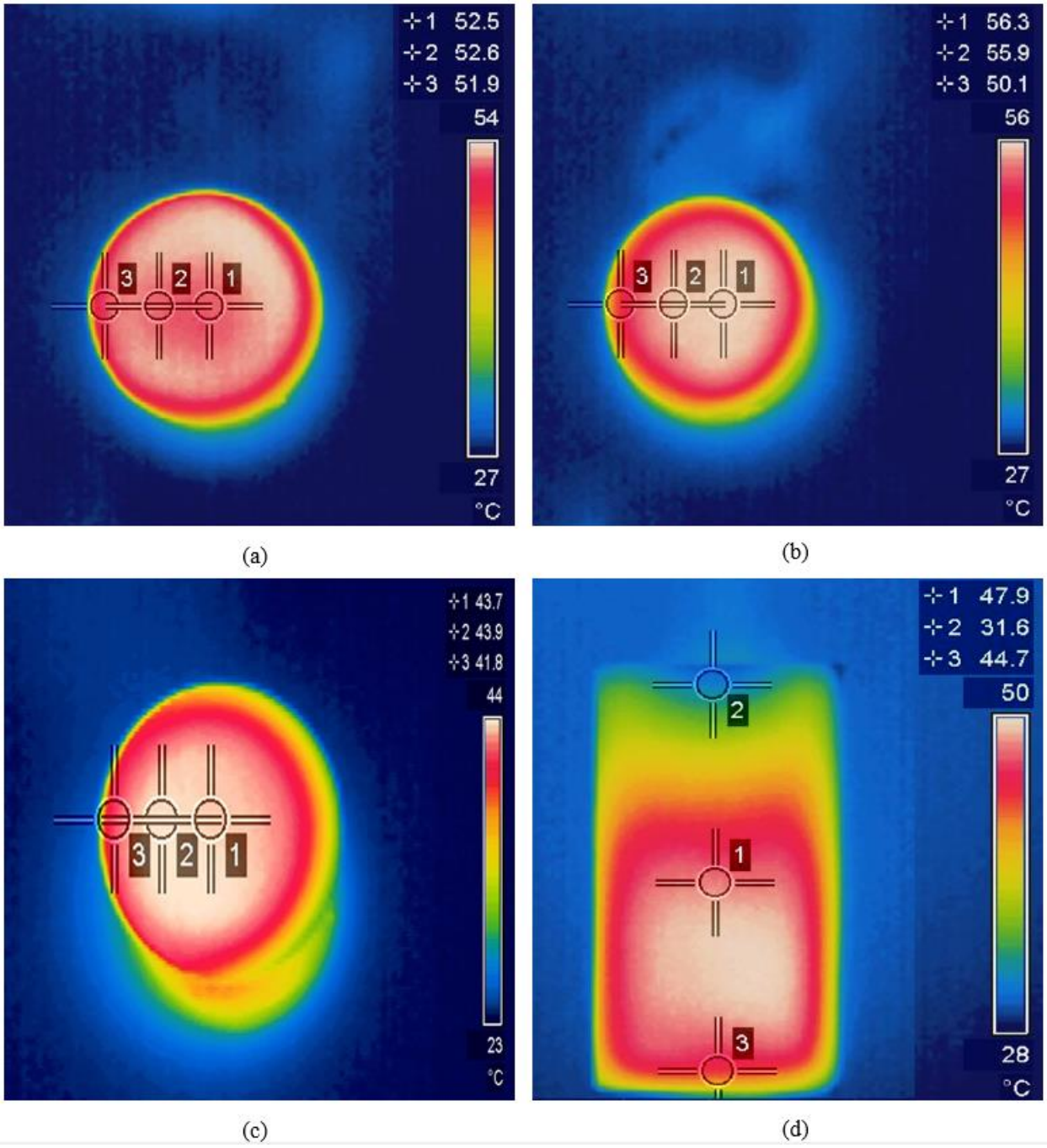

Figure 3. 7. Temperature profile of 2% agar gel (small holder) at *h*1 (10.0 mm) (a), *h*2 (50.0 mm) (b), *h*3 (90.0 mm) (c) surfaces and vertical surface (25.0 mm from holder-wall) (d) after RF heating.

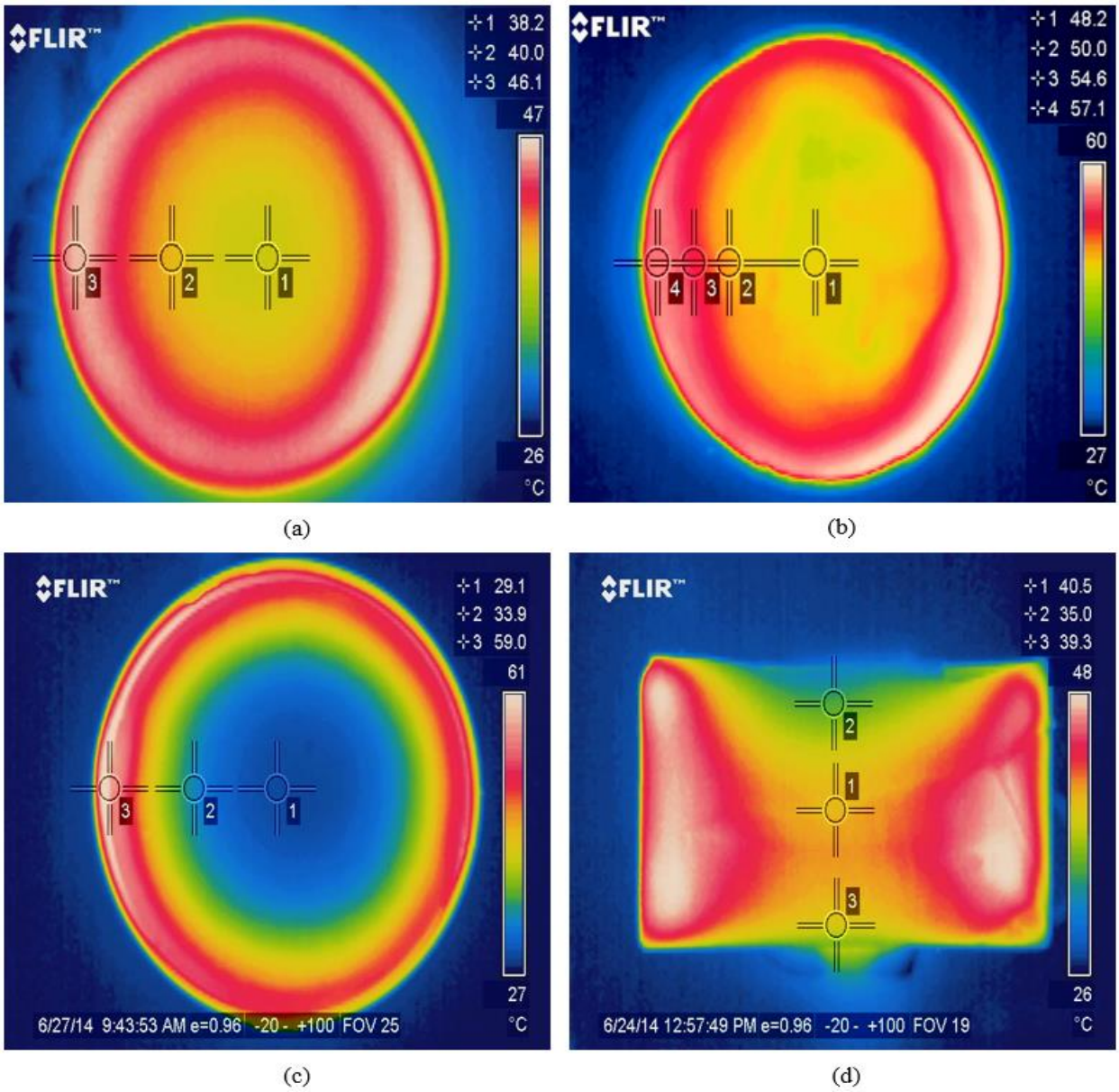

Figure 3. 8. Temperature profile of 2% agar gel (medium holder) at *h*1 (10.0 mm) (a), *h*2 (50.0 mm) (b), *h*3 (90.0 mm) (c) surfaces and vertical surface (75.0 mm from holder-wall) (d) after RF heating.

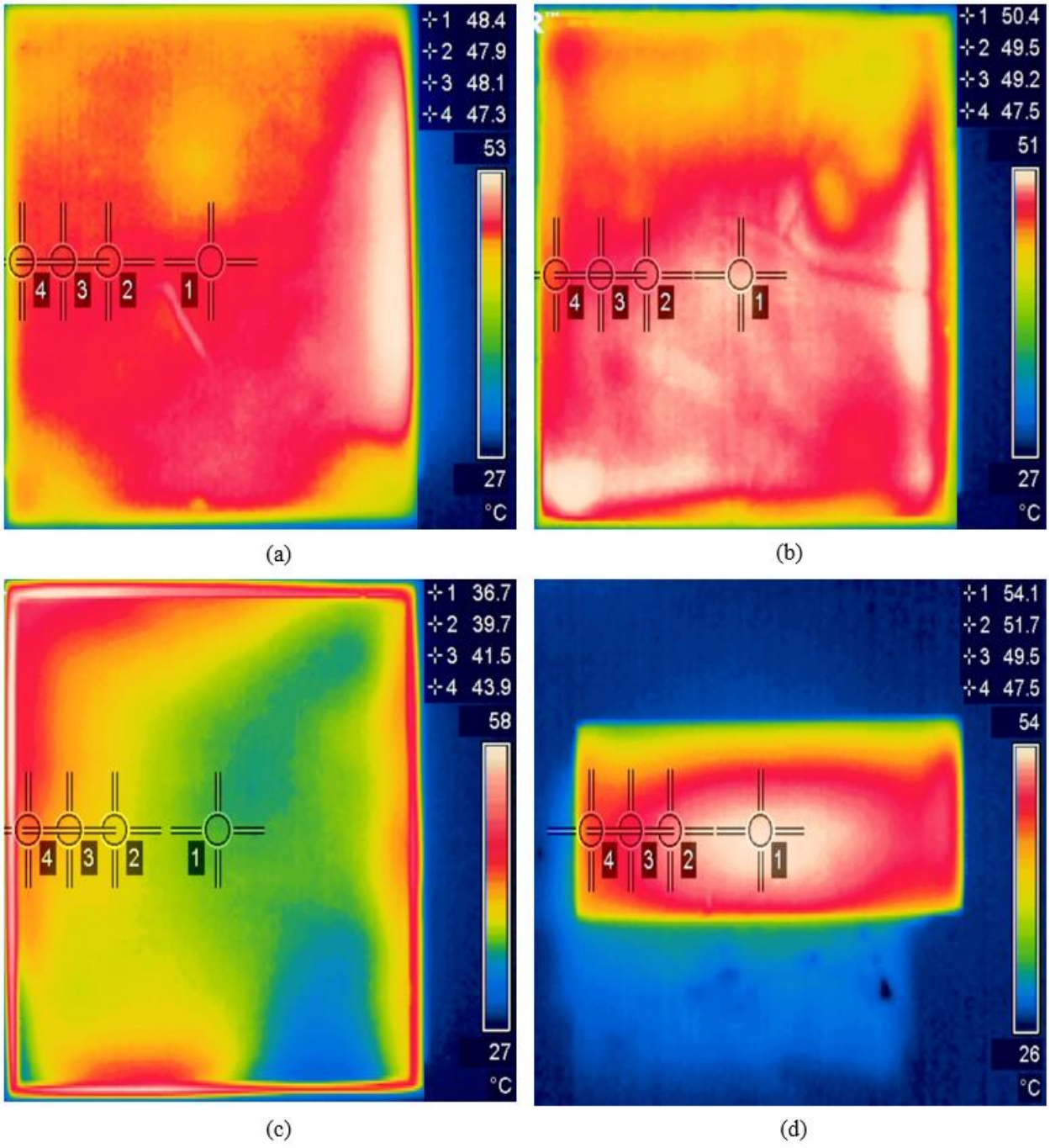

Figure 3. 9 Temperature profiles of 2% agar gel (large holder) at *h*1 (10.0 mm) (a), *h*2 (50.0 mm) (b), *h*3 (90.0 mm) (c) surfaces and vertical surface (128 mm from the holder-wall) (d) after the RF heating.

3.5.2 Temperature uniformity of canola seeds

The temperature uniformities of the canola seeds by RF heating along the horizontal and the vertical planes at different MCs and volumes are summarized in Table 3. 3. As shown in Fig. 3. 10 (a), the θ (horizontal direction) for the samples of small volume is higher than that for other volumes regardless of MCs and height. It was due to higher $\Delta\sigma$. The average uniformities along horizontal direction for small, medium, and large volumes were 0.35, 0.27, and 0.30 respectively. More uniform RF heating was observed in the samples of medium volume in spite of the edge effect. It was resulted from the lower $\Delta\sigma$. The highest and the lowest θ values were 0.40 (small volume at *h*2 of 11% MC) and 0.17 (medium volume at *h*3 of 9% MC) respectively. The θ values in this study with the canola seeds were higher than those reported by others with RF heating of almonds, chestnuts, coffee beans, lentils, soybeans, walnuts, and wheats (Gao et al., 2010; Pan et al., 2012; Hou et al., 2014). It might be attributed that our final target temperature (80℃) was higher than those (48℃, 55℃, 60℃, and 63℃) in RF heating by the others. Spatial temperature difference can be propagated more with higher final temperature resulting in lower heating uniformity. Moreover, other researchers combined forced hot air (48℃, 55℃, and 63℃), mixing (single and twice), and temperature holding (5 min) with their RF heating systems to improve heating uniformity. It is obvious that RF heating uniformity can be enhanced using properly designed hybrid RF systems (Hou et al. 2014). The average θ values along vertical direction for small, medium, and large volumes were 0.15, 0.18, and 0.17 respectively. The highest and lowest θ values were 0.33 and 0.03 for the samples of large volumes at 7% and 11% MCs ($M2^{L}$ and W^{L}). Based on θ, the bulk canola seeds could be heated more uniformly along vertical direction than horizontal direction by RF energy. Considering the correlation coefficients, temperature uniformities of the canola seeds by RF heating seemed to be more affected by seeds MCs than seeds volume for both directions. Many researchers have used hot air, stirring, tumbling, and polyetherimide (PEI) blocks combined with RF heating process to achieve lower θ (Wang et al. 2007; Wang et al. 2010; Jiao et al. 2015). However, there is still a large room for further improvement to achieve more uniform RF heating.

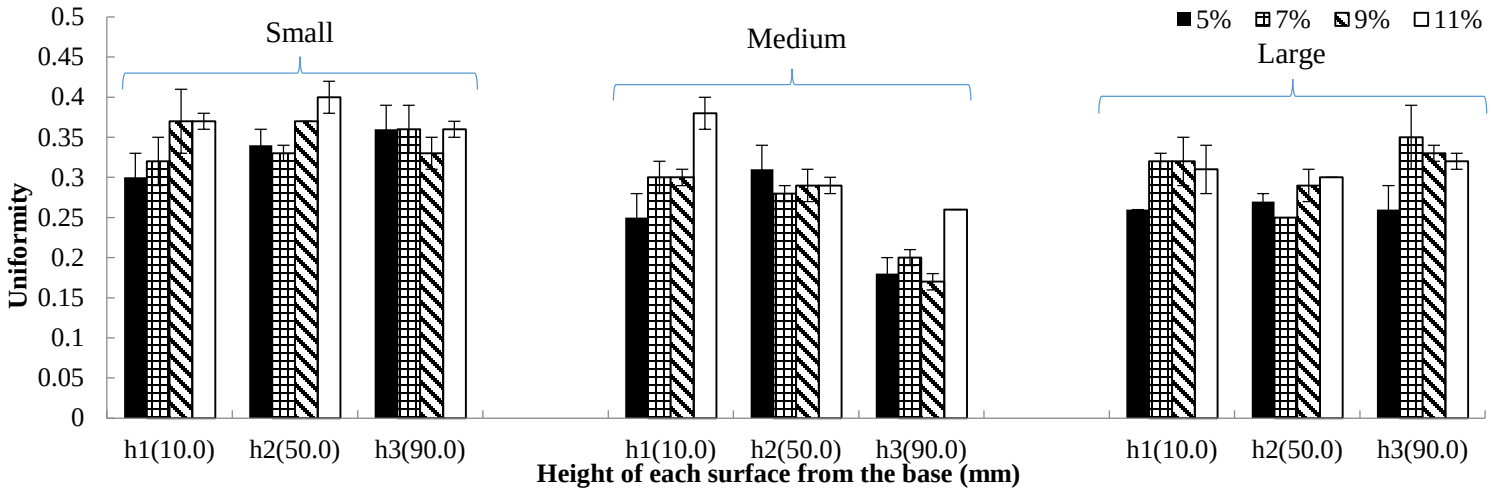

(a)

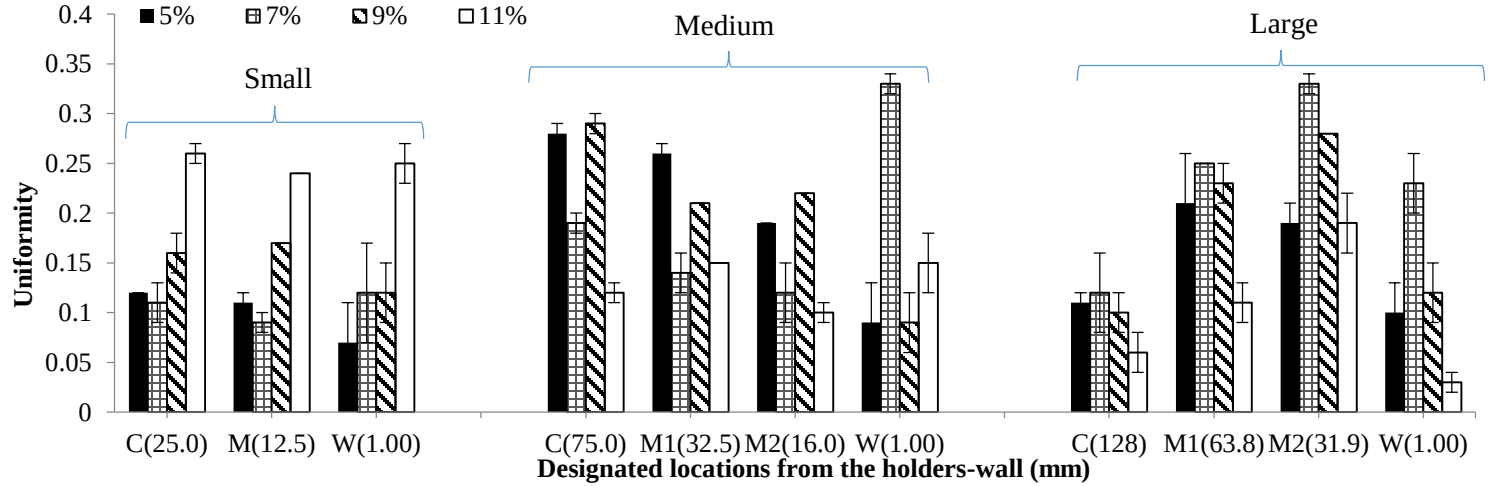

(b)

Figure 3. 10. The θ of the canola seeds by the RF heating under various MCs in different sizes of holder at horizontal (a) and vertical (b) directions when the temperature of hottest spot reached up to 80°C (n = 3).

Table 3. 3. The θ values of the canola seeds by RF heating at different MCs and volumes along the horizontal and vertical directions when the temperature of hottest spot reached up to 80°C.

Size of holder	MC (%)	Horizontal direction (mm)			Vertical direction (mm)			
		$h1$ (10.0)	$h2$ (50.0)	$h3$ (90.0)	C^{S} (25.0)	M^{S} (12.5)	W^{S} (1.00)	
Small	5	0.30 ± 0.03	0.34 ± 0.02	0.36 ± 0.03	0.12 ± 0.00	0.11 ± 0.01	0.07 ± 0.04	
	7	0.32 ± 0.03	0.33 ± 0.01	0.36 ± 0.03	0.11 ± 0.02	0.09 ± 0.01	0.12 ± 0.05	
	9	0.37 ± 0.04	0.37 ± 0.00	0.33 ± 0.02	0.16 ± 0.02	0.17 ± 0.04	0.12 ± 0.03	
	11	0.37 ± 0.01	0.40 ± 0.02	0.36 ± 0.01	0.26 ± 0.01	0.24 ± 0.00	0.25 ± 0.02	
		$h1$ (10.0)	$h2$ (50.0)	$h3$ (90.0)	C^{M} (75.0)	$M1^{M}$ (37.5)	$M2^{M}$ (18.8)	W^{M} (1.00)
Medium	5	0.25 ± 0.03	0.31 ± 0.29	0.18 ± 0.22	0.28 ± 0.01	0.26 ± 0.01	0.19 ± 0.00	0.09 ± 0.04
	7	0.30 ± 0.02	0.28 ± 0.01	0.20 ± 0.01	0.19 ± 0.01	0.14 ± 0.02	0.12 ± 0.03	0.33 ± 0.09
	9	0.30 ± 0.01	0.29 ± 0.02	0.17 ± 0.01	0.29 ± 0.01	0.21 ± 0.00	0.22 ± 0.00	0.09 ± 0.06
	11	0.38 ± 0.02	0.29 ± 0.01	0.26 ± 0.00	0.12 ± 0.01	0.15 ± 0.00	0.10 ± 0.01	0.15 ± 0.03
		$h1$ (10.0)	$h2$ (50.0)	$h3$ (90.0)	C^{L} (128)	$M1^{L}$ (64.0)	$M2^{L}$ (32.0)	W^{L} (1.00)
Large	5	0.26 ± 0.00	0.27 ± 0.01	0.26 ± 0.03	0.11 ± 0.01	0.21 ± 0.05	0.19 ± 0.02	0.10 ± 0.03
	7	0.32 ± 0.01	0.25 ± 0.00	0.35 ± 0.04	0.12 ± 0.04	0.25 ± 0.00	0.33 ± 0.09	0.23 ± 0.06
	9	0.32 ± 0.03	0.29 ± 0.02	0.33 ± 0.01	0.10 ± 0.02	0.23 ± 0.02	0.28 ± 0.00	0.12 ± 0.04
	11	0.31 ± 0.03	0.30 ± 0.00	0.32 ± 0.01	0.06 ± 0.02	0.11 ± 0.02	0.19 ± 0.05	0.03 ± 0.01

*n = 3

3.6 Conclusion

The temperature distribution in the packed-bed of canola seeds was observed at different MCs and volumes during RF heating (1.5 kW, 27.12 MHz). Edge effect was observed due to the deflected electric fields at the edge and the corners of the packed-bed. It increased with the volumes of the sample. This effect was not observed in the bulk canola seeds of large volume. It implied that the electric field is more uniform at the corners and the edges of the samples with surface areas greater than that of the electrode. The hottest spot of the bulk canola seeds was the geometric center for the small and large volumes of bulk canola, and it was shifted toward the edge for the sample of medium volume due to the edge effect. The temperature profile of the agar gel were in good agreement with those of the canola seeds. Based on the θ values, the canola seeds of medium volume was heated more uniformly in spite of the edge effect. Hybrid RF heating can be designed to improve RF heating uniformity accommodating hot air heating, sample movement and mixing,

and different angle of the electrode into typical RF heating (Wang et al. 2010; Tiwari et al. 2011a; Hou et al. 2014). The results of this work lay a foundation for designing and simulating a RF heating system/process to achieve more uniform heating of bulk canola seeds.

3.7 References

Armstrong, J. W., J. Tang, and S. Wang. 2009. Thermal death kinetics of Mediterranean, Malaysian, melon, and oriental fruit fly (Diptera: Tephritidae) eggs and third instars. *Journal of economic entomology* 102 (2): 522-532.

ASAE. 2002. ASAE S352.2, moisture measurements-unground grains and seeds. In ASAE standards. St. Joseph, MI: ASAE.

Birla, S. L., S. Wang, and J. Tang. 2008a. Computer simulation of radio frequency heating of model fruit immersed in water. *Journal of Food Engineering* 84 (2): 270-280.

Birla, S. L., S. Wang, J. Tang, G. Tiwari. 2008b. Characterization of radio frequency heating of fresh fruits influenced by dielectric properties. *Journal of Food Engineering* 89 (4): 390-398.

Canola Watch. 2015. http://www.canolawatch.org/2011/05/09/estimating-flea-beetle-damage-in-canola/. (Feb, 9, 2016).

Choi, C. T. M., and A. Konrad. 1991. Finite element modeling of the RF heating process. *Magnetics, IEEE Transactions on* 27 (5): 4227-4230.

Gao, M., Tang, J., Y. Wang, J. Powers, and S. Wang. 2010. Almond quality as influenced by radio frequency heat treatments for disinfestation. *Postharvest Biology and Technology* 58(3): 225-231.

Heather, N. W., and G. J. Hallman. 2008. Phytosanitation with ionizing radiation. *Pest management and phytosanitary trade barriers* : 132-152.

Hou, L., B. Ling, and S. Wang. 2014. Development of thermal treatment protocol for disinfesting chestnuts using radio frequency energy. *Postharvest Biology and Technology* 98: 65-71.

Jiao, Y., H. Shi, J. Tang, F. Li, and S. Wang. 2015. Improvement of radio frequency (RF) heating uniformity on low moisture foods with Polyetherimide (PEI) blocks. *Food Research International* 74: 106-114.

Johnson, J. A., K. A. Valero, S. Wang, and J. Tang. 2004. Thermal death kinetics of red flour beetle (Coleoptera: Tenebrionidae). *Journal of economic entomology* 97(6): 1868-1873.

Mitcham, E. J., R. H. Veltman, X. Feng, E. De Castro, J. A. Johnson, T. L. Simpson, W. V. Biasi, S. Wang, and J. Tang. 2004. Application of radio frequency treatments to control insects in in-shell walnuts. *Postharvest Biology and Technology* 33 (1): 93-100.

Neter, J., M. Kutner, W. Wasserman, and C. Nachtsheim. 1996. *Applied Linear Statistical Models.* 4th ed. McGraw-Hill/Irwin, New York.

Pan, L., S. Jiao, L. Gautz, K. Tu, and S. Wang. 2012. Coffee bean heating uniformity and quality as influenced by radio frequency treatments for postharvest disinfestations. *Transactions of the ASABE* 55(6): 2293-2300.

Romano, V., and F. Marra. 2008. A numerical analysis of radio frequency heating of regular shaped food stuff. *Journal of Food Engineering* 84 (3): 449–457.

Roussy, G., and J. A. Pearce. 1995. Foundations and industrial applications of microwave and radio frequency fields: physical and chemical processes. John Wiley and Sons, New York.

Shrestha, B., D. Yu, and O. D. Baik. 2013. Elimination of Cruptolestes Ferrungineus S. in Wheat by Radio Frequency Dielectric Heating at Different Moisture Contents. *Progress In Electromagnetics Research* 139: 517-538.

Tiwari, G., S. Wang, J. Tang, and S. L. Birla. 2011a. Analysis of radio frequency (RF) power distribution in dry food materials. *Journal of Food Engineering* 104 (4): 548-556.

Tiwari, G., S. Wang, J. Tang, and S. L. Birla. 2011b. Computer simulation model development and validation for radio frequency (RF) heating of dry food materials. *Journal of Food Engineering* 105 (1): 48-55.

USDA Foreign Agricultural Service. 2015. Production, Supply and Distribution Online Database, query for Commodity: "Oilseed, Rapeseed"; Data Type: "Production"; Country: "All countries"; Year: "2015", (Feb, 9, 2016).

Wang, S., J. N. Ikediala, J. Tang, and J. D. Hansen. 2002. Thermal death kinetics and heating rate effects for fifth-instar *Cydia pomonella* (L.)(Lepidoptera: Tortricidae). *Journal of Stored Products Research* 38(5): 441-453.

Wang, S., M. Monzon, J. A. Johnson, E. J. Mitcham, and J. Tang. 2007. Industrial-scale radio frequency treatments for insect control in walnuts: I: Heating uniformity and energy efficiency. *Postharvest Biology and Technology* 45 (2): 240-246.

Wang, S., and J. Tang. 2004. Radio frequency heating: a potential method for post-harvest pest control in nuts and dry products. *Journal of Zhejiang University Science* 5(10): 1169-1174.

Wang, S., G. Tiwari, S. Jiao, J. A. Johnson, and J. Tang. 2010. Developing postharvest disinfestation treatments for legumes using radio frequency energy. *Biosystems engineering* 105 (3): 341-349.

Wang, S., J. Yue, B. Chen, and J. Tang. 2008. Treatment design of radio frequency heating based on insect control and product quality. *Postharvest Biology and Technology* 49 (3): 417-423.

Wang, Y., L. Zhang, M. Gao, J. Tang, and S. Wang. 2014. Evaluating radio frequency heating uniformity using polyurethane foams. *Journal of Food Engineering* 136: 28-33.

Yang, H. W., and S. Gunasekaran. 2001. Temperature profiles in a cylindrical model food during pulsed microwave heating. *Journal of Food Science*, 66(7): 998-1004.

Yang, H. W., and S. Gunasekaran. 2004. Comparison of temperature distribution in model food cylinders based on Maxwell's equations and Lambert's law during pulsed microwave heating. *Journal of Food Engineering* 64 (4): 445-453.

Yu, D., B. Shrestha, and O. Baik. 2016. Radio frequency (RF) control of red flour beetle (*Tribolium castaneum*) in stored rapeseeds (*Brassica napus* L.). Submitted to *biosystems engineering* 151: 248-260.

CHAPTER 4

RADIO FREQUENCY (RF) CONTROL OF RED FLOUR BEETLE (*TRIBOLIUM CASTANEUM*) IN STORED CANOLA SEEDS (*BRASSICA NAPUS* L.)

Published, *Biosystems Engineering* 151 (2016) 248-260.

Contribution of this paper to overall study

A research on the RF disinfestation of the red flour beetle in the stored canola seeds has not been pursued. In this paper, the mortalities of the insects infesting the seeds were determined during RF heating as functions of MC, volume, and final temperature of the infested seeds (specific objectives 5 and 6) and physicochemical qualities and germination rate of the seeds was compared before and after RF treatment (specific objective 7). The determined adult insect mortalities were used for developing the thermal death kinetics of the adult red flour beetle in Chapter 5. All the experiments in this chapter were conducted and the journal paper manuscript was drafted by myself.

4.1 Abstract

Absolute and relative mortalities of red flour beetle (*Tribolium castaneum*) infesting the canola seeds (*Brassica napus* L.) of a small (196.3 cm^3) and a medium (1766 cm^3) volumes during RF heating (1.5 kW, 27.12 MHz) were determined at different end temperatures (30 to 80℃) and initial seed moisture contents (5%, 7%, 9%, and 11% wet basis). 100% absolute and relative mortalities of the adult insects were achieved at 80℃ for the small volume of the seeds at all MCs and at 60℃ and 9% and 11% MCs, and 70℃ and 5% and 7% MCs for the medium volume. Over 80% and 96% of the absolute and the relative mortalities of the adult insects were achieved at over 60℃ for both volumes of the seeds. 100% mortalities of larvae infesting the small and the medium volume seeds were achieved at 55℃ at all MCs. Germination, major and minor axes, roundness,

colour of the seeds and qualities of the canola seed oil were not affected significantly by RF treatment temperature at entire MCs. Therefore, a complete mortality of the red flour beetle infesting the canola seeds with acceptable thermal degradation to qualities of the seeds could be achieved at under 60℃ by the RF treatment with a proper design of RF disinfestation.

4.2 Nomenclature

a^*	colour value (green - red)	L^*	colour value (black - white)
AV	P - Anisidine	MC	moisture content (%, wet basis)
b^*	colour value (blue – yellow)	meq	milliequivalent
df	degree of freedom	*p*	p - value
d	diameter (mm)	PV	peroxide value
F	*F* - value	RF	radio frequency
h	height (mm)	RH	relative humidity (%)
$I\ O^{-1}$	input $output^{-1}$	Totox	total oxidation value
IV	iodine value		

4.3 Introduction

The USDA Foreign Agricultural Service reported 71.7 million tons of the canola seed were produced in the 2013 - 2014 season around the world (USDA Foreign Agricultural Service 2015). The canola seed is produced mainly in Canada as well as other countries such as the United States, European Union, Australia, India, and China. Around 90% of the canola seed is exported from Canada to markets around the world. It contributes $ 19.3 billion each year to the Canadian economy including more than $ 12.5 billion in wages, and 249,000 jobs (Canola Council of Canada 2014a).

Insect pest can cause average 8 to 10% losses of oilseeds production in annual crop yield, and it causes hundreds of millions of dollars damage to the economy (Canola Watch 2015). All plant-based food products (vegetables, cereals, dried or fresh fruit, etc) hold insects, in spite of protective measures taken during a harvesting stage (Ben-Lalli et al. 2011). Insect pest infestations are a

major concern in the process of all food products that make barriers to export (Gao et al. 2010). To guarantee quarantine security from pests, postharvest treatments of all food products have been demanded the norm for interstate and international markets (such as the United States, India, Korean, Spain, etc) and trade regulations (Birla et al. 2008; Jiao et al. 2011).

The red flour beetle (*Tribolium castaneum*) is one of the most common insect pests of stored grains, oilseeds, and food-processing facilities worldwide (Mills and Pedersen 1990). It can quickly build up to huge populations at warm and humid facilities (Canadian Grain Commission 2013). Serious infestations can cause oilseed to spoil and decompose. The adult is a small reddish brown beetle about 4 mm long. Each female lays 400 – 500 eggs at over 20℃. It takes 28 days to develop from egg to adult under optimal conditions (32℃ to 35℃ and over 65% RH) and the adult can fly at over 25℃ (Canadian Grain Commission 2013).

The fumigation with methyl bromide has been regarded as one of the practical methods for the disinfestation and has been widely used to disinfest various insect pests found in the oilseeds and cereal grains. However it has been banned since the Montreal Protocol due to excessive insecticide residues causing health hazards and destructive effect to the ozone layer (Birla et al. 2008; Griffin 1988; Wang and Tang 2004). Other conventional treatments such as the hot air, the ionizing radiation, and the cold storage are the possible substitutes without using the chemicals, however the slow and inefficient heating by the hot air method, live insects found by inspectors or consumers in the product treated with the ionizing radiation, and the requirement of a long treatment time with cold storage technique are the major drawbacks associated with these methods (Heather and Hallman 2008; Wang and Tang 2004).

The RF heating based on electromagnetic radiation is one of the alternative treatments for the disinfestation. A fast volumetric and selective heating are the main advantages of the RF heating, and it is one of the ways to overcome a thermal gradient driven conventional heating treatment (Tang et al. 2000). Depending upon the insect pests and the host grains, there is a potential of killing the insects with lethal temperature by using the RF heating with an acceptable thermal degradation to the grain quality. However, the RF heating usually generates non-uniform heating of the material, but it can be minimized with a proper design of an RF applicator.

The RF heating (12 kW, 27.12 MHz) with preheated water was used to disinfest codling moths (*Cydia pomonella*) in apples after harvest (Wang et al. 2006). Samples were heated up to 48℃ after preheating in 45℃ water for 30 min. They found that the most effective and practical

condition was 48℃ for 15 min considering the mortality and the quality of the test samples. However, the properties of other agricultural products such as grains, vegetables, and meats might be changed easily by this combination of heating. Lagunas et al. (2007) conducted RF heating to disinfest lesser grain borers (*Rhyzopertha dominica*) and Angoumois grain moths (*Sitotroga cerealella*) in rough rice without chemical treatment. Over 99% mortality of Angoumois grain moths (*Sitotroga cerealella*) at 55 to 60℃ for 5 min and 100% mortality of lesser grain borers (*Rhyzopertha dominica*) at 60℃ for 1 h were achieved respectively, without moisture loss or sacrificing milling quality of rice. Shrestha et al. (2013) studied elimination of rusty grain beetles (*Cryptolestes ferrungineus*) in stored wheat by RF heating (1.5 kW, 27.12 MHz). Hou et al. (2015) reported that 100% mortality of fifth – instar *C. punctiferalis* was achieved by RF heating combined with forced hot air at 55℃ for 5 min holding time. The result indicated that all life stages of insect pest can be controlled by the uniform temperature of 60℃ without significant degradation of the product quality. However, no comprehensive research has been pursued in applying the RF heating to disinfest insect pest (red flour beetle) in stored canola seeds. Other researchers have also reported the disinfestation of the insects (Indian meal moth and rice weevil) in other grains (soybean and milled rice) with RF heating (Huang et al. 2015; Zhou et al. 2015).

The objectives of this study were (1) to determine the immediate and the delayed mortalities of the red flour beetle infesting the stored canola seeds, (2) to analyze the effect of MC, the bulk volume, and the final temperature of the infested canola seeds on the mortality of the test insect, and (3) to compare the physicochemical qualities and germination rate of stored canola seeds before and after RF treatment.

4.4 Materials and methods

4.4.1 Canola seed sample

Top quality canola seeds (B. *napus* L.) at initial MC of 7% wet weight basis (w.b.) was supplied by our industrial partner Viterra Inc., Canada. The seeds were transported in polypropylene bags and were stored in a cold storage at 4^{o}C before using them.

The MC of the bulk canola seeds was determined by drying 10 g of canola seeds in a hot air oven (Despatch, Despatch Industries, MN, USA) for 24 h at 103℃ in five replicates (ASAE 2002; Brusewitz 1975).

Bulk canola seeds at different MCs, 5%, 7%, 9%, and 11% were prepared. Those MCs were determined based on that the MC of stored canola seed is normally around 10%, but for long-term storage, under 8% MC is required (Canola Council of Canada 2014b). Samples at 5% were prepared by drying a known mass of canola seeds at initial MC (7%) to the pre-calculated weight in the hot air oven set up at 40℃ followed by storing them at the cold storage (4℃) until used. Samples at 9% and 11% were prepared by spraying a pre-calculated amount of distilled water on the known mass of the seeds at initial MC contained in a glass jar. The glass jar was continuously shook and rotated while spraying the distilled water. The air-tight glass jars were left at room temperature (24℃) for 3 days with periodic shaking to achieve an equilibrium MC followed by storing them at the cold storage (4℃) until used. A digital scale with an accuracy of ± 0.01 g (Symmetry, PR4200, Cole-Parmer Instrument Co., Niles, IL, USA) was used for all weighing. The samples from the storage were left at room temperature for 2 h and the final MC of samples were measured before using them for experiments.

4.4.2 Insect cultures

The test insects were reared and handled following the procedure described by Shrestha et al. (2013). The adult red flour beetle (*Tribolium castaneum*) collected from Agriculture and Agri-Food Canada in University of Manitoba, Canada were reared in a mixture of wheat kernels (14% MC) and wheat germs in a proportion of 70 to 30% by weight. A total of 100 adult insects were moved into a glass jar (2 L) containing 1.5 kg of the rearing mixture. The jar was covered using a lid with a fabric for better ventilation. Four cultures were prepared and grown in a temperature and humidity chamber maintained at 30℃ and 70% RH. These cultures were used to prepare another batch of new cultures after 10 weeks. The insects with the rearing mixture were sieved using the Canadian standard sieve # 40 assembled with the bottom tray. Then insects were sucked through a suction pipe into a glass vial which was closed with a # 5 rubber cap with two holes, one connected to the suction pipe, and the other to the vacuum device with the rubber tube. The hole connecting to the vacuum was covered with a fine wire net on the inside of the collecting vial to stop the insects sucking away from the vial. The insects were exposed to carbon dioxide gas for 1 min and frozen at -18℃ for 1 h to anesthetize them before measuring their MC. The larvae (second and third instars) were collected with a fine bristle brush (Wild Heerbrugg M3Z, Switzerland).

4.4.3 Measurement of insect MC

About 1 g of insects in each of five aluminum dishes were dried in the oven for 16 h at 105℃. At the end of drying, the dishes containing the insects were covered with lids before removing them out from the oven, and were cooled in the desiccator before weighing. The averages of five replicates were reported.

4.4.4 RF heating system

A 1.5 kW, 27.12 MHz RF system (Strayfield Fastran, Berkshire, England) was used for heating infested canola seeds (Fig. 4. 1). The size of the parallel electrode plates was 250 mm × 250 mm. The gaps between the upper electrode and top of the sample holder were set at 1 mm and 15 mm respectively for a small (d = 50 mm, h = 100 mm) and a medium (d = 150 mm, h = 100 mm) cylindrical holders made of RF transparent polycarbonate to prevent electric arcing. A cylindrical shape was chosen based on our preliminary tests to minimize edge effects. The upper electrode was adjusted to a required height by turning the crank on the top of the enclosure. As shown in Fig. 4. 1, the infested canola seeds in the sample holder was placed in between electrodes housed in a metallic enclosure.

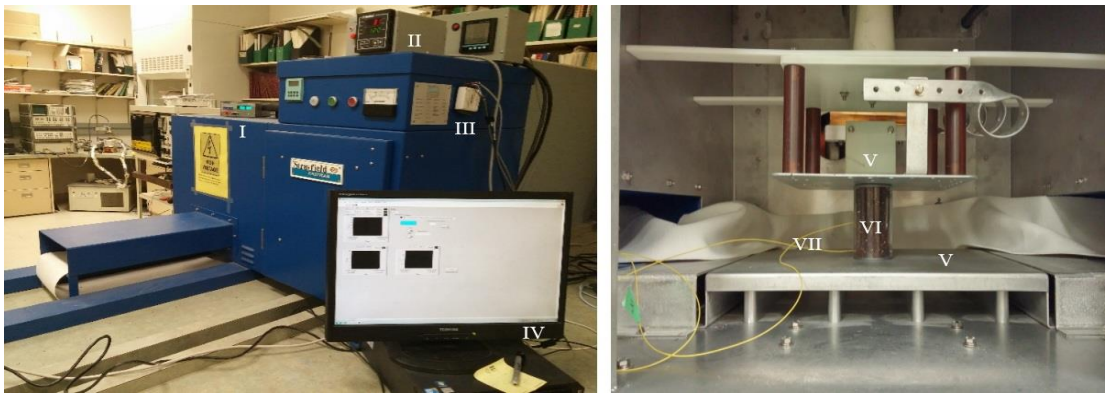

(a) (b)

Figure 4. 1. The back (a) and the inside (b) aspects of the RF heating system ; I : optic fiber thermometer device, II : temperature controller, III : I O^{-1} device, IV : data acquisition software, V : electrodes, VI : canola seed samples, VII : T1^{TM} fibre optic temperature sensors.

Temperature distributions in the canola seeds over the MC and the volume during the RF heating (1.5 kW, 27.12 MHz) were obtained from another study of ours (Yu et al. 2016). They

were used to determine the hottest spots of the small and the medium volumes of the canola seeds. The procedures to determine the temperature distributions in the canola seeds were described in detail in Yu et al. (2016). A T1^{TM} fiber optic temperature sensor (Neoptix, Québec, Canada) was inserted at the hottest spot of the seeds to monitor and record the temperatures of the seeds with a ReFlex^{TM} Signal Conditioner with an accuracy of ± 0.8℃ (Neoptix, Québec, Canada) (Fig. 4. 2). The hottest spot of the small volume of the canola seeds was found at 25 mm from the wall and 50 mm from the holder-base for all MCs. The hottest spots of the medium volume of the canola seeds were found at 75 mm from the wall and 50 mm from the holder-base for 5% and 7% MCs and at 16.25 mm from the wall and 50 mm from the holder-base for 9% and 11% MCs. The instantaneous current (A), voltage (V) and power (kW) being used by the RF system were sensed by using a multifunction power meter (Acuvim-I Accuenergy Corp., LA). All data were recorded at a predefined interval of time.

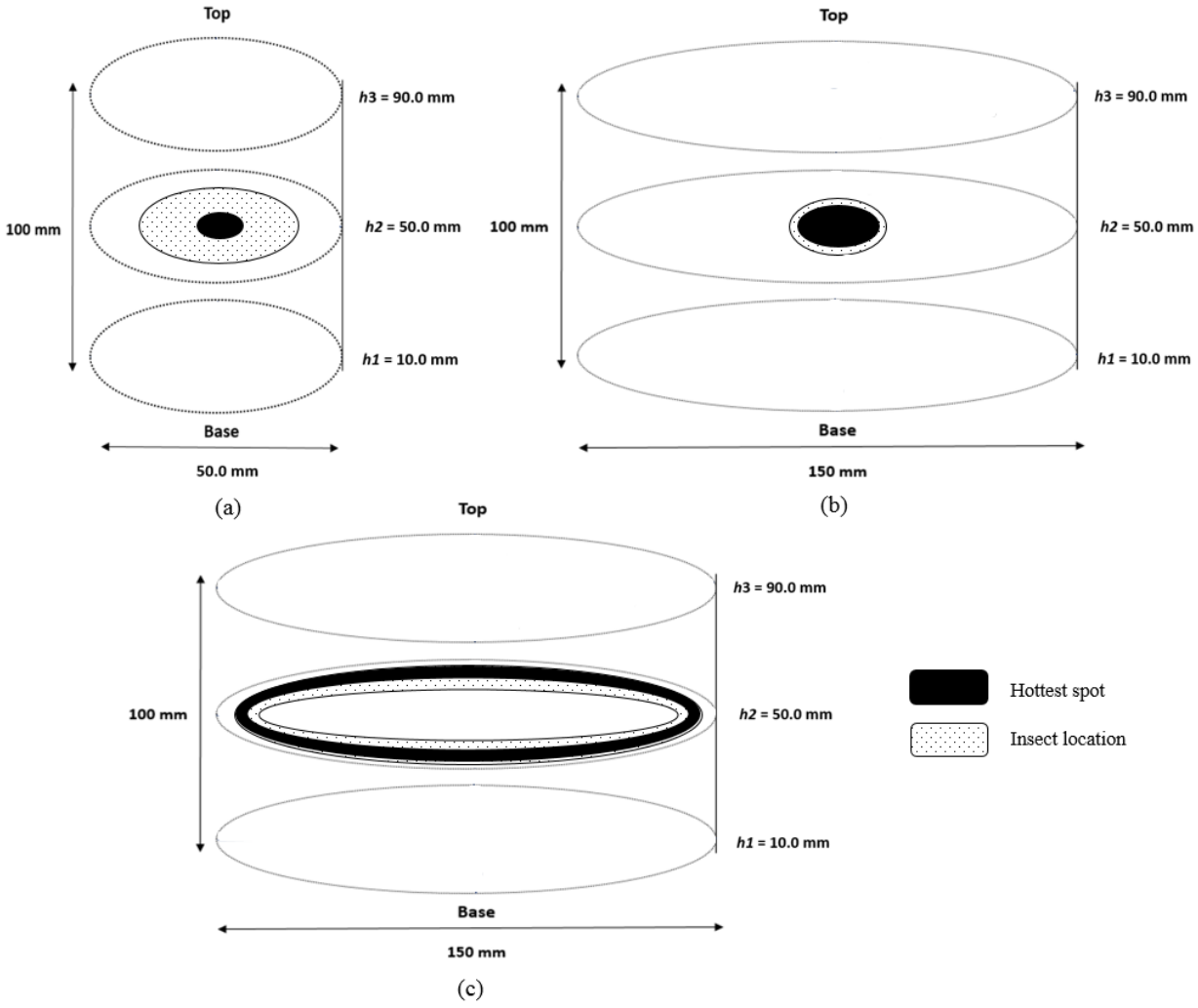

Figure 4. 2. Locations of the hottest spots and insects and the dimensions of small (a) and medium volumes (5 % and 7 % MCs (b) and 9 % and 11 % MCs (c) of the canola seeds).

4.4.5 Determination of insect mortality

To determine the thermal mortality of adult insects, 30 and 90 adult insects were transferred to the hottest spot and its vicinity (approximate diameter of 10 mm) of the small bulk volume canola seeds and the exact hottest spot of the medium volume canola seeds, respectively (Fig. 4. 2). It was technically hard to place the insects to the exact hottest spot of the small volume canola seeds as the hottest spot was too tiny compared to that of the medium volume canola seeds (ball vs doughnut shown in Fig. 4. 2). The adult insects (3 - 4 mm long) were not allowed to diffuse themselves randomly through the canola seeds (approximate seed diameter of 1.8 mm) due to insufficient space between seeds during RF heating (BPCA 2016). The hottest spot was chosen to

show how effectively insects can be killed with optimally designed RF heating systems. Furthermore, the determined mortalities of the insects at the hottest spot of the canola seeds have been used for our further research on thermal death kinetics reflecting the temperature history of the hottest spot. To determine lethal temperatures of 100% thermal mortalities for all life stages of the insects by the RF heating, the insects with the bulk canola seeds were heated up to 30℃, 40℃, 50℃, 60℃, 70℃, and 80℃ (end temperatures of the hottest spot), respectively. The initial temperature of the seeds was approximately 24℃. The RF heating unit was turned off when the temperature of the seeds at the hottest spot reached the desired temperature. The RF exposure time of the sample without holding and cooling times is listed in Table 4. 1. Lethal temperatures of other insects at all life stages were reported within these temperature ranges by other researchers (Armstrong et al., 2009; Johnson et al., 2004; Shrestha et al., 2013). The live insects were counted immediately, 1 day, and every week after the RF heating up to 5 weeks (quarantine period) to calculate the absolute and the relative mortalities. All the heated insects and 100 g of the heated canola seeds were mixed with wheat germs in a proportion of 8 : 2 by weight, and then poured into a glass jar (250 g) covered by a fabric screen lid for ventilation. The glass jars was stored in a growth chamber (30℃ and 70% RH) for the quarantine period (5 weeks) for absolute mortalities. Abbott's formula was used to calculate the relative mortalities (Abbott 1925).

$$\text{The relative mortality } (\%) = \left(1 - \frac{\text{percent living in treated sample}}{\text{percent living in control}}\right) \times 100 \qquad (4.1)$$

The averages of the triplicate were used for the absolute and the relative mortalities.

Table 4. 1. The RF exposure time (s) of the canola seeds of the small and the medium volumes without holding and cooling time at the indicated MCs and temperatures.

MC (%, w. b.)	Volume	Temperature (℃)					
		30	40	50	60	70	80
5	Small	56	215	403	597	820	1080
	Medium	196	345	545	677	910	1200
7	Small	35	178	316	478	540	720
	Medium	135	278	425	539	671	870
9	Small	30	119	200	275	337	390
	Medium	125	190	310	333	381	510
11	Small	25	60	86	106	125	140
	Medium	118	160	185	218	248	270

To protect larvae from external physical damage during the RF heating and to ease locating them in the bulk canola seeds, an RF transparent polyethylene capsule was used to determine the mortality of the larvae. A tiny capsule (d = 30 mm, h = 30 mm) including 30 larvae and a few canola seeds was placed at the hottest spots of the small and the medium bulk volumes of the canola seeds. The capsule was almost fully filled with larvae and canola seeds to minimize experimental error. The capsule might have affected the RF heating of the larvae. We speculated, however, that the effect might be minimal as the capsule was tiny and made of RF transparent polycarbonate to minimize the effect of the capsule on the electric field. Other researchers also have used similar RF transparent materials (polypropylene and polycarbonate) as a sample holder (Hou et al. 2015; Shrestha et al. 2013; Yin et al. 2006). The fiber optic temperature sensor was inserted inside the capsule to measure the inner temperature of the capsule at 100% immediate mortality of larvae, and the average of triplicate was reported as the lethal temperature of the larvae.

Other life stages (egg and pupae) of the red flour beetle have relatively less heat tolerance compared to their adult and larvae stages (Johnson et al. 2004), and therefore it was assumed that the eggs and pupae would be destroyed at the temperature of 100% mortality of the adult insect and the larvae. To determine 100% mortality of eggs and pupae, 8 weeks old culture with a great number of the eggs and the pupae (it can be confirmed under microscope) was separated into 5 sub-samples after gently mixing it. It is technically hard to collect the eggs and the pupae of the red flour beetle from the rearing material as their sizes are too tiny and they reside inside the wheat

kernels (BioNet-EAFRINET 2011). The sub-samples were heated to the temperature that would achieve 100% mortalities for the adult and larvae, then it was stored in the growth chamber for 5 weeks to observe an emergence of new adult insects.

4.4.6 Seed quality analysis

The bulk canola seeds at 5%, 7%, 9%, and 11% MCs were heated to desired temperatures (60℃, 70℃, and 80℃) at the hottest spot of the seeds. These temperatures determined from our preliminary tests had destroyed 100 % of all life stages of the test insects. The seeds after RF heating were gently mixed before the following quality tests.

4.4.6.1 Germination test

A total of 50 RF treated canola seeds were placed on two moistened Whatman # 3 filter papers with 5 mL of distilled water in a 90 mm-*d* plastic petri dish. The seeds sample was kept in a Ziploc® bag to prevent moisture loss. It was then subjected to germination in a temperature and humidity chamber at 25℃ and 75% RH. The seeds sample was classified into germinated and dead seeds by naked eyes each day according to whether sprout came out or not. Then, the germinated seeds were counted everyday up to 7 days. An average of five replicates was used.

4.4.6.2 Shape, colour, and mass

A total of 100 test seeds were placed manually on a petri dish. The sample was then placed on the stage of the stereomicroscope with a virtual ruler (Leica Wild M3Z, Wild, Heerbrugg, Switzerland) to measure the major and minor axes of the individual seeds. The roundness of the canola seed was calculated as :

$$\text{Roundness} = \frac{\text{Minor axis}}{\text{Major axis}} \tag{4.2}$$

The surface colour of the canola seeds was measured using a HunterLab ColorFlex^{TM} 45^{o}0$^{o\text{-}1}$ Spectrophotometer (HunterLab ColorFlex, Hunter Associated Inc., Reston, VA, USA). The seeds were poured on the petri dish and then placed on the stage of the colorimeter. The colour of the seeds was expressed with Hunter L^* (black-white), a^* (green-red), and b^* (blue-yellow) parameters. The average and the standard deviation were calculated from five replications.

The mass of 100 canola seeds was determined by weighing with Ohaus analytical scale with an accuracy of ± 0.0001 g. The average and the standard deviation were calculated from three replications.

4.4.6.3 Oil quality

150 g of the canola seeds were ground into fine particles using a coffee grinder (Braun Coffee Grinder, KMS2 model, Frankfurt, Germany). The flour was then transferred into a 500 ml glass beaker, and 200 ml of n-hexane was added into it. The solution was left for overnight to defat the flour. The solution was filtered through a Whatman # 1 filter paper. The filtrate was defatted again, and more solution was collected following the same procedure. The filtered solution was distilled off in a rotary evaporator (Rotavapor R-210, Buchi Corp., New Castle, Del., USA) under vacuum at 60℃ for extraction of canola seed oil, which was stored in the refrigeration (4℃) until used.

To evaluate the oxidative stability of the extracted oil, the peroxide value (PV) and the *p*-Anisidine value (AV) were measured following the American Oil Chemists' Society (AOCS) Official Methods Cd 8-53 and Cd 18-90 (AOCS 1993) respectively. Then the overall oxidative stability was reported as the Totox value ;

$$\text{Totox} = 2\text{PV} + \text{AV} \tag{4.3}$$

Low Totox values indicate better quality of oil.

The iodine value (IV) was also measured following the AOCS, Cd 1-25 (AOCS 1993) to determine the amount of unsaturated fatty acid in the extracted oil.

4.4.7 Statistical analysis

The stepwise regression analysis in SPSS 20.0 (SPSS Inc., Chicago, IL, USA) was used to determine the statistical significances of the MC and the temperatures of the bulk canola seeds on the mortality of the red flour beetle, and the physicochemical qualities of the seeds.

4.5 Results and discussion

4.5.1 Mortality

Mortalities of the adult red flour beetles infesting the small and the medium volumes of the canola seeds at various seed MCs (5%, 7%, 9%, and 11%) without RF treatment are shown in

Table 4. 2. After 35 days of storage the number of adult insects naturally reduced by an average of 5.9% and 3.2% for the small and the medium volumes of the canola seeds. Table 4. 3 shows the absolute mortalities of the adult insects (48.12 ± 0.78% MC) infesting the small volume of canola seeds at various seed MCs and temperatures (30℃ to 80℃) after RF treatments. All adult insects were killed at 80℃ at the tested MCs. The absolute mortality rate increased with MC and temperature. Over 81% and 76% absolute mortalities of the adult insects were achieved at over 60℃ and 50℃ for 5%, 7%, and 9% MCs and 11% MC. Table 4. 4 shows the relative mortalities of the adult test insects infesting the small volume canola seeds at various seed MCs and the temperatures after the RF treatments. The relative mortality trends were similar to those observed with the absolute mortality. The complete relative mortality of the insects was achieved at 80℃ at any MCs. Over 80% and 75% relative mortalities of the insects were achieved at over 60℃ and 50℃ for 5%, 7%, and 9% MCs and 11% MC. Other researchers have found similar thermal mortalities of other insects infesting various crops. Woodworms were killed by microwave heating (2450 MHz) at 52 to 53℃ in 3 min (Andreuccetti et al. 1994). The best parameters of RF heat treatment (12 kW, 27.12 MHz) for disinfesting the codling moth (*Cydia pomonella*) in harvested apples considering insect control and sample quality, simultaneously was 48℃ for 15 min (Wang et al. 2006). Johnson et al. (2004) reported that 95% mortalities of the red flour beetle (*Tribolium castaneum*) were achieved at 50℃ and 52℃ for 8 min and 1.3 min respectively, by a heating block system (15℃ min^{-1}) which was selected to simulate RF heating. The mortalities of the red flour beetle reported by Johnson et al. (2004) were higher than ours. They heated the insects by a heating block system (non-dielectric heating) with the holding time at the end temperature. In this study, however, the temperature of the infested canola seeds was continuously increased up to the assigned end temperatures by RF heating without establishing the holding and cooling times. The relative mortalities of the adult test insects were lower than those of the absolute mortalities due to the decreasing number of live adult insects in the control during the quarantine period. A decreasing - increasing pattern of the absolute and the relative mortalities at early stages of the quarantine period (immediate to 1 or 2 weeks) were observed at certain MC and temperature. This was due to the partially damaged insects, which were revived or dead in this period. Dowdy (1999) reported that the adult survival of the red flour beetle exposed to 15 to 30 min (50℃) was significantly enhanced when the RF treated insects were quarantined in the rearing material.

Table 4. 2. The mortalities (%) of the adult red flour beetles infesting the small and the medium volumes of the canola seeds at the indicated MCs without RF treatment.

Volume	MC (%, w. b.)	Quarantine Period (days)						
		0	1	7	14	21	28	35
Small	5	0.0	0.0	3.3	5.6	5.6	5.6	5.6
	7	0.0	0.0	2.2	4.4	5.6	5.6	5.6
	9	0.0	0.0	2.2	5.6	5.6	5.6	6.7
	11	0.0	0.0	3.3	3.3	5.6	5.6	5.6
medium	5	0.0	0.0	2.2	2.2	2.6	3.0	3.0
	7	0.0	0.0	1.1	2.2	2.6	3.0	3.0
	9	0.0	0.0	1.5	2.2	2.6	3.0	3.3
	11	0.0	0.0	1.5	2.2	2.2	3.0	3.3

Table 4. 3. The absolute mortalities (%) of the adult red flour beetles infesting the small volume of canola seeds at the indicated MCs and temperatures after RF treatment.

Temperature (℃)	MC (%, w. b.)													
	5							7						
	Quarantine Period (days)													
	0	1	7	14	21	28	35	0	1	7	14	21	28	35
30	0.00	0.00	3.33	5.56	5.56	6.67	6.67	0.00	0.00	2.22	4.44	5.56	5.56	5.56
40	1.11	1.11	4.44	6.67	6.67	6.67	6.67	1.11	1.11	3.33	5.56	6.67	6.67	6.67
50	10.0	8.89	8.89	8.89	10.0	11.1	11.1	11.1	13.3	13.3	13.3	13.3	14.4	14.4
60	84.4	83.3	81.1	81.1	81.1	81.1	81.1	85.6	83.3	84.4	84.4	84.4	84.4	84.4
70	92.2	90.0	91.1	91.1	91.1	91.1	91.1	95.6	92.2	92.2	92.2	92.2	92.2	92.2
80	100	100	100	100	100	100	100	100	100	100	100	100	100	100
Temperature (℃)	MC (%, w. b.)													
	9							11						
	Quarantine Period (days)													
	0	1	7	14	21	28	35	0	1	7	14	21	28	35
30	0.00	0.00	3.33	5.56	5.56	5.56	6.67	0.00	0.00	3.33	3.33	5.56	5.56	5.56
40	2.22	3.33	4.44	6.67	7.78	7.78	7.78	4.44	4.44	5.56	7.78	8.89	10.0	10.0
50	36.7	32.2	30.0	32.2	34.4	35.6	35.6	84.4	81.1	77.8	76.7	78.9	78.9	78.9
60	87.8	86.7	85.6	85.6	85.6	85.6	85.6	95.6	96.7	94.4	94.4	94.4	94.4	94.4
70	98.9	98.9	97.8	96.7	96.7	96.7	96.7	95.6	97.8	97.8	97.8	98.9	98.9	98.9
80	100	100	100	100	100	100	100	100	100	100	100	100	100	100

Table 4. 4. The relative mortalities (%) of the adult red flour beetles infesting the small volume of canola seeds at the indicated MCs and temperatures after RF treatment.

Temperature (℃)	MC (%, w. b.)													
	5							7						
	Quarantine Period (days)													
	0	1	7	14	21	28	35	0	1	7	14	21	28	35
30	0.00	0.00	0.00	0.00	0.00	1.18	1.18	0.00	0.00	0.00	0.00	0.00	0.00	0.00
40	1.11	1.11	1.15	1.18	1.18	1.18	1.18	1.11	1.11	1.14	1.16	1.18	1.18	1.18
50	10.0	8.89	5.75	3.53	4.71	5.88	5.88	11.1	13.3	11.4	9.30	8.24	9.41	9.41
60	84.4	83.3	80.5	80.0	80.0	80.0	80.0	85.6	83.3	84.1	83.7	83.5	83.5	83.5
70	92.2	90.0	90.8	90.6	90.6	90.6	90.6	95.6	92.2	92.1	91.9	91.8	91.8	91.8
80	100	100	100	100	100	100	100	100	100	100	100	100	100	100
Temperature (℃)	MC (%, w. b.)													
	9							11						
	Quarantine Period (days)													
	0	1	7	14	21	28	35	0	1	7	14	21	28	35
30	0.00	0.00	1.14	0.00	0.00	0.00	0.00	0.00	0.00	0.00	0.00	0.00	0.00	0.00
40	2.22	3.33	2.27	1.18	2.35	2.35	1.19	4.44	4.44	2.30	4.60	3.53	4.71	4.71
50	36.7	32.2	28.4	28.2	30.6	31.8	31.0	84.4	81.1	77.0	75.9	77.7	77.7	77.7
60	87.8	86.7	85.2	84.7	84.7	84.7	84.5	95.6	96.7	94.3	94.3	94.1	94.1	94.1
70	98.9	98.9	97.7	96.5	96.5	96.5	96.4	95.6	97.8	97.7	97.7	98.8	98.8	98.8
80	100	100	100	100	100	100	100	100	100	100	100	100	100	100

The mortality of the insect could be caused by a sudden heat shock when the insect was exposed to a high temperature in which the insects would not get sufficient time for thermal adaptation (Mahroof et al. 2003). In general, thermal mortality results from thermal degradation of proteins, DNA, RNA, lipids, and carbohydrates of the insects (Hallman and Denlinger 1998). Susceptibility of the insects to thermal degradation (mortality) is different at different developmental stages of the insects (Bursell 1964; Davison 1969).

Tables 4.5 and 4.6 describe the absolute and the relative mortalities of the adult insects infesting the medium volume of the canola seeds at various seed MCs and temperatures after the RF treatment. The increasing trend of mortality was similar to that of the small volume of the canola seeds. The 100% absolute and relative mortalities of the adult insects were achieved at over 60℃ for 9% and 11% MCs and over 70℃ for 5% and 7% MCs. Over 95% absolute and relative mortalities of the adult insects were achieved at over 60℃ of the canola seeds at any MCs. The mortalities of the adult insects infesting the medium volume of the canola seeds were higher than those of the small volume during quarantine period due to the transferring location of the insects in the canola seeds. The insects were transferred to the exact hottest region in the medium volume canola seeds, but in case of the small volume of the canola seeds, the insects were transferred on the vicinity region of hottest spot due to tiny space of hottest spot before the RF heating. Therefore, the mortality of the adult insects infesting the small volume of the canola seeds would be increased as much as that of medium volume of the canola seeds when the insects transferred on the area of exact hottest spot. Therefore, there is potential to achieve complete mortality of the adult red flour beetle infesting the canola seeds at 60℃ by RF heating regardless of the volume of the seeds sample, with proper design. Proper design utilizing a specialized applicator with a sample mixing system (like a RF transparent helix), different shape of top electrode, etc, could achieve more uniform temperature distribution and shorter RF heating time. Wang et al. (2007a) reported mixing system (a riffle-type sample splitter) improved RF heating uniformity in walnuts. Gao et al. (2010) also found that RF heating uniformity in almonds improved by applied conveyor (moving back and forth) and mixing by hands. Different bending positions and angles of top electrode were tested to improve RF power uniformity by Tiwari et al. (2011). They found that optimum RF power uniformity was obtained when the top electrode bending position and top electrode bending angle were 200 mm from the symmetrical edge and 20 ° respectively. The RF exposure time could affect the mortality of the adult red flour beetle infesting the canola seeds. Table 4. 1 contains the RF

exposure times of the canola seeds without holding and cooling times at different MCs and volumes. The RF heating times for the seed samples at 11% MC of the canola seeds were approximately 7 times shorter than that for the seed samples at 5% MC in the case of small volume seed samples; it was 4.5 times for the medium volume of the seed samples. A synthesis of heat shock proteins within the cells of the insect at high temperature enhances its heat tolerance, thus preventing them from heat damage. More heat shock proteins could be generated from longer heat exposure times (Yin et al. 2006). However, susceptibility of the mortality of the red flour beetle to heat could be affected by differences in adapting to slowly increasing temperatures during heating depending upon its life stage (Mahroof et al. 2003). The adult red flour beetles infesting the seed samples at 11% MC had less time to generate heat shock proteins compared to that at 5% MC. Therefore, a short RF heating time could be one of the main reasons for higher mortality of the adult red flour beetle infesting the canola seeds at 11% MC.

Table 4. 5. The absolute mortalities (%) of the adult red flour beetles infesting the medium volume of canola seeds at the indicated MCs and temperatures after RF treatment.

Temperature (℃)	MC (%, w. b.)													
	5							7						
	Quarantine Period (days)													
	0	1	7	14	21	28	35	0	1	7	14	21	28	35
30	0.00	0.00	2.59	2.59	2.59	2.96	3.33	0.00	0.00	1.11	2.59	2.59	2.96	3.33
40	0.00	2.59	4.44	4.44	8.89	8.89	8.89	0.74	4.07	6.30	6.30	9.63	10.4	10.4
50	30.4	34.4	34.4	33.7	34.1	36.3	37.0	30.7	34.4	35.6	36.7	36.7	37.8	38.5
60	100	95.6	95.9	99.3	99.3	99.3	99.3	99.6	99.6	99.6	99.6	99.6	99.6	99.6
70	100	100	100	100	100	100	100	100	100	100	100	100	100	100
80	100	100	100	100	100	100	100	100	100	100	100	100	100	100
Temperature (℃)	MC (%, w. b.)													
	9							11						
	Quarantine Period (days)													
	0	1	7	14	21	28	35	0	1	7	14	21	28	35
30	0.00	0.00	1.48	2.59	2.59	2.96	3.33	0.00	0.37	1.48	2.59	2.96	2.96	3.33
40	7.78	6.67	8.52	10.7	10.7	11.1	11.5	9.26	8.52	11.1	13.7	13.7	16.7	17.0
50	38.9	38.2	40.7	43.7	43.7	45.9	47.8	42.2	41.5	45.2	46.3	46.3	48.9	51.1
60	99.6	100	100	100	100	100	100	100	100	100	100	100	100	100
70	100	100	100	100	100	100	100	100	100	100	100	100	100	100
80	100	100	100	100	100	100	100	100	100	100	100	100	100	100

Table 4. 6. The relative mortalities (%) of the adult red flour beetles infesting the medium volume of canola seeds at the indicated MCs and temperatures after RF treatment.

Temperature (℃)	MC (%, w. b.)													
	5							7						
	Quarantine Period (days)													
	0	1	7	14	21	28	35	0	1	7	14	21	28	35
30	0.00	0.00	0.38	0.38	0.00	0.00	0.38	0.00	0.00	0.00	0.38	0.00	0.00	0.38
40	0.00	2.59	2.27	2.27	6.46	6.11	6.11	0.74	4.07	5.24	4.17	7.22	7.63	7.63
50	30.4	34.4	33.0	32.2	32.3	34.4	35.1	30.7	34.4	34.8	35.2	35.0	35.9	36.6
60	100	95.6	95.8	99.2	99.2	99.2	99.2	99.6	99.6	99.6	99.6	99.6	99.6	99.6
70	100	100	100	100	100	100	100	100	100	100	100	100	100	100
80	100	100	100	100	100	100	100	100	100	100	100	100	100	100
Temperature (℃)	MC (%, w. b.)													
	9							11						
	Quarantine Period (days)													
	0	1	7	14	21	28	35	0	1	7	14	21	28	35
30	0.00	0.00	0.00	0.38	0.00	0.00	0.00	0.00	0.37	0.00	0.38	0.76	0.00	0.00
40	7.78	6.67	7.14	8.71	8.37	8.40	8.43	9.26	8.52	9.77	11.7	11.7	14.1	14.2
50	38.9	38.2	39.9	42.4	42.2	44.3	46.0	42.2	41.5	44.4	45.1	45.1	47.3	49.4
60	99.6	100	100	100	100	100	100	100	100	100	100	100	100	100
70	100	100	100	100	100	100	100	100	100	100	100	100	100	100
80	100	100	100	100	100	100	100	100	100	100	100	100	100	100

The MC of the canola seed can significantly affect the mortality of the adult red flour beetles infesting the canola seeds. The adult red flour beetles fully surrounded by the canola seeds were exposed to the evaporated hot steam from the wet canola seeds by RF energy. The mortality of the adult insects in the seed samples at 11% MC was higher than that in 5% MC seed samples at the same end temperature because of more evaporated steam from the seed samples of 11% MC. The heating temperature had the most significant effect ($P \approx 0$) on the absolute and the relative mortalities of the canola seeds of the small and the medium volumes.

The 100% mortalities of the larvae infesting the small and the medium volumes of the canola seeds were achieved at 55℃ regardless of MC. No emergence of new adult insects from the 5 sub-samples of the 8 week old culture with a great number of the eggs and the pupae was observed during the quarantine period (5 weeks), thus confirming 100% delayed mortalities.

4.5.2 Quality of canola seeds

The RF exposure times of the canola seeds for quality tests when the temperature of the seeds reached to the desired temperature (60℃, 70℃, and 80℃) at the hottest spot of the seeds were the same as those of the small volume shown in Table 4. 1.

4.5.2.1 Germination

Fig. 4. 3 illustrates the effect of RF heating on germination of the test canola seeds at different MCs (5%, 7%, 9%, and 11%) and temperatures (60℃, 70℃, and 80℃). A germination rate of the RF treated canola seeds decreased with increasing initial seed MC and RF heating temperature. Sutherland and Ghaly (1982) reported similar patterns on germination of oilseeds (canola seed, Sunflower, etc). Comparing to the controls, the germination rate decreased by 10.0%, 16.4%, 28.8%, and 36.8% for 5%, 7%, 9%, and 11% MCs, respectively when the seeds were heated to 80℃. Physicochemical qualities of the canola seed affecting germination might have been changed by the RF heating once the temperature of the seeds exceed including some degree of heat damage at over certain temperature (Shrestha et al. 2013). The reduction rate of the germination at 60℃ were 0.80%, 3.60%, 4.40%, and 10.4% for 5%, 7%, 9%, and 11% MCs. No substantial loss of germination occurred at temperature up to 60℃ for each of seed MCs. The germination ability of the canola seeds at 80℃ was significantly reduced by RF energy compared to that at 60℃ regardless of the seed MC. The germination rates at 80℃ dropped by 9.2%, 12.8%, 24.4% and

26.4% more for 5%, 7%, 9%, and 11% MCs compared to those at 60℃. The RF heating resulted in less heat damage to the germination ability of the canola seed compared to other heat treatments. Canola seeds and sunflower seeds did not germinate at all when they were heated at 60℃ for 4 h in a fluidized bed (Sutherland and Ghaly 1982). On the contrast, in our research, the canola seed germinated over around 60% even it heated at 80℃ by the RF energy. The effects of the MC and the temperature on the germination rate were significant for the canola seeds treated to 60℃ ($p \approx 0$, $F = 20.2$, $df = 2$), 70℃ ($p \approx 0$, $F = 30.1$, $df = 2$), and 80℃ ($p \approx 0$, $F = 157$, $df = 2$) for the MC and 5% ($p \approx 0$, $F = 10.6$, $df = 2$), 7% ($p \approx 0$, $F = 14.5$, $df = 2$), 9% ($p \approx 0$, $F = 32.0$, $df = 2$), and 11% ($p = 0$, $F = 101$, $df = 2$) for the temperature.

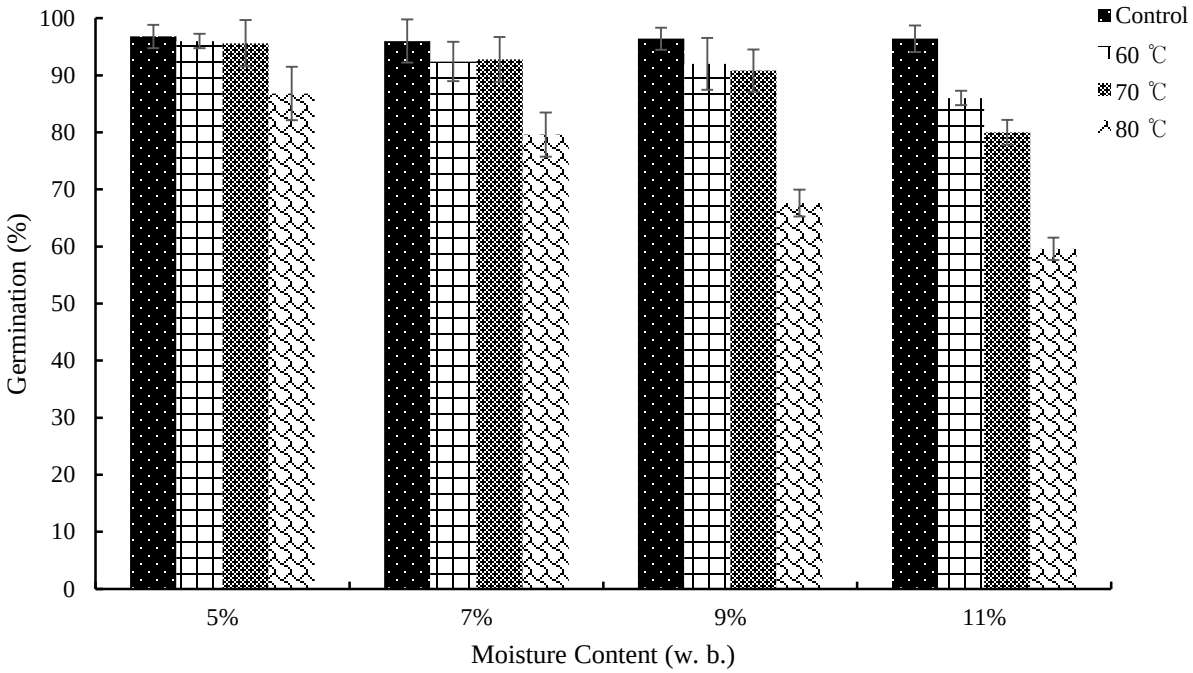

Figure 4. 3. The effect of the RF heating on germination of canola seeds at various MCs and temperatures.

4.5.2.2 Shape, colour, and mass

Figure 4. 4 shows the changes in the canola seeds mass after RF heating, and Table 4. 7 compares the major and the minor axes, roundness and the colour of the canola seed at different MCs and temperatures before and after RF treatment. The minimum and maximum differences of the mass of 100 canola seeds between the control and the treated seeds were 9.81% and 23.6%

over the ranges of temperature and MC. The average mass of the 100 seeds was 0.373 g over the ranges of temperature and MC. The RF heating had effect on the mass of 100 canola seeds at entire MCs. More mass loss was observed with higher initial seed MC and heating temperature. It was attributed to increasing moisture diffusion rate at higher heating temperature resulting in higher drying rate (Gazor and Mohsenimanesh 2010). Similar results were found by Gazor and Mohsenimanesh (2010) for canola seeds. The minimum and maximum differences of the major and minor axes, and roundness of a canola seed between the control and the treated seeds were 1.37% and 5.36% for major axis, 0.62% and 9.38% for minor axis, and 0.16% and 4.50% for roundness over the ranges of temperature and MC. The average of the major and the minor axes, and the roundness of the canola seed were 1.78 mm, 1.51 mm, and 0.86 over the ranges of temperature and MC in this study. The major and minor axes of the canola seeds increased with increasing temperature. It might be caused by expansion of constituents (carbohydrate, protein, etc) of the seeds and trapped air inside of the seeds by RF heating. The minimum and maximum differences of the L^*, a^*, and b^* of the canola seeds between the control and the treated seeds were 0.006% and 0.428% for L^*, 0.004% and 0.652% for a^*, and 0.010% and 0.794% for b^* over the ranges of temperature and MC. The average of the L^*, a^*, and b^* were 22.6, 4.72, and 2.82 over the ranges of temperature and MC. The major and the minor axes, the roundness, and the colour were not affected significantly by the RF heating at entire MCs.

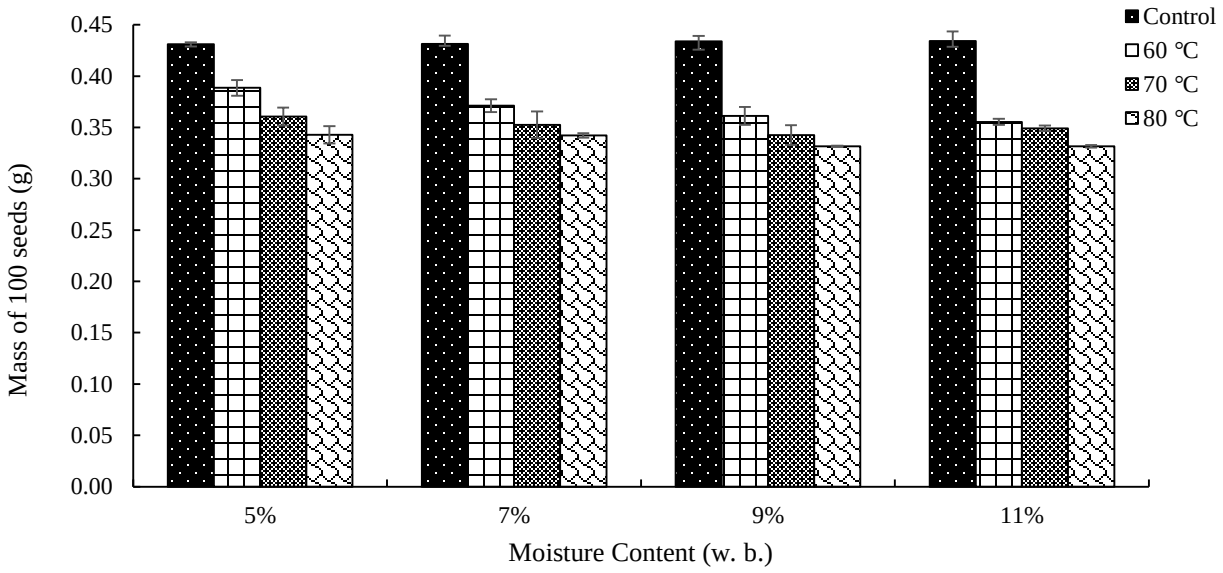

Figure 4. 4. The effect of the RF heating on mass of the 100 canola seeds at various MCs and temperatures.

Table 4. 7. The effect of the RF heating on the dimensions and the colour values of the canola seeds at various MCs as a function of temperature.

MC (%, w. b.)	Dimension		Temperature (°C)			
			Control	60	70	80
5	Major Axis (mm)		1.80 ± 0.01	1.82 ± 0.02	1.84 ± 0.00	1.71 ± 0.01
	Minor Axis (mm)		1.52 ± 0.02	1.55 ± 0.00	1.57 ± 0.01	1.42 ± 0.01
	Roundness		0.85 ± 0.01	0.88 ± 0.02	0.85 ± 0.00	0.85 ± 0.00
	Colour values	L^*	21.7 ± 0.30	21.6 ± 0.27	22.2 ± 0.20	22.0 ± 0.26
		a^*	3.99 ± 0.10	3.82 ± 0.16	3.74 ± 0.22	3.34 ± 0.18
		b^*	2.54 ± 0.19	2.58 ± 0.30	2.61 ± 0.21	2.53 ± 0.24
7	Major Axis (mm)		1.75 ± 0.01	1.70 ± 0.01	1.81 ± 0.02	1.80 ± 0.01
	Minor Axis (mm)		1.46 ± 0.03	1.44 ± 0.01	1.50 ± 0.00	1.50 ± 0.01
	Roundness		0.86 ± 0.01	0.85 ± 0.00	0.82 ± 0.01	0.85 ± 0.02
	Colour values	L^*	23.0 ± 0.27	23.0 ± 0.15	23.1 ± 0.24	23.2 ± 0.15
		a^*	4.38 ± 0.18	4.57 ± 0.10	4.62 ± 0.17	4.83 ± 0.35
		b^*	2.61 ± 0.20	2.68 ± 0.23	2.56 ± 0.30	2.71 ± 0.08
9	Major Axis (mm)		1.76 ± 0.03	1.72 ± 0.01	1.70 ± 0.01	1.82 ± 0.01
	Minor Axis (mm)		1.51 ± 0.02	1.45 ± 0.01	1.50 ± 0.01	1.54 ± 0.02
	Roundness		0.87 ± 0.01	0.85 ± 0.01	0.88 ± 0.00	0.84 ± 0.00
	Colour values	L^*	22.3 ± 0.23	22.6 ± 0.21	22.4 ± 0.32	22.5 ± 0.28
		a^*	5.16 ± 0.13	5.16 ± 0.22	5.14 ± 0.20	5.52 ± 0.22
		b^*	2.67 ± 0.30	3.04 ± 0.41	3.05 ± 0.12	3.46 ± 0.20
11	Major Axis (mm)		1.72 ± 0.03	1.81 ± 0.02	1.75 ± 0.02	1.94 ± 0.01
	Minor Axis (mm)		1.47 ± 0.01	1.60 ± 0.01	1.51 ± 0.02	1.62 ± 0.03
	Roundness		0.85 ± 0.01	0.88 ± 0.00	0.87 ± 0.00	0.85 ± 0.01
	Colour values	L^*	22.7 ± 0.24	22.7 ± 0.15	22.8 ± 0.20	22.9 ± 0.24
		a^*	5.30 ± 0.23	5.16 ± 0.09	5.37 ± 0.16	5.37 ± 0.19
		b^*	2.92 ± 0.29	3.18 ± 0.08	3.04 ± 0.35	3.01 ± 0.38

4.5.2.3 Quality of canola seed oil

The effect of the RF heating on the quality of the canola seed oil at various MCs and temperatures is shown in Table 4. 8. The qualities of the oil extracted from the RF treated canola

seeds was not significantly different from that extracted from the controls. The PV, AV, Totox, and IV values varied between 0.28 meq kg^{-1} and 0.34 meq kg^{-1}, 0.33 and 0.38, 0.91 and 1.03, and 109 g $100g^{-1}$ oil and 112 g $100g^{-1}$ oil, respectively. Our measured values of PV and IV were in close agreement with those reported by Hawrysh et al. (1995) and Wang et al. (2007b). The AV and IV values of canola seed oil measured by Beig et al. (2012) were also in good agreement with our measured data. There were no significant differences in our measured values of AV and PV comparing to that reported by Crapiste et al. (1999) for sunflower oil.

Table 4. 8. The effect of the RF heating on the qualities of the canola seed oil at various MCs and temperatures.

MC (%, w. b.)	Characteristics	Temperature (℃)			
		Control	60	70	80
5	PV (meq kg^{-1})	0.28 ± 0.01	0.31 ± 0.00	0.30 ± 0.01	0.30 ± 0.01
	AV	0.35 ± 0.03	0.36 ± 0.01	0.33 ± 0.01	0.34 ± 0.01
	Totox	0.91 ± 0.02	0.98 ± 0.01	0.94 ± 0.03	0.94 ± 0.03
	IV (g 100g oil^{-1})	110 ± 0.31	110 ± 1.12	109 ± 1.84	110 ± 1.67
7	PV (meq kg^{-1})	0.29 ± 0.22	0.29 ± 0.00	0.31 ± 0.02	0.28 ± 0.03
	AV	0.33 ± 0.02	0.36 ± 0.02	0.34 ± 0.00	0.36 ± 0.02
	Totox	0.91 ± 0.06	0.93 ± 0.02	0.96 ± 0.03	0.93 ± 0.05
	IV (g 100g oil^{-1})	110 ± 1.23	110 ± 1.35	110 ± 0.97	111 ± 0.56
9	PV (meq kg^{-1})	0.31 ± 0.02	0.33 ± 0.01	0.34 ± 0.01	0.32 ± 0.00
	AV	0.36 ± 0.01	0.35 ± 0.02	0.36 ± 0.02	0.37 ± 0.02
	Totox	0.97 ± 0.03	1.01 ± 0.04	1.03 ± 0.04	1.02 ± 0.02
	IV (g 100g oil^{-1})	109 ± 3.01	110 ± 1.01	111 ± 0.62	110 ± 1.41
11	PV (meq kg^{-1})	0.30 ± 0.01	0.31 ± 0.02	0.29 ± 0.02	0.31 ± 0.00
	AV	0.35 ± 0.00	0.38 ± 0.01	0.34 ± 0.03	0.37 ± 0.05
	Totox	0.96 ± 0.01	0.99 ± 0.02	0.92 ± 0.06	0.99 ± 0.05
	IV (g 100g oil^{-1})	109 ± 2.53	111 ± 1.17	112 ± 1.06	111 ± 1.84

4.6 Conclusion

The absolute and the relative mortalities of the red flour beetles infesting the canola seeds during RF heating were determined at different MCs of seeds and treatment temperatures. The

mortality rate of insects increased with increasing MC of seed and heating temperature. The 100% absolute and the relative mortalities of the adult insects were achieved at 80℃ for the small volume of the seeds at all MCs. In the case of medium volumes of the seeds, the 100% absolute and the relative mortalities of the adult insects were achieved at 60 ℃ for 9 % and 11 % MCs and at 70 ℃ for 5 % and 7 % MCs of the seeds respectively. Over 80% and 96% of the absolute and the relative mortalities of the adult insects were achieved at over 60℃ for both volumes of the canola seeds. The 100% mortalities of the larvae infesting the small and the medium volumes of the canola seeds were achieved at 55℃ regardless of MC. There was no significant change in the germination of the seeds treated to 60℃. The major and the minor axes, the roundness, the colour of the canola seeds and the quality of the seed oil from the treated seeds were not significantly different between before and after RF heating. Therefore, there is potential to achieve a complete mortality of the red flour beetle infesting canola seeds with acceptable thermal degradation of the canola seeds at 60℃ by RF heating with proper design. Future research will be mainly focused on an accurate instantaneous heat transfer (conduction and convection) from high temperature steam evaporating from the canola seeds at higher MC to the tiny red flour beetle to investigate the kinetics of thermal death of the insects during RF heating.

4.7 References

Abbott, W. S. 1925. A method of computing the effectiveness of an insecticide. *Journal of economic entomology* 18(2): 265-267.

Andreuccetti, D., M. Bini, A. Ignesti, A. Gambetta, and R. Olmi. 1994. Microwave destruction of woodworms. *Journal of Microwave Power and Electromagnetic Energy* 29(3): 153-160.

AOCS. 1993. Official methods and recommended practices of the American oil chemists' society . Methods : Cd 8-53, Cd 18-90, Cd 1-25 (4th ed).

Armstrong, J. W., J. Tang, and S. Wang. 2009. Thermal death kinetics of Mediterranean, Malaysian, melon, and oriental fruit fly (Diptera: Tephritidae) eggs and third instars. *Journal of economic entomology* 102(2): 522-532.

ASAE. 2002. ASAE S352.2, moisture measurements-unground grains and seeds. In ASAE standards. St. Joseph, MI: ASAE.

Beig Mohammadi, Z., Y. Maghsoudlou, H. Safafar, and A. R. Sadeghi Mahoonak. 2012. Physicochemical properties and stability of oil extracted from three canola cultivars grown in Golestan province of Iran. *Journal of Agricultural Science and Technology* 14(3).

Ben-Lalli, A., J. M. Méot, A. Collignan, and P. Bohuon. 2011. Modelling heat-disinfestation of dried fruits on "biological model" larvae Ephestia kuehniella (Zeller). *Food research international* 44(1): 156-166.

Bio – EAFRINET. 2011. http://keys.lucidcentral.org/keys/v3/eafrinet/maize_pests/key/maize_pests/Media/Html/Triboliu m_castaneum_(Herbst_1797)_-_Red_Flour_Beetle.htm. (Feb, 3, 2016)

Birla, S. L., S. Wang, J. Tang, and G. Tiwari. 2008. Characterization of radio frequency heating of fresh fruits influenced by dielectric properties. *Journal of Food Engineering* 89(4): 390-398.

BPCA. 2016. http://www.bpca.org.uk/pages/?page_id=170. (Feb, 3, 2016)

Brusewitz, G. H. 1975. Density of rewetted high moisture grains. *Transactions of the ASAE* 18(5): 935-0938.

Bursell, E. 1964. Environmental aspects: temperature. *The physiology of Insecta* 1: 283-321.

Canadian Grain Commission. 2013. http://www.grainscanada.gc.ca/storage-entrepose/pip-irp/rfb-trf-eng.htm/. (Oct, 31, 2015).

Canola Council of Canada. 2014a. http://www.canolacouncil.org/markets-stats/industry-overview/. (Oct, 31, 2015).

Canola Council of Canada. 2014b. http://www.canolacouncil.org/canola-encyclopedia/crop-establishment/seed-quality/. (Feb, 3, 2016)

Canola Watch. 2015. http://www.canolawatch.org/2011/05/09/estimating-flea-beetle-damage-in-canola/. (Oct, 31, 2015).

Crapiste, G. H., M. I. Brevedan, and A. A. Carelli. 1999. Oxidation of sunflower oil during storage. *Journal of the American Oil Chemists' Society* 76(12): 1437-1443.

Davison, T. F. 1969. Changes in temperature tolerance during the life cycle of Calliphora erythrocephala. *Journal of Insect Physiology* 15(6): 977-988.

Dowdy, A. K. 1999. Mortality of red flour beetle, *Tribolium castaneum* (Coleoptera: Tenebrionidae) exposed to high temperature and diatomaceous earth combinations. *Journal of Stored Products Research* 35(2): 175-182.

Gao, M., J. Tang, Y. Wang, J. Powers, and S. Wang. 2010. Almond quality as influenced by radio frequency heat treatments for disinfestation. *Postharvest Biology and Technology* 58: 225–231.

Gazor, H. R., and A. Mohsenimanesh. 2010. Modelling the drying kinetics of canola in fluidised bed dryer. *Czech Journal of Food Sciences* 28(6): 531-537.

Griffin, J. P. 1988. Montreal Protocol on Substances That Deplete the Ozone Layer. *In Int'l L.* (Vol. 22, p. 1261).

Hallman, G. J., and D. L. Denlinger. 1998. Temperature sensitivity in insects and application in integrated pest management. Westview Press, Inc., pp. 7-53.

Hawrysh, Z. J., M. K. Erin, S. S. Kim, and R. T. Hardin. 1995. Sensory and chemical stability of tortilla chips fried in canola oil, corn oil, and partially hydrogenated soybean oil. *Journal of the American Oil Chemists' Society* 72(10): 1123-1130.

Heather, N. W., and G. J. Hallman. 2008. Pest management and phytosanitary trade barriers. CABI.

Hou, L., J. Hou, Z. Li, J. A. Johnson, and S. Wang. 2015. Validation of radio frequency treatments as alternative non-chemical methods for disinfesting chestnuts. *Journal of Stored Products Research* 63: 75-79.

Huang, Z., L. Chen, and S. Wang. 2015. Computer simulation of radio frequency selective heating of insects in soybeans. *International Journal of Heat and Mass Transfer* 90: 406-417.

Jiao, S., J. A. Johnson, J. Tang, G. Tiwari, and S. Wang. 2011. Dielectric properties of cowpea weevil, black-eyed peas and mung beans with respect to the development of radio frequency heat treatments. *biosystems engineering* 108(3): 280-291.

Johnson, J. A., K. A. Valero, S. Wang, and J. Tang. 2004. Thermal death kinetics of red flour beetle (Coleoptera: Tenebrionidae). *Journal of Economic Entomology* 97(6): 1868-1873.

Lagunas-Solar, M. C., Z. Pan, N. X. Zeng, T. D. Truong, R. Khir, and K. S. P. Amaratunga. 2007. Application of radiofrequency power for non-chemical disinfestation of rough rice with full retention of quality attributes. *Applied Engineering in Agriculture* 23(5): 647.

Mahroof, R., B. Subramanyam, and D. Eustace. 2003. Temperature and relative humidity profiles during heat treatment of mills and its efficacy against *Tribolium castaneum* (Herbst) life stages. *Journal of Stored Products Research* 39(5): 555-569.

Mills, R., and J. Pedersen. 1990. A flour mill sanitation manual. Eagen Press.

Shrestha, B., D. Yu, and O. D. Baik. 2013. Elimination of *Cruptolestes Ferrungineus S*. in Wheat by Radio Frequency Dielectric Heating at Different Moisture Contents. *Progress In Electromagnetics Research* 139: 517-538.

Sutherland, J. W., and T. F. Ghaly. 1982. Heated-air drying of oilseeds. *Journal of Stored Products Research* 18(2): 43-54.

Tang, J., J. N. Ikediala, S. Wang, J. D. Hansen, and R. P. Cavalieri. 2000. High-temperature-short-time thermal quarantine methods. *Postharvest Biology and Technology* 21(1): 129-145.

Tiwari, G., S. Wang, J. Tang, and S. L. Birla. 2011. Analysis of radio frequency (RF) power distribution in dry food materials. *Journal of Food Engineering* 104(4): 548-556.

USDA Foreign Agricultural Service. 2015. Production, Supply and Distribution Online Database, query for Commodity: "Oilseed, Rapeseed"; Data Type: "Production"; Country: "All countries"; Year: "2014", (Oct, 31, 2015).

Wang, S., S. L. Birla, J. Tang, and J. D. Hansen. 2006. Postharvest treatment to control codling moth in fresh apples using water assisted radio frequency heating. *Postharvest Biology and Technology* 40(1): 89-96.

Wang, S., M. Monzon, J. A. Johnson, E. J. Mitcham, and J. Tang. 2007a. Industrial-scale radio frequency treatments for insect control in walnuts: I: Heating uniformity and energy efficiency. *Postharvest Biology and Technology* 45(2): 240-246.

Wang, S., M. Monzon, J. A Johnson, E. J. Mitcham, and J. Tang. 2007b. Industrial-scale radio frequency treatments for insect control in walnuts: II: Insect mortality and product quality. *Postharvest Biology and Technology* 45(2): 247-253.

Wang, S., and J. Tang. 2004. Radio frequency heating: a potential method for post-harvest pest control in nuts and dry products. *Journal of Zhejiang University Science* 5(10): 1169-1174.

Yin, X., S. Wang, J. Tang, J. D. Hansen, and S. Lurie. 2006. Thermal conditioning of fifth-instar Cydia pomonella (Lepidoptera: Tortricidae) affects HSP70 accumulation and insect mortality. *Physiological Entomology* 31(3): 241-247.

Yu, D., B. Shrestha, and O. Baik. 2016. Temperature distribution in a packed-bed of canola seeds during radio frequency (RF) heating with seed moisture content and bulk volume. *biosystems engineering* 148: 55-67.

Zhou, L., B. Ling, A. Zheng, B. Zhang, and S. Wang. 2015. Developing radio frequency technology for insect control in milled rice. *Journal of Stored Products Research* 62: 22-31.

CHAPTER 5

THERMAL DEATH KINTICS OF ADULT RED FLOUR BEETLE (*TRIBOLIUM CASTANEUM*) IN STORED CANOLA SEEDS (*BRASSICA NAPUS* L.) BY RADIO FREQUENCY (RF) HEATING

Accepted in *International Journal of Food Properties* (2016).

Contribution of this paper to overall study

Thermal death kinetics of the adult red flour beetle infesting the canola seeds has not been developed based on the dynamic temperature history of the infested seeds and immediate mortality of the insect during RF heating. Therefore, thermal death kinetics of the adult insect infesting stored canola seeds at various MCs and volumes of the seeds was developed in this paper (specific objective 8). The developed thermal death kinetics of the adult insect would be helpful in designing RF thermal processes to control red flour beetles and similar insects in stored-canola seeds and other commodities. All the experiments in this chapter were conducted and the journal paper manuscript was drafted by myself.

5.1 Abstract

Thermal mortalities of adult red flour beetles (*Tribolium castaneum*) infesting canola seeds (*Brassica napus* L.) at various moisture contents and volumes were determined after radio frequency (RF) heating (i. e. temperature between 30 and 80℃) the infested seeds between 303K (30℃) and 353K (80℃). The mortality of 92% was achieved at the end temperature of 343K for small volume (1.96×10^{-4} m^3, 0.250 kg) seeds, and the mortality of 99% at 333K for medium volume (1.77×10^{-3} m^3, 2.26 kg) seeds. Regardless of sample volume, the thermal mortalities of

the test insects increased significantly after the seed temperature reached 333K (60℃). The kinetic parameters of the thermal death of the adult *T. castaneum* were estimated using inverse simulation. The ordinary differential equation based kinetic model with the Arrhenius temperature dependent reaction rate constant was solved using the 4th order Runge-Kutta method. The kinetics followed first-order reaction with the activation energy of 100 kJ/mol. Good agreements were observed between the mortalities predicted using the kinetic model and the experiments (R^2 = 0.972 to 0.987) except for the small volume seeds at 11% MC (11 g/100 g raw materials)(R^2 = 0.741). The predicted lethal times (s) to achieve 95 and 99% mortalities using the kinetic model were well matched with those determined from the experiments.

5.2 Nomenclature

Cal	data calculated from the kinetic models	n	order of the reaction
d.f.	degree of freedom for error	N	number of live insects
E_a	activation energy (J/mol)	N_0	initial numbers of the insects
Exp	data calculated from the experimental values	R	universal gas constant (8.314 J/mol·K)
k	reaction rate constant (1/s)	ODE	ordinary differential equation
k_0	frequency factor	RMSE	root mean square error
LT	lethal time (s)	RF	radio frequency
LT_{95}	lethal time to achieve 95% mortalities	t	heating time (s)
LT_{99}	lethal time to achieve 99% mortalities	T	temperature of the bulk canola seeds (K)
m	number of data	x_i	measured value
MC	moisture content (%, wet basis)	x_i'	predicted value using the kinetic model

5.3 Introduction

The world's total production of canola seeds in 2015 - 2016 was 67.7 million metric tons (USDA Foreign Agricultural Service 2016). Major canola producing countries are Canada, Austria, China, European Union, India, and the United States. Over 90% of the canola produced

in Canada is exported to markets around the world. The canola industries had injected $19.3 billion to the Canadian economy including 249,000 jobs and $12.5 billion in wages (Canola Council of Canada 2014).

In Canada, the losses of oilseed production average out 8 to 10% in annual crop yield due to insect pest causing hundreds of millions of dollars loss in the Canadian economy (Canola Watch 2015). Insect pest infestations that make barriers to export are a major concern in the production, storage, and the process of all food products (Gao et al. 2010). The trade regulations of domestic and international markets have required postharvest treatments of all food products to ensure quarantine security from insect pests (Birla et al. 2008; Jiao et al. 2011). One of the most common insect pests in the stored grains and oilseeds around the world is *T. castaneum* (Sinha and Watters 1990).

The fumigation with methyl bromide has been widely used and regarded as one of the practical methods to disinfest various insect pests found in grains and oilseeds (Sinha and Watters 1990). However, it was prohibited since Montreal Protocol because of the health hazards caused by excessive insecticide residues and the destructive effect to the ozone layer (Birla et al. 2008; Griffin 1988; Wang et al. 2004). The other nonchemical treatments to control insect pests such as ionizing radiation, hot air, and cold storage have disadvantages. These techniques require a long treatment time and a substantial capital investment, and may leave live insect pests after the treatments (Heather and Hallman 2008; Want et al. 2004). RF heating based on electromagnetic radiation is volumetric and selective heating, and this technique may avoid the problems posed by the aforementioned nonchemical treatments (Tang et al. 2000). There is a possibility to destroy the insect pests using RF heating without significant thermal degradation of the grain. Lagunas-Solar et al. (2007) reported the mortalities of Angoumois grain moths, *Sitotroga cerealella* (Olivier) and lesser grain borers, *Rhyzopertha dominica* (Fabricius) in rice using RF heating. A mortality of 99% of *S. cerealella* was achieved at 55 to 60°C for 5 min of heating, and 100% mortality of *R. dominica* at 60°C for 1 h of heating. There were no significant changes in moisture level and milling quality of the rice. Shrestha et al. (2013) have achieved 100% mortality for all the life stages of rusty grain beetles, *Cryptolestes ferrugineus* (Stephens) in stored wheat at 60°C with RF heating (1.5 kW, 27.12 MHz) without significant degradation of the wheat qualities.

Several kinetic models for the mortalities of insect pests have been studied for thermal processing. Tang et al. (2000) demonstrated a possibility of developing high – temperature – short

time thermal treatments to control larvae of codling moth, *Cydia pomenella* (Linnaeus) with a minimal thermal impact on fruit quality using the thermal death kinetics of the insect. Wang et al. (2002a) reported thermal death kinetic parameters for the fifth-instar *C. pomenella*, which were heated to four temperatures (46, 48, 50, and 52℃) using a heating block system. The thermal death kinetics of the insects followed a 0.5^{th} order reaction with an activation energy of 472 kJ/mol at a heating rate of 18℃/min. Johnson et al. (2003) estimated the lethal exposure times for the fifth-instar larvae of Indian meal moth, *Plodia interpunctella* (Hubner) at 44 to 52℃ during RF heating using a 0.5^{th} order kinetics model. They obtained the RF heating time of less than 5 min to achieve 95% mortalities at 50℃ and 52℃. A thermal death kinetic model of *T. castaneum* at larvae stage (the most heat - tolerant life stage of the insect) with 0.5^{th} order reaction was developed to estimate lethal exposure times at 48, 50, and 52℃ during RF heating (Johnson et al. 2004). They reported the lethal times (LTs) to achieve 99% mortalities were 1.6 min, 9.1 min, and 76.8 min at the constant temperatures of 52℃, 50℃, and 48℃, respectively. The thermal death kinetics were determined based on experiments at constant system temperatures, and only applied for the larvae stage of the insect. These kinetic models could not be used in this study. The target life stage of the insect in this study was adult, the heating process was transient (the temperature of the infested sample was continuously increased), and the immediate mortality (the mortality determined immediately after the RF heating) was considered.

Thermal death kinetics of the adult *T. castaneum* based on the immediately determined mortalities and temperature histories of host material (canola seeds) will be helpful. The determined kinetic parameters and model can predict mortalities at specific RF heating times without knowing insect body temperatures. They can be also used to determine proper RF heating conditions for disinfestation of the adult *T. castaneum*. Therefore, in this study, the thermal death kinetics of the adult *T. castaneum* infesting canola seeds at various moisture contents and volumes of the seeds was characterized based on dynamic temperature changes of the canola seeds and the experimental data of insect mortalities during RF heating.

5.4 Materials and methods

5.4.1 RF heating system

The RF heating system used in this work is shown in Fig. 5. 1. A 1.5 kW, 27.12 MHz RF system (Strayfield Fastran, Berkshire, England) with two parallel electrode plates (250 mm × 250 mm) was used to heat the samples.

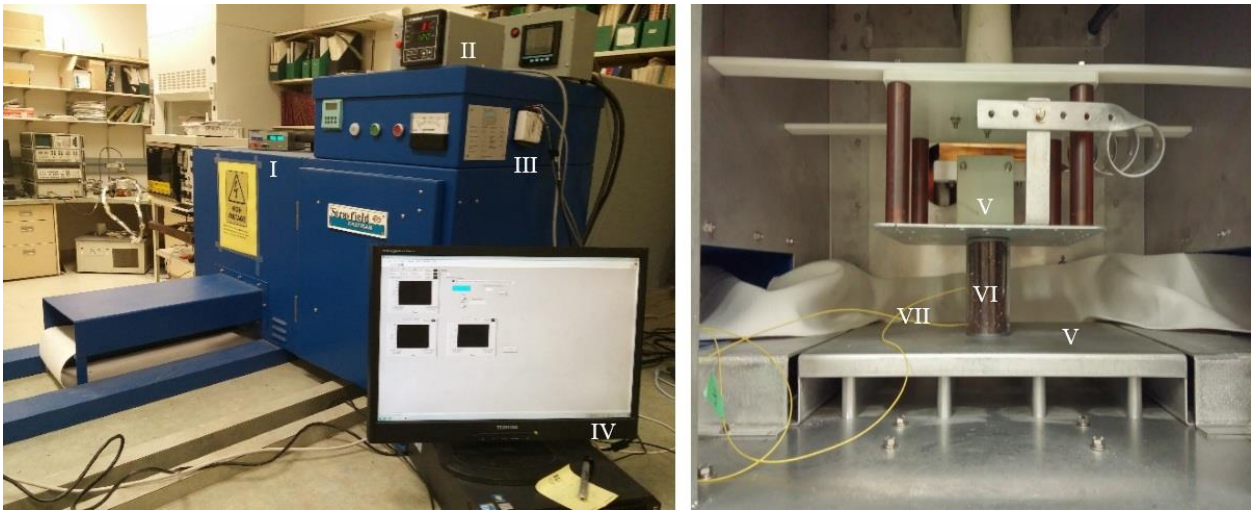

(a) (b)

Figure 5. 1. The side and the rear view of the RF heating system (a) and the interior view of the RF heating system (b) showing the I : reflex signal conditioner, II : temperature controller, III : data acquisition device, IV : data acquisition software, V : electrodes, VI : canola seeds, VII : fibre optic temperature sensors (Yu et al. 2016a).

The upper electrode can be adjusted vertically up or down by turning the crank attached to the plate, and the bottom plate was fixed and grounded. The electric arcing was observed when air gap between the upper electrode and the top surface of the samples was less than 1 mm and 15 mm for the small and medium volume samples due to evaporated moisture from the sample during RF heating. To prevent the electric arcing, the air gaps of 1 mm and 15 mm for the small and medium volume samples were set. The larger air gap for the medium volume samples was determined due to intensified electric arcing by more evaporated moisture from the seeds compared to that of the small volume samples. Those air gap sized were determined from our previous work (Yu et al. 2016b).

5.4.2 Canola seed samples

Top quality canola seeds (B. *napus* L.) at the initial moisture content (MC) of 7% wet basis (w.b.) were provided by our industrial partner, Viterra Inc., Regina, SK, Canada. The standard

method (ASAE 2002; Brusewitz 1975) was used to determine the MC of the canola seeds. Four different MCs (5%, 7%, 9%, and 11%) of the bulk canola seeds were prepared. The seed samples at 5% MC was prepared by drying the original canola seeds in a hot air oven. The seed samples at 9% and 11% MCs were prepared by adding pre-calculated amounts of distilled water to the seeds at the initial MC. A sprayer was used to do that. The prepared canola seed samples were stored in a cold storage at 4℃ before using them. The details on preparing the seed samples at the required MCs can be found in Yu et al. (2016b).

5.4.3 RF exposure time of the canola seeds

Small volume (1.96×10^{-4} m^3, 0.250 kg) seed samples were contained in a RF transparent polycarbonate sample holder which can minimize the effect of the holder on RF heating, measuring 50 mm and 100 mm of diameter and height, and larger volume (1.77×10^{-3} m^3, 2.26 kg) seed samples were contained in a sample holder made of the identical material measuring 150 mm and 100 mm of diameter and height. The former and the latter were referred to small volume sample and medium volume sample respectively in this work.

A Reflex^{TM} signal conditioner and the fiber optic temperature sensors with an accuracy of ± 0.8℃ (Neoptix, Québec City, Québec, Canada) were used to measure and monitor the temperatures of samples. The fiber optic temperature sensors were located at the hottest spot of the seed samples. The hottest spot for the small volume samples was at the geometric center regardless of MC of the seeds. But, for the medium volume samples, the hottest spot was shifted from the geometric center to near the inner wall of the sample holder as the MCs of the samples were changed from 5% and 7% to 9% and 11% at as illustrated in Fig. 5. 2.

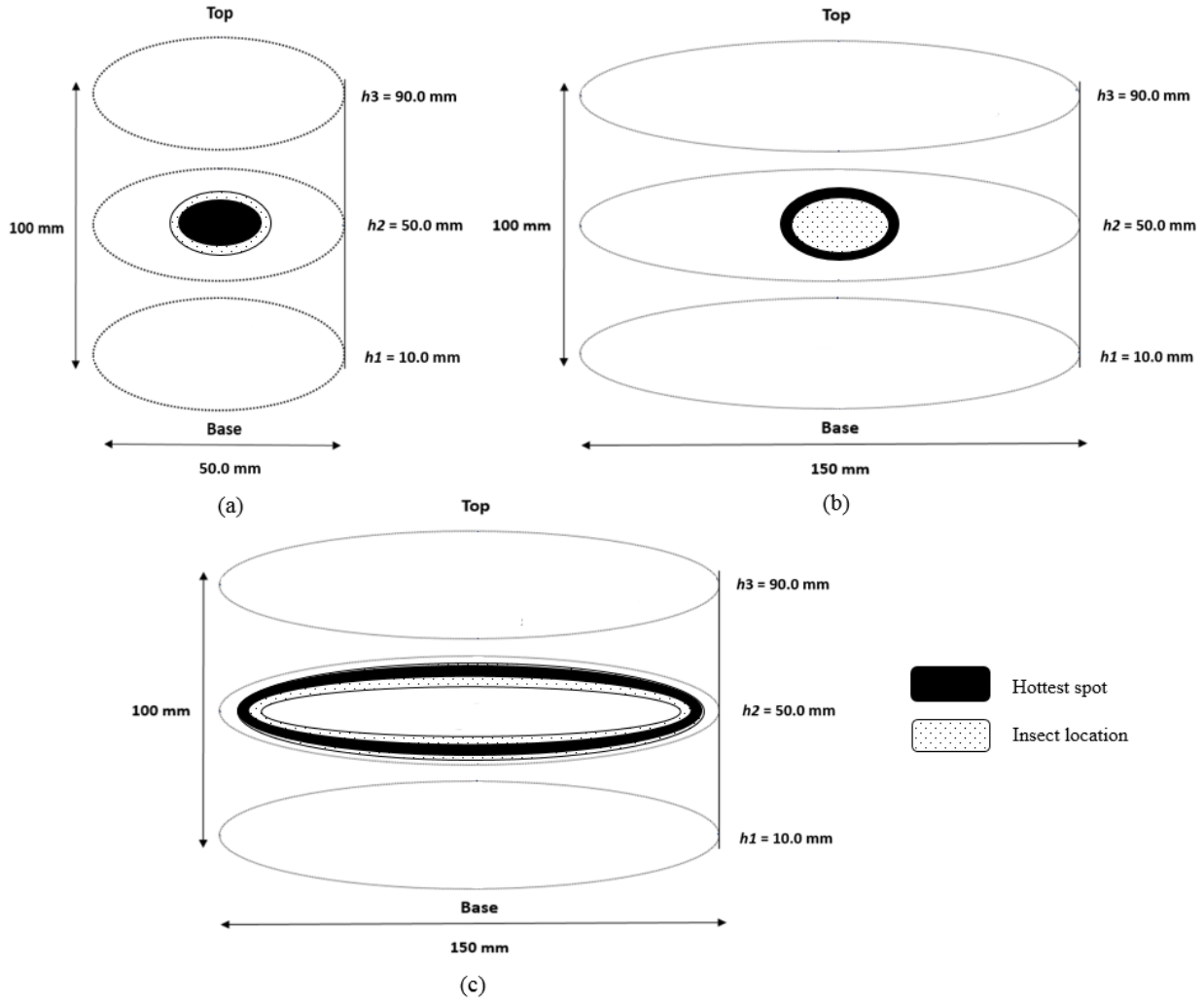

Figure 5. 2. The location of the hottest spot of the small volume samples (a), and the medium volume samples at MCs of 5% and 7% (b), and 9% and 11% (c) (Yu et al. 2016a).

Those hottest spots were obtained from our previous research (Yu et al. 2016b). A dedicated Labview (2010v.10) program was developed to interface with the data acquisition device connected to the temperature sensors. The temperatures of the sample were displayed and recorded every 2 s. RF exposure times (s) of the canola seeds were determined when the temperature of the hottest spot of the bulk seeds reached up to each desired temperature (303K, 313K, 323K, 333K, 343K, and 353K) from 297K (initial temperature) for each MC (5%, 7%, 9%, and 11%) of the seeds. Three different batches of the canola seeds in total were used for the each MC. The same amount of the seeds was used for each batch with the same operating condition of the RF unit. The RF exposure times (s) were obtained from our previous research (Yu et al. 2016a). The average of

triplicate measurements was used for the RF exposure time (s) of the seeds. Then regression models were developed for the temperature (K) of the seeds as a function of RF exposure time (s) for input data in the kinetic model used in this study.

5.4.4 Test insect culture

The adult *T. castaneum* were collected from the Agriculture and Agri - Food Canada / University of Manitoba, Canada. The insects were cultured following the procedure adopted by Shrestha et al. (2013). In brief, a total of 500 adult insects were reared in the jar (2 L) containing 1.5 kg of a mixture of wheat at MC of 14% and wheat germs in a proportion of 7 : 3 by weight. The jar was covered with a fabric for better ventilation and placed in a temperature and humidity chamber (30 ℃ and 70 % RH) for 70 days. The insects with the rearing mixture were separated using the Canadian standard sieve # 40 and collected using a suction assembly. The insects were exposed to carbon dioxide gas at various stages of the experiment when it was required to stop them from moving around. The details on the procedures of rearing and handling the test insects can be found in Yu et al. (2016a).

5.4.5 Insect mortality

The insect mortalities were determined by introducing the adult insects in small and medium seed samples. A total of 30 adult insects (70-72 days old from the time of hatching from eggs) were introduced at the hottest spot (ball shape) of the small volume samples and its vicinity, and 90 adult insects at the hottest spot (doughnut shape) of the medium volume samples as shown in Fig. 1. The hottest spot was chosen to show how effectively insects can be killed with optimally designed RF heating systems. The vicinity of the hottest spot was also taken by the adult insects for the small volume samples as the hottest spot was too tiny to hold 30 adult insects at the exact hottest spot. The infested canola seeds were heated until the hottest spot of the bulk seeds reached up to the each desired temperature (303K, 313K, 323K, 333K, 343K, and 353K) from 297K (initial temperature) for the each MC (5%, 7%, 9%, and 11%) of the seeds. The dead and the live insects were counted to calculate mortalities. The immediate mortalities of the adult *T. castaneum* at each desired temperature were tested in triplicate and then averaged for each MC of the seeds. The more detailed procedures of the insect mortality are available in Yu et al. (2016b).

5.4.6 Kinetics modeling

The thermal death rate of the adult *T. castaneum* can be modeled using the following kinetic model.

$$\frac{d\,(N/N_0)}{dt} = -k\,(N/N_0)^n \tag{5.1}$$

where t is the heating time (s), N and N_0 are respectively the number of live insects at time and the initial number of the insects, k is the reaction rate constant (1/s), and n is the order of the reaction (Datta 2002).

The temperature dependent reaction rate constant can be expressed using the Arrhenius relationship as follows:

$$k = k_0 \exp(-\frac{E_a}{R\mathrm{T}}) \tag{5.2}$$

where k_0 is the frequency factor, E_a is the activation energy (J/mol), R is the universal gas constant (8.314 J/mol·K), and T is the temperature of the bulk canola seeds (K) (Datta 2002). Temperature histories of the canola seeds during RF heating were used instead of those of the insects as measuring the insect-body temperatures was extremely difficult due to their tiny size (3 - 4 mm) and mobility. This makes the activation energy and frequency factor as apparent or effective values as the temperature of the insects is not the same to that of the canola seeds during RF heating. It is, however, assumed that the canola seeds had similar heating patterns as those of the insects even if their heating speed were slower. Using the temperature of the canola seeds instead of the insect-body temperature was the limitation of this study, however at the same time this approach would be more practical for real world applications. Only a limited mobility of the insects in the seed sample during the RF heating was observed due to the natural compactness of the tiny seeds (The diameter of the seed is approximately 1.8 mm).

Substitution of the value of k from Eq. (5.2) into Eq. (5.1) results in the thermal death rate of the adult *T. castaneum* as shown in Eq. (5.3).

$$\frac{d(N/N_0)}{dt} = -k_0 \left\{\exp\left(-\frac{E_a}{R\mathrm{T}}\right)\right\} (N/N_0)^n \tag{5.3}$$

The ordinary differential equation, Eq. (5.3) was solved using ODE 45 solver based on the 4th order Runge-Kutta method in MATLAB R2013a (The MathWorks Inc., Natick, MA, USA). The optimum values of k_0, E_a, and n were determined by minimizing the root mean square error (RMSE)

between the values predicted from the kinetic model and the experimental data as depicted in Eq (5.4).

$$\text{RMSE} = \sqrt{\frac{1}{m}\sum_{i=1}^{m}(x_i - x_i')^2} \quad (5.4)$$

where, m is number of data, x_i is the measured value, and x_i' is the value predicted using the kinetic model, Eq (5.3). The unknown parameters, k_0, E_a, and n were determined by trial and error from 8 different sets of time-temperature data (6 points per each set) depending on RF heating rates. As n was found to be 1 ± 0.01 in our preliminary parameter estimation, we set the order of kinetics (n) as 1 for all of the estimation. Then, only the other two unknown parameters k_0, and E_a were estimated. The kinetic model was also used to estimate LTs to achieve 95% (LT_{95}) and 99% (LT_{99}) mortalities of the insects infesting the canola seeds at different MCs and volumes.

5.4.7 Statistical analysis

The stepwise regression and bi-variate correlation analysis in SPSS (SPSS Inc., Chicago, IL, USA) was used to derive regression models for temperature of the canola seeds vs. RF exposure time, and to investigate the correlation between the mortalities of the insects from the kinetic model and the experiments.

5.5 Results and discussion

5.5.1 Temperature profiles of canola seed samples

Figure 5. 3 shows the temperature histories of the canola seed samples at various MCs during RF heating.

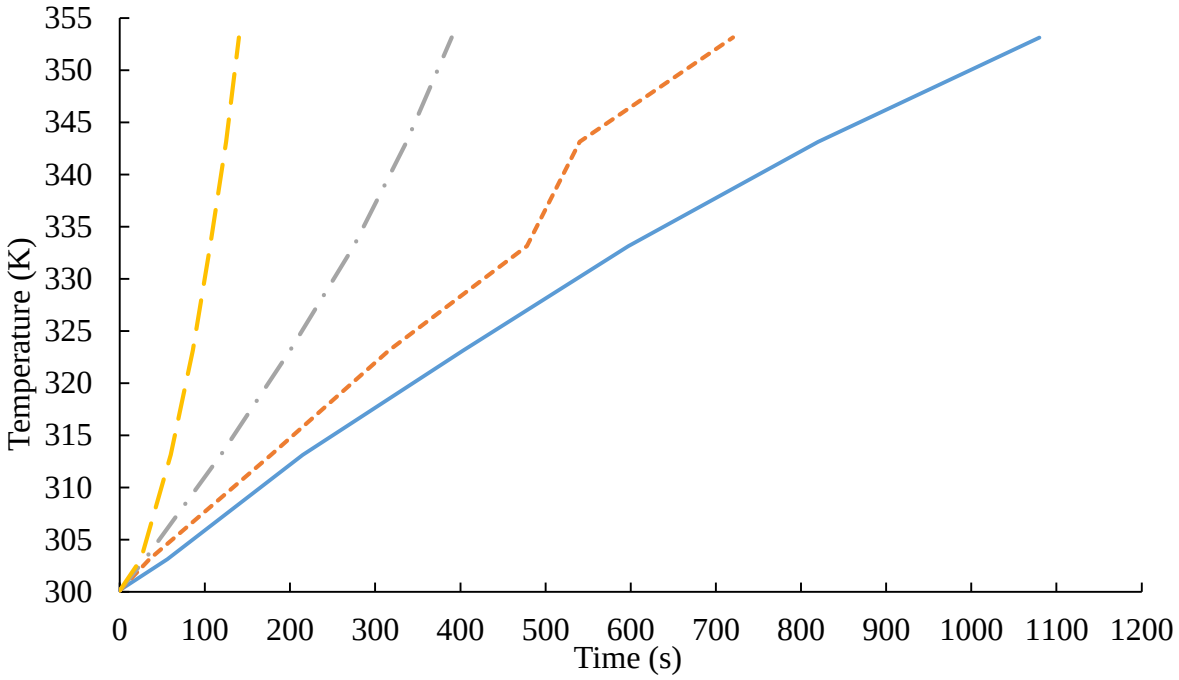

(a)

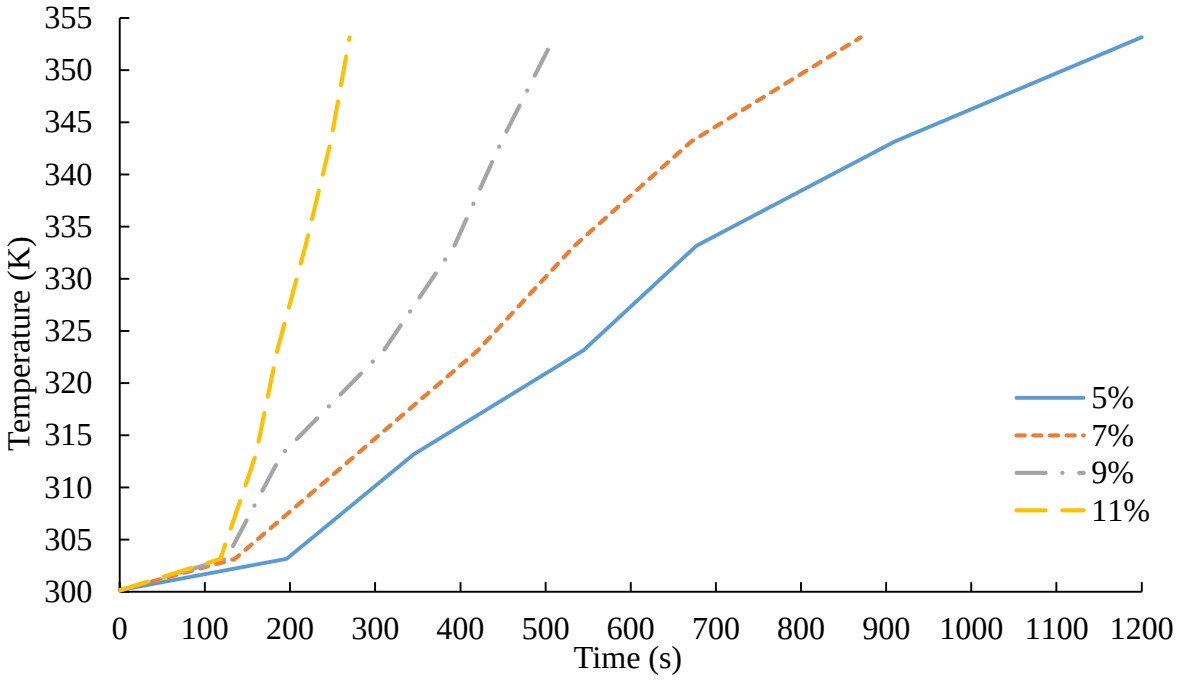

(b)

Figure 5. 3. The temperature histories of the small (a) and the medium (b) volume samples at the indicated MCs of the seeds during the RF heating (Note: The experimental data points are connected with simple straight lines for visual presentation.)

The rate of the temperature increment of the seeds was apparently proportional to the MC of the seeds. It was attributed to the higher dielectric loss factor of the seeds due to the enhanced conductivity of dipoles and ions in the material with higher MC causing higher dissipation of electromagnetic energy (Shrestha et al. 2013). In case of the medium volume samples, the temperatures were increased significantly faster after 303K. The RF exposure times to reach the end temperatures for the small and the medium volume samples at different MCs are presented in Table 5. 1.

Table 5. 1. The RF exposure time (s) to reach the end temperatures for the small and the medium volume samples at different MCs (Yu et al. 2016a).

MC (%)	Volume	Temperature K (℃)					
		303 (30)	313 (40)	323 (50)	333 (60)	343 (70)	353 (80)
5	Small	55.98 ± 3.68	215.0 ± 12.5	403.0 ± 1.41	597.0 ± 11.4	820.0 ± 16.7	1080 ± 24.3
	Medium	73.00 ± 4.08	301.0 ± 9.98	485.0 ± 20.4	765.0 ± 17.2	984.5 ± 13.5	1200 ± 29.0
7	Small	34.98 ± 8.52	178.0 ± 10.4	316.0 ± 11.0	478.0 ± 16.0	540.0 ± 17.1	720.0 ± 23.3
	Medium	50.00 ± 2.16	223.0 ± 8.52	337.0 ± 6.80	570.0 ± 12.3	726.0 ± 10.2	870.0 ± 13.0
9	Small	30.00 ± 0.47	119.0 ± 3.27	200.0 ± 6.94	275.0 ± 11.6	337.0 ± 13.0	390.0 ± 16.3
	Medium	34.00 ± 0.47	148.5 ± 3.30	255.5 ± 4.92	355.5 ± 4.92	444.5 ± 4.19	510.0 ± 9.50
11	Small	25.02 ± 0.82	60.00 ± 2.05	85.98 ± 4.08	106.0 ± 8.18	125.0 ± 10.3	140.0 ± 4.11
	Medium	25.00 ± 2.45	92.50 ± 3.74	149.5 ± 4.50	198.5 ± 7.13	241.0 ± 8.16	270.0 ± 1.00

The RF exposure time ranged from 25 to 1200 s. The differences between the RF exposure times to attain the same temperature for the small and the medium volume samples ranged from 0.024 to 186 s. The small and the medium volume samples at 5% MC took approximately 8 and 4 times longer RF exposure times than those at 11% MC to reach 353K, respectively. The regression models for the temperatures (K) of the canola seeds as a function of the RF exposure time (s) at the interested MCs for both the small and the medium volume samples are listed in Table 5. 2.

Table 5. 2. Regression models for the temperature of the canola seeds as a function of the RF exposure time (s) at different seed MCs and volumes during the RF heating.

Volume	MC[b] (%, w. b.)	Regression Model	*p* value	*d.f.*[a]	R^2
Small	5	$T^c_{5S} = -1.0 \cdot 10^{-5} \cdot t^2 + 0.063 \cdot t + 300.0$	< 0.00001	6	0.999
	7	$T_{7S} = 3.0 \cdot 10^{-6} \cdot t^2 + 0.072 \cdot t + 300.3$		6	0.994
	9	$T_{9S} = 1.0 \cdot 10^{-4} \cdot t^2 + 0.090 \cdot t + 300.4$		6	0.999
	11	$T_{11S} = 2.0 \cdot 10^{-3} \cdot t^2 + 0.096 \cdot t + 299.9$		6	0.999
Medium	5	$T_{5L} = -2.0 \cdot 10^{-6} \cdot t^2 + 0.042 \cdot t + 300.1$		6	0.999
	7	$T_{7L} = 7.0 \cdot 10^{-6} \cdot t^2 + 0.054 \cdot t + 300.4$		6	0.999
	9	$T_{9L} = 6.0 \cdot 10^{-5} \cdot t^2 + 0.073 \cdot t + 300.5$		6	0.999
	11	$T_{11L} = 3.0 \cdot 10^{-4} \cdot t^2 + 0.098 \cdot t + 300.5$		6	0.999

[a] *d.f.* = degree of freedom for error.

[b] MC = moisture content (%)

[c] T = temperature (℃)

The developed regression models were used as input data in Eq. (5.3) to determine the thermal death kinetics of the adult *T. castaneum*.

5.5.2 Thermal mortality of the insects

Figure 5. 4 shows the measured survival rates (100%-mortality %) of the adult *T. castaneum* in the small and the medium volume samples when the samples at MCs of 5%, 7%, 9%, and 11% were RF heated from 303K to 353K by RF energy.

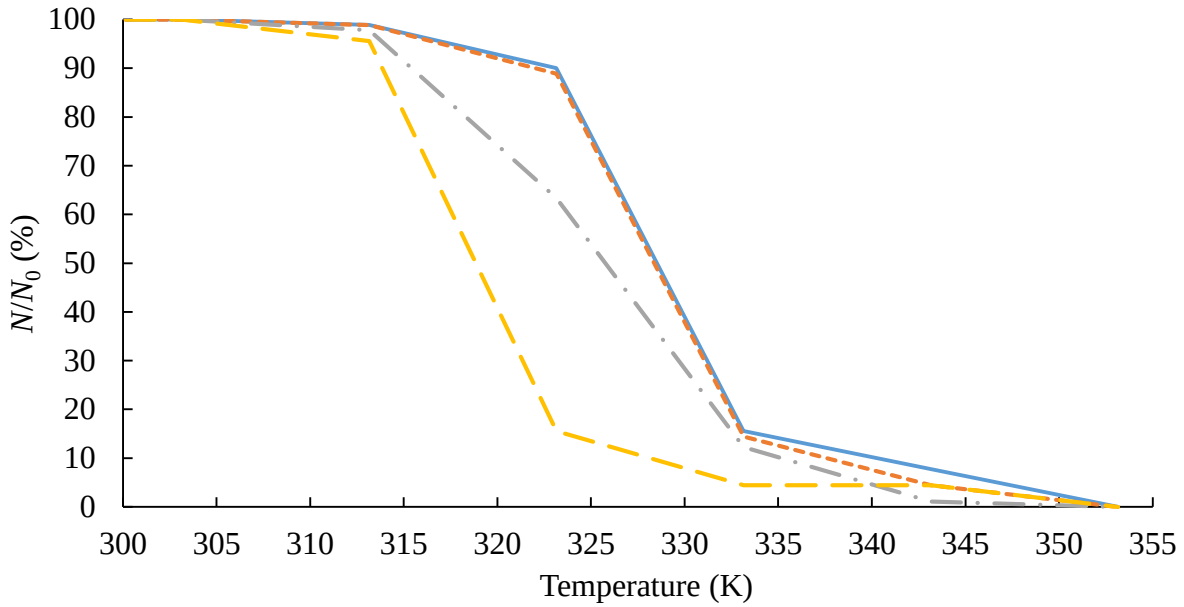

(a)

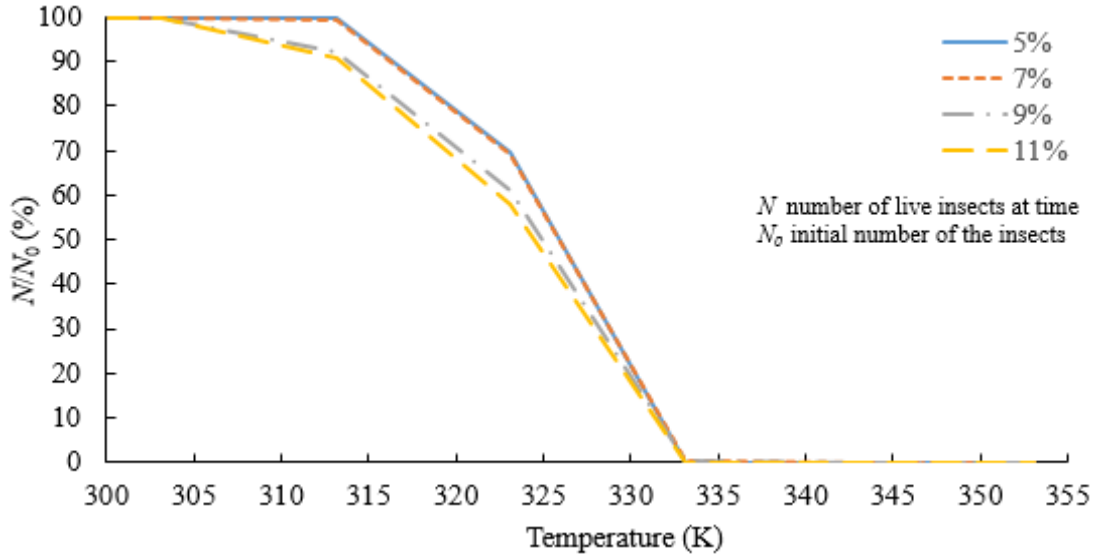

(b)

Figure 5. 4. The survival rates (N/N_0, %) of the adult *T. castaneum* infesting the small (a) and the medium (b) volume samples at different seeds MCs during the RF heating. (Note: The experimental data points are connected with simple straight lines for visual presentation)

In general, the survival rate of the insect decreased with increasing temperature. At any end temperatures of the seeds, the survival rate of the insect decreased with increasing MC of the seeds. The insects thoroughly surrounded by the seeds are exposed to the evaporated hot steam from the wet seeds by RF heating. The survival rate of the insects in the seed samples at high MC (11%) was lower than that at low MC (5%) at the same end RF heating temperature due to the more evaporated moisture from the seeds of high MC (11%). The survival rates of the insect in the medium volume samples had significantly dropped over the temperature compared to that in the small volume samples due to the more evaporated moisture from the medium volume samples. Placement locations of the adult *T. castaneum* in the small and medium volume samples (mentioned in section 2.4) could be one of the reasons for the difference of the survival rates between the small and the medium volume samples. Over 84% and 99% mortalities of the insects were achieved at 333K for the small and the medium volume samples, respectively. Those mortalities required RF exposure times of 106.0 to 597.0 s and 198.5 to 765.0 s for the small and the medium volume samples at 5 to 11% MC. The thermal effect on the insect mortality was attributed to the thermal degradation of carbohydrates, proteins, DNA, RNA, and lipids of the insects (Hallman and Denlinger 1998). Yu et al. (2016a) reported that 100% mortality of *T. castaneum* infesting the canola seeds at MCs of 5%, 7%, 9%, and 11% could be achieved without significant degradation of the seed quality at 333K (60℃) with proper design of RF heating applicators.

5.5.3 Thermal death kinetics

The best fitted kinetic model of thermal death of the adult *T. castaneum* infesting the canola seeds during RF heating was as follows.

$$\frac{d(N/N_0)}{dt} = -6.73 \times 10^{13} \cdot \exp\left(\frac{-1.00 \times 10^5}{R\mathrm{T}}\right)(N/N_0)^1 \quad (5.5)$$

The performance of the model in predicting the mortalities for both the small and the medium volume samples is summarized in Table 5. 3.

Table 5. 3. Performance of the kinetic model (Eq. 5.5) in predicting the mortalities of the adult T. *castaneum* during the RF heating.

E_a (kJ / mol)	k_0 (1 / s)	n	Volume	MC (%, w. b.)	R^2	RMSE[a]	*d.f.*
100	6.73×10^{13}	1	Small	5	0.958	16.20	6
				7	0.978	11.55	6
				9	0.972	12.84	6
				11	0.741	43.32	6
			Medium	5	0.975	12.30	6
				7	0.987	8.745	6
				9	0.979	11.02	6
				11	0.908	25.73	6

[a] RMSE = root mean square error, Eq. (5.5).

The mortalities determined from the kinetic model agreed reasonably well with the experimental values resulting in R^2 values of 0.958, 0.978, 0.972, and 0.741, and RMSE of 16.20, 11.55, 12.84, and 43.32 for 5%, 7%, 9%, and 11% MCs of the small volume samples, respectively. In case of the medium volumes samples, the R^2 values were 0.975, 0.987, 0.979, and 0.908, and the RMSE values were 12.30, 8.745, 11.02, and 25.73 for 5%, 7%, 9%, and 11% MCs, respectively. The kinetic parameters should be independent of MC and volume of samples if the effect of steam release is not reflected in the thermal death kinetics. Relatively high RMSE (43.32) and low R^2 (0.741) for the small volume samples at 11% MC were caused by sharply dropped survival rate of insects. Figure 5. 5 compares the survival rates of insects determined from the kinetic model with those from the experiments for the small and the medium volume samples at 5%, 7%, 9%, and 11% MCs during the RF heating.

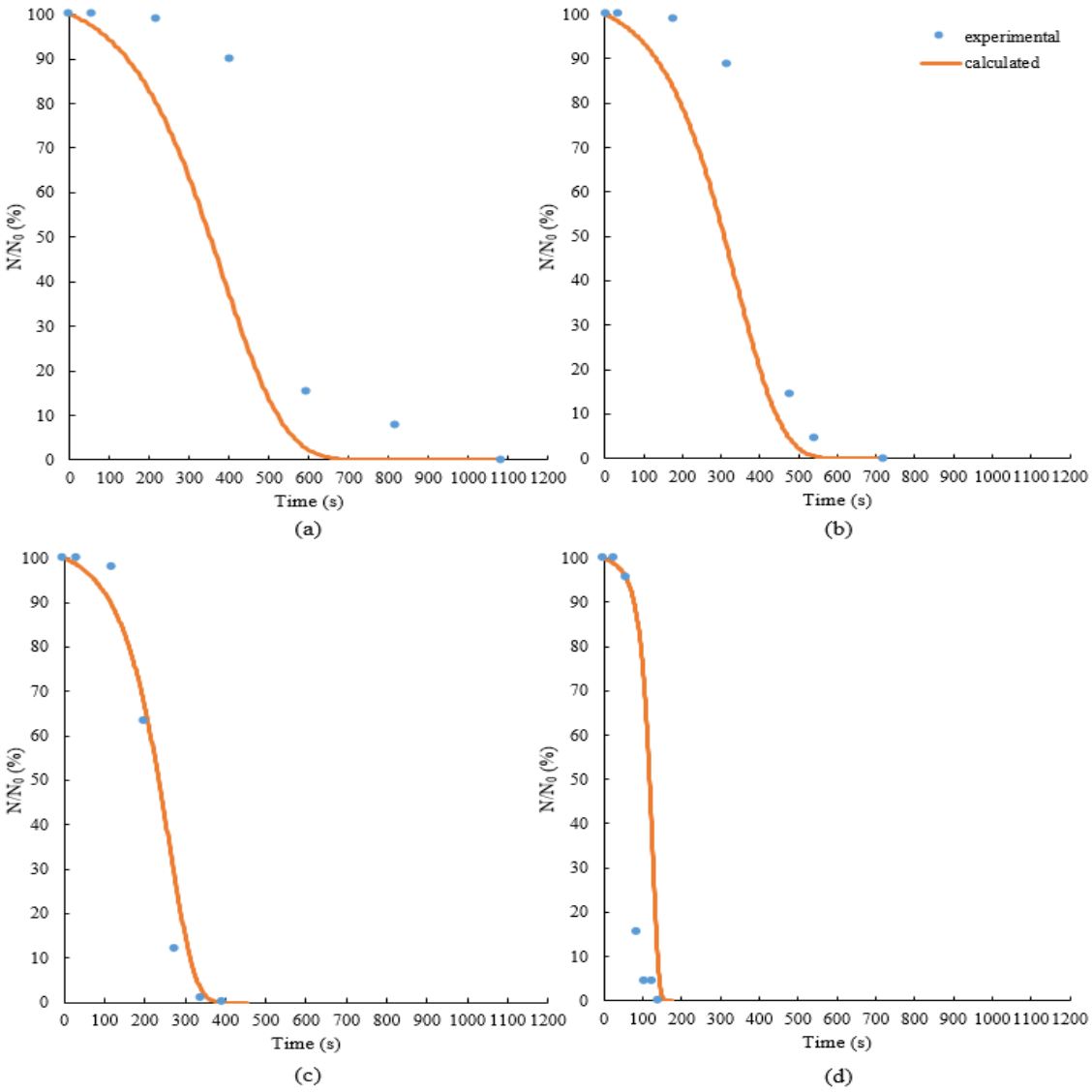

(A)

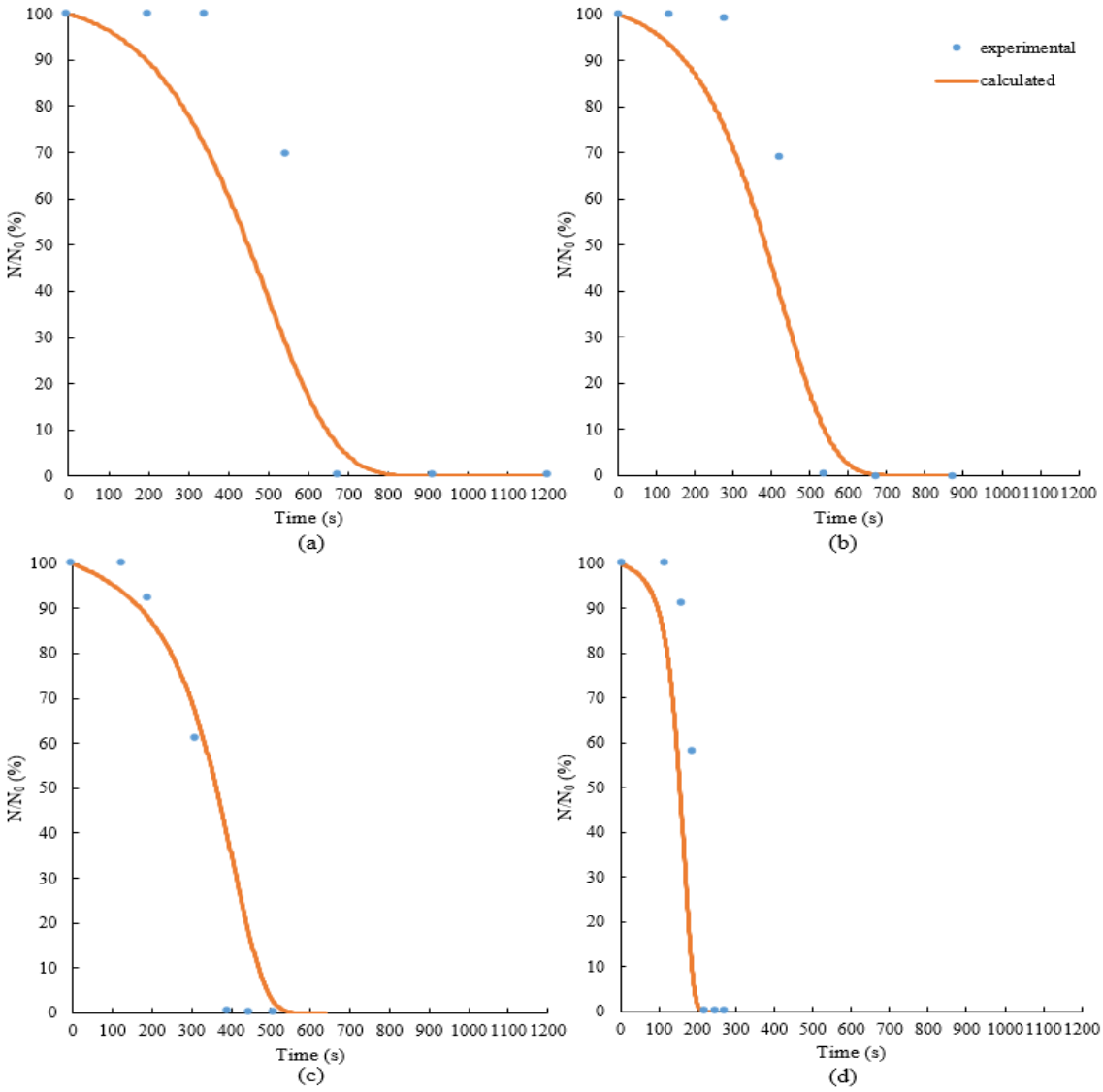

(B)

Figure 5. 5. Survival rates (*N/N*$_0$, %) of the adult *T. castaneum* infesting the small (A) and the medium (B) volume samples at 5% (a) , 7% (b), 9% (c), and 11% (d) seed MCs during the RF heating.

In Fig. 5. 5, the scatter data present the experimental values, and the continuous lines represent the calculated values from the kinetic model. The first order kinetic model was much more suitable to describe the thermal death kinetics of the insect than 0.5th order which was used by Wang et al. (2002a) and Johnson et al. (2003, 2004) for thermal death kinetics of other insects. Shimoda et al. (2001) reported the inactivation of *Saccharomyces cerevisiae* by combinations of dissolved CO_2

and heating (30 to 38℃) followed first-order kinetics. First-order reaction was the most suitable to describe the thermal death kinetics of eggs of Mediterranean flour moth, *Ephestia kuehniella* (Zeller) which were heated in hot water at constant temperatures (46 to 75℃) for 5 to 1200 s (Ben-Ialli et al., 2009). Our determined activation energy of 100 kJ/mol for the adult *T. castaneum* infesting the canola seeds was similar to that of eggs of *E. kuehniella* (102 kJ/mol) (Ben-Ialli et al., 2009) and lower than that for the fifth-instar of *C. pomonella* (472 kJ/mol) (Wang et al., 2002a), the fifth-instar of *P. interpunctella* (506.3 kJ/mol) (Johnson et al., 2003), and the fifth-instar navel orangeworm, *Amyelois transitella* (Walker) (510 kJ/mol to 520 kJ/mol) (Wang et al., 2002b). The lower activation energy indicated that the adult *T. castaneum* was more susceptible to the thermal death by the RF heating than the other insects infesting the food commodities. It should be, however, noted that in our study for kinetic parameter estimation the temperatures of the canola seeds were used instead of the adult insect body temperatures.

5.5.4 Lethal time (LT)

The developed kinetics model was reversibly used to estimate the LT_{95} and the LT_{99} for each MC and volume. Table 5. 4 shows the experimental LT required to kill 100% of the insect as well as the LT_{95} and the LT_{99} determined from the experiments and the kinetics model.

Table 5. 4. The RF exposure times (s) to achieve 100% mortality and the LTs (s) determined from the experimental and simulated data for the adult *T. castaneum* at the indicated seed MCs and volumes.

Volume	MC (%, w. b.)	RF exposure time (sec) for 100% mortality	LT_{95}		LT_{99}	
			Experimentally determined	Numerically simulated	Experimentally determined	Numerically simulated
Small	5	1080	912.9	625.7	1047	698.0
	7	720.0	536.6	519.2	679.5	571.4
	9	390.0	315.3	354.1	342.3	381.0
	11	140.0	123.0	149.2	136.6	156.1
Medium	5	762.0	745.4	774.3	758.7	859.0
	7	726.0	558.4	623.1	568.4	686.2
	9	445.0	348.4	513.5	355.0	513.6
	11	199.0	194.8	272.3	198.1	272.3

The predicted LT_{95} and LT_{99} from the kinetic model were in good agreement with those from the experiments except the small volume seeds at 5% MC. This exception was caused by the slow heating rate of the seeds at the lower moisture level. Complete destruction of the adult insect in the canola seeds was achieved with the RF exposure time ranging 140 to 1080 s and 199 to 762 s for the small and the medium volume samples at 5 to 11% MC, respectively. The differences between LT_{95} and LT_{99} determined from the experiments and the kinetic model ranged from 17.40 to 287.1 s, and 19.49 to 348.6 s respectively. Similar discrepancies of LT_{95} and LT_{99} of mortalities of fifth-instar of *A. trasitella* were observed by Wang et al. (2002b). The LT_{95} and LT_{99} from the experiments for the small volume samples at 5% MC were 7.41 times and 7.66 times longer than those at 11% MC. This means disinfestation of the insect by RF could be done more effectively with higher MC seeds due to shorter RF heating time and steam release effect to achieve the specific mortalities compared to seeds at lower MC.

5.6 Conclusion

The survival rate of the adult *T. castaneum* infesting the canola seeds at different seed MCs (5%, 7%, 9%, and 11%) and volumes (small and medium) decreased with temperature (303 to

353K) during RF heating. The kinetic parameters of the thermal death of the adult *T. castaneum* were estimated using an inverse simulation. The kinetics followed first-order reaction with the activation energy of 100 kJ / mol and it produced the insect mortalities that were comparable to the experiments. The determined LT_{95} and LT_{99} from the experiments and the kinetic model were in good agreement. The thermal death kinetic model developed in this research would be useful in designing post-harvest RF thermal processes to control *T. castaneum* and similar insects in stored canola seeds and other commodities.

5.7 References

ASAE. 2002. ASAE S352.2, moisture measurements-unground grains and seeds. In ASAE standards. St. Joseph, MI, USA.

Ben-Ialli, A., J. M. Méot, P. Bohuon, and A. Collignan. 2009. Survival kinetics of Ephestia kuehniella eggs during 46–75 C heat treatment. *Journal of Stored Products Research* 45 (3): 206-211.

Birla, S. L., S. Wang, J. Tang, and G. Tiwari. 2008. Characterization of radio frequency heating of fresh fruits influenced by dielectric properties. *Journal of Food Engineering* 89(4): 390-398.

Brusewitz, G. H. 1975. Density of rewetted high moisture grains. *Transactions of the ASAE* 18 (5): 935-938.

Canola Council of Canada. 2014. http://www.canolacouncil.org/markets-stats/industry-overview/. (Oct, 23, 2015).

Canola Watch. 2015. http://www.canolawatch.org/2011/05/09/estimating-flea-beetle-damage-in-canola/. (Oct, 23, 2015).

Gao, M., J. Tang, Y. Wang, J. Powers, and S. Wang. 2010. Almond quality as influenced by radio frequency heat treatments for disinfestation. *Postharvest Biology and Technology* 58: 225–231.

Griffin, J. P. 1988. Montreal Protocol on Substances That Deplete the Ozone Layer. In Int'l L. (Vol. 22, p. 1261).

Hallman, G. J., and D. L. Denlinger. 1998. Temperature sensitivity in insects and application in integrated pest management. Westview Press, Inc., NY, USA, p. 7-53.

Heather, N. W., and G. J. Hallman. 2008. Pest management and phytosanitary trade barriers. CABI, Oxfordshire, UK.

Jiao, S., J. A. Johnson, J. Tang, G. Tiwari, and S. Wang. 2011. Dielectric properties of cowpea weevil, black-eyed peas and mung beans with respect to the development of radio frequency heat treatments. *biosystems engineering* 108 (3): 280-291.

Johnson, J. A., S. Wang, and J. Tang. 2003. Thermal death kinetics of fifth-instar Plodia interpunctella (Lepidoptera: Pyralidae). *Journal of Economic Entomology* 96 (2): 519-524.

Johnson, J. A., K. A. Valero, S. Wang, and J. Tang. 2004. Thermal death kinetics of red flour beetle (Coleoptera: Tenebrionidae). *Journal of economic entomology* 97 (6): 1868-1873.

Lagunas-Solar, M. C., Z. Pan, N. X. Zeng, T. D. Truong, E. Khir, and K. S. P. Amaratunga. 2007. Application of radio frequency power for non-chemical disinfestations of rough rice with full retention of quality attributes. *Applied Engineering in Agriculture* 23 (5): 647–654.

Shimoda, M., J. Cocunubo-Castellanos, H. Kago, M. Miyake, Y. Osajima, and I. Hayakawa. 2001. The influence of dissolved CO2 concentration on the death kinetics of Saccharomyces cerevisiae. *Journal of Applied Microbiology* 91 (2): 306-311.

Shrestha, B., D. Yu, and O. D. Baik. 2013. Elimination of Cruptolestes Ferrungineus S. in Wheat by Radio Frequency Dielectric Heating at Different Moisture Contents. *Progress In Electromagnetics Research* 139: 517-538.

Sinha, R. N., and F. L. Watters. 1985. Insect pests of flour mills, grain elevators, and feed mills and their control. Agriculture Canada, Ottawa, Canada (No. 1776).

Tang, J., J. N. Ikediala, S. Wang, J. D. Hansen, and R. P. Cavalieri. 2000. High-temperature-short-time thermal quarantine methods. *Postharvest Biology and Technology* 21 (1): 129-145.

USDA Foreign Agricultural Service. 2015. Production, Supply and Distribution Online Database, query for Commodity: "Oilseed, Rapeseed"; Data Type: "Production"; Country: "All countries"; Year: "2015", (Feb, 9, 2016).

Wang, S., J. N. Ikediala, J. Tang, and J. D. Hansen. 2002a. Thermal death kinetics and heating rate effects for fifth-instar Cydia pomonella (L.) (Lepidoptera: Tortricidae). *Journal of Stored Products Research* 38 (5): 441-453.

Wang, S., J. Tang, J. A. Johnson, and J. D. Hansen. 2002b. Thermal-death kinetics of fifth-instar Amyelois transitella (Walker) (Lepidoptera: Pyralidae). *Journal of Stored Products Research* 38 (5): 427-440.

Wang, S., and J. Tang. 2004. Radio frequency heating: a potential method for post-harvest pest control in nuts and dry products. *Journal of Zhejiang University Science* 5 (10): 1169-1174.

Yu, D., B. Shrestha, and O. Baik. 2016a. Radio frequency (RF) control of red flour beetle (*Tribolium castaneum*) in stored rapeseeds (*Brassica napus* L.). Submitted to *biosystems engineering* 151: 248-260.

Yu, D., B. Shrestha, and O. D. Baik. 2016b. Temperature distribution in a packed-bed of canola seeds with various moisture contents and bulk volumes during radio frequency (RF) heating. *biosystems engineering* 148: 55-67.

CHAPTER 6

COMPUTER SIMULATION OF HEAT TRANSFER FOR DISINFESTATION OF RED FLOUR BEETLE (*TRIBOLIUM CASTANEUM*) IN STORED CANOLA SEEDS (*BRASSICA NAPUS* L.) BY RADIO FREQUENCY HEATING

Submitted to *Engineering in Agriculture, Environment and Food* (2016).

Contribution of this paper to overall study

A feasibility study based on computer simulation for RF selective heating of the red flour beetle in the stored canola seeds has not been reported yet. Therefore, in this paper a computer simulation model for the RF heating of the stored canola seeds infested with the red flour beetles was developed (specific objective 9), the simulated and the measured temperature profiles of the stored canola were compared (specific objective 10), and the selective RF heating of the red flour beetle in the stored canola seeds was analyzed using simulation concepts (specific objective 11). The developed simulation model was useful for further simulations in improving the RF heating uniformity in the seeds in Chapter 7 and the model can be used to determine the optimum condition of the scaled-up RF heating unit equipped with auxiliary equipment (a rotating helix, different shapes and sizes of the sample holders and electrodes, etc) for improving RF heating uniformity in the canola seeds. All the simulation works in this chapter were conducted and the journal paper manuscript was drafted by myself.

6.1 Abstract

The RF selective heating of red flour beetle (*Tribolium castaneum*) in two different volumes of bulk canola seeds (*Brassica napus* L.) at 5%, 7%, 9%, and 11% moisture contents (MC) using a 1.5 kW, 27.12 MHz RF heating unit was simulated using a finite element method-based commercial simulation package (COMSOL Multi-physics). The electric field formation, dielectric heat generation, non-isothermal fluid flow, and heat transfer including surface to surface radiation were coupled. The simulated and the measured temperatures of the seeds were compared with the different MCs and volumes of the seeds. Similar comparison was also conducted for the insects and the seeds. The differences between the simulated and the measured temperatures of the seeds were not more than 17.4%, 13.4%, 8.08%, and 19.0% for the small volume seeds and 14.8%, 15.6%, 19.5%, and 18.8% for the medium volume seeds at 5%, 7%, 9%, and 11% MCs, respectively. Non-uniform RF heating of the seeds was observed regardless of the MC and the volume of the seeds. The RF selective heating of the insects was most effective for the small volume seeds at 11% MC. The temperature of the insects was 14.6℃ (maximum) higher than the temperature of the seeds. The RF selective heating of *T. castaneum* in the canola seeds could be improved with a proper design of RF applicator that minimizes the non-uniformity of heating.

6.2 Nomenclature

A	electrode area (m^2)		
C_p	specific heat ($J \cdot kg^{-1} \cdot K^{-1}$)	nitf	conjugate heat transfer
BiCGStab	biconjugate gradient stabilized	p	pressure (Pa)
d	diameter (mm)	RF	radio frequency
DTF	dielectric test fixture	R_p	resistance
ec	electric current	SS	small volume of the seeds
F	frequency (MHz)	t	electrode gap (m)
F	buoyancy force vector ($N \cdot m^{-3}$)	T	Temperature of the sample (K)
F_{amb}	ambient view factor	T_{amb}	ambient temperature in directions included in F_{amb}

G	irradiative flux from both the ambient surroundings and from other surfaces ($W \cdot m^{-2}$)	u	velocity field in the x-direction ($m \cdot s^{-1}$)
G_m	mutual irradiation coming from other objects ($W \cdot m^{-2}$)	V	electric potential between two electrodes (V)
GMRES	generalized minimum residual	w. b.	wet basis
h	height (mm)	*Greek symbols*	
I	identity matrix	ε	surface emissivity of the sample
j	$\sqrt{-1}$	ε'	dielectric constant
J	Surface radiosity of the sample ($W \cdot m^{-2}$)	ε''	dielectric loss factor
k	thermal conductivity ($W \cdot m^{-1} \cdot K^{-1}$)	ρ	density ($kg \cdot m^{-3}$)
MS	medium volume of the seeds	σ	electric conductivity of the sample ($S \cdot m^{-1}$)
MDSC	modulated differential scanning calorimetry	σ	Stefan-Bolzmann constant (5.6704×10^{-8}, $W \cdot m^{-2} \cdot K^{-4}$)
MC	moisture content (%, wet basis)	$\|E\|$	electric field strength ($W \cdot m^{-1}$)

6.3 Introduction

Canola (*Brassica Sp*.) is one of the major oilseeds produced and consumed worldwide. Approximately 67.7 million metric tons of canola seeds were produced in 2015 – 2016 around the world (USDA Foreign Agricultural Service 2015). Major producing countries of the canola seeds are Austria, Canada, China, European Union, India, and the United States. Around 90% of the canola seeds produced in Canada is exported to worldwide markets. This accounts for $ 19.3 billion (including 249,000 jobs and $ 12.5 billion in wages) of the Canadian economy (Canola Council of Canada 2014). Insect pest infestation is a major consideration in international trade of the food products that make hurdles to export market (Gao et al. 2010). An annual loss of 8 to 10% of the oilseeds due to insect pest resulting in millions of dollars losses in the Canadian economy has been reported (Canola Watch 2015). One of the most harmful insect pest in the oilseeds worldwide is *T. castaneum* (size ca. 3×0.5×0.3 mm) (Canadian Grain Commission 2013; Mills and Pedersen 1990). These insect pests spoil and decompose the oilseeds.

To disinfest the insect pest in the grains, many practical methods including chemical (pesticides and fumigants) and non-chemical (hot air method, cold storage, and mechanical pressure) have been applied. The chemical fumigation with methyl bromide has been traditionally regarded as one of the practical treatments for disinfestation of various insect pest due to its cost effectiveness (Barreveld 1993). It has, however, been prohibited since Montreal Protocol due to destructive effect to the ozone layer and health hazards from excessive insecticide residues (Birla et al., 2008a; Griffin 1988; Wang and Tang 2004). On the top of that, the conventional non-chemical methods are slow and inefficient (hot air method), or takes long treatment time (cold storage technique) or requires to identify insect and grains (insecticides) (Heather and Hallman, 2008; Wang and Tang, 2004).

Radio frequency (RF) heating provides volumetric and selective heating, and it can be used as an alternative to the existing disinfestation methods for various agricultural products (Jiao et al. 2011; Tang et al. 2000). The volumetric heating by RF energy can achieve faster heating resulting in shorter heating time than the conventional heating methods. The selective heating of insects depends upon the electrical, physical and thermal properties of the grain and the insects themselves. Usually, grains have lower dielectric properties than those of the insect pest, and it leads to a relatively faster heating of the insects compared to the treated grains (Guo et al. 2010). There is potential for disinfestation of the insect pest using the RF heating without significant quality degradation of the host grain. Wang et al. (2007) achieved 100% mortality of orangeworm larvae in walnuts keeping most of its initial quality at 52℃ for 5 min using RF heating (25 kW, 27 MHz). Lagunas-Solar et al. (2007) reported that 99% mortality of Angoumois grain moths and 100% mortality of lesser grain borers were achieved at 55 to 60℃ for 5 min and 60℃ for 1 h of the RF heating (100 W, 27.18 MHz) in rice without significant changes of the rice qualities. The RF heating was effectively used to control cowpea weevil in chickpea, lentil and green pea without serious thermal degradation of the product quality (Jiao et al. 2012; Wang et al. 2010).

The RF heating is governed by the electrical, the physical, and the thermal properties of the materials and the features of the electromagnetic energy. The effect of those properties on the RF selective heating of the insects can be studied by actual experiments requiring enormous amounts of effort, time, and resources. On the other hand, computer simulation is a useful tool as rapid, cost-effective, and flexible analysis to understand the effect of materials' and insects' properties on the RF selective heating of the insects. It has been conducted to help understand the complexity

of RF heating of various food materials. Alfaifi et al. (2014) simulated RF dielectric heating (6 kW, 27.12 MHz) of dry raisins using commercially available finite element method-based software, COMSOL Multiphysics and validated the simulation model with actual experiment data. Chen et al. (2015) analyzed mixing effects on the temperature distribution of wheat samples during RF heating (6 kW, 27.12 MHz) by the help of computer simulation. Huang et al (2015) conducted computer simulation to study feasibility of RF selective heating of larvae of Indianmeal moth in soybeans using a 6 kW, 27.12 MHz RF heating system. Jiao et al. (2015) developed a computer simulation model to study influences of the wheat kernel size and position on RF heating (12 kW, 27.12 MHz) uniformity using COMSOL and to explore a possibility of controlling insects or microorganisms in wheat kernel. Uyar et al. (2015) also conducted computer simulation to study temperature distributions during defrosting of frozen lean beef with phase change which was treated by a custom built RF system (50Ω). However, a feasibility study based on computer simulation for RF selective heating of *T. castaneum* in stored canola seeds has not reported yet.

Therefore, the objectives of this research were 1) to develop a computer simulation model for the RF heating of the stored canola seeds infested with *T. castaneum*, 2) to compare the simulated and the measured temperature profiles of the stored canola and 3) to investigate the RF selective heating of *T. castaneum* in the stored canola seeds via simulation.

6.4 Materials and methods

6.4.1 Materials and sample preparation

6.4.1.1 Canola seed

The top quality Canadian canola seeds (B. *napus* L.) at 7% (wet basis, w. b.) MC was supplied by our industrial partner Viterra Inc., Canada. MC of the seeds was determined using the standard method (ASAE 2002; Brusewitz 1975). The canola seeds at 5% MC was prepared drying the seeds at the initial MC using a hot air oven (Despatch, Despatch Industries, MN, USA) at 40℃, and the seeds at 9% and 11% MCs were prepared by uniformly spraying pre-calculate amounts of distilled water to the seeds at the initial MC. The prepared seeds were stored at 4℃ in a cold storage until used. Two sample holders (small : d = 50 mm, h = 100 mm and medium : d = 150 mm, h = 100 mm) made of RF transparent material (polycarbonate) were used for RF heating. The cylindrical

sample holders were chosen because the preliminary tests showed that the cylindrical shape resulted in better heating uniformity during the RF heating.

6.4.1.2 Insect cultures

The adult *T. castaneum* collected from the Agriculture and Agri-Food Canada / University of Manitoba, Canada were reared for 10 weeks in a mixture of wheat (15% MC) and wheat germs in a ratio of 7 to 3 by weight. The reared insects were collected using a suction assembly, and carbon dioxide gas was used to anesthetize the insects as required such as in measuring dielectric properties. The procedures of insect cultures were described in details in Shrestha & Baik (2013). To calculate the initial MC of the insect, five empty aluminum dishes were placed in a hot air oven at 105℃ for an hour and cooled in a desiccator before weighing them. Each of the five dishes containing 1 g of insects was heated at 105℃ for 16 h. The dishes with dried insects were covered with lids before taking out of the oven. The samples were then cooled in the desiccator before weighing. The weight of the dried insects was measured with an Ohaus analytical scale with an accuracy of ± 0.0001 g. An average of five replicates was used.

6.4.1.3 Properties of the insect

6.4.1.3.1 Density

The tapped-bulk density (ρ) of the insects was calculated by measuring mass of a known volume of the insects in a precision graduated cylinder of the known volume (1 mL ± 0.05 mL). The mass of the insects was measured after dropping the cylinder five times onto the ground from a 10 mm height and leveling out the top surface with a little shake. An average of quintuplicate was used.

6.4.1.3.2 Specific heat and thermal conductivity

A modulated differential scanning calorimetry (MDSC) (Q2000, TA Instruments, Inc., New Castle, Del) was used to measure the specific heat (C_p) of the insects as a rapid and accurate method (Yu et al., 2015a). The MDSC was calibrated using a standard sapphire at the temperature of interest. A ratio of the measured specific heat of the sapphire to its standard specific heat was used to calculate a calibration constant. A blank aluminum pan for reference and an identical hermetically sealed aluminum pan including 10 mg (± 0.01 mg) of anesthetized insects were placed

into the MDSC. Heating rate of 5°C min^{-1} was determined from the preliminary tests. The specific heat of the insects was measured at 30 to 80°C. An average of quintuplicate was used.

A KD2 thermal properties analyzer (Decagon Devices, Inc., Pullman, WA) was used to measure the thermal conductivity (k) of the insects at bulk density as a function of temperature. The analyzer was calibrated using a calibration factor - the ratio of the measured to the standard value of k of 0.5% agar-water mixture (Ochsner et al. 2003). A brass sample holder (d = 25.3 mm × h = 153 mm) was filled with a known mass of the anesthetized insects. The mass was calculated using the volume of the sample holder and the density of the insects at a desired temperature. The holder was softly tapped three times on the ground before placing it in a temperature and humidity chamber with an accuracy of ± 0.1°C (SH-641, Espec Corp., Osaka, Japan). The sample was heated to the desired temperature. From the preliminary experiments it was found that an hour was sufficient to heat the samples to the target temperatures regardless of their MCs. The KD2 was inserted into the sample at the desired temperature, and turned it on to measure the k values of the samples.

6.4.1.3.3 Dielectric properties

A computer controlled precision LCR (Inductance, Capacitance, and Resistance) device (4285A, Agilent Technologies, Palo Alto, CA), a dielectric test fixture (DTF) (16452, Agilent Technologies, Palo Alto, CA), and other peripheral devices were used to measure the capacitance (C_p) and the resistance (R_p) of the insects at different temperatures (Fig. 6. 1).

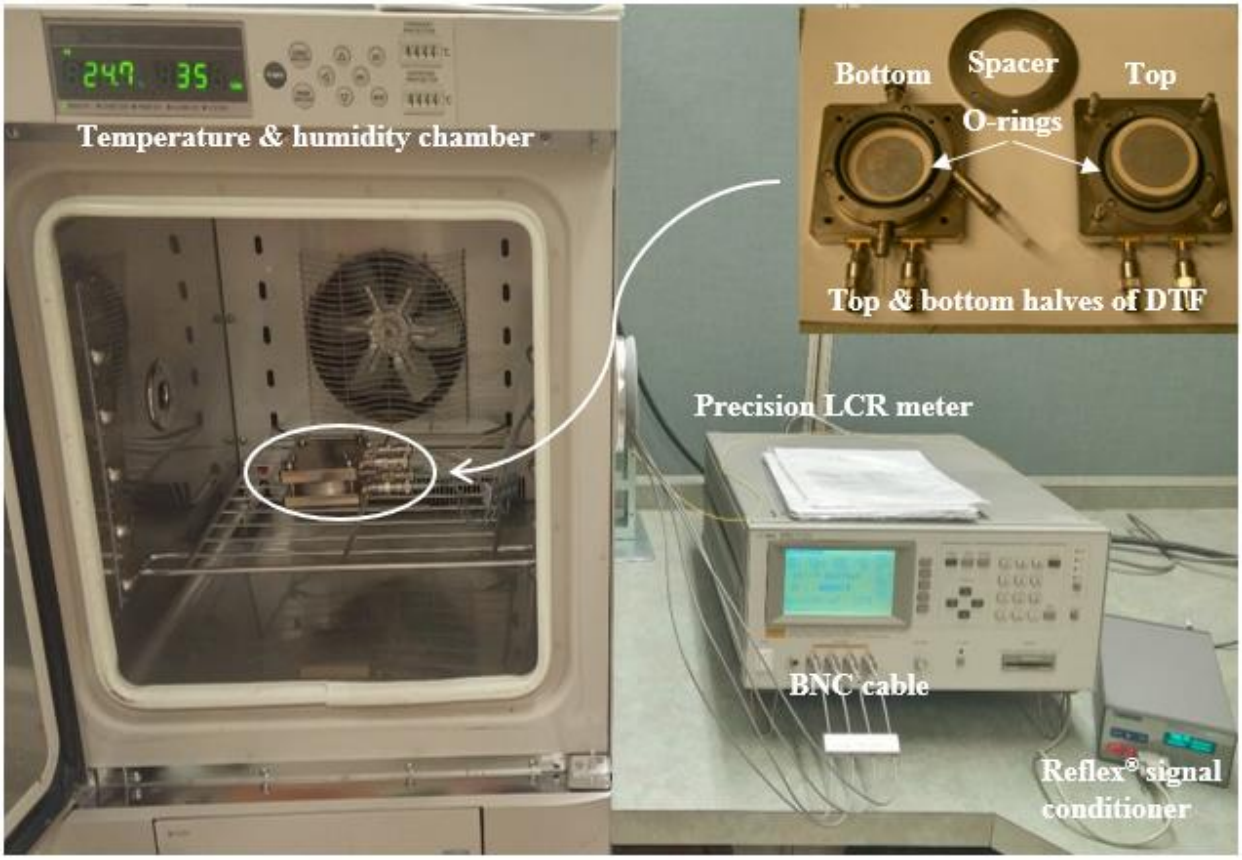

(a)

(b)

(c)

Figure 6. 1. The precision LCR (Inductance, Capacitance, and Resistance) device, the temperature and humidity chamber, the Reflex® signal conditioner, the top and bottom halves of the dielectric test fixture (a), *T. castaneum* in the bottom half of the dielectric test fixture (b), and the closed assembled dielectric test fixture (c).

A 1.5 mm thick factory supplied spacer was used to measure dielectric properties of 0.5 mL bulk insects. The LCR device was calibrated using a 1 m cable and a short termination to minimize biased errors (Agilent 2001). The fixture including two O-rings, and the spacer were washed and rinsed using warm soap and the distilled water, and then completely dried before they were used. The anesthetized insects were uniformly spread in the bottom fixture (Fig. 6. 1), and the fixture was tightly closed. The fixture containing the insects was placed on the shelf inside the temperature and humidity chamber followed by properly connected to a 1 m 4-terminal BNC cable (16452-61601, Agilent Technologies, Palo Alto, CA). The other ends of the cable were connected to the LCR device. The fixture was left in the chamber for an hour at the desired temperature for a thermal equilibrium.

The dielectric constant (ε') and the dielectric loss factor ($\varepsilon^{"}$) were calculated using the measured C_p and R_p as shown in Eq. (6.1) and (6.2).

$$\varepsilon' = \mathrm{t}C_p/\mathrm{A}\varepsilon_0 \tag{6.1}$$

$$\varepsilon^{"} = \mathrm{t}/2\pi f \mathrm{A}\varepsilon_0 R_p \tag{6.2}$$

where t = the electrode gap (m), C_p = the parallel capacitance (F), A = the electrode area (m^2), ε_0 = the air permittivity (8.85×10^{-12} F·m^{-1}), f = the frequency (MHz), and R_p = the parallel resistance (Ω). Average of triplicate was used to minimize the random error.

6.4.1.4 RF heating system

A 1.5 kW, 27.12 MHz RF system (Strayfield Fastran, Berkshire, England) with the square shaped parallel electrode (top: 250 mm × 250 mm) was used to disinfest the canola seeds (Fig. 6. 2).

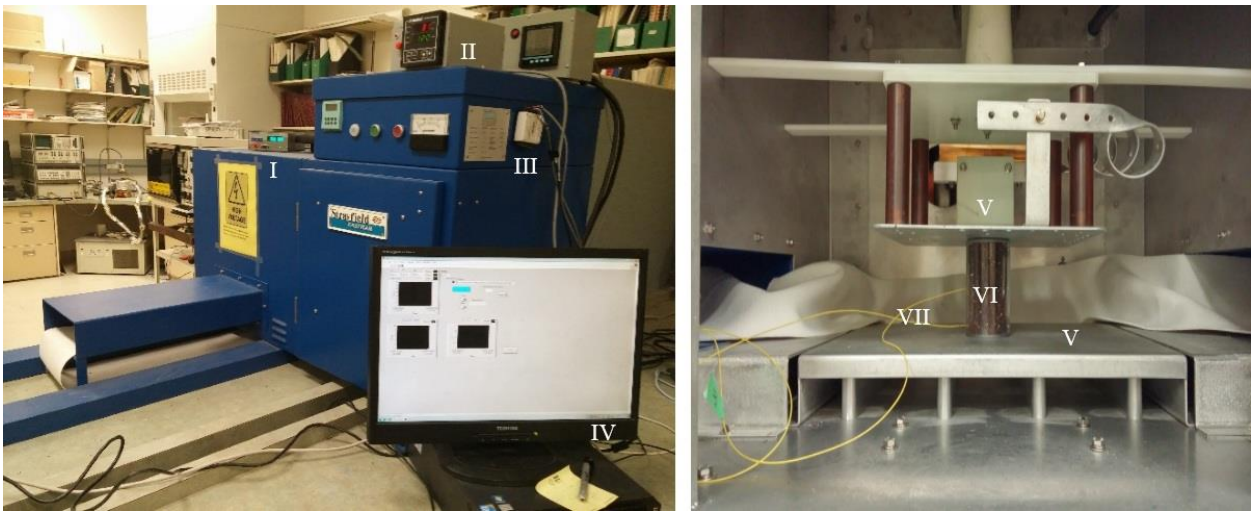

(a) (b)

Figure 6. 2. The side and back (a) and the inside (b) view of the RF heating unit ; I : the Reflex® signal conditioner, II : the multifunction power meter, III : the $I \cdot O^{-1}$ device, IV : the data acquisition software, V : the two electrodes, VI : the canola seeds in a small sample holder, VII : T1™ fibre optic temperature sensors (Yu et al. 2015a).

The sample was placed at the center of the bottom electrode which was grounded (0 Volt). The top electrode was attached to a crank of which the handle was accessible from the top of the enclosure. The desired gap between the electrodes was acquired by turning the crank. The RF source was connected to the top electrode through a metallic stripe. The airgap of 1 mm between the small sample holder and the top electrode prevented the electric arcing. The airgap of 15 mm was required for the medium holder. The T1™ fibre optic temperature sensors and the Reflex® signal conditioner with an accuracy of ± 0.8℃ (Neoptix, Québec City, Québec, Canada) were used to measure the temperature of the seeds. The sensors were inserted at nine (small holder) and twelve (medium holder) locations as shown in Fig. 6. 3.

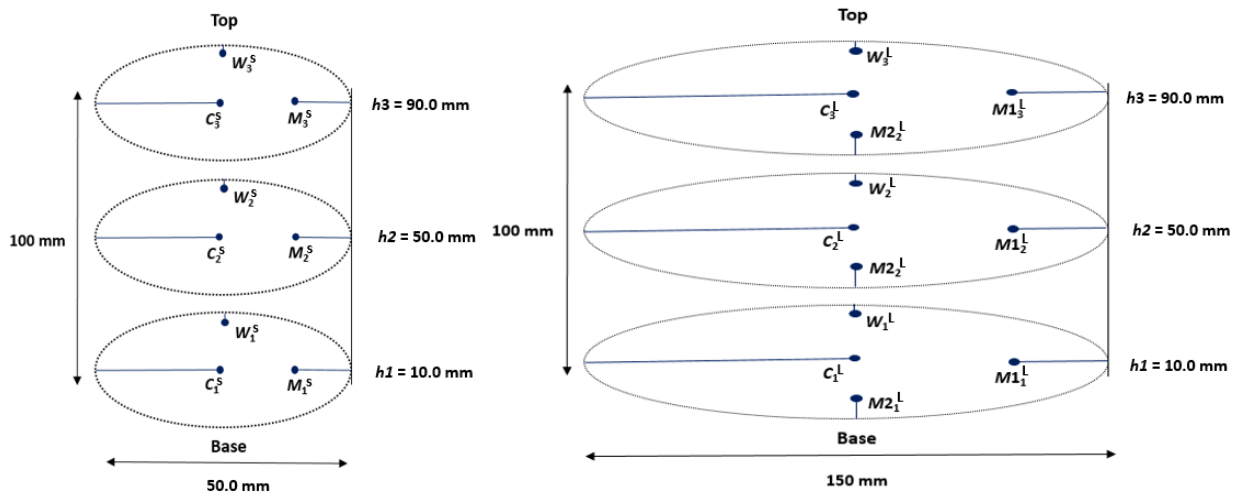

(a) (b)

Figure 6. 3. The locations of the temperature sensors and the dimensions of the small (a) and the medium (b) sample holders : $W^S = W^L = 1$ mm, $M^S = 12.5$ mm, $M2^L = 16$ mm, $M1^L = 32.5$ mm, $C^S = 25$ mm, and $C^L = 75$ mm away from the inner wall of the sample holder at the heights of $h1 = 10$ mm, $h2 = 50$ mm, and $h3 = 90$ mm from the base (Yu et al. 2016a).

The seeds infested with the insects were heated from 25 (initial temperature) to 80℃ (end temperature) by RF heating without holding time and its temperature was measured during RF heating. This temperature range was chosen to consider that 100% mortalities of all life stages of *T. castaneum* infesting the bulk canola seeds were achieved at the end temperature range (60 to 80℃) of the hottest spot of the seeds by RF heating (Yu et al. 2016a). RF exposure times of the canola seeds were measured while the seeds were heated up to the end temperature. The temperature of the sample was transferred automatically to the data acquisition software (NI LabVIEW, National Instruments, TX) through the I/O device (NI USB 6008, National Instruments, TX). All readings were displayed and recorded every 2 s. More information on the RF heating system and the measurement of the temperatures of the bulk canola seeds can be found in Yu et al. (2016b).

6.4.2 Development of the computer simulation model

6.4.2.1 Geometry

Only one quadrant of the RF heating unit was considered due to a 3D axial symmetry to save simulation time, and the top half of the empty metallic enclosure was excluded with a negligible change in the electric fields. The geometries of the RF heating unit with the small and the medium holders containing the canola seeds and *T. castaneum* that were used for the simulation are illustrated in Fig. 6. 4. The locations of the insects were the same as those shown for the temperature sensors in Fig. 6. 3.

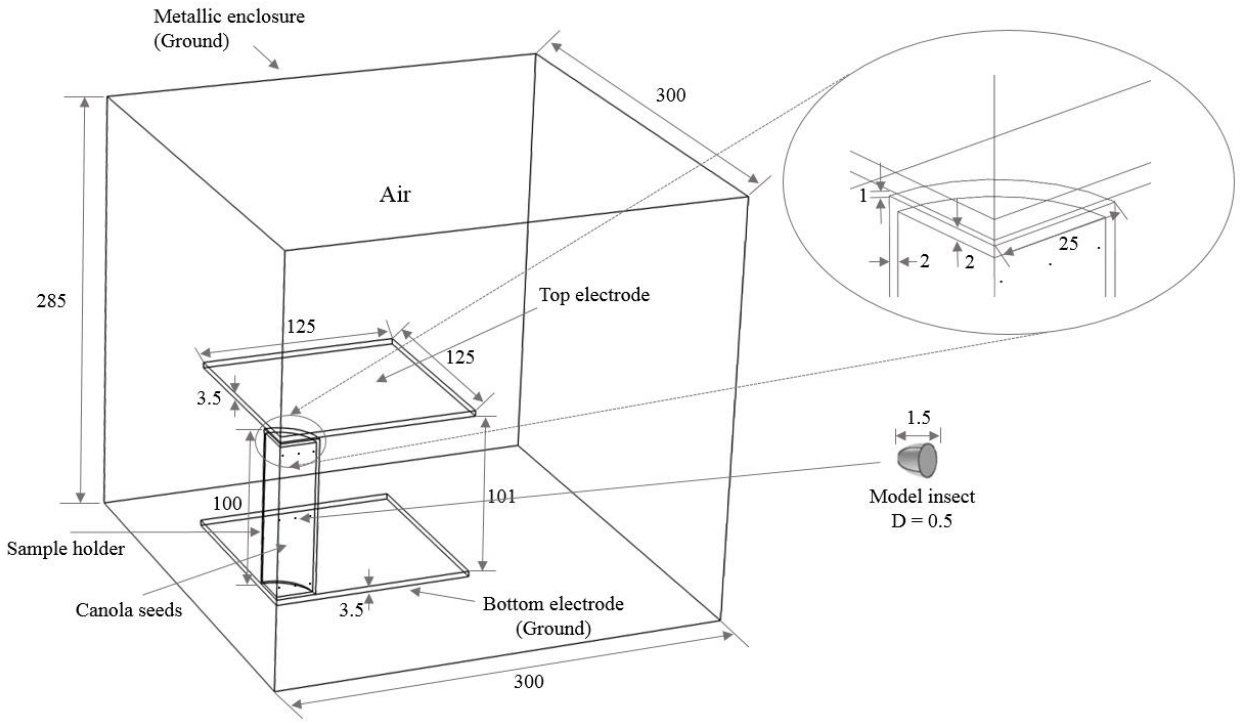

(a)

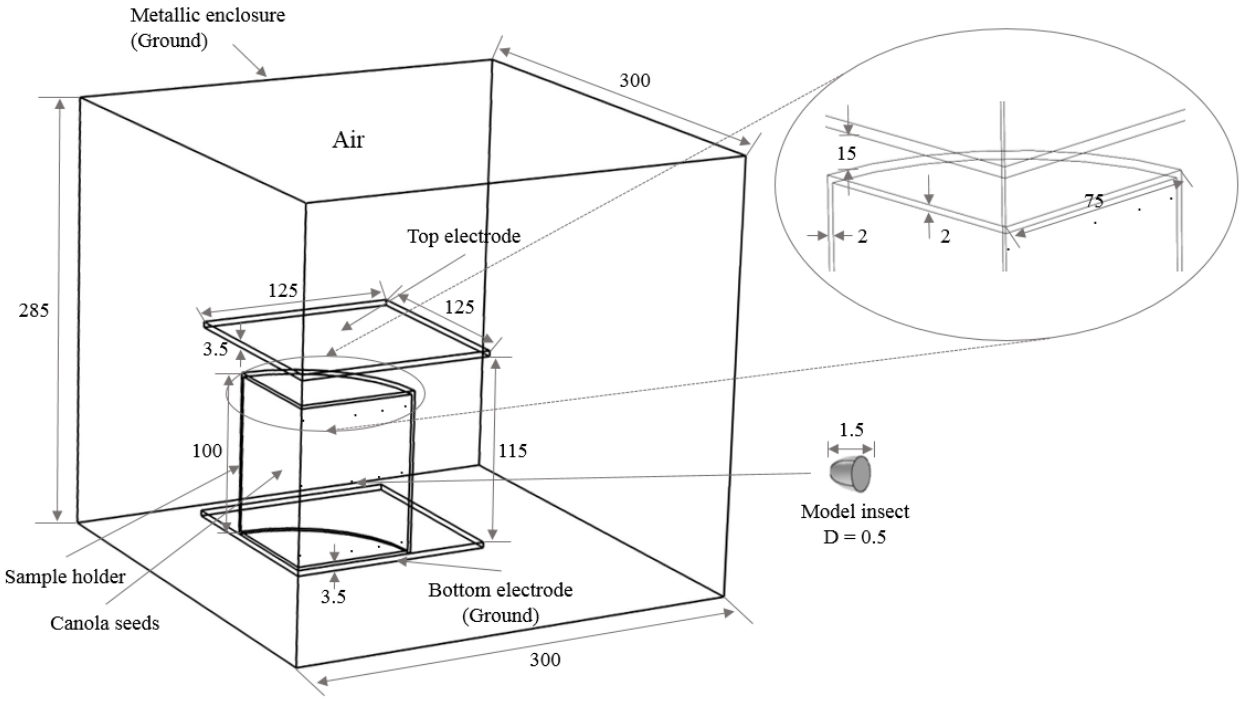

(b)

Figure 6. 4. The one quadrant of the RF heating chamber with the small (a) and the medium (b) volumes infested canola seeds with *T. castaneum* in the sample holders (unit : mm).

6.4.2.2 Material properties

The dielectric and the thermo-physical properties of the canola seeds were obtained from Yu et al. (2015a, b, and 2016b), and the properties of air and aluminum at room temperature (25℃) were taken from the COMSOL material library file. The properties of polycarbonate was obtained from Shrestha et al. (2016).

6.4.2.3 Governing equations

The combined multi-physics models – coupling of an electric current (*ec*) model and a conjugate heat transfer (*nitf*) model (non-isothermal flow/heat and surface-to-surface radiation) were used in the simulations.

6.4.2.3.1 Electric current (*ec*)

A Laplace equation with a quasi-static assumption can be obtained by simplifying the full Maxwell's equation when RF wavelength (11 m) is larger than the RF cavity size (0.6 m × 0.6 m × 0.56 m) (Birla et al. 2008b) :

$$-\nabla \cdot \left((\sigma + j2\pi f \varepsilon_0 \varepsilon')\nabla \mathrm{V}\right) = 0 \tag{6.3}$$

where σ = the electric conductivity of the sample (S·m^{-1}), $j = \sqrt{-1}$, f = the frequency (Hz), ε_0 = the vacuum permittivity (8.854 × 10^{-12}, F·m^{-1}), ε' = the dielectric constant of the sample, and V = the electric potential between two electrodes (V) (Choi et al., 1991). The electric potential (V) within the system was calculated using the Laplace equation, and was used to determine the electric field ($E = -\nabla \mathrm{V}$). The RF power absorbed into the dielectric sample per volume (Q_{abs}, W·m^{-3}) was given by Choi et al. (1991):

$$Q_{abs} = 2\pi f \varepsilon_0 \varepsilon'' |E|^2 \tag{6.4}$$

where ε'' = the dielectric loss factor of the sample, $|E|$ = the electric field strength (W·m^{-1}).

6.4.2.3.2 Conjugate heat transfer

A temperature increment in the treated material can be described by the unsteady heat transfer equation as shown in Eq. 6.5.

$$\rho C_p u \nabla \mathrm{T} = \nabla \cdot (k \nabla \mathrm{T}) + Q_{abs} \tag{6.5}$$

where ρ = the density (kg·m^{-3}), C_p = the specific heat at the constant pressure (J·kg^{-1}·K^{-1}), u = the velocity field in the x-direction (m·s^{-1}), T = the temperature of the sample (K), and k = the thermal conductivity (W·m^{-1}·K^{-1}). The non-isothermal flow of the air in the system was determined using the continuity (Eq. 6.6) and the momentum transport (Eq. 6.7).

$$\nabla \cdot (\rho \mathrm{u}) = 0 \tag{6.6}$$

$$\rho(\mathrm{u} \cdot \nabla)\mathrm{u} = \nabla \cdot \left[-\mathrm{pI} + \mu\left(\nabla \mathrm{u} + (\nabla \mathrm{u})^{\mathrm{T}} - \frac{2}{3}\mu(\nabla \cdot \mathrm{u})\mathrm{I}\right)\right] + \mathrm{F} \tag{6.7}$$

where p = the pressure (Pa), I = the identity matrix, and F = the buoyancy force vector (N·m^{-3}). Eqs. (6.5) and (6.7) can be applied to y and z-directions by substitution of v and w for u, respectively. The Boussinesq approximation was applied to calculate the buoyancy force vector in the z-direction where the air density varied due to the change in the volume force by temperature difference of the flow fields. The prescribed radiosity which was chosen from the subcategory of the surface to surface radiation of the conjugate heat transfer model was applied to solve the radiative heat transfer between the sample and the electrodes and the metallic enclosure.

$$J = \rho G + \varepsilon \sigma T^4 \quad (6.8)$$

$$G = G_m + F_{amb}\, \sigma T_{amb}^4 \quad (6.9)$$

Substitution of the G from Eq. (6.9) into Eq. (6.8) yields

$$J = \rho(G_m + F_{amb}\, \sigma T_{amb}^4) + \varepsilon \sigma T^4 \quad (6.10)$$

Eq. (6.10) was transformed into Eq. (6.11) based on the assumption that the sample is a gray body

$$J = (1 - \varepsilon)(G_m + F_{amb}\, \sigma T_{amb}^4) + \varepsilon \sigma T^4 \quad (6.11)$$

where J = the surface radiosity of the sample ($W \cdot m^{-2}$), G = the irradiative flux from both the ambient surroundings and from other surfaces ($W \cdot m^{-2}$), ε = the surface emissivity of the sample, σ = the Stefan-Bolzmann constant (5.6704×10^{-8}, $W \cdot m^{-2} \cdot K^{-4}$), G_m = the mutual irradiation coming from other objects ($W \cdot m^{-2}$), F_{amb} = The ambient view factor, and T_{amb} = The ambient temperature in the directions included in F_{amb} (initial ambient temperature was 298.15K). The G_m and F_{amb} values were automatically determined in the simulation using geometry factors (the distance and the angle between the samples, and the surface area of the samples) and the local temperature of the surrounding.

6.4.2.4 Initial and boundary conditions

As mentioned above only one quadrant of the RF heating unit was considered in the simulations (Fig. 4). The boundary conditions of thermal insulation ($\nabla T = 0$) and electrical insulation ($\nabla E = 0$) were assigned to vertical cut sections of the RF heating unit with the samples in the *nitf* and *ec* models, respectively. The metallic enclosure was assigned as the electrical and the thermal insulations ($\nabla E = 0$ and $\nabla T = 0$). The heat loss during RF heating from the outer boundary of the sample holder to the surrounding air was simulated by the external natural convection (convection through the surrounding air) setting which was selected from the subcategories of the conjugate heat transfer model. The electric potential distribution on the electrodes was assumed to be uniform because the dimension (0.25 m × 0.25 m) of the electrodes was sufficiently smaller than the 30% (3.3 m) of the RF wavelength (11 m) used in the RF heating system (Tiwari et al. 2011a).

The top electrode was set at an arbitrary potential V_0, and the bottom electrode connected to the enclosure was set at ground potential (V = 0). The measurement of the actual electric voltage on the top electrode was difficult during the RF heating without interference to the electric field (Marshall and Metaxas 1998). Therefore, preliminary simulations were run with different electric voltages on the top electrode for different volumes and MCs of the seeds. The electric potentials

which produced the closest actual dielectric properties of the seeds at the hottest spot were assumed the right electric potentials as the dielectric properties of the sample mainly affect the temperature increments of the sample (Tiwari et al. 2011a; Birla et al. 2008b). The initial temperature and pressure were set as 25℃ and 101,300 Pa.

6.4.2.5 Mesh generation

The intrinsic normal type of mesh in the COMSOL package was adopted for meshing the geometry of the RF heating region containing the samples. Meshing size affects the accuracy of simulation results. Normally, more accurate results would be obtained by a smaller element. But it would require much longer computation time. Therefore, the normal size of the mesh was chosen among 9 different sizes (coarse, normal, fine, etc) of the mesh as the computation time was the shortest compared to that with finer sizes of the mesh and the difference of the simulated maximum seed temperatures between using the normal size and finer sizes (fine, finer, extra finer, and extremely finer) of the mesh was lower than 0.1%, respectively. (Tiwari et al. 2011a). Coarser sizes of the mesh produced higher differences of the simulated maximum seed temperatures than 0.1%. The finer mesh was generated near the corner and within the narrow region for better accuracy of the simulation results.

6.4.2.6 Simulation process

A commercial package, COMSOL Multiphysics (v4.2, Burlington, MA, USA) based on a finite element method was used to simulate the RF selective heating of *T. castaneum* in the stored canola seeds. The simulation package was installed and run on a ThinkCentre M90p with dual-core, 3.2 GHz Intel® Core™ i5 processors and 8 GB memory running on a Window 7 Professional operating system (64 bit). The time dependent setting and the fixed frequency domain were applied to the *nitf* and the *ec* models, respectively. The generalized minimum residual (GMRES) and the biconjugate gradient stabilized (BiCGStab) iterative methods were used to solve the *nitf* and the *ec* models. The relative and the absolute tolerances were set as 0.001 for both and the initial and the maximum time steps were 0.001 and 0.1 s, respectively.

6.4.3 Regression models

The stepwise regression analysis in SPSS 20.2 (SPSS Inc., Chicago, IL, USA) was used to develop regression models for each density, specific heat, thermal conductivity, and dielectric properties of the canola seeds and *T. castaneum* as input parameters in COMSOL simulations. The regression models were functions of temperature only as mass transfer was not considered in this study. Each regression model was separately developed for each MC of the seeds using each data set of seed MC.

6.5 Results and discussion

6.5.1 Properties of materials

The measured dielectric properties, C_p, k, and ρ of the insect are presented in Table 6. 1.

Table 6. 1. The dielectric, physical, and thermal properties of *T. castaneum* at various temperatures.

Temp (℃)	ε'	ε''	C_p (J·kg^{-1}·K^{-1})	k (W·m-1·K^{-1})	ρ (kg·m^{-3})
30	10.97 ± 0.005	2.786 ± 0.005	3.797 ± 0.401	0.030 ± 0.001	484.4 ± 9.125
40	12.50 ± 0.020	5.183 ± 0.028	4.405 ± 0.420	0.043 ± 0.005	433.4 ± 7.283
50	16.22 ± 0.035	7.652 ± 0.001	5.013 ± 0.495	0.053 ± 0.005	389.0 ± 4.312
60	24.43 ± 0.026	14.39 ± 0.159	5.940 ± 2.930	0.073 ± 0.005	332.1 ± 15.46
70	27.42 ± 0.040	20.25 ± 0.276	6.475 ± 0.693	0.093 ± 0.005	258.7 ± 1.101
80	31.50 ± 0.033	24.62 ± 0.182	8.480 ± 5.677	0.113 ± 0.005	221.3 ± 2.747

The MC of *T. castaneum* was 48.1 ± 0.78%. It was close to those of other insects (the adult rice weevil and the rusty grain beetle) which were 48.9% and 49.6%, respectively (Nelson et al. 1996; Shrestha and Baik 2013). The C_p and k of the insect increased with increasing temperature whereas the opposite was true for the ρ. At high temperatures, ions and dipoles in the insect exhibit higher lattice vibrations resulting in high k value (Sweat 1986). The C_p, k, and ρ varied from 3.80 to 8.48 $J \cdot kg^{-1} \cdot K^{-1}$, 0.030 to 0.113 $W \cdot m^{-1} \cdot K^{-1}$, and 221 to 484 $kg \cdot m^{-3}$, respectively. The ρ of sawtoothed grain beetle and the lesser grain borer were 462 $kg \cdot m^{-3}$and 490 $kg \cdot m^{-3}$ (Nelson et al. 1998). The measured ε' and ε'' of *T. castaneum* increased with increasing temperature. The increased ε' of the insect at higher temperature was due to an increased ionic conductivity resulting in the increased level of the dielectric dispersion (Nelson and Bartley 2002; Tang et al. 2002). The increased ε'' of the insect at higher temperature was attributed to the higher movement of ions and oscillation of dipoles (Yu et al. 2015b). The ε' and ε'' of the insect ranged from 11.0 to 31.5 and 2.79 to 24.6 over the temperature range of 30 to 80°C, respectively. Similar trends have been reported for lesser grain borers (Nelson 2005), chestnut weevil slurry (Guo et al. 2011), and rusty grain beetles (Shrestha and Baik 2013). The regression models for the dielectric, the physical, and the thermal properties of the canola seed and *T. castaneum* are listed in Table 6. 2 along with the constant values for air, aluminum and polycarbonate.

Table 6. 2. The dielectric, physical, and thermal properties of the materials used in the simulations.

Materials	Properties					
	ε'	ε''	C_p (J·kg^{-1}·K^{-1})	k (W·m-1·K^{-1})	ρ (kg·m^{-3})	ε
Canola seed (5% MC)	-8.469+0.0404*T	67.95-0.434*T+0.0007*T^2	-15541+93.97*T-0.121*T^2+8.685*10^{-7}*T^3	0.092-5.300*10^{-4}*T+1.365*10^{-6}*T^2	1023-1.583*T+4.425*10^{-6}*T3	1.283-0.0009*T
Canola seed (7% MC)	-8.019+0.0397*T	65.30-0.425*T+0.0007*T^2	-15541+93.86*T-0.121*T^2+1.216*10^{-6}*T^3	0.092-7.420*10^{-4}*T+2.009*10^{-6}*T^2	1026-1.583*T+4.332*10^{-6}*T3	1.277-0.0009*T
Canola seed (9% MC)	-7.569+0.0391*T	62.65-0.416*T+0.0007*T^2	-15541+93.68*T-0.121*T^2+1.563*10^{-6}*T^3	0.092-9.540*10^{-4}*T+2.709*10^{-6}*T^2	1032-1.583*T+4.168*10^{-6}*T3	1.271-0.0009*T
Canola seed (11% MC)	-7.119+0.0384*T	60.01-0.407*T+0.0007*T^2	-15541+93.38*T-0.121*T^2+1.911*10^{-6}*T^3	0.092-1.166*10^{-3}*T+3.465*10^{-6}*T^2	1040-1.583*T+3.911*10^{-6}*T3	1.266-0.0009*T
Air[a]	1	0	1200	0.025	1.2	-
Aluminum[a]	1	0	900	160	2700	0.055
Insect	-125.4+0.4461*T	-138.6+0.4603*T	-25.32+0.0947*T	0.0091+0.0168*T	2058-5.191*T	-
Polycarbonate[a]	2.3	0.0028	1250	0.13	1210	0.23

[a] COMSOL material library, V 4.2 (2011)

6.5.2 RF exposure time of canola seeds and meshing the RF heating unit

The RF exposure times for the canola seeds at different MCs and volumes are listed in Table 6. 3.

Table 6. 3. The RF exposure time (s) for the temperature of the hottest spot of the bulk canola seeds reached 80°C.

MC (%, w. b.)	Volume of the canola seeds	
	Small (d = 50 mm × h = 100 mm)	Medium (d = 50 mm × h = 100 mm)
5	1080	1200
7	720	870
9	390	510
11	140	270

The RF exposure time decreased with the seed MC, and increased with the volume of the seeds for the seed samples to reach 80℃ (the hottest spot). These phenomena were attributed to the enhanced ionic conductivity and dipoles in the seeds resulting in increasing ε'' of the seeds. The increased ε'' of the seeds can cause higher RF power dissipation in the seeds (Shrestha and Baik 2013). Total numbers of elements were 84883 (without insects) and 96258 (with insects) for small volume seeds and 96140 (without insects) and 120593 (with insects) for medium volume seeds.

6.5.3 Estimated electric voltage and simulated dielectric properties of canola seeds

The estimated electric voltage on the top electrode is listed in Table 6. 4.

Table 6. 4. The determined electric voltages (V) on the top electrode in the simulations with the volume and the MC of the canola seeds.

MC (%, w. b.)	Volume of canola seeds	
	Small (d = 50 mm × h = 100 mm)	Medium (d = 150 mm × h = 100 mm)
5	1094	1482
7	1071	1467
9	1272	1650
11	1843	1992

The electric voltage increased with the MC (except at 7%) and the volume of the seeds. The voltage ranged from 1094 to 1843 V and 1482 to 1992 V for the small and the medium volumes of the seeds, respectively. The comparison of the dielectric properties of the canola seeds measured at the estimated voltages and from the experiments are shown in Table 6. 5.

Table 6. 5. The measured and the simulated dielectric properties of the canola seeds.

Dielectric constant (ε')												
Temp (℃)	MC (%, w. b.)											
	5%			7%			9%			11%		
	Measured	Simulated	Difference (%)	Measured	Simulated	Difference (%)	Measured	Simulated	Difference (%)	Measured	Simulated	Difference (%)
30	3.84	3.78	1.57	4.21	4.03	4.37	4.37	4.28	2.08	5.03	4.85	3.64
40	4.20	4.19	0.24	4.74	4.52	4.75	4.73	4.70	0.64	5.16	4.92	4.76
50	4.96	4.69	5.60	5.15	4.94	4.16	5.17	5.07	1.95	5.22	5.31	1.71
60	5.23	5.00	4.50	5.33	5.24	1.70	5.68	5.51	3.04	5.76	5.67	1.57
70	5.40	5.39	0.19	5.74	5.61	2.29	6.11	5.85	4.35	6.24	6.11	2.11
80	5.92	5.78	2.39	5.91	6.00	1.51	6.60	6.28	4.97	6.60	6.49	1.68
Dielectric loss factor (ε'')												
Temp (℃)	MC (%, w. b.)											
	5%			7%			9%			11%		
	Measured	Simulated	Difference (%)	Measured	Simulated	Difference (%)	Measured	Simulated	Difference (%)	Measured	Simulated	Difference (%)
30	0.12	0.14	19.7	0.25	0.29	16.6	0.41	0.44	6.44	0.75	0.63	17.2
40	0.20	0.24	15.9	0.43	0.43	0.65	0.61	0.58	4.84	0.96	0.85	12.5
50	0.57	0.48	18.0	0.91	0.75	19.2	0.97	0.84	14.0	1.41	1.21	14.8
60	0.83	0.68	19.8	1.23	1.04	16.5	1.53	1.31	15.6	2.05	1.77	14.3
70	1.23	1.03	17.8	1.70	1.47	14.6	2.26	1.89	17.8	2.75	2.31	17.6
80	1.62	1.41	13.6	1.73	1.94	11.1	2.93	2.46	17.4	3.44	3.08	11.3

The measured dielectric properties of the seeds increased with temperature and MC of the seeds. At the higher MC of the seeds, the enhanced dipole and ionic polarizations, and increased number of free ions and dipoles by added moisture resulting in increasing the storage of electrical charges and movements of ions and dipoles (Wang et al. 2003; Guan et al. 2004). It caused the higher dielectric properties of the seeds at higher MC of the seeds. The reasons for increasing dielectric properties of the seeds with temperature was the same as those for the insect in section 6.3.1. The simulated dielectric properties of the seeds were in good agreement with the measured values with the difference in percentage ranging from 0.19 to 5.60 and 0.65 to 19.8 for the ε' and the ε'', respectively.

6.5.4 Simulated potential and electric filed distribution

The patterns of simulation results for the small and medium volumes canola seeds at 5%, 7%, and 9% MCs were also similar to those at 11% MCs described in figures below except the scale differences of the parameters. Fig. 6. 5 illustrates the simulated electric field distribution in contour (A) and arrow (B) within the RF unit with the small (a) and the medium (b) volumes canola seeds at 11% MC after 140 s and 270 s of RF heating, respectively.

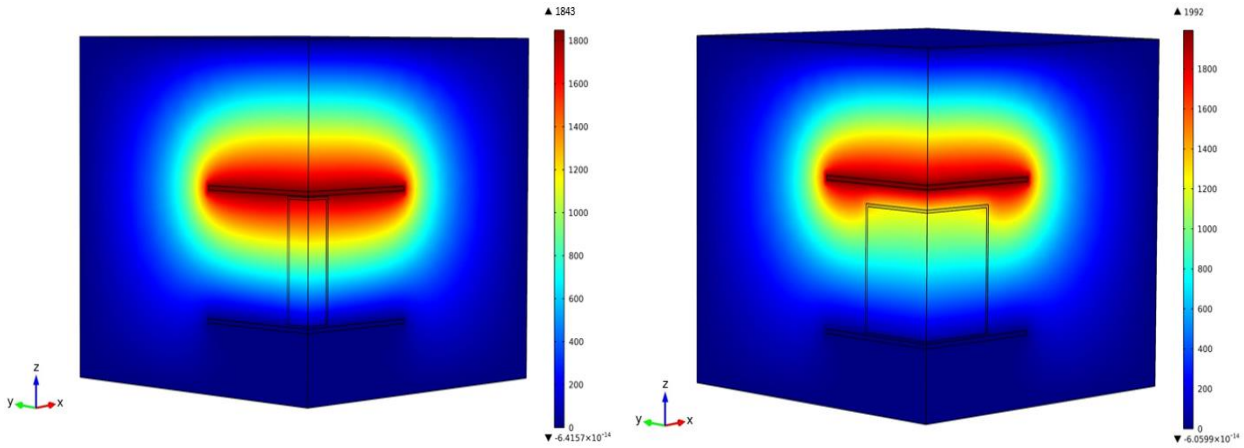

(a) (b)

(A)

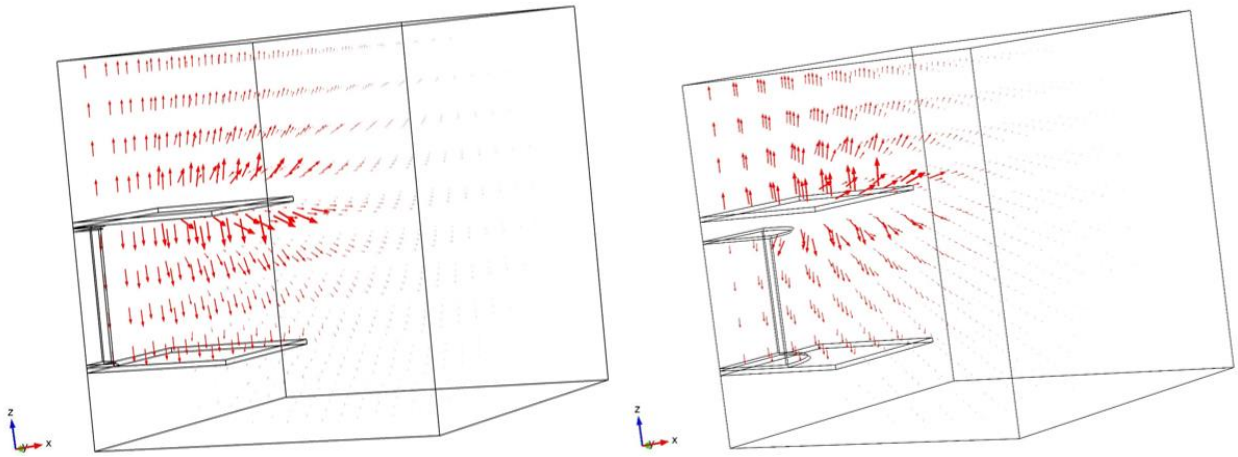

(a) (b)

(B)

Figure 6. 5. The simulated electric distributions in contour (A) and arrow (B) within the RF heating unit with the small (a) and the medium (b) volume samples of the canola seeds at 11% MC after 140 s and 270 s of RF heating.

The arrow and its length in Fig. 6. 5 (B) present the direction and the magnitude of the electric field. The electric potential gradually diminished from the top electrode towards the bottom electrode and the enclosure regardless of the volume of the seeds. The fringing electric field was clearly observed at the edge of the top and the bottom electrodes. It was gradually faded away from the top electrode. In case of the medium volume seeds (MS), the electric field was deflected to the edge and corner of the sample holder resulting in the quantity of the electric field is relatively larger at the outer areas of the sample compared to that in the inner areas. It caused the electric field concentration at the edges and the corners of the sample. (Roussy and Pearce 1995). The edge effect has been reported in other researches (Birla et al. 2008b; Tiwari et al. 2011a, b; Yu et al. 2016b).

6.5.5 Comparison of simulated and experimental temperature profiles of canola seeds

Fig. 6. 6 illustrates the simulated temperature distributions of the small (a) and the medium (b) volume canola seeds at 11% MC in the RF unit after 140 s and 270 s of RF heating, respectively.

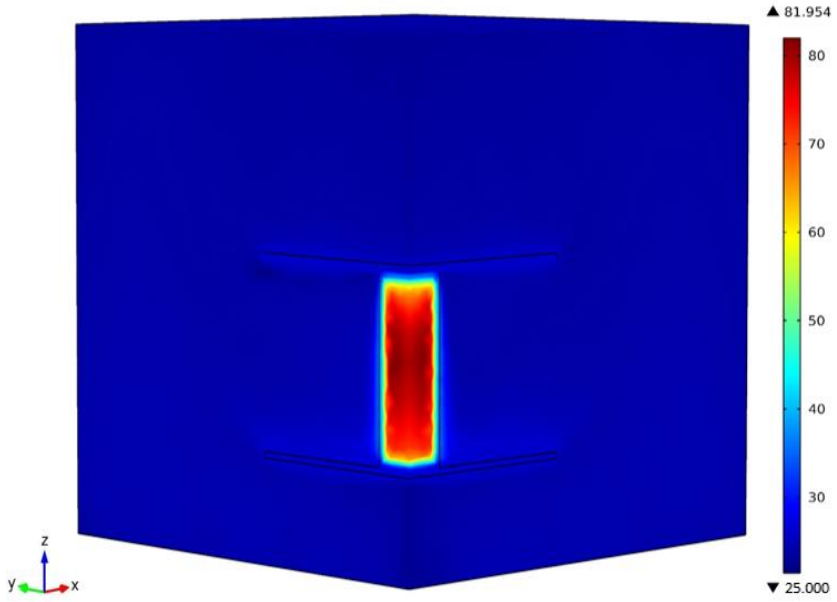

(a)

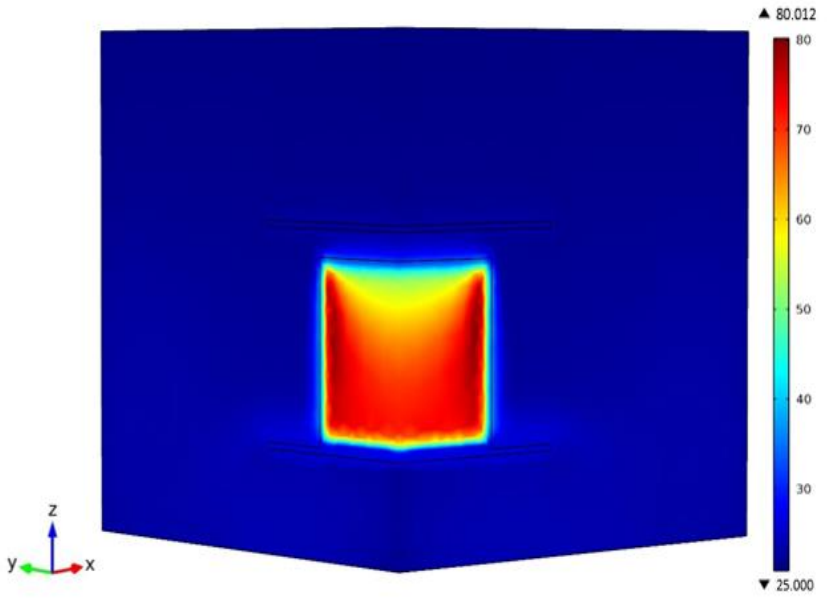

(b)

Figure 6. 6. The simulated temperature distributions of the small (a) and the medium (b) volume canola seeds at 11% MC after 140 s and 270 s of RF heating, respectively.

The higher simulated temperature was observed at the geometric center and its vicinity of the small volume seeds (SS). The simulated temperature of the SS was gradually decreased towards the outer

boundary of the sample holder due to the heat loss to the surroundings. In case of the MS, the higher simulated temperature was observed at the edge and the corner of the holder due to the edge effect. The simulated temperature of the MS was gradually decreased towards the center and the outer boundary of the sample holder. Fig. 6. 7 shows the simulated dielectric loss factor distributions of the SS and the MS at 11% MC after 140 s and 246 s of RF heating, respectively.

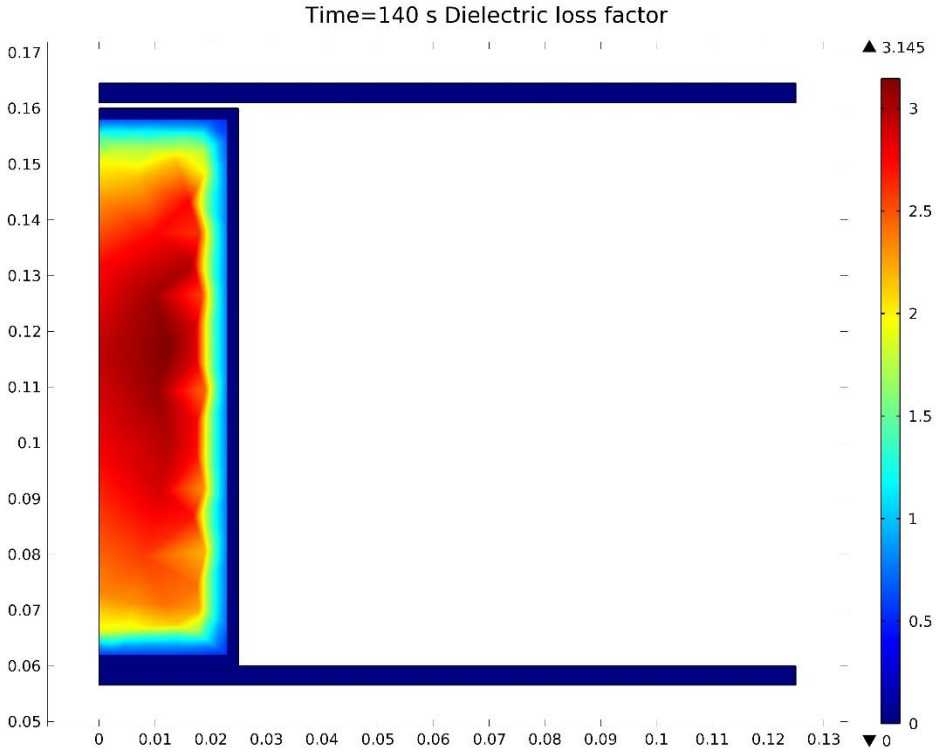

(a)

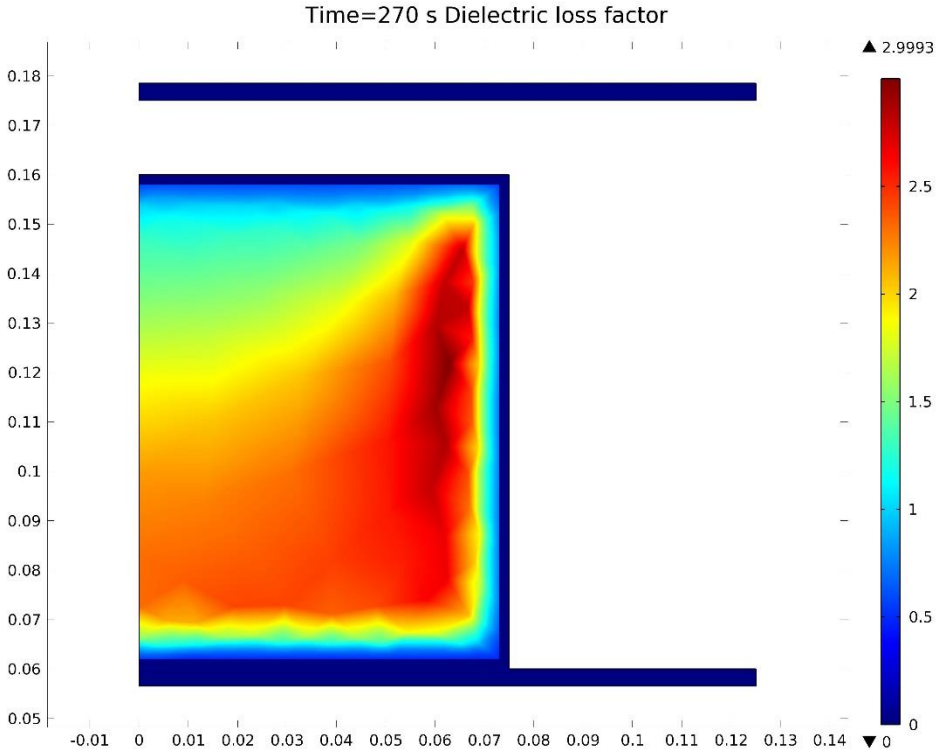

(b)

Figure 6. 7. The determined dielectric loss factor distributions of the small (a) and the medium (b) volume canola seeds at 11% by simulation after 140 s and 246 s of RF heating, respectively.

The pattern was similar to the simulated temperature distribution of the seeds as the ε'' mainly affected to the temperature increment of the sample at the constant electric field strength (Shrestha and Baik 2013; Yu et al. 2015b). The non-uniformity of the ε'' of the seeds was consecutively increased by the non-uniform heat generation due to non-uniform electric field distribution in the seeds during RF heating even though the ε'' of the seeds was uniform at the beginning. Therefore, different dielectric loss factors of the seeds were observed at different locations in the seeds. The simulated temperature distributions of the seeds were similar to the temperature distributions of the 2% agar gel contained in the same sample holders, and are shown in Fig. 6. 8.

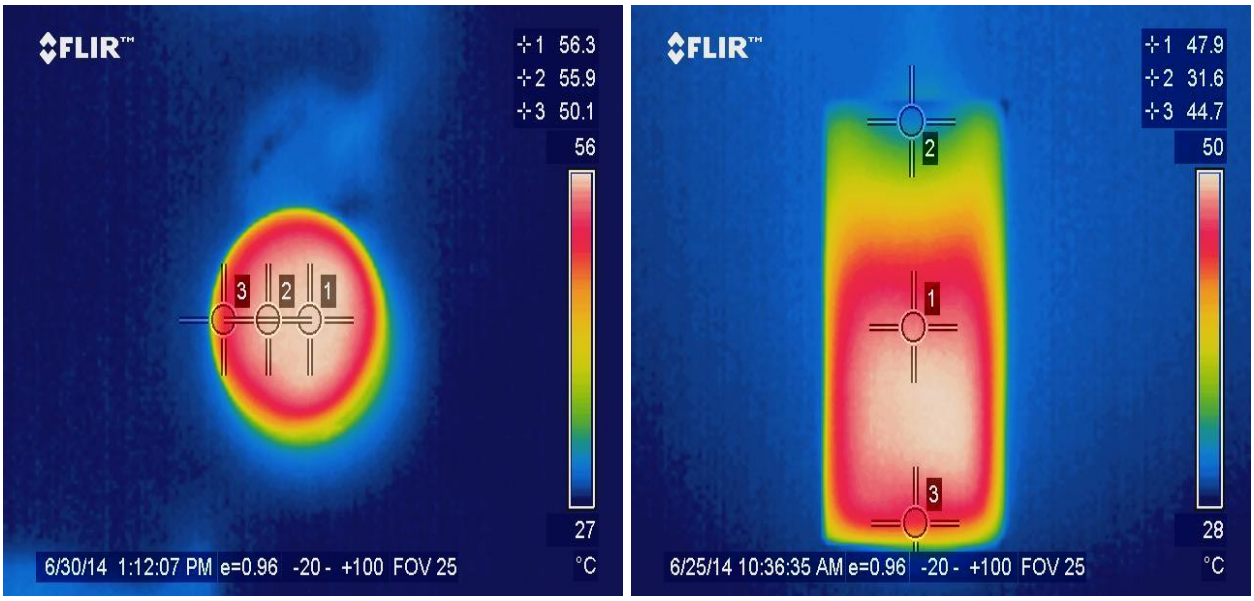

(a) (b)

(A)

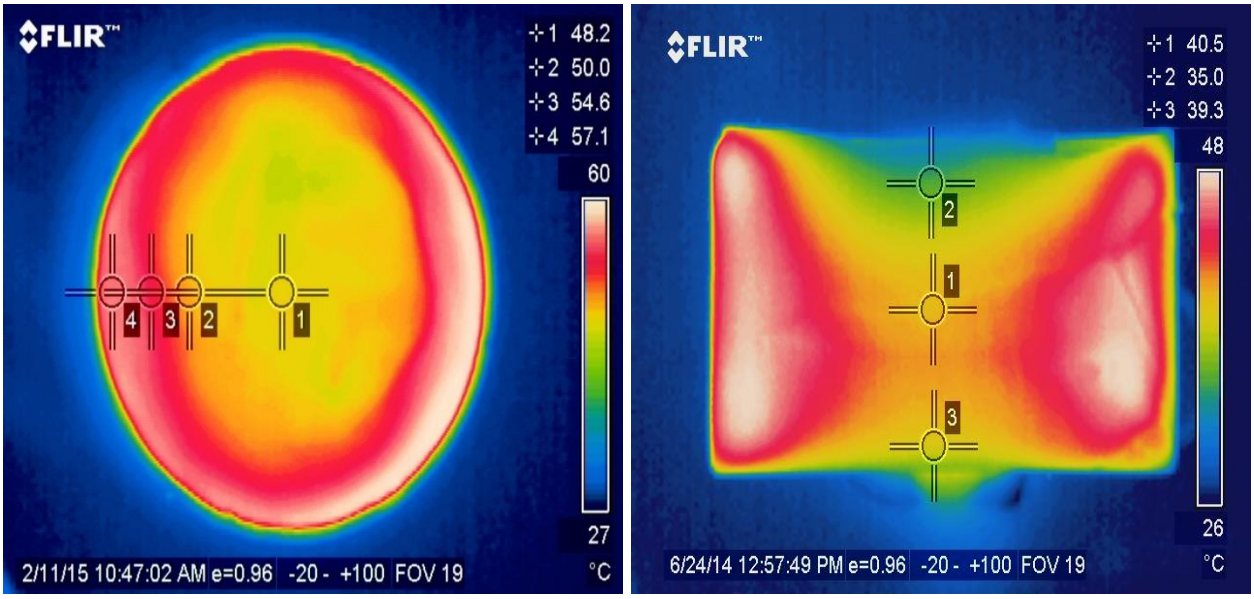

(a) (b)

(B)

Figure 6. 8. The temperature distributions of the small (A) and the medium (B) volume 2% agar gels after RF heating: horizontal profiles at the *h*2 (50 mm from the bottom) surface (a) and a vertical (b) profiles at 25 mm (small volume) and 75 mm (large volume) from the holder wall, respectively (Yu et al. 2016a).

Those were obtained from our previous research (Yu et al. 2016b). The 2% agar gel, chemically and structurally homogenous object, was used to demonstrate the effect of the sample volume on characterizing the electric field formation affecting RF heating pattern. The edge effect was also observed in the medium volume 2% agar gel sample.

In the seed samples, the simulated temperature of the surrounding air gradually increased from the top to the bottom and decreased from the outer surface of the sample holder towards the enclosure for both holders. The heat losses from the seeds to the surrounding can be explained by the natural convection of the surrounding air and the heat conduction of the bottom electrode. The magnitude of the determined convective heat transfer coefficient from the simulation is shown in Fig. 6. 9.

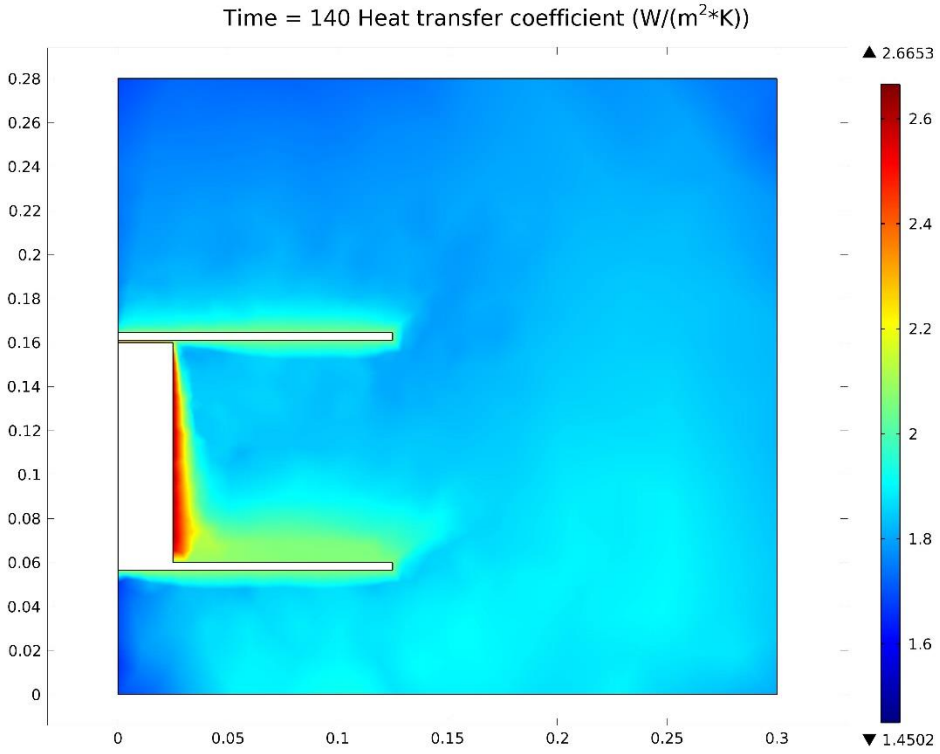

(a)

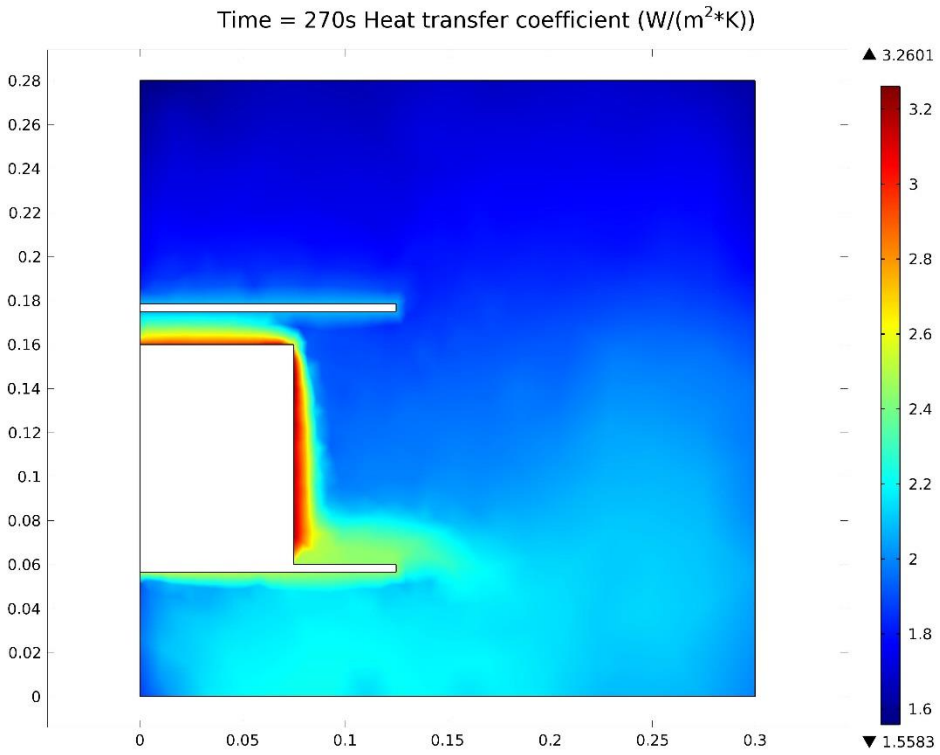

(b)

Figure 6. 9. A x-z cross section of the simulated convective heat transfer coefficient distributions within the RF heating chamber containing the small (a) and the medium (b) volume canola seeds at 11% MC after 140 s and 270 s of RF heating, respectively.

It gradually increased from near the top of the outer surface of the sample holder to the bottom and decreased with the distance from the outer surface of the sample holder to the enclosure regardless of the volume of the seeds. The simulated non-isothermal flow-fields of the air surrounding the SS and the MS were observed to explain accurate heat loss from the seeds to the surrounding (Fig. 6. 10).

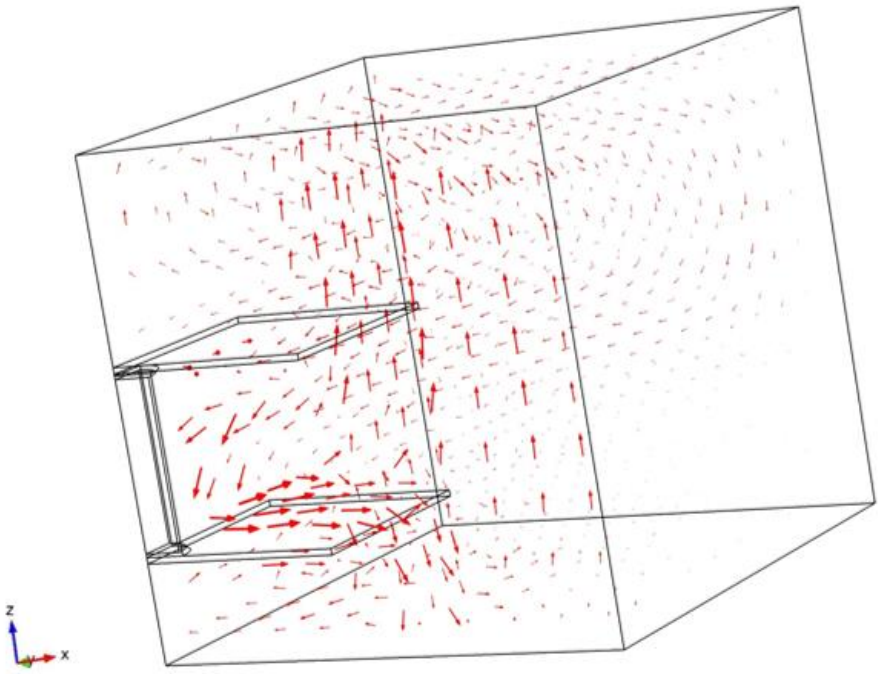

(a)

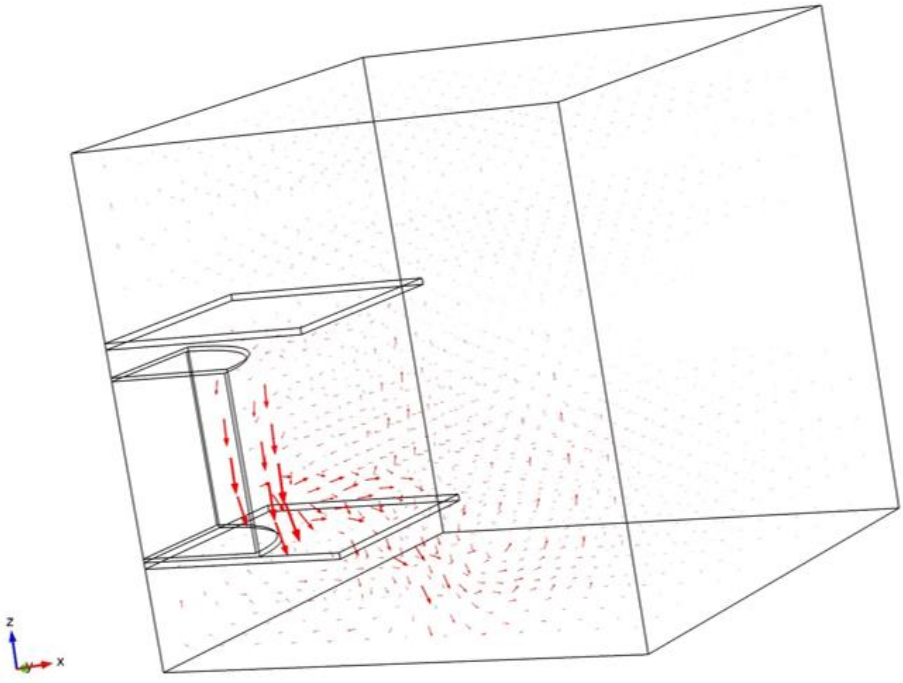

(b)

Figure 6. 10. The simulated flow-fields of the air surrounding the small (a) and medium (b) volume canola seeds at 11% MC within the RF heating chamber after 140 s and 270 s of RF heating, respectively.

The relatively cooler air flowed down along the outer surface of the holder, and then it flowed away along the bottom electrode toward the enclosure. The relatively warmer air flowed up toward the top of the enclosure. The relatively cooler air flowed into under the top electrode to fill the voids initially created. The determined convective heat transfer coefficient distributions (Fig. 6. 10) were almost the same as the pattern of the flow-field of the surrounding air within the RF heating unit. Table 6. 6 lists the measured and the simulated temperatures of the SS and the MS at 5%, 7%, 9%, and 11% MCs and their differences in percentage.

Table 6. 6. The measured and the simulated temperatures of the canola seeds and their differences at various MCs and volumes.

Vol	MC (%)	Height (mm)	RF exposure (s)	Sensor location (mm)								
				Measured (℃)			Simulated (℃)			Difference (%)		
				Distance from the sample holder wall (mm)								
				C^S (25.0)	M^S (12.5)	W^S (1.00)	C^S (25.0)	M^S (12.5)	W^S (1.00)	C^S (25.0)	M^S (12.5)	W^S (1.00)
Small	5	*h*1 (10.0)	1080	66.5	62.8	46.1	57.3	54.5	38.5	14.9	14.2	12.9
		*h*2 (50.0)		80.0	72.6	48.6	80.3	72.9	43.0	0.37	0.41	12.2
		*h*3 (90.0)		74.9	63.4	45.4	59.9	56.2	38.9	17.4	12.0	15.4
	7	*h*1 (10.0)	720	67.9	63.7	44.4	62.5	61.6	42.1	8.28	3.35	5.32
		*h*2 (50.0)		80.0	72.2	48.7	80.5	76.2	46.7	0.62	5.39	4.19
		*h*3 (90.0)		72.3	67.3	44.2	63.2	61.3	42.2	13.4	9.33	4.63
	9	*h*1 (10.0)	390	69.2	62.9	42.4	64.2	65.8	45.3	7.50	4.51	6.61
		*h*2 (50.0)		80.0	75.2	46.3	80.4	78.7	50.2	0.50	4.55	8.08
		*h*3 (90.0)		62.8	59.8	42.0	63.6	64.0	45.3	1.27	6.79	7.56
	11	*h*1 (10.0)	140	55.0	55.3	37.7	68.7	69.1	46.6	17.7	18.8	19.0
		*h*2 (50.0)		80.0	71.1	44.3	80.1	79.2	51.4	0.12	10.8	14.8
		*h*3 (90.0)		77.1	78.8	46.9	66.2	67.8	49.4	15.2	15.0	5.19
				C^L (75.0)	$M1^L$ (37.5)	$M2^L$ (18.8)	W^L (1.00)	C^L (75.0)	$M1^L$ (37.5)	$M2^L$ (18.8)	W^L (1.00)	C^L (75.0)	$M1^L$ (37.5)	$M2^L$ (18.8)	W^L (1.00)
Medium	5	*h*1 (10.0)	1200	54.9	60.4	58.5	43.0	58.1	58.8	57.9	39.3	5.83	2.65	1.03	8.60
		*h*2 (50.0)		80.0	79.0	73.9	47.0	72.3	76.0	80.2	44.7	9.63	3.80	8.53	4.89
		*h*3 (90.0)		62.3	56.5	59.3	46.1	53.3	54.6	57.4	40.8	14.4	3.36	3.20	11.5
	7	*h*1 (10.0)	870	60.7	66.0	65.2	42.8	63.9	65.4	65.4	43.5	5.3	0.9	0.31	1.64
		*h*2 (50.0)		80.0	79.3	78.3	50.1	71.5	75.1	80.1	48.1	10.6	5.30	2.30	3.99
		*h*3 (90.0)		66.8	67.7	70.8	51.4	54.3	55.7	59.7	44.8	18.7	17.7	15.7	12.8
	9	*h*1 (10.0)	510	56.1	69.3	67.8	45.0	63.7	65.7	65.6	44.4	13.5	5.2	3.2	1.33
		*h*2 (50.0)		77.9	78.5	80.0	47.8	69.7	73.5	80.2	49.2	10.5	6.37	0.25	2.93
		*h*3 (90.0)		55.4	57.3	57.8	46.4	53.3	55.8	60.2	47.0	3.8	2.6	4.2	1.29
	11	*h*1 (10.0)	270	55.6	71.4	73.2	41.9	66.2	67.7	67.9	46.2	19.1	5.2	7.2	10.3
		*h*2 (50.0)		70.1	73.1	80.0	48.6	67.7	72.4	80.1	51.4	3.42	0.96	0.12	5.76
		*h*3 (90.0)		66.4	59.8	68.4	46.3	52.4	58.0	60.1	49.5	21.1	3.0	12.1	6.91

The highest temperatures were observed at the geometric center of the SS for both the actual measurements and the simulations regardless of the seed MC. In case of the MS at 5% and 7% MCs, the highest temperatures were observed at the geometric center of the seeds for the actual measurements, but the simulation results showed the highest temperature at the mid-height ($h2$) and 18.8 mm away from the inner surface of the holder ($M2^{L}$). This discrepancy was addressed as follows. In the actual measurement, the evaporated water vapor (steam) from the hotter regions of the MS near the wall might have been migrated to the inner colder regions of the seeds through the pore between the seeds during the RF heating. In the simulation, however, the effect of the steam flow were not reflected as the bulk canola seeds were treated as a single solid cylindrical material for simplification. This discrepancy was not observed at 9% and 11% MCs of the MS because the evaporated moisture from the hotter region of the seeds near the wall might not have enough time to migrate into the inner colder regions of the seeds due to the relatively short RF exposure times compared to those for seeds at 5% and 7% MCs. The highest temperatures for the MS at 9% and 11% MCs were observed at $h2$ - $M2^{L}$ for both the actual measurements and the simulations. The relative differences between the measured and the simulated temperatures of the seeds at 5%, 7%, 9%, and 11% MCs ranged from 0.37 to 17.4%, 0.62 to 13.4%, 0.50 to 8.08%, and 0.12 to 19.0% for the small volume and from 1.03 to 14.4%, 0.31 to 18.7%, 0.25 to 13.5%, and 0.12 to 21.1% for the medium volume, respectively. The largest temperature differences were observed at $h3$ - W^{S} and $h3$ - C^{L} for the SS and the MS at 11% MC respectively.

6.5.6 Comparison of simulated temperatures of the insects and canola seeds

Simulated temperature distributions of the infested canola seeds with *T. castaneum* at 11% MC after 140 s and 246 s of RF heating are shown in Fig. 6. 11.

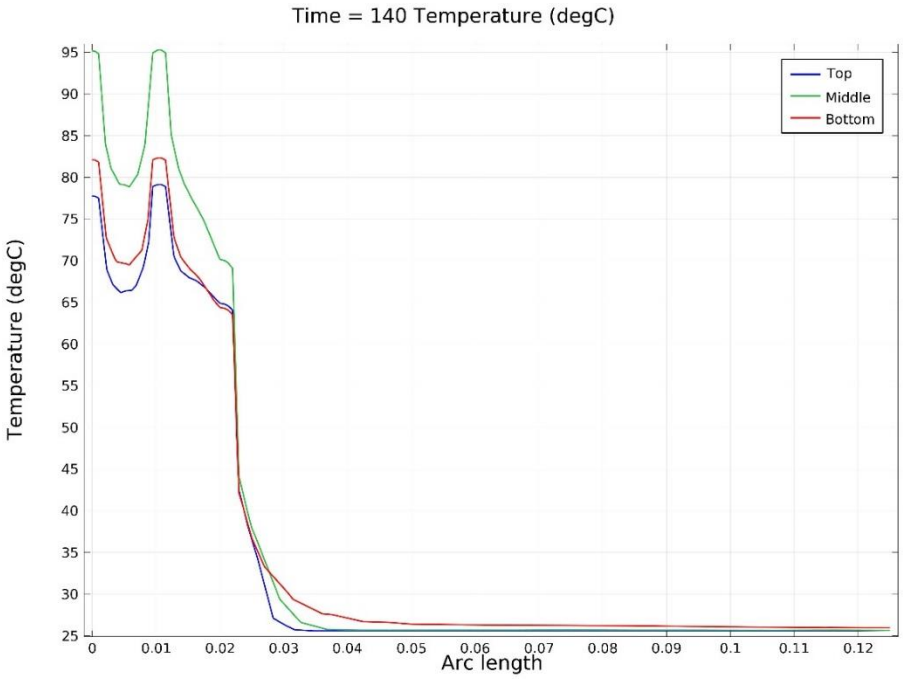
Time = 140 Temperature (degC)
Temperature (degC)
Arc length
Top
Middle
Bottom

(a)

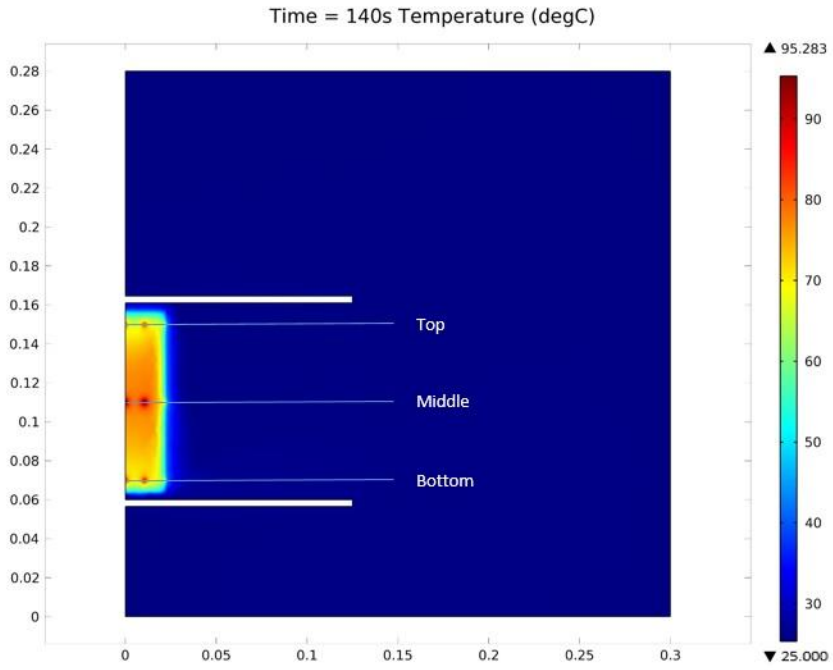
Time = 140s Temperature (degC)
▲ 95.283
▼ 25.000
Top
Middle
Bottom

(b)

(A)

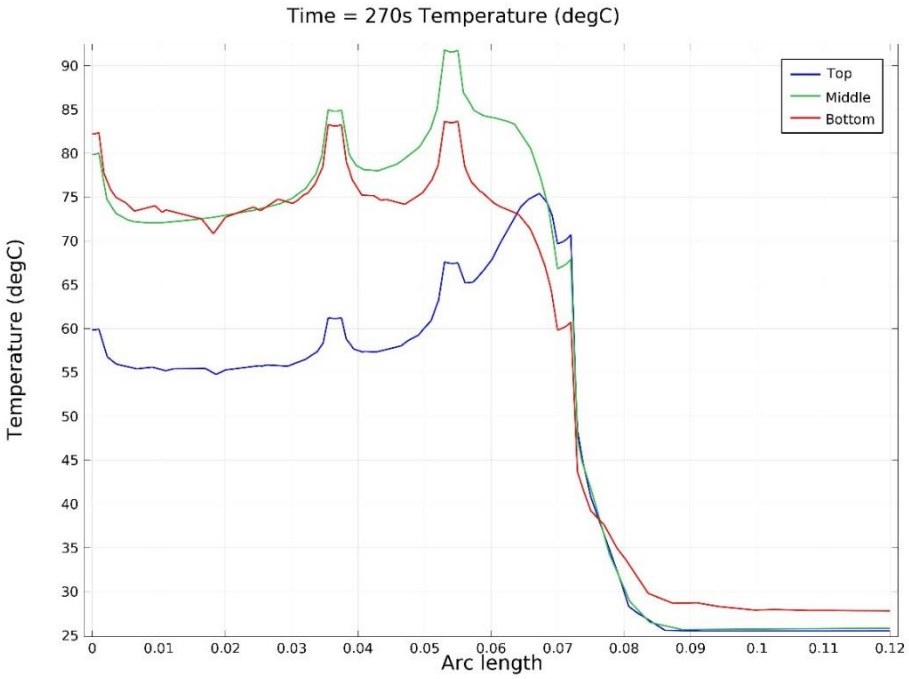

(a)

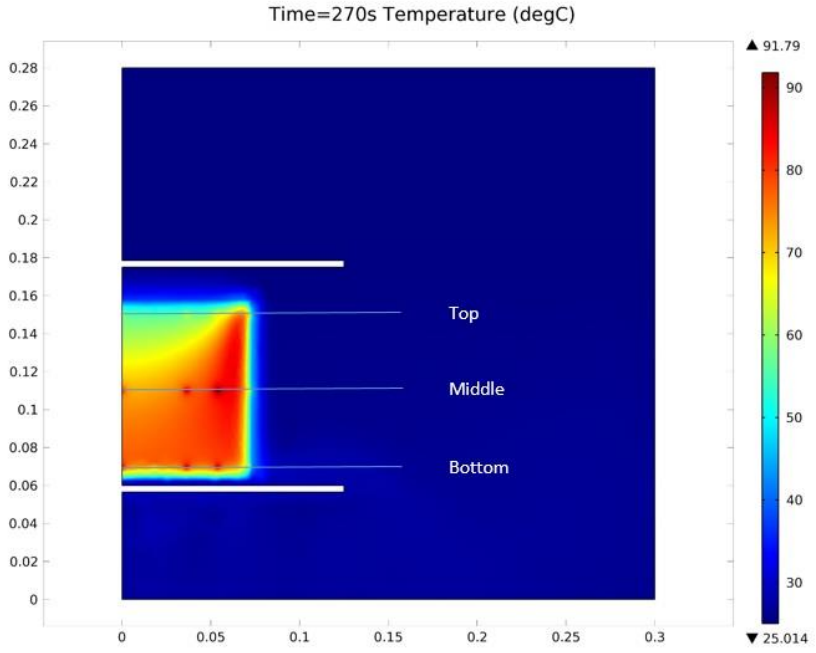

(b)

(B)

Figure 6. 11. The temperature distributions of the infested the small (A) and the medium (B) volume canola seeds with *T. castaneum* at 11% MC within the RF heating chamber at different heights (top, middle, and bottom) in graph (a) and contour (b) after 140 s and 246 s of RF heating, respectively.

Three horizontal lines (top, middle, and bottom) pass through the simulated insects - there were three and four insects on each line for the small and the medium volumes of the seeds respectively. In the figure, some insects have been blended into the surrounding seeds due to the negligible temperature difference between them. In case of the SS, the temperature difference gradually decreased from the geometric center of the seed samples to the outer boundary of the sample holder. The temperature difference was mainly affected by the difference of ε'' between the insects and the seeds (Shrestha and Baik 2013; Yu et al. 2015b). In case of the medium volume, the largest temperature difference was observed at $M2^{L}$ - $h2$ for 5% and 7% MCs and at $M2^{L}$ - $h1$ for 9% and 11% MCs. In horizontal direction, the temperature difference gradually decreased from $M2^{L}$ towards the center of the seeds and the outer boundary of the sample holder at $h2$ and $h1$ and from the outer boundary of the sample holder towards the center of the seeds at $h3$. In the vertical direction, the temperature difference decreased from $h2$ towards $h1$ and $h3$ regardless of the volume of the seeds. As depicted in Fig. 6. 12, the ε'' of *T. castaneum* was 3.72 to 25.9 times higher than that of the canola seeds depending upon the MC of the seeds and the temperature of the seeds and the insects.

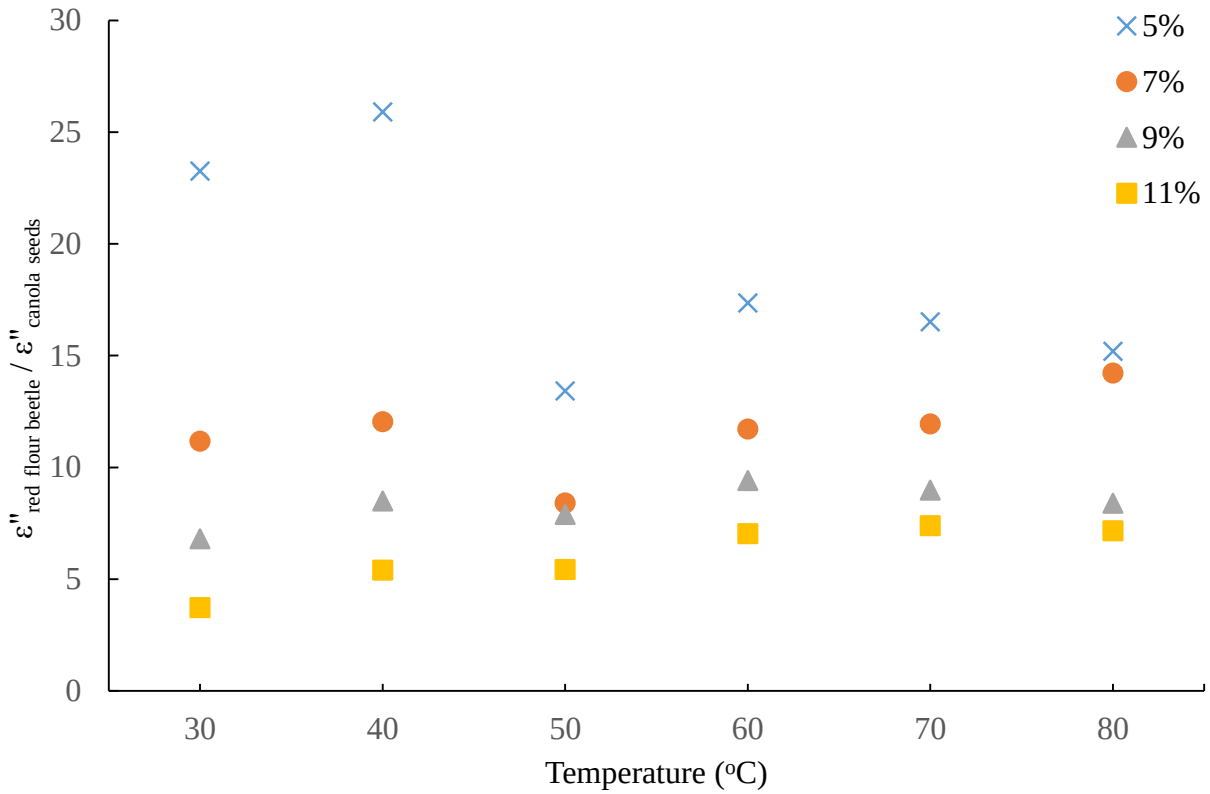

Figure 6. 12. The ratio of the ε'' of *T. castaneum* to that of the canola seeds as functions of the MC and the temperature of the seeds at 27.12 MHz.

Simulated temperatures of the insects were not compared to measured temperatures of the insects from actual experiments as measuring the temperature of actual insects infesting the canola seeds was extremely difficult due to their mobility and tiny size (3 – 4 mm). The simulated temperatures of the red flour beetles and surrounding canola seeds, and their differences (℃) as functions of the MC and the volume of the seeds are presented in Table 6.7.

Table 6. 7. The simulated temperatures (°C) of *T. castaneum* and the surrounding canola seeds and their differences at various MCs and volumes of the seeds.

Volume	MC (%)	Height (mm)	RF exposure (s)	Sensor location (mm)								
				Canola seeds (℃)			Insects (℃)			Difference (℃)		
				Distance from the sample holder wall (mm)								
				C^S (25.0)	M^S (12.5)	W^S (1.00)	C^S (25.0)	M^S (12.5)	W^S (1.00)	C^S (25.0)	M^S (12.5)	W^S (1.00)
Small	5	*h*1 (10.0)	1080	55.2	52.6	38.7	61.5	58.1	40.7	6.30	5.50	2.00
		*h*2 (50.0)		80.8	71.9	42.9	88.2	78.9	45.9	7.40	7.00	3.00
		*h*3 (90.0)		57.2	54.2	38.4	63.8	60.1	40.8	6.60	5.90	2.40
	7	*h*1 (10.0)	720	60.9	59.1	41.7	67.5	65.1	44.3	6.60	6.00	2.60
		*h*2 (50.0)		79.9	75.2	46.4	88.4	83.6	50.3	8.50	8.40	3.90
		*h*3 (90.0)		62.4	61.2	41.0	68.0	66.1	44.3	5.60	4.90	3.30
	9	*h*1 (10.0)	390	67.1	66.5	47.0	73.9	73.1	51.0	6.80	6.60	4.00
		*h*2 (50.0)		80.2	79.7	52.1	90.8	89.3	57.2	10.6	9.60	5.10
		*h*3 (90.0)		66.0	66.2	46.7	72.2	72.4	51.3	6.20	6.20	4.60
	11	*h*1 (10.0)	140	70.5	71.0	57.1	82.1	82.3	64.2	11.6	11.3	7.10
		*h*2 (50.0)		80.7	80.9	61.6	95.3	95.3	69.9	14.6	14.4	8.30
		*h*3 (90.0)		67.4	69.2	57.0	77.8	79.1	64.7	10.4	9.90	7.70
				C^L (75.0)	$M1^L$ (37.5)	$M2^L$ (18.8)	W^L (1.00)	C^L (75.0)	$M1^L$ (37.5)	$M2^L$ (18.8)	W^L (1.00)	C^L (75.0)	$M1^L$ (37.5)	$M2^L$ (18.8)	W^L (1.00)
Medium	5	*h*1 (10.0)	1200	75.0	74.0	73.1	45.0	80.6	79.5	79.1	48.7	5.57	5.53	6.00	3.73
		*h*2 (50.0)		81.8	87.6	92.1	53.8	87.3	92.7	98.2	58.7	5.47	5.07	6.13	4.90
		*h*3 (90.0)		51.4	51.9	58.7	51.2	54.4	54.9	60.4	56.4	3.03	3.00	1.70	5.23
	7	*h*1 (10.0)	870	76.0	77.1	76.0	48.1	80.8	81.8	81.7	51.1	4.80	4.70	5.70	3.00
		*h*2 (50.0)		87.2	95.1	102	56.9	92.3	99.5	109	61.4	5.10	4.40	7.00	4.50
		*h*3 (90.0)		60.4	62.2	70.1	50.9	63.1	64.8	71.7	55.2	2.70	2.60	1.60	4.30
	9	*h*1 (10.0)	510	73.4	74.3	74.3	50.3	78.6	79.5	79.8	53.9	5.20	5.20	5.50	3.60
		*h*2 (50.0)		76.4	82.0	88.7	57.5	81.5	86.7	93.9	62.2	5.10	4.70	5.20	4.70
		*h*3 (90.0)		56.9	58.3	66.0	55.2	59.7	61.1	67.4	60.2	2.80	2.80	1.40	5.00
	11	*h*1 (10.0)	270	75.5	76.4	76.7	55.6	82.2	83.1	83.5	59.9	6.70	6.70	6.80	4.30
		*h*2 (50.0)		73.7	78.7	85.4	61.7	79.9	84.8	91.6	67.2	6.20	6.10	6.20	5.50
		*h*3 (90.0)		56.3	57.6	65.3	63.6	60.2	61.2	67.4	70.0	3.90	3.60	2.10	6.40

The simulated temperature of the insects was higher than that of the surrounding seeds at all locations of the seeds regardless of the volume and the MC of the seeds. In the case of the SS, the highest and the lowest simulated temperatures of the insects were observed at the geometric center and at $h1$ - W^S of the seeds at all MCs. The largest simulated temperature differences between the insects and the surrounding seeds were obtained at $h2$ - M^S for all MCs. The simulated temperature differences between the insects and the surrounding seeds in the SS ranged from 2.00 to 7.40℃, 2.60 to 8.50℃, 4.00 to 10.6℃, and 7.10 to 14.6℃ for the seeds at 5%, 7%, 9%, and 11% MCs. In case of the MS, the highest and the lowest simulated temperatures of the insects were observed at $h2$ - $M2^L$ and at $h1$ - W^L for all MCs. The largest simulated temperature differences between the insects and the surrounding seeds in the MS were obtained at $h2$ - $M2^L$ and $h1$ - $M2^L$ for the seeds at 5% and 7%, and 9% and 11% MCs respectively. The simulated temperature differences between the insects and the surrounding seeds in the MS ranged from 1.70 to 6.13℃, 1.60 to 7.00℃, 1.40 to 5.50℃, and 2.10 to 6.80℃ for 5%, 7%, 9%, and 11% MCs. Based on the simulated temperature differences, *T. castaneum* was most selectively heated in the SS at 11% MC after 140 s of RF heating.

6.6 Conclusion

The C_p, k, ε', and ε'' of *T. castaneum* increased with the increasing temperature, and the ρ decreased with the increasing temperature. The electric potential of the top electrode depended on the MC and the volume of the seeds, and it gradually diminished towards the bottom electrode and the enclosure regardless of the volume of the seeds.

Non-uniform RF heating was observed in the actual and the simulated RF heating of the canola seeds regardless of the MC and the volume of the seeds. The simulated temperature of *T. castaneum* was higher than that of the seeds. The simulated temperature differences between the insects and the seeds ranged from 1.40 to 14.6℃ over the range of the volume and the MC of the seeds. The selective heating of *T. castaneum* was most effective (14.6℃ higher than the temperature of the surround seeds) in the SS at 11% MC. The selective heating of the insects was not strong enough even though the huge difference in the dielectric loss factor between the seeds and the insects. It might be attributed to heat loss from the tiny insects to the surroundings by conduction. Unavailable actual electric potential and no consideration of the mass transfer in the simulation were the limitation of this study. From the separate experiments on the mortality of the

insects, it was found that 100% of *T. castaneum* can be selectively destroyed while keeping the seed temperature below thermal degradation (60℃) (Yu et al. 2016a). Therefore, RF heating systems equipped with a hot air flow, a rotating helix, and/or electrodes with different shapes, sizes and angles can be designed to achieve uniform seed temperature of 60℃ to control *T. castaneum* completely without compromising the seed physico-chemical qualities. This simulation can be used to determine the optimum condition of the industrial scale of the RF heating unit by testing different designs of applicators equipped with a rotating helix, different shapes and sizes of the sample holders and electrodes, etc for selective heating of the insects in the canola seeds.

6.7 References

Agilent, H. P. 2001. 4285A Precision LCR Meter-Operation Manual, (Chap 7), Agilent Technologies, Inc.: Tokyo, Japan.

Alfaifi, B., J. Tang, Y. Jiao, S. Wang, B. Rasco, S. Jiao, and S. Sablani. 2014. Radio frequency disinfestation treatments for dried fruit: Model development and validation. *Journal of Food Engineering* 120: 268-276.

ASAE. 2002. ASAE S352.2, moisture measurements-unground grains and seeds. In ASAE standards. St. Joseph, MI:ASAE.

Barreveld, W. H. 1993. Date palm products. FAO Agricultural Services Bulletin No. 101. Rome, Italy.

Birla, S. L., S. Wang, J. Tang, and G. Tiwari. 2008a. Characterization of radio frequency heating of fresh fruits influenced by dielectric properties. *Journal of Food Engineering* 89(4): 390-398.

Birla, S. L., S. Wang, and J. Tang. 2008b. Computer simulation of radio frequency heating of model fruit immersed in water. *Journal of Food Engineering* 84(2): 270-280.

Brusewitz, G. H. 1975. Density of rewetted high moisture grains. *Transactions of the ASAE* 18(5): 935-938.

Canola Council of Canada. 2014. http://www.canolacouncil.org/markets-stats/industry-overview/. (July. 15. 2016)

Canadian Grain Commission. 2013. http://www.grainscanada.gc.ca/storage-entrepose/pip-irp/rfb-trf-eng.htm. (July. 15. 2016)

Canola Watch. 2015. http://www.canolawatch.org/2011/05/09/estimating-flea-beetle-damage-in-canola/. (July. 15. 2016)

Chen, L., K. Wang, W. Li, and S. Wang. 2015. A strategy to simulate radio frequency heating under mixing conditions. *Computers and Electronics in Agriculture* 118: 100-110.

Choi, C. T. M., and A. Konrad. 1991. Finite element modeling of the RF heating process. *Magnetics, IEEE Transactions on* 27(5): 4227-4230.

Gao, M., J. Tang, Y. Wang, J. Powers, and S. Wang. 2010. Almond quality as influenced by radio frequency heat treatments for disinfestation. *Postharvest Biology and Technology* 58: 225–231.

Guan, D., M. Cheng, Y. Wang, and J. Tang. 2004. Dielectric properties of mashed potatoes relevant to microwave and radio-frequency pasteurization and sterilization processes. *Journal of Food Science -Chicago-* 69(1): FEP30-FEP30.

Guo, W., S. Wang, G. Tiwari, J. A. Johnson, and J. Tang. 2010. Temperature and moisture dependent dielectric properties of legume flour associated with dielectric heating. *LWT-Food science and technology* 43(2): 193-201.

Guo, W., X. Wu, X. Zhu, and S. Wang. 2011. Temperature-dependent dielectric properties of chestnut and chestnut weevil from 10 to 4500 MHz. *Biosystems Engineering* 110(3): 340-347.

Griffin, J. P. 1988. Montreal Protocol on Substances That Deplete the Ozone Layer. In International Lawyer. (Vol. 22, p. 1261).

Heather, N. W., and G. J. Hallman. 2008. Pest management and phytosanitary trade barriers. Wallingford: CABI Publishing.

Huang, Z., L. Chen, and S. Wang. 2015. Computer simulation of radio frequency selective heating of insects in soybeans. *International Journal of Heat and Mass Transfer* 90: 406-417.

Jiao, S., Y. Deng, Y. Zhong, D. Wang, and Y. Zhao. 2015. Investigation of radio frequency heating uniformity of wheat kernels by using the developed computer simulation model. *Food Research International* 71: 41-49.

Jiao, S., J. A. Johnson, J. Tang, and S. Wang. 2012. Industrial-scale radio frequency treatments for insect control in lentils. *Journal of Stored Products Research* 48: 143-148.

Jiao, S., J. Tang, J. A. Johnson, G. Tiwari, and S. Wang. 2011. Determining radio frequency heating uniformity in mixed beans for disinfestations. *Transactions of the ASABE* 54(5): 1847-1855.

Lagunas-Solar, M. C., Z. Pan, N. X. Zeng, T. D. Truong, R. Khir, and K. S. P. Amaratunga. 2007. Application of radiofrequency power for non-chemical disinfestation of rough rice with full retention of quality attributes. *Applied Engineering in Agriculture* 23(5): 647.

Marshall, M. G., and A. C. Metaxas. 1998. Modeling of the radio frequency electric field strength developed during the RF assisted heat pump drying of particulates. *Journal of Microwave Power and Electromagnetic Energy* 33(3): 167-177.

Mills, R., and J. Pedersen. 1990. A flour mill sanitation manual. ST. Paul, MN: Eagan Press.

Nelson, S. O. 2005. Dielectric spectroscopy in agriculture. *Journal of Non-crystalline Solids* 351(33): 2940-2944.

Nelson, S. O., and P. G. Bartley. 2002. Frequency and temperature dependence of the dielectric properties of food materials. *Transactions of the ASAE* 45(4): 1223.

Nelson, S. O., P. G. Bartley Jr, and K. C. Lawrence. 1996. Measuring RF and microwave permittivities of stored-grain insects. In *Instrumentation and Measurement Technology*

Conference, 1996. IMTC-96. Conference Proceedings. Quality Measurements: The Indispensable Bridge between Theory and Reality., IEEE (Vol. 2, pp. 1108-1113). IEEE.

Nelson, S. O., P. G. Bartley, and K. C. Lawrence. 1998. RF and microwave dielectric properties of stored-grain insects and their implications for potential insect control. *Transactions of the ASAE* 41(3): 685.

Ochsner, T. E., R. Horton, and T. Ren. 2003. Use of the dual-probe heat-pulse technique to monitor soil water content in the vadose zone. *Vadose Zone Journal* 2(4): 572-579.

Roussy, G., and J. A. Pearce. 1995. Foundations and industrial applications of microwave and radio frequency fields: physical and chemical processes. Chichester, U.K: John Wiley & Sons Inc.

Shrestha, B., and O. D. Baik. 2013. Radio frequency selective heating of stored-grain insects at 27.12 MHz: a feasibility study. *Biosystems Engineering* 114(3): 195-204.

Shrestha, B., D. U. Yu, and O. D. Baik. 2016. Multi-physics computer simulation of radio frequency heating to control pest insects in stored-wheat. Submitted to *Engineering in Agricultural Environment and Food*.

Sweat, V. E. 1986. Thermal properties of foods. Engineering properties of foods (pp. 49-87), New York: Marcel Dekker Inc.

Tang, J., H. Feng, and M. Lau. 2002. Microwave heating in food processing. *Advances in Bioprocessing Engineering*, 1-43.

Tang, J., J. N. Ikediala, S. Wang, J. D. Hansen, and R. P. Cavalieri. 2000. High-temperature-short-time thermal quarantine methods. *Postharvest Biology and Technology* 21(1): 129-145.

Tiwari, G., S. Wang, J. Tang, and S. L. Birla. 2011. Computer simulation model development and validation for radio frequency (RF) heating of dry food materials. *Journal of Food Engineering* 105(1): 48-55.

USDA Foreign Agricultural Service. 2015. Production, Supply and Distribution Online Database, query for Commodity: "Oilseed, Rapeseed"; Data Type: "Production"; Country: "All countries"; Year: "2015" (July. 15. 2016)

Uyar, R., T. F. Bedane, F. Erdogdu, T. K. Palazoglu, K. W. Farag, and F. Marra. 2015. Radio-frequency thawing of food products–a computational study. *Journal of Food Engineering* 146: 163-171.

Wang, S., M. Monzon, J. A. Johnson, E. J. Mitcham, and J. Tang. 2007. Industrial-scale radio frequency treatments for insect control in walnuts: II: Insect mortality and product quality. *Postharvest Biology and Technology* 45 (2): 247-253.

Wang, S., and J. Tang. 2004. Radio frequency heating: a potential method for post-harvest pest control in nuts and dry products. *Journal of Zhejiang University Science* 5(10): 1169-1174.

Wang, S., J. Tang, R. P. Cavalieri, and D. C. Davis. 2003. Differential heating of insects in dried nuts and fruits associated with radio frequency and microwave treatments. *Transactions of the ASAE* 46(4): 1175.

Wang, S., G. Tiwari, S. Jiao, J. A. Johnson, and J. Tang. 2010. Developing postharvest disinfestation treatments for legumes using radio frequency energy. *Biosystems Engineering* 105(3): 341-349.

Yu, D., Shrestha, B., and O. D. Baik, 2015a. Thermal conductivity, specific heat, thermal diffusivity, and emissivity of stored canola seeds with their temperature and moisture content. *Journal of Food Engineering* 165: 156-165.

Yu, D., B. Shrestha, and O. D. Baik. 2015b. Radio Frequency Dielectric Properties of Bulk Canola Seeds under Different Temperatures, Moisture Contents, and Frequencies for Feasibility of Radio Frequency Disinfestation. *International Journal of Food Properties* 18(12): 2746-2763.

Yu, D., B. Shrestha, and O. Baik. 2016a. Radio frequency (RF) control of red flour beetle (*Tribolium castaneum*) in stored rapeseeds (*Brassica napus* L.). Submitted to *biosystems engineering* 151: 248-260.

Yu, D., B. Shrestha, and O. D. Baik. 2016b. Temperature distribution in a packed-bed of canola seeds with various moisture contents and bulk volumes during radio frequency (RF) heating. *Biosystems Engineering* 148: 55-67.

CHAPTER 7

GENERAL DISCUSSION

This chapter is aimed at integrating the findings of the preceding chapters to discuss the achievements of this research work. Application of the developed simulation model for demonstrating the effect of electric voltage of the hot electrode on the RF heating uniformity and the RF selective heating of the insects, improvement of RF heating uniformity (specific objective 12), contributions to knowledge development, and potential works for future research on the scaled-up RF disinfestation system (specific objective 13) are described below. All the simulation works in this chapter were conducted by myself.

7.1 Properties of the bulk canola seeds and the red flour beetles

The red flour beetle (*Tribolium castaneum*) is one of the most common insect pests in stored grains, oilseeds, and food-processing facilities worldwide (Mills and Pedersen 1990). The adult is a small reddish brown beetle about 4 mm long. Each female lays 400 – 500 eggs at over 20℃. It takes 28 days to develop from egg to adult under optimal conditions (32℃ to 35℃ and over 65% RH) and the adult can fly at over 25℃ (Canadian Grain Commission 2013).

7.1.1 C_p, ρ, porosity, k and α, ε, and dielectric properties of the bulk canola seeds

Properties of the bulk canola seeds were measured as functions of temperature (30 to 80℃) and MC (5 to 11% w.b.) over the frequency range of 5 to 30 MHz for dielectric properties and temperature (40 to 90℃) and MC (5 to 11% w.b.) for thermal-physical properties. The C_p of stored canola seeds increased with temperature and MC.

Increased particle size of canola seed increased the total volume air voids and decreased mass of canola seed due to the evaporation of moisture resulting in decreasing densities. The canola seed continued to expand its volume with temperature, it resulted in increasing the particle volume. The bulk and particle densities ranged from 655 to 670 kg·m^{-3} and 1064 to 1137 kg·m^{-3}, respectively. The porosity of canola seeds ranged from 38.3 to 41.6. It decreased with temperature and MC due to decreasing ratio of ρ_b to ρ_p.

The C_p of stored canola seeds ranged from 2180 to 3498 $J \cdot kg^{-1} \cdot ℃^{-1}$. The k of stored canola seeds increased with temperature and MC, because of large number of ions and dipoles present at higher MC, and these entities exhibit higher lattice vibrations at high temperatures facilitating heat transfer (Sweat 1986). At all times, the k_p was higher than the k_b. This was attributed to the fact that the canola seeds in the compacted form transferred heat better due to less air voids in the matrix. The thermal diffusivity at bulk density (α_b) increased with temperature and MC. This was attributed to the fact that the increment rate of k_b with temperature and MC were higher than that of C_p and ρ_b. The descending-ascending trends of thermal diffusivity at particle density (α_p) were observed with increasing MC at different temperatures except at 40℃. The descending trend of α_p with MC was due to the fact that the increment rate of C_p with MC were higher than that of k_p. The ascending trend can be explained by the fact that the increment rate of k_p with MC were higher than that of C_p. The ε decreased with temperature and MC. The ε of stored canola seeds is higher than other metallic materials (copper : 0.07, iron : 0.6 ~ 0.7, and stainless steel : 0.45) that means canola seeds can absorb or emit more thermal radiation from its surroundings (Bramson 1968).

The ε' and ε'' ranged from 3.82 to 7.85 and 0.11 to 13.0, respectively. The ε' decreased almost linearly with increasing frequency for all MCs. It was attributed to rapidly alternating EM fields at higher frequencies significantly diminishing reorientation of the dipoles, distortion of ionic bonds, and the interfacial polarization mechanism within the test material resulting in less polarization (Shrestha and Baik 2011). The ε' increased with increasing temperature and MC at different frequencies. It was attributed to increased level of dielectric dispersion because of higher ionic conductivity at higher temperatures (Nelson and Bartley 2002). Ionic conductivity normally increases with increasing temperature (Tang et al. 2002). The added moisture enhanced the ionic, and dipole polarizations in the bulk canola seeds resulting in increasing storage of electrical charges under the applied EM field.

The ε'' decreased with increasing frequency with a dramatic drop to over 50% at 5 MHz to 13.56 MHz regardless of temperature and MC. Diminishing movements of the dipoles and ions due to the rapidly alternating EM fields with increasing frequency resulted in lower ionic conductivity and less conservation of EM energy to heat, consequently decreasing its values. Further increase of frequency to 30 MHz exhibited almost linear decrease of the ε''.

The ε'' linearly increased in proportion to increasing temperature and MC. The increased ε'' at higher temperature was attributed to higher oscillation of the dipoles and movement of the ions resulting from higher thermal agitation of the molecules and ions (Tang et al. 2002; Sipahioglu et al. 2003; Wang et al. 2003; Koskiniemi et al. 2013).

7.1.2 Thermal and dielectric properties of the red flour beetle

The C_p and the k of the insect increased and the ρ of the insect decreased with increasing temperature. At high temperature, ions and dipoles in the insect exhibit higher lattice vibrations resulting in high k value (Sweat 1986). Those properties of the insect ranged from 3.80 to 8.48 $J \cdot kg^{-1} \cdot K^{-1}$, 0.030 to 0.113 $W \cdot m^{-1} \cdot K^{-1}$, and 221 to 484 $kg \cdot m^{-3}$ for the C_p, the k, and the ρ, respectively. Similar ρ of other insects (462 $kg \cdot m^{-3}$and 490 $kg \cdot m^{-3}$ for the sawtoothed grain beetle and the lesser grain borer) were observed (Nelson et al. 1998).

The measured ε' and ε'' of the red flour beetle increased with increasing temperature. The increased ε' of the insect at high temperature was due to increased ionic conductivity resulting in increased level of the dielectric dispersion (Nelson and Bartley 2002; Tang et al. 2002). The increased ε'' of the insect at higher temperatures was attributed to the higher movement of ions and oscillation of dipoles (Yu et al. 2015).

7.2 Temperature distribution in the bulk canola seeds

7.2.1 Temperature distribution in the bulk canola seeds

The temperature distribution in a packed-bed of canola seeds at various MCs (5%, 7%, 9%, and 11% w.b.) and bulk volumes (small – 196.3 cm^3, medium – 1766 cm^3, and large – 6503 cm^3) during RF heating was investigated. The RF exposure time decreased with seed MC to reach the same core temperature of 80 ℃. It is due to the enhanced conductivity of ions and dipoles in the bulk canola seeds, which in turn, increased the dielectric loss factor of the material resulting in higher RF power dissipation in the material (Shrestha et al. 2013). It ranged from 2.3 to 24 min. In general, the sample temperatures decreased from the center towards the wall region due to the heat losses from the outer boundary of the sample. In the case of medium volume of the seeds (Fig. 3. 2 in the section 3.3.3), relatively higher temperatures of the bulk canola seeds at the region between the middle and outer boundary were observed compared to those for small and large

volumes. It was attributed to the edge effect. The edge effect is occurred due to an increasing electric field concentration at the edges and the corners of the container. The net electric field at the outer regions of a sample is larger than that in the inner regions due to the deflected electric fields. The intensity of the edge effect increased with increasing sample volume. It might be affected by increasing surface of the edges and corners of the sample. Interestingly, the edge effect was not observed in the large volume of the seeds which has relatively lager surface area than the electrode. It implied that the electric field is more uniform at the corners and edges of the sample which has relatively larger surface area than the electrode.

7.2.2 Temperature profile of the 2% agar gel

The hottest spot of the gel of the small volume was observed near the geometrical center similar to bulk canola seeds. Near the edge and at the corners of the gel were heated faster than other regions. The reason could be the same as in the case of bulk canola seeds. Interestingly, the edge effect was not observed for the gel of large volume. This result was similar with that of bulk canola seeds. It proved that the electric field near the edge and the corner regions were bent toward the sample resulting in an increasing electric field concentration therein irrespective of the material in hand. Overall, the temperature profiles of the gels were in good agreement with those of the bulk canola seeds.

7.2.3 Temperature uniformity (θ) of the bulk canola seeds

More uniform RF heating was observed in the samples of medium volume in spite of the edge effect. Based on θ, the bulk canola seeds could be heated more uniformly along vertical direction than horizontal direction by RF energy. It is obvious that RF heating uniformity can be enhanced using properly designed hybrid RF systems (Hou et al. 2014).

7.3 RF control of red flour beetle in stored canola seeds

7.3.1 Mortalities of the red flour beetles

The 100% absolute and relative mortalities of the adult insects were achieved at over 60℃ for 9% and 11% MCs and over 70℃ for 5% and 7% MCs. Over 95% absolute and relative mortalities of the adult insects were achieved at over 60℃ of the seeds at any MCs. The mortality of the insect could be caused by a sudden heat shock when the insect was exposed to a high temperature in

which the insects would not get sufficient time for thermal adaptation (Mahroof et al. 2003). The mortalities of the adult insects infesting the medium volume of the seeds were higher than those of the small volume during quarantine period due to the transferring location of the insects in the seeds. Before the RF heating, the insects were transferred to the exact hottest region in the medium volume canola seeds, but in case of the small volume of the canola seeds, the insects were transferred to the hottest spot and it vicinity due to the tiny space of the hottest spot. The adult red flour beetles infesting the seed samples at 11% MC had less time to generate heat shock proteins compared to that at 5% MC (Yin et al. 2006). Therefore, a short RF heating time could be one of the main reasons for higher mortality of the adult red flour beetle infesting the seeds at 11% MC. The mortality of the adult insects in the seed samples at 11% MC was higher than that in 5% MC seed samples at the same end temperature because of more evaporated steam from the seed samples of 11% MC. The 100% mortalities of the larvae infesting the small and the medium volumes of the seeds were achieved at 55℃ regardless of MC. No emergence of new adult insects from the 5 sub-samples of the 8 week old culture with a great number of the eggs and the pupae was observed during the quarantine period (5 weeks) confirming 100% delayed mortalities. There is potential to realize a complete mortality of all life stages of the insect infesting the seeds at 60℃ by RF heating regardless of the volume of the seeds sample with proper design to achieve more uniform temperature distribution and shorter RF heating time.

7.3.2 Quality of the canola seeds

A germination rate of the RF treated seeds decreased with increasing initial seed MC and RF heating temperature. Physicochemical qualities of the seed affecting germination might have been changed by the RF heating once the temperature of the seeds exceed including some degree of heat damage at over certain temperature (Shrestha et al. 2013). No substantial loss of germination occurred at temperatures up to 60℃ for all seed MCs. More mass loss was observed with higher initial seed MC and heating temperature. It was attributed to increasing moisture diffusion rate at higher heating temperature resulting in higher drying rate (Gazor and Mohsenimanesh 2010). The major and minor axes of the seeds increased with increasing temperature. It might be caused by expansion of constituents (carbohydrate, protein, etc) of the seeds and trapped air inside of the seeds by RF heating. The major and the minor axes, the roundness, and the colour were not affected significantly by the RF heating at entire MCs. The qualities of the oil extracted from the RF treated

seeds was not significantly different from that extracted from the controls. The PV, AV, Totox, and IV values varied between 0.28 meq kg^{-1} and 0.34 meq kg^{-1}, 0.33 and 0.38, 0.91 and 1.03, and 109 g $100g^{-1}$ oil and 112 g $100g^{-1}$ oil, respectively.

7.4 Thermal death kinetics of adult red flour beetle by RF heating

7.4.1 Thermal death kinetics

The temperature increment rate of the seeds proportional to the MC of the seeds and the survival rate of the insect decreasing with the increasing seeds temperature were used to develop the thermal death kinetics model. The best thermal death kinetics model for the adult red flour beetles infesting the canola seeds is as follows.

$$\frac{d(N/N_0)}{dt} = -6.73 \times 10^{13} \cdot \exp\left(\frac{-1.00 \times 10^5}{R\mathrm{T}}\right)(N/N_0)^1 \quad (7.1)$$

The mortality values determined from the kinetics model agreed well with the experimental values.

The first order of reaction model was the most satisfactory to describe the thermal death kinetics of the adult red flour beetle. The determined activation energy of 100 kJ / mol for the adult red flour beetles infesting the canola seeds was lower than that of other insects. It indicated that the adult red flour beetle was more susceptible to the thermal death by the RF heating than the other insects infesting the food commodities. The predicted LT_{95} and LT_{99} from the kinetics model were in good agreement with those from the experiments.

7.5 Computer simulation of heat transfer for disinfestation of red flour beetle in the stored canola seeds by RF heating

7.5.1 Estimated electric voltage and simulated electric filed distribution

The electric voltage on the top electrode in the simulation increased with the MC (except at 7%) and the volume of the seeds. The voltage ranged from 1094 to 1843 V and 1482 to 1992 V for the small and the medium volumes of the seeds, respectively. The electric potential gradually diminished from the top electrode towards the bottom electrode and the enclosure regardless of the volume of the seeds. The fringing electric field was clearly observed at the edge of the top and the bottom electrodes. It was gradually faded away from the top electrode. In case of the medium volume seeds (MS), the electric field was deflected to the edge and corner of the sample holder

resulting in the quantity of the electric field is relatively larger at the outer areas of the sample compared to that in the inner areas. It caused the electric field concentration at the edges and the corners of the sample.

7.5.2 Comparison of simulated and experimental temperature profiles of the canola seeds

The higher simulated temperature was observed at the geometric center and its vicinity of the small volume seeds (SS). The simulated temperature of the SS was gradually decreased towards the outer boundary of the sample holder due to the heat loss to the surroundings. The highest temperatures were observed at the geometric center of the SS for both the actual measurements and the simulations regardless of the seed MC. In case of the MS, the higher simulated temperature was observed at the edge and the corner of the holder due to the edge effect. The simulated temperature of the MS was gradually decreased towards the center and the outer boundary of the sample holder. The ε'' mainly affected to the temperature increment of the sample at the constant electric field strength (Shrestha and Baik 2013). The non-uniformity of the ε'' of the seeds was consecutively increased by the non-uniform heat generation due to non-uniform electric field distribution in the seeds during RF heating even though the ε'' of the seeds was uniform at the beginning. The highest temperatures were observed at the geometric center of the seeds at 5% and 7% MCs for the actual measurements, but the simulation results showed the highest temperature at the mid-height ($h2$) and 18.8 mm away from the inner surface of the holder ($M2^{L}$). This discrepancy was not observed at 9% and 11% MCs of the MS because the evaporated moisture from the hotter region of the seeds near the wall might not have enough time to migrate into the inner colder regions of the seeds due to the relatively short RF exposure times compared to those for seeds at 5% and 7% MCs. The highest temperatures for the MS at 9% and 11% MCs were observed at $h2$ - $M2^{L}$ for both the actual measurements and the simulations. The largest temperature differences were observed at $h3$ - W^{S} and $h3$ - C^{L} for the SS and the MS at 11% MC respectively.

7.5.3 Comparison of simulated temperatures of the red flour beetles and the surrounding seeds

The simulated temperature of the insects was higher than that of the surrounding seeds at all locations of the seeds regardless of the volume and the MC of the seeds. The temperature

difference was mainly affected by the difference of ε'' between the insects and the seeds (Shrestha and Baik 2013). In case of the SS, the temperature difference between the insects and the seeds gradually decreased from the geometric center of the seed samples to the outer boundary of the sample holder. The highest and the lowest simulated temperatures of the insects were observed at the geometric center and at $h1$ - W^S of the seeds at all MCs. The largest simulated temperature differences between the insects and the surrounding seeds were obtained at $h2$ - M^S for all MCs. In case of the medium volume, the largest temperature difference was observed at $M2^L$ - $h2$ for 5% and 7% MCs and at $M2^L$ - $h1$ for 9% and 11% MCs. The highest and the lowest simulated temperatures of the insects were observed at $h2$ - $M2^L$ and at $h1$ - W^L for all MCs. The largest simulated temperature differences between the insects and the surrounding seeds in the MS were obtained at $h2$ - $M2^L$ and $h1$ - $M2^L$ for the seeds at 5% and 7%, and 9% and 11% MCs respectively. The maximum temperature difference (14.6℃) between the seeds and the insects was observed in the SS at 11% MC after 140 s of RF heating.

7.6 Electricity cost of treatment

Based on the RF exposure time (20 min) of the medium volume (1.2 kg) of the seeds at 5% MC to achieve 100% mortality of the insects, the throughput of the 1.5 kW RF unit was 3.6 kg/h. Based on the average retail electricity price of Canadian $ 0.0704/kWh in Saskatoon for commercial loads not exceeding 75 kWh, the total electrical cost was C$ 0.1056/h for 1.5 kW RF units or C$ 0.0293/kg for treating the canola seeds (City of Saskatoon 2016).

7.7 Application of developed simulations

7.7.1 Simulated temperatures of the canola seeds and insects with different electric voltages

The effect of electric voltage on RF heating uniformity and selective RF heating was determined in simulations by comparing the simulated temperature distributions of the canola seeds at 11% MC and the insects. The number and the location of the insects in the seeds were the same as those which were described in Chapter 6. 4. 6. Other conditions (properties of the samples, distance between the container and top electrode, etc) of the RF heating were the same as Chapter 6 except the electric voltage on the top electrode.

The RF exposure times of the canola seeds and electric voltage values at different volume of the seeds are listed in Table 7. 1.

Table 7. 1. The RF exposure time (s) of the canola seeds at 11% MC when the temperature of the hottest spot of the seeds reached 80°C with different electric voltages.

Electric voltage	Volume of the canola seeds			
	Small (d = 50 mm × h = 100 mm)		Medium (d = 150 mm × h = 100 mm)	
	Voltage (V)	RF exposure time (s)	Voltage (V)	RF exposure time (s)
Lower (half times)	922	610	996	1085
Estimated	1843	140	1992	270
Higher (two times)	3686	31	3984	56

Fig. 7. 1 shows the comparison of simulated temperature distributions of the infested canola seeds at 11% MC with the red flour beetles within the RF heating chamber with half and double the control (the estimated electric voltage from Chapter 6).

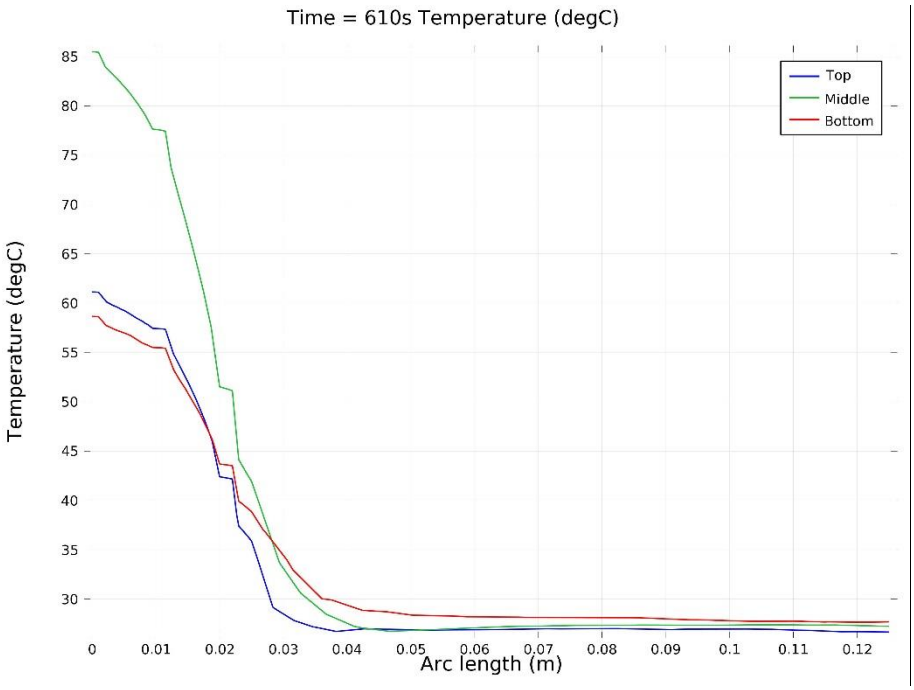
Time = 610s Temperature (degC)
Top
Middle
Bottom
Temperature (degC)
Arc length (m)
85
80
75
70
65
60
55
50
45
40
35
30
0
0.01
0.02
0.03
0.04
0.05
0.06
0.07
0.08
0.09
0.1
0.11
0.12

(a)

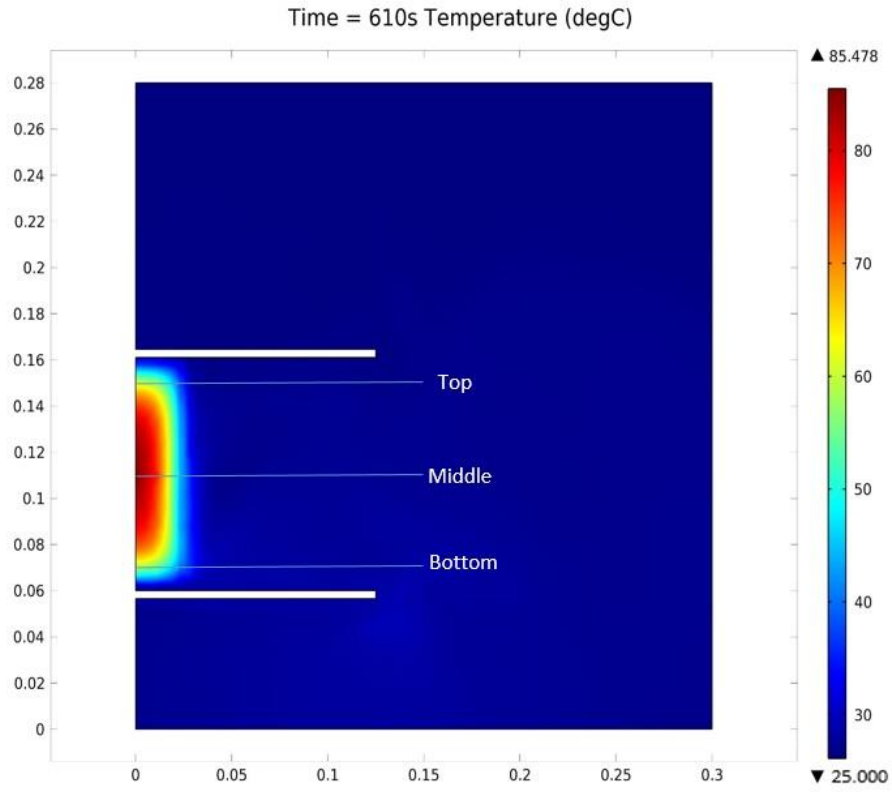
Time = 610s Temperature (degC)
▲ 85.478
▼ 25.000
Top
Middle
Bottom
0.28
0.26
0.24
0.22
0.2
0.18
0.16
0.14
0.12
0.1
0.08
0.06
0.04
0.02
0
0
0.05
0.1
0.15
0.2
0.25
0.3
80
70
60
50
40
30

(b)

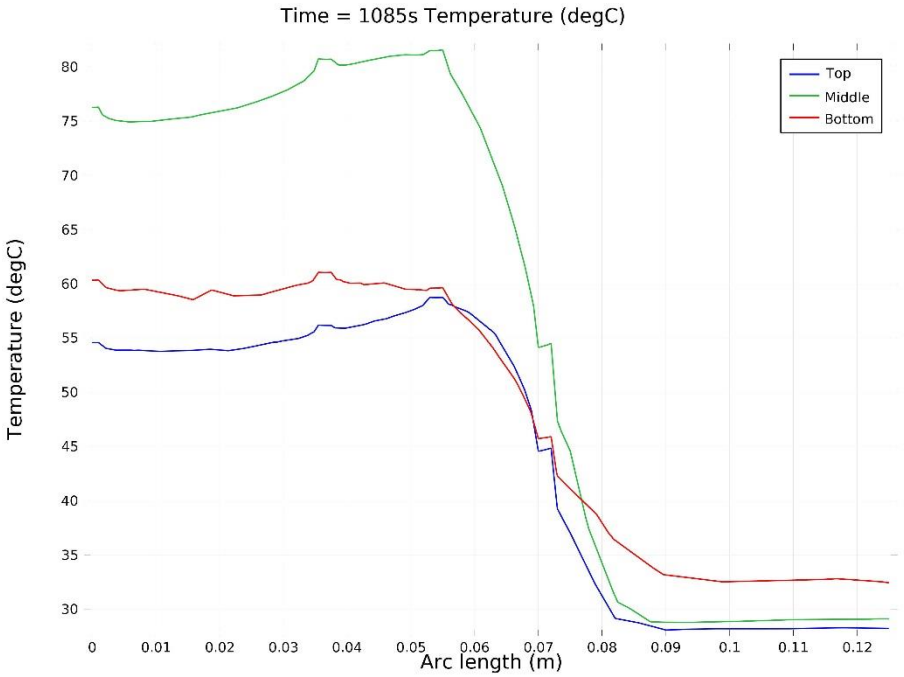
Time = 1085s Temperature (degC)
Top
Middle
Bottom
Temperature (degC)
Arc length (m)
80
75
70
65
60
55
50
45
40
35
30
0
0.01
0.02
0.03
0.04
0.05
0.06
0.07
0.08
0.09
0.1
0.11
0.12

(c)

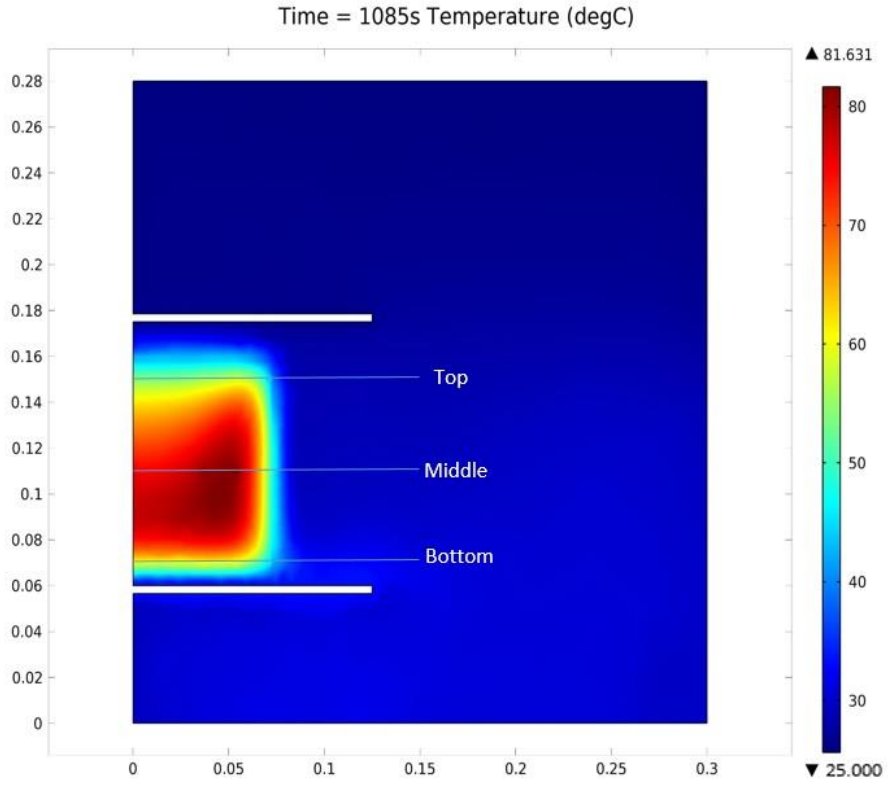
Time = 1085s Temperature (degC)
▲ 81.631
▼ 25.000
Top
Middle
Bottom
0.28
0.26
0.24
0.22
0.2
0.18
0.16
0.14
0.12
0.1
0.08
0.06
0.04
0.02
0
0.05
0.15
0.25
0.3
80
70
60
50
40
30

(d)

(A)

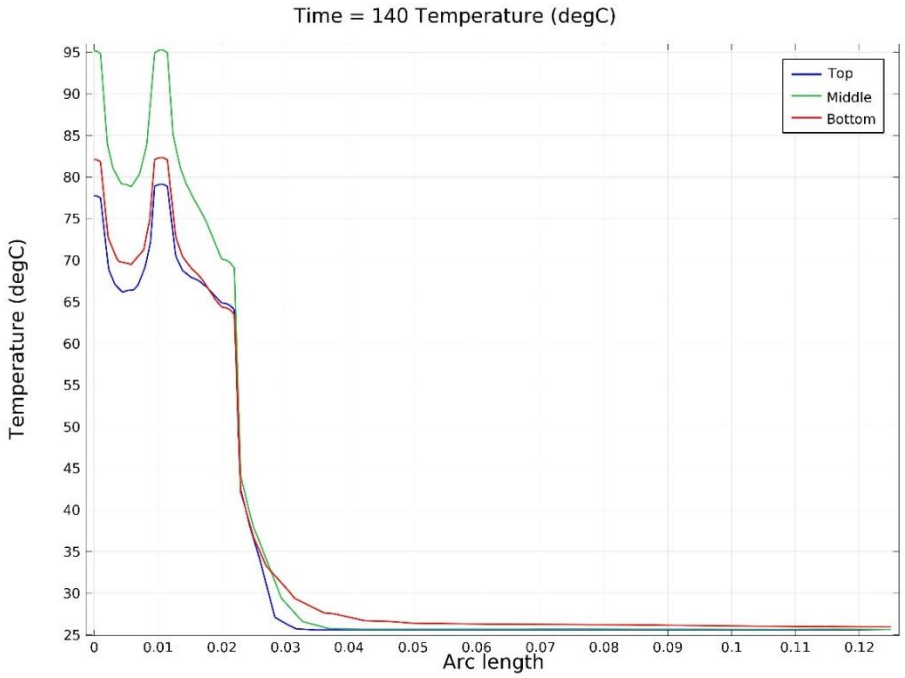
Time = 140 Temperature (degC)
Top
Middle
Bottom
Temperature (degC)
Arc length
95
90
85
80
75
70
65
60
55
50
45
40
35
30
25
0
0.01
0.02
0.03
0.04
0.05
0.06
0.07
0.08
0.09
0.1
0.11
0.12

(a)

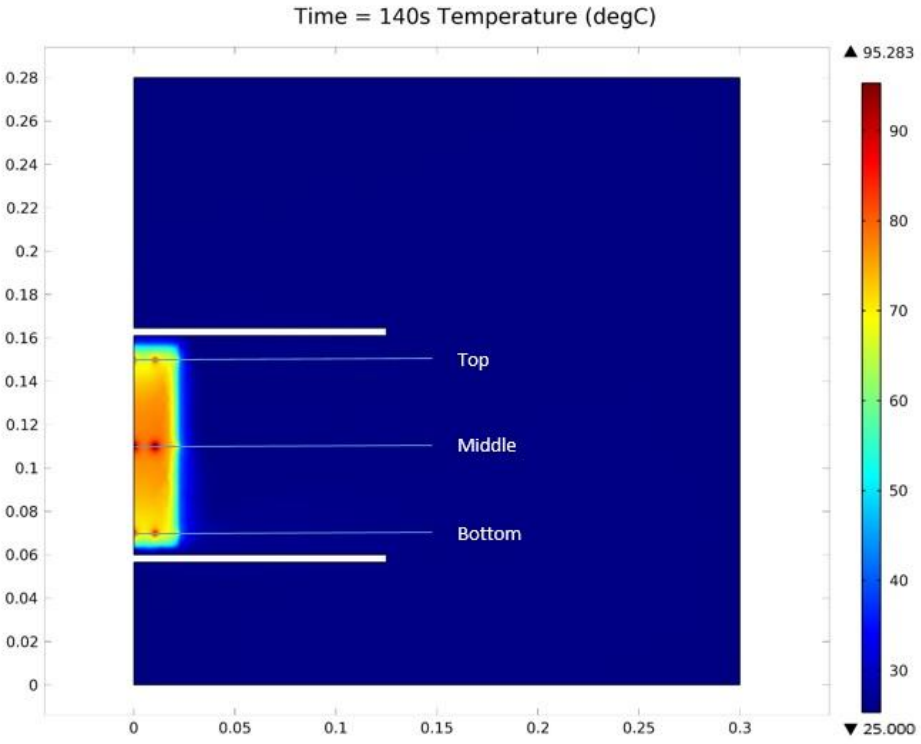
Time = 140s Temperature (degC)
▲ 95.283
▼ 25.000
Top
Middle
Bottom
0.28
0.26
0.24
0.22
0.2
0.18
0.16
0.14
0.12
0.1
0.08
0.06
0.04
0.02
0
0
0.05
0.1
0.15
0.2
0.25
0.3
90
80
70
60
50
40
30

(b)

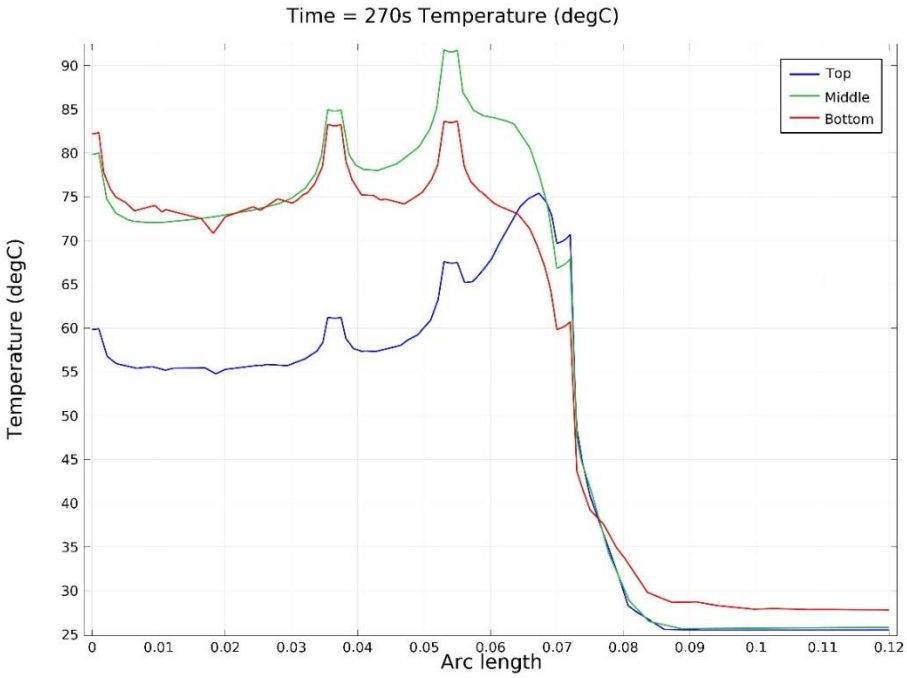
Time = 270s Temperature (degC)
Top
Middle
Bottom
Temperature (degC)
Arc length
90
85
80
75
70
65
60
55
50
45
40
35
30
25
0
0.01
0.02
0.03
0.04
0.05
0.06
0.07
0.08
0.09
0.1
0.11
0.12

(c)

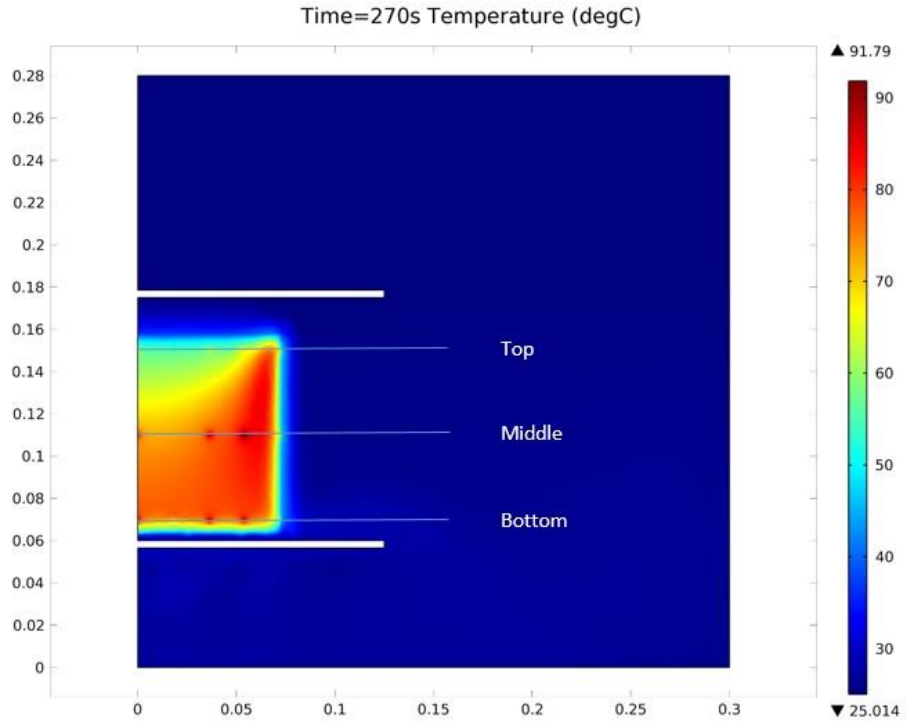
Time=270s Temperature (degC)
Top
Middle
Bottom
▲ 91.79
▼ 25.014
90
80
70
60
50
40
30
0.28
0.26
0.24
0.22
0.2
0.18
0.16
0.14
0.12
0.1
0.08
0.06
0.04
0.02
0
0
0.05
0.1
0.15
0.2
0.25
0.3

(d)

(B)

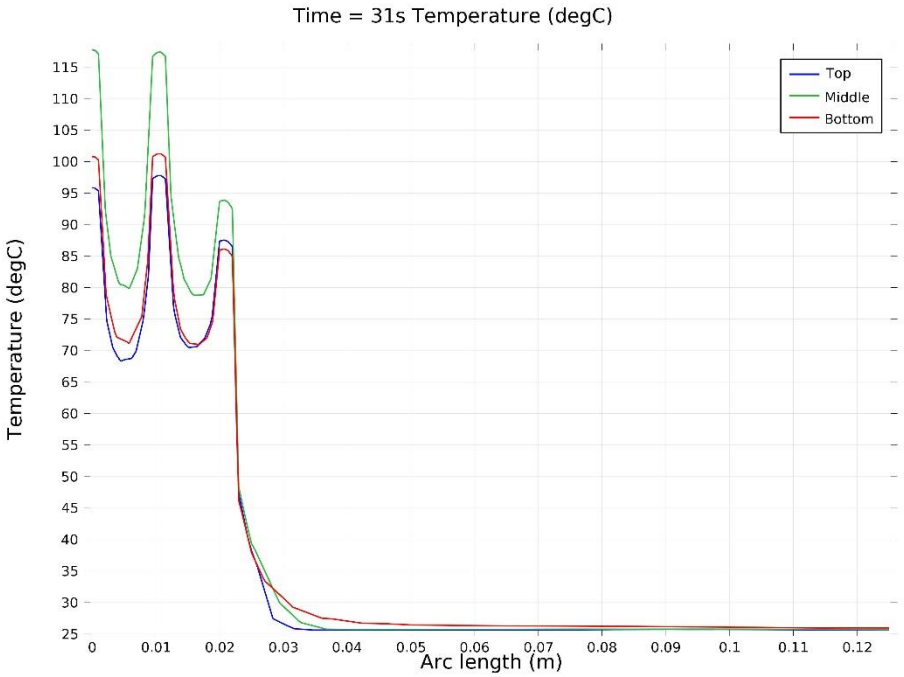
Time = 31s Temperature (degC)
Top
Middle
Bottom
Temperature (degC)
Arc length (m)

(a)

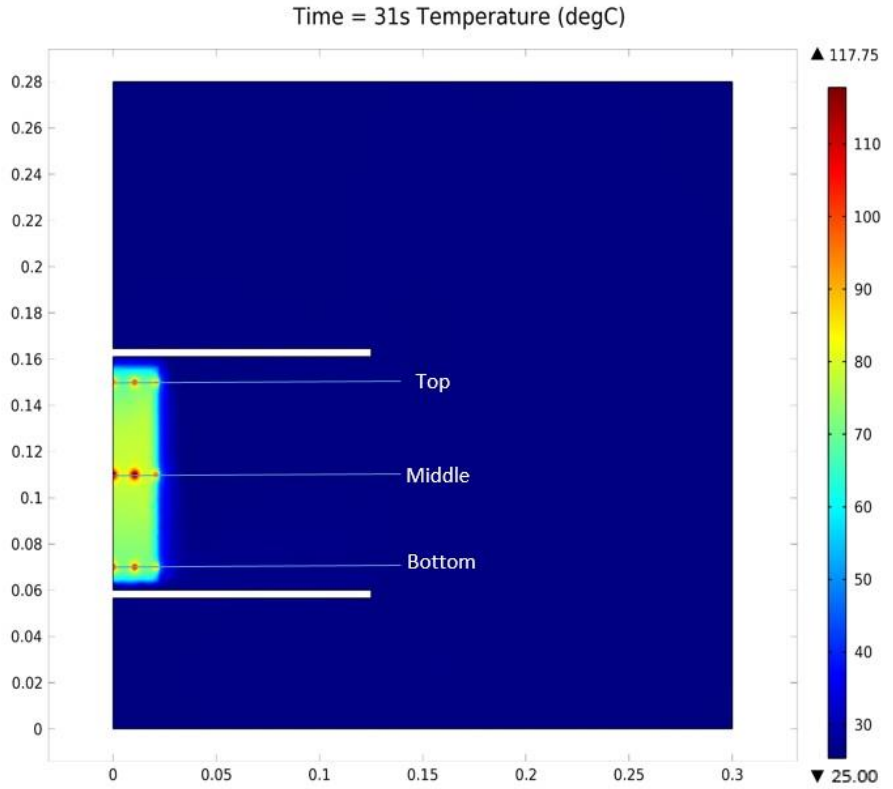
Time = 31s Temperature (degC)
▲ 117.75
▼ 25.00
Top
Middle
Bottom

(b)

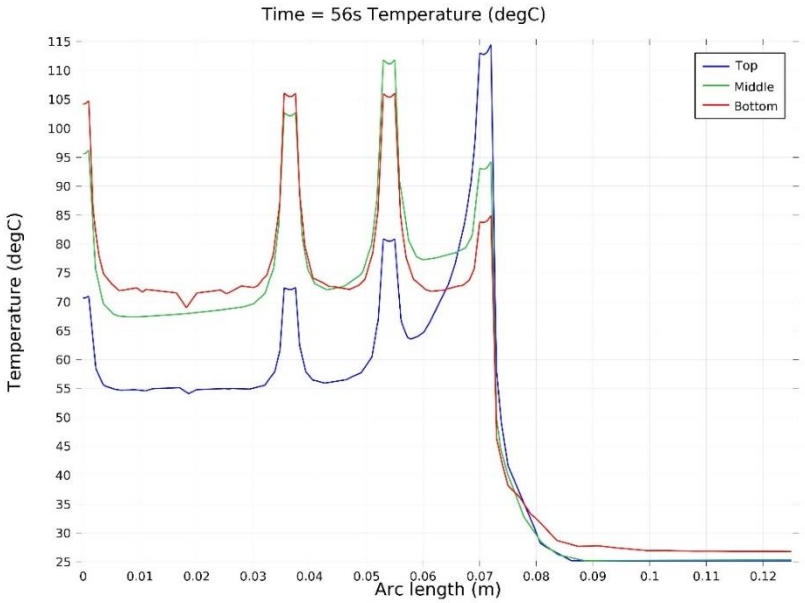

(c)

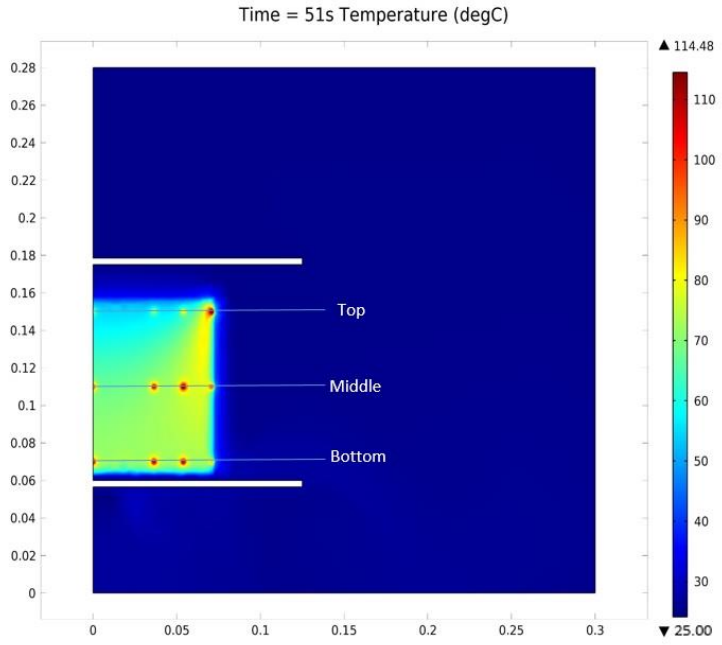

(d)

(C)

Figure 7. 1. The simulated temperature distributions of the infested the small (a and b) and the medium (c and d) volume canola seeds at 11% MC with the red flour beetles within the RF heating chamber with half times lower (A) and two times higher (C) electric voltages than the estimated electric voltage (B) from chapter 6 at difference heights (top, middle, and bottom) in graph (a and c) and contour (b and d), respectively.

In the contour plot (Fig. 7. 1. b and d), some insects have been blended into the surrounding seeds due to the negligible temperature difference between them. As shown in Fig. 7. 1, the RF heating uniformity in the seeds increased with increasing electric voltage on the top electrode regardless of the seeds volume. The temperature difference in the seeds increased with decreasing the electric voltage. The simulated temperature of the insects was higher than that of the surrounding seeds at all locations of the seeds regardless of the electric voltage and the volume of the seeds. The selective RF heating of the insects was enhanced with increasing the electric voltage on the top electrode regardless of the seeds volume. The simulated temperatures of the red flour beetles and surrounding canola seeds, and their differences (℃) are presented with the volume of the seeds and electric voltage in Table 7. 2.

Table 7. 2. The simulated temperatures (℃) of the red flour beetles and the surrounding canola seeds at 11% MC and their differences at different electric voltages and volumes of the seeds.

Volume	Voltage (V)	Height (mm)	RF exposure (s)	Sensor location (mm)								
				Canola seeds (℃)			Insects (℃)			Difference (℃)		
				Distance from the sample holder wall (mm)								
				C^S (25.0)	M^S (12.5)	W^S (1.00)	C^S (25.0)	M^S (12.5)	W^S (1.00)	C^S (25.0)	M^S (12.5)	W^S (1.00)
Small	Lower (922)	*h*1 (10.0)	610	57.5	54.5	43.5	58.6	55.4	43.6	1.10	0.90	0.10
		*h*2 (50.0)		80.9	78.4	51.0	85.5	79.5	52.1	4.60	1.10	1.10
		*h*3 (90.0)		60.0	56.5	42.3	61.1	57.4	42.3	1.10	0.90	0.00
	Control (1843)	*h*1 (10.0)	140	70.5	71.0	57.1	82.1	82.3	64.2	11.6	11.3	7.10
		*h*2 (50.0)		80.7	80.9	61.6	95.3	95.3	69.9	14.6	14.4	8.30
		*h*3 (90.0)		67.4	69.2	57.0	77.8	79.1	64.7	10.4	9.90	7.70
	Higher (3686)	*h*1 (10.0)	31	80.1	80.2	79.9	101	101	88.0	20.9	20.8	8.10
		*h*2 (50.0)		80.9	80.7	79.7	118	117	93.8	37.1	36.3	14.1
		*h*3 (90.0)		80.3	80.6	79.4	95.8	97.7	87.4	15.5	17.1	8.00
				C^L (75.0)	$M1^L$ (37.5)	$M2^L$ (18.8)	W^L (1.00)	C^L (75.0)	$M1^L$ (37.5)	$M2^L$ (18.8)	W^L (1.00)	C^L (75.0)	$M1^L$ (37.5)	$M2^L$ (18.8)	W^L (1.00)
Medium	Lower (996)	*h*1 (10.0)	1085	59.9	60.1	59.2	45.5	60.3	61.1	59.6	45.8	0.40	1.00	0.40	0.30
		*h*2 (50.0)		75.9	81.3	80.8	50.7	76.3	81.6	81.6	54.3	0.40	0.30	0.80	3.60
		*h*3 (90.0)		54.6	56.1	56.9	45.6	55.5	56.2	58.7	46.6	0.90	0.10	1.80	1.00
	Control (1992)	*h*1 (10.0)	270	75.5	76.4	76.7	55.6	82.2	83.1	83.5	59.9	6.70	6.70	6.80	4.30
		*h*2 (50.0)		73.7	78.7	85.4	61.7	79.9	84.8	91.6	67.2	6.20	6.10	6.20	5.50
		*h*3 (90.0)		56.3	57.6	65.3	63.6	60.2	61.2	67.4	70.0	3.90	3.60	2.10	6.40
	Higher (3984)	*h*1 (10.0)	56	74.4	74.3	75.3	73.7	104	106	106	83.8	29.6	31.7	30.7	10.1
		*h*2 (50.0)		71.6	73.8	77.4	81.1	96.8	103	112	94.1	25.2	29.2	34.6	13.0
		*h*3 (90.0)		61.6	61.8	63.2	76.4	72.7	73.2	80.5	114	11.1	11.4	17.3	37.6

The maximum differences of the seed temperatures with the lower, control, and higher electric voltages were 38.6℃, 23.9℃, and 1.5℃ for the small volume seeds and 35.8℃, 29.8℃, and 19.5℃ for the medium volume seeds, respectively. The maximum temperature differences between the insects and surrounding seeds were 4.60℃, 14.6℃, and 37.1℃ for the small seeds volume and 3.60℃, 6.80℃, and 37.6℃ for the medium seeds volume, respectively. In the case of the lower electric voltage, the temperature differences between the insects and the surrounding seeds were lower than those with the control regardless of the seeds volume. Differences of the simulated temperature differences (between the insects and surrounding seeds) between with the control and lower electric voltages ranged from 7.10 to 10.0℃ and from 2.00 to 3.20℃ for the small and medium volume seeds. In the case of the higher electric voltage, the temperature differences between the insects and surrounding seeds were higher than those with the control electric voltage regardless of the seeds volume. Differences of the simulated temperature differences (between the insects and surrounding seeds) between with the estimated and higher electric voltages ranged from 1.00 to 22.5℃ and from 8.00 to 30.8℃ for the small and medium seeds volumes. Based on the effect of electric voltage on the temperature distribution of the seeds and the temperature differences between the insects and surrounding seeds, the RF heating uniformity and the selective heating of the insects would be enhanced by increasing the electric voltage on the top electrode of the RF heating unit.

7.7.2 Improvement of RF heating uniformity

Non-uniform RF heating of the canola seeds due to the edge effect is one of main obstacles. To improve RF heating uniformity, the RF heating systems can be designed by equipping a hot air flow, a rotating auger (RF transparent polycarbonate), and a different shape and angle of the electrode. Among the assisting equipment, the effect of seed mixing on the RF heating uniformity was determined in the simulations.

The increased sizes of the electrodes ($500 \times 500 \times 3.5$ mm^3) and the sample container (tubular shape, diameter = 150 mm, length = 600 mm, and thickness = 3 mm) were assigned in the simulations as shown in Fig. 7. 2.

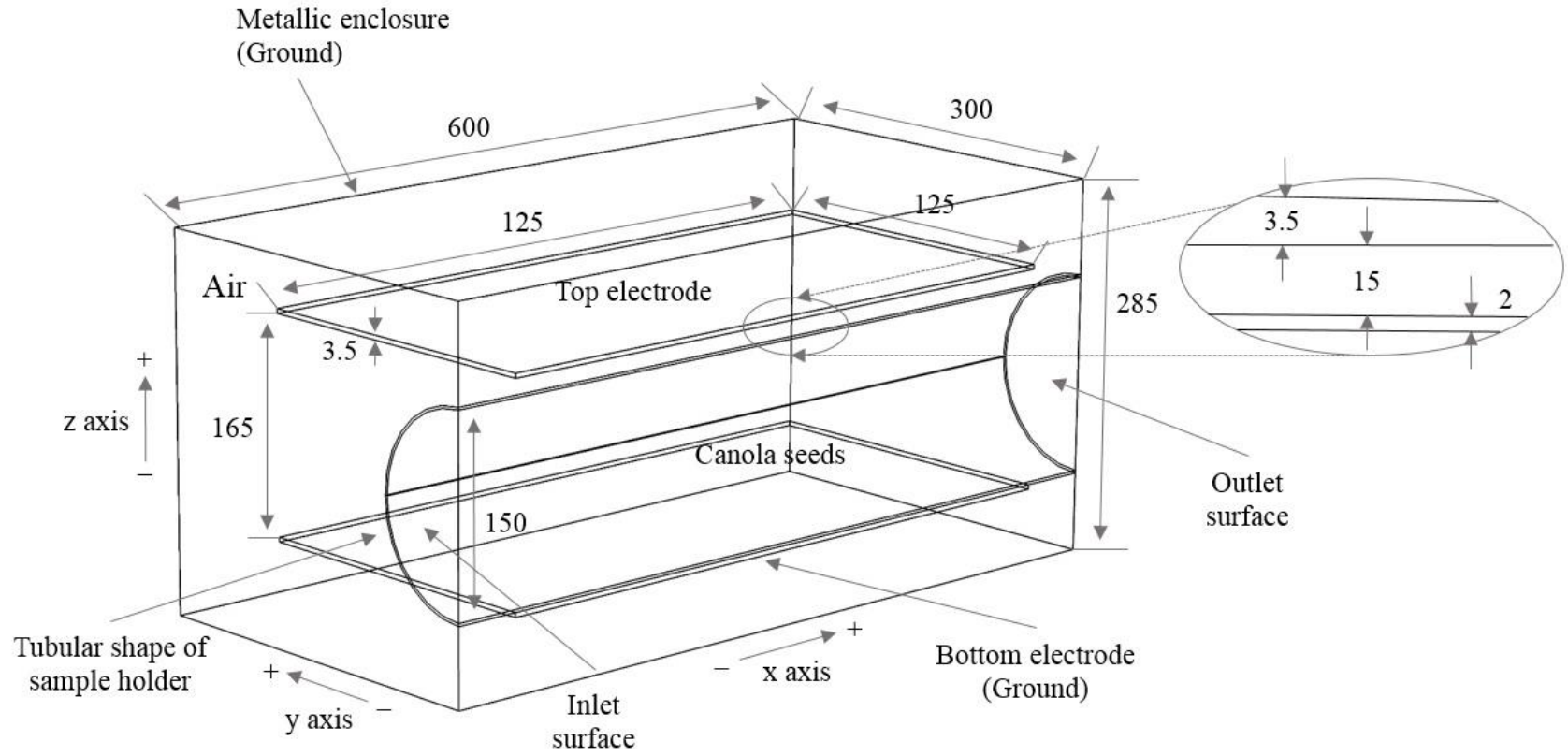

Figure 7. 2. The half of the RF heating chamber with the canola seeds in the tubular shape of the sample holder (unit : mm).

The tubular shape of the container was considered to be the best for applying a rotating auger. The bulk canola seeds at 11% MC were assumed to be fluid with a viscosity (10 Pa*s which was assumed only to observe the mixing effect via simulation based on our guess that the viscosity of the canola seeds might be the similar to that of honey, however it has not been verified) and velocities on the x, y, and z axes of the seeds sample were assigned to make a vortex (mixing effect) for improving the RF heating uniformity, instead of the equipping the rotating auger due to technical the difficulties and limited scope of this thesis. The seeds sample was continuously fed through inlet boundary and exited through outlet boundary with the velocities. Adequate velocities were determined by simulating different combinations of the velocities. Only half of the RF heating unit was considered due to the 3D axial symmetry to save simulation time, and the top half of the empty metallic enclosure was excluded for a negligible change in the electric fields. The properties of the seeds, the electrodes, and the sample container were the same as Table 6.2. The combined multi-physics models – coupling of the electric current (*ec*) model and the conjugated heat transfer (*nitf*) model (laminar flow/heat) were used in the simulations. Eqs. (6.3) and (6.4) of chapter 6. 3. 2. 3. 1 were used to describe the electric potential (V) within the system and the RF power absorbed into the dielectric samples per volume. A temperature increment in the treated materials was described by the unsteady heat transfer equation as described in Eq. 6.5 of chapter 6. 3. 2. 3. 2. The laminar flow of the seeds sample was determined using Eqs. (6.6) and (6.7) of chapter 6. 3. 2. 3. 2. The same electric voltage (1992 V, Table 6.4) estimated for the medium volume of the seeds at 11% MC was assigned on the top electrode. The initial temperature and pressure were set as 25℃ and 101300 Pa. The normal size of the mesh was used. Other conditions of the simulations except the mentioned above were the same as chapter 6. 3. 2.

The optimum velocities to achieve improved RF heating uniformity in the seeds were 0.0045 $m \cdot s^{-1}$, 0.00005 $m \cdot s^{-1}$, and -0.0003 $m \cdot s^{-1}$ in x, y, and z directions, respectively (+ and – directions were depicted in Fig. 7. 2). The RF exposure time of the seeds was 2410 s when the hottest temperature of the seeds reached 80℃. Simulated temperature distributions of the seeds (11% MC) on different cross sections are shown with different RF heating durations in Fig. 7. 3.

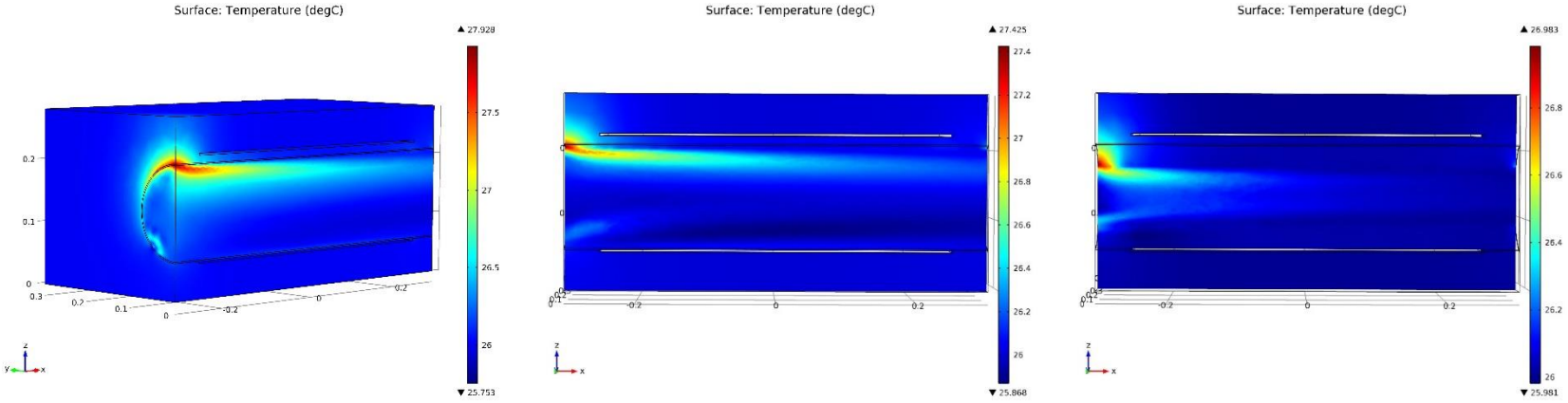
Surface: Temperature (degC)
▲ 27.928
27.5
27
26.5
26
▼ 25.753
Surface: Temperature (degC)
▲ 27.425
27.4
27.2
27
26.8
26.6
26.4
26.2
26
▼ 25.868
Surface: Temperature (degC)
▲ 26.983
26.8
26.6
26.4
26.2
26
▼ 25.981

(a) (b) (c)

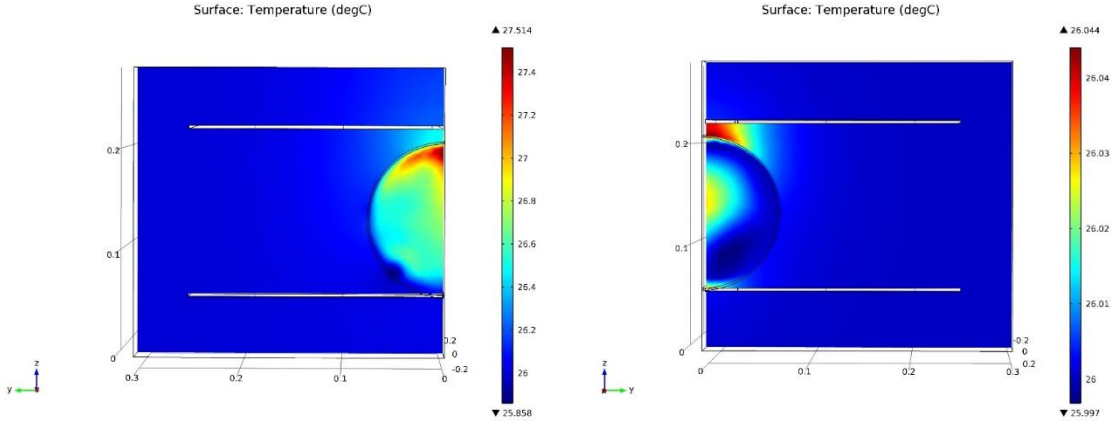
Surface: Temperature (degC)
▲ 27.514
27.4
27.2
27
26.8
26.6
26.4
26.2
26
▼ 25.858
Surface: Temperature (degC)
▲ 26.044
26.04
26.03
26.02
26.01
26
▼ 25.997

(d) (e)

(A)

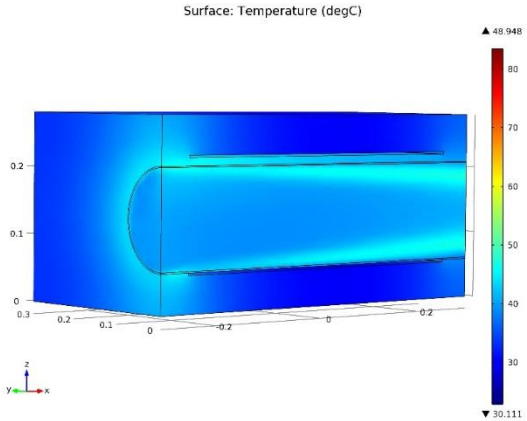
Surface: Temperature (degC)
▲ 48.948
▼ 30.111

(a)

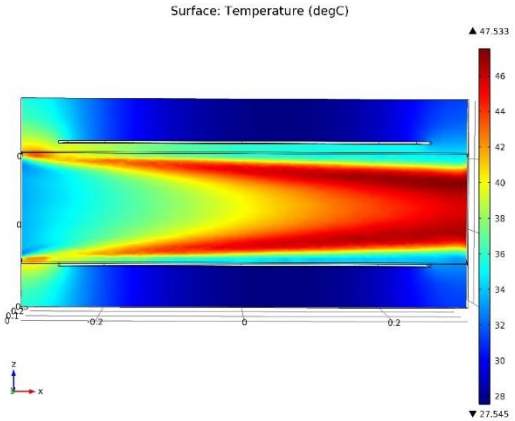
Surface: Temperature (degC)
▲ 47.533
▼ 27.545

(b)

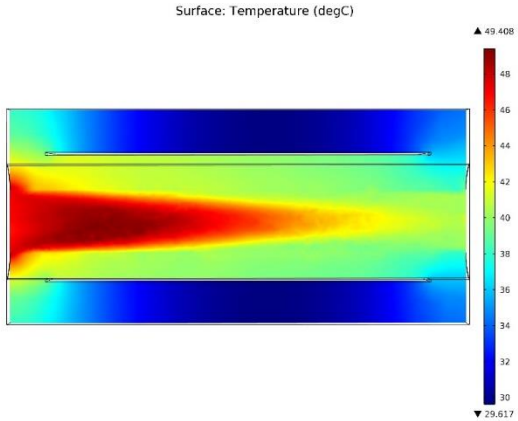
Surface: Temperature (degC)
▲ 49.408
▼ 29.617

(c)

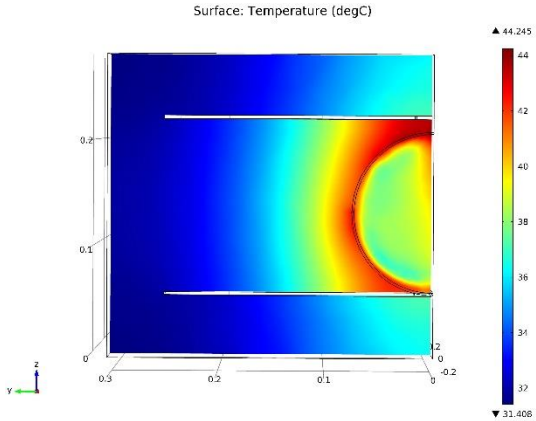
Surface: Temperature (degC)
▲ 44.245
▼ 31.408

(d)

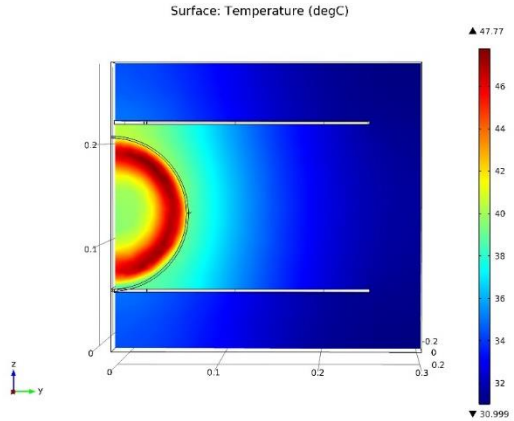
Surface: Temperature (degC)
▲ 47.77
▼ 30.999

(e)

(B)

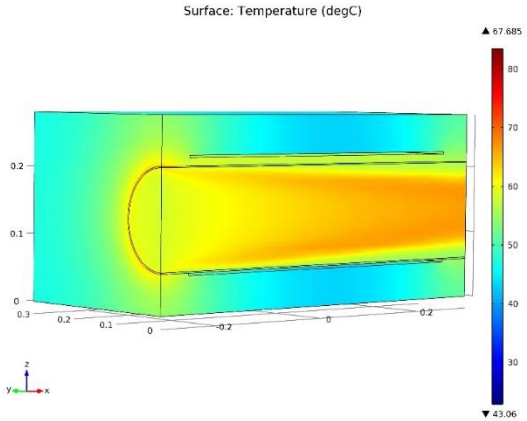
Surface: Temperature (degC)
▲ 67.685
80
70
60
50
40
30
▼ 43.06

(a)

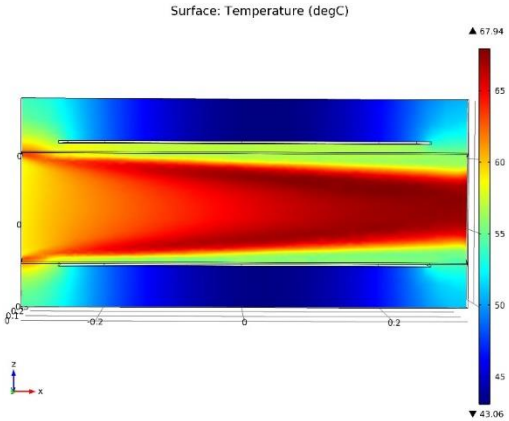
Surface: Temperature (degC)
▲ 67.94
65
60
55
50
45
▼ 43.06

(b)

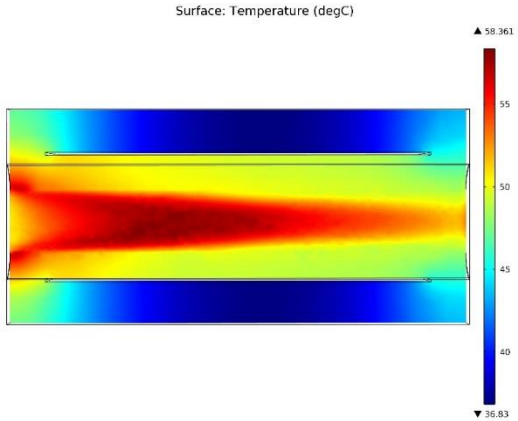
Surface: Temperature (degC)
▲ 58.361
55
50
45
40
▼ 36.83

(c)

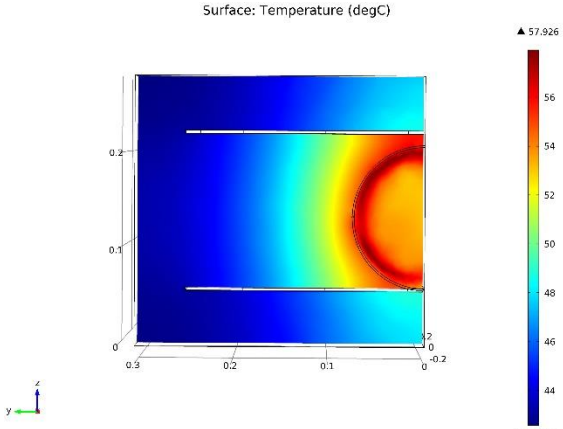
Surface: Temperature (degC)
▲ 57.926
56
54
52
50
48
46
44
▼ 42.578

(d)

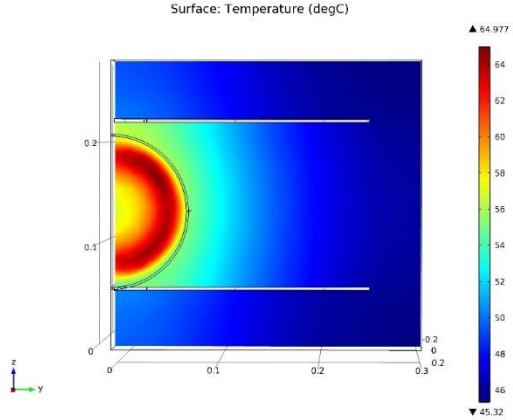
Surface: Temperature (degC)
▲ 64.977
64
62
60
58
56
54
52
50
48
46
▼ 45.32

(e)

(C)

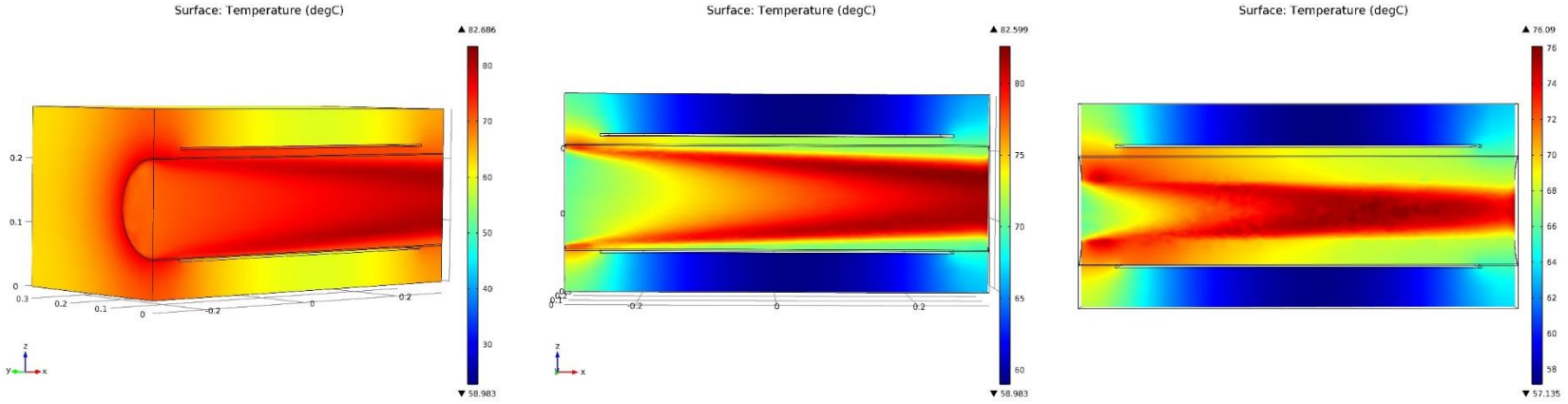

(a) (b) (c)

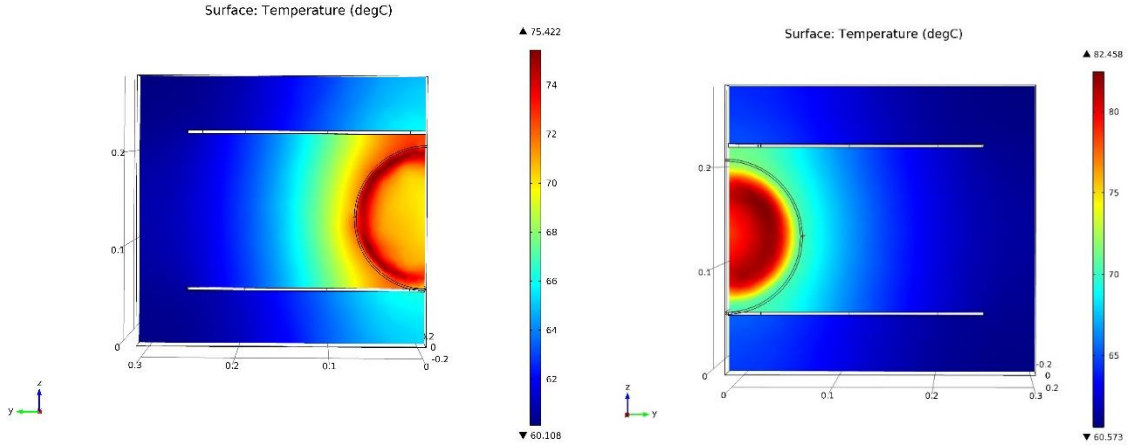

(d) (e)

(D)

Figure 7. 3. The simulated temperature distribution profiles of the canola seeds (11% MC) at half-cut surface of RF heating chamber (a), x-z cross section surfaces at 37.5 mm (b) and 70.0 mm (c) from center of the seeds, and y-z cross section surfaces of the seeds at 60 mm from inlet (d) and outlet (e) boundaries in the tubular shape of the sample container after 100 s (A), 1510 s (B), 2050 s (C), and 2410 s (D).

As depicted in Fig. 7. 3. (A), the seeds at top surface and outer boundary of the sample holder were intensively heated due to the edge effect at the beginning of RF heating. The deflected electric fields at the outer boundary of the seeds during the RF heating were observed in the simulations (Fig. 7. 4. (a)) and the phenomenon refers to the edge effect.

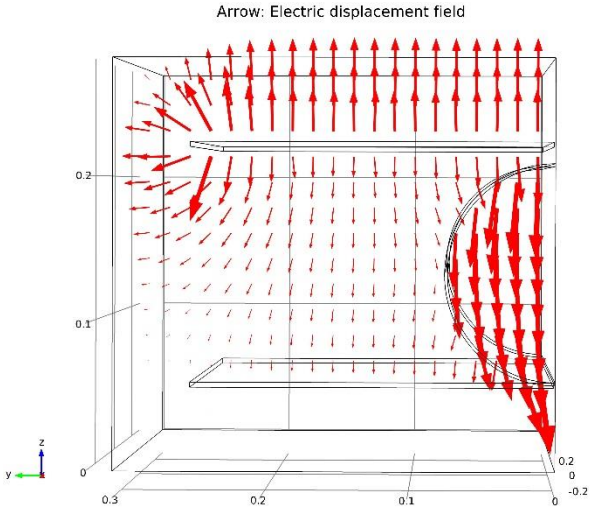

(a)

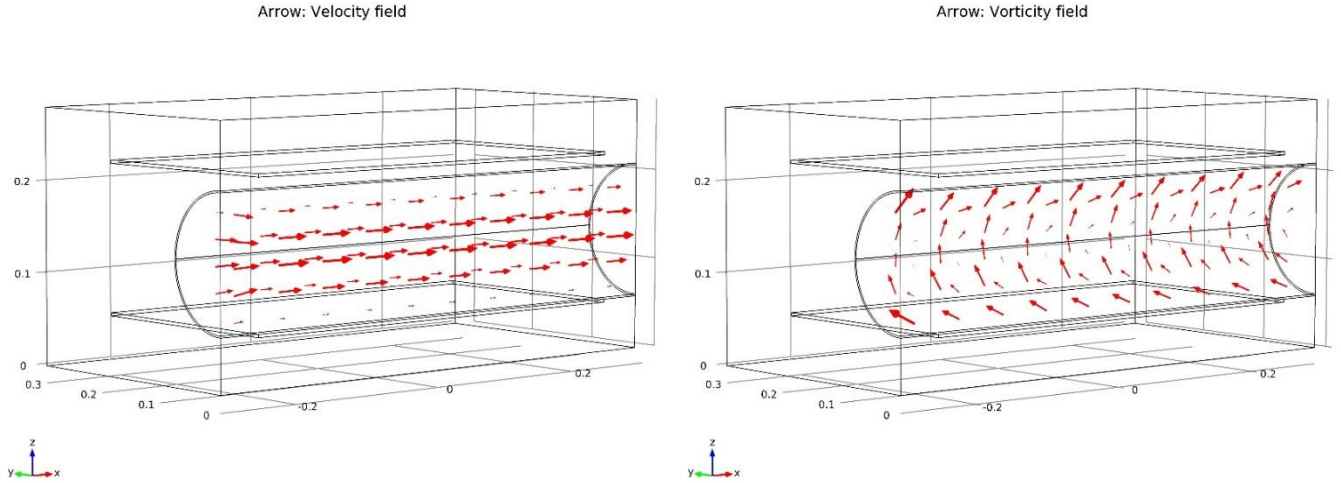

(b) (c)

Figure 7. 4. The simulated electric displacement (a), velocity (b) and vorticity (c) field distributions in the canola seeds at 11% MC during the RF heating.

As the RF heating continues, the intensively heated seeds (hotter temperature) at the top surface and outer boundary of the container were uniformly distributed to inner areas (relatively colder temperature) by the assigned forces (mixing effect) in the x, y, and z directions of the seeds (Fig. 7. 3). The simulated velocity and vorticity field distributions in the seeds during the RF heating were described in Fig. 7. 4. The assigned forces formed the vortex flows which push the relatively colder seeds at the bottom and inner areas to the top surface and outer boundary of the sample container. By the help of mixing effect, uniform RF heating of the seeds were observed near the exit (distributions in Fig. 7. 3. (D)). The maximum temperature difference between the hottest and coldest spots of the seeds was less than 8.73℃. It was much lower (approximately four times) than that for the medium volume seeds at 11% MC (34.1℃) in Table 3. 2. The temperature difference of the seeds in the tubular container was mainly caused by convective heat loss from the sample container to surrounding air in the RF heating unit. Therefore, to achieve more uniform RF heating, the convective heat loss can be minimized with forced hot air flowing over the sample container using a hot air blast system during the RF heating.

7.8 Contributions to knowledge development

No comprehensive research has been done on the measurement of the dielectric properties and the thermal-physical properties of the canola seeds at various temperatures and MCs and the demonstration of the feasibility of RF disinfestation based on selective heating principle. Therefore, measured dielectric properties and thermal-physical properties of the seeds as functions of temperature and MC (chapters 1 and 2) would be useful to estimate and simulate those properties at given temperature and MC of the seeds, to evaluate feasibility of RF disinfestation, and to design various RF heating processes with the seeds.

The determined temperature distributions in the seeds at various bulk volumes and MCs during RF heating and the demonstrated effect of the sample volume and shape of the seeds on the formation of the electric field using 2% agar gel (chapter 3) could lay a broad foundation for designing and simulating RF heating process. The discovery should be useful to improve RF heating uniformity for the canola seeds and other grains.

The mortalities of the red flour beetles infesting the canola seeds during RF heating at various MCs, volumes, and final temperatures of the infested seeds (chapter 4) and the developed thermal death kinetics of the adult red flour beetles (chapter 5) using the determined temperature histories

of the seeds (chapter 3) and the corresponding mortalities of the insects would be helpful to control red flour beetles and similar insects in the stored canola seeds and other similar grains by RF heating.

The feasibility study of selective RF heating of the insects (chapter 6), the improved RF heating uniformity in the seeds with mixing, and the demonstrated effect of the electric voltage on the RF heating uniformity and selective heating (chapter 7.7), all by the help of computer simulations would be useful to determine the optimum condition of the scaled-up RF heating process with mixing equipment for improving global heating uniformity and local selective heating.

7.9 General conclusions

Based on the experiments and analysis of this research, the following general conclusions were achieved.

1. Thermal, physical and dielectric properties of the bulk canola seeds and the red flour beetle were determined.

- The C_p of the canola seeds increased with temperature and MC. The densities of the seeds decreased with temperature. These resulted in decreasing porosity of the seeds with temperature and MC. The k and α of the seeds increased with temperature and MC. The ε decreased with temperature and MC. The ε' and the ε'' decreased with increasing frequency regardless of temperature and MC and increased in proportion to increasing temperature and MC.
- The C_p and the k of the insect increased and the ρ of the insect decreased with increasing temperature. The ε' and the ε'' of the insect increased with increasing temperature.

2. The temperature distribution in the bulk canola seeds was determined during RF heating. The temperature of the seeds decreased from the center towards the wall region for the small and the large volumes. In case of the medium volume of the seeds, relatively higher temperatures of the seeds at the region between the middle and outer boundary were observed due to the edge effect. The intensity of the edge effect increased with increasing sample volume. However, the edge effect was not observed, once the surface of the seeds was larger than the electrode. The 2% agar gel was used to demonstrate the effect of the sample volume on the formation of electric field affecting the RF heating pattern. The temperature profiles of the gels were in good agreement with those of the

bulk canola seeds. More uniform RF heating was observed in the samples of medium volume in spite of the edge effect.

3. The mortality of the insect infesting the seeds (small and medium volumes) during RF heating were determined. The complete mortalities of the insects were achieved at over 60℃ for 9% and 11% MCs and over 70℃ for 5% and 7% MCs. A complete mortality of all life stages of the insect infesting the seeds can be achieved at 60℃ of the seeds by RF heating regardless of the volume of the seeds with proper design with acceptable thermal degradation to qualities of the seeds.

4. Thermal death kinetics of the adult red flour beetles infesting the bulk canola seeds was characterized. The best thermal death kinetics model for the adult insects is as follows.

$$\frac{d(N/N_0)}{dt} = -6.73 \times 10^{13} \cdot \exp\left(\frac{-1.00 \times 10^5}{R\mathrm{T}}\right)(N/N_0)^1$$

The adult red flour beetle was more susceptible to the thermal death by the RF heating than the other insects infesting the food commodities based on the determined activation energy (100 KJ/mol).

5. The RF selective heating of red flour beetle in the bulk canola seeds was simulated. The selective heating of the red flour beetles was most effective (14.6℃ higher than the temperature of the surround seeds) in the small volume seeds at 11% MC. Based on the mortality of the insects, the RF heating systems equipped with a hot air flow, a rotating helix, and/or electrodes with different shapes, sizes and angles can be designed to achieve uniform seed temperature of 60℃ to control the red flour beetles completely without compromising the seed physico-chemical qualities.

6. The RF heating uniformity in the seeds and the selective RF heating of the insects increased with increasing the electric voltage regardless of the seeds volume in the simulation. The RF heating uniformity in the seeds was improved by mixing effect (equipped rotating auger) in the simulation.

Based on the mortality of the insect and the simulation result, the complete mortality of the red flour beetles infesting the canola seeds without thermal degradation of the seeds at 60℃ would be achieved by improved RF heating uniformity in the canola seeds by combination of equipped the rotating auger and the hot air system with the continuous RF heating process (increased electric voltage) including tubular shape of the sample holder.

7.10 Recommendations for future studies

No consideration of actual temperature changes of the insects during the RF heating in developing thermal death kinetics of the insects, and mass transfer in the computer simulation was limitation of this study. The non-uniform RF heating of the canola seeds was a major obstacle controlling the red flour beetles effectively without significant thermal degradation of the seed quality. Therefore, the following investigations are recommended to analyse thermal death kinetics of the insects more accurately, improve simulation models, minimize temperature gradients in the seeds during RF heating, and suggest effective designs for scaled-up RF disinfestation unit as future studies.

7.10.1 Measuring the mass changes of the seeds and the insects and temperature changes of the insects during RF heating

In general, heat and mass transfer occur simultaneously during heating process. During RF disinfestation process, the mass of the canola seeds and the adult red flour beetles decreased due to evaporated moisture. Measurement of the mass changes of the samples and the temperature changes of the insects are needed to simulate RF selective heating of the insects more realistically.

7.10.2 Minimizing non-uniform RF heating

The non-uniform RF heating was observed in this research irrespective of the MCs and volumes of the canola seeds. From the further simulations, RF heating uniformity of the seeds was improved by the mixing in the simulation. To improve the RF heating uniformity further, the effect of combination of the rotating auger and the hot air system needs to be simulated and validated. The simulation results will be helpful for designing scaled-up RF disinfestation processes and it should be compared with actual experimental data.

7.10.3 Designing conceptual scaled-up RF disinfestation units

Conceptual scaled-up RF disinfestation processes combining with auxiliary equipment (a gravity chute, a rotating auger, a hot air system, and a conveyer belt) are illustrated in Fig. 7. 5. The rotating auger made of RF transparent polycarbonate to avoid the electric arcing can be assembled between the two electrodes to achieve more uniform RF heating by mixing the infested seeds and to push the seeds forward to the destination during an operation as Fig. 7. 5. (a). The slope of electrodes in Fig. 7. 5. (b) can be adjusted to control RF heating rate and change input

quantity of the infested seeds. Dead insects would be selectively separated and the seeds can be cooled down by forced cold air from a fan through holes on the shaking perforated conveyer belt as a sieve. Optimum conditions (flow rate, angle of the slope, auger speed, etc) for conceptual scaled-up RF disinfestation process can be determined with computer in the simulation. Thus, the red flour beetles infesting the canola seeds can be more effectively controlled in the conceptual scaled-up RF disinfestation process with the optimum conditions. An economic analysis of the scaled-up RF disinfestation process can be conducted considering the retail electricity price in Saskatoon, the capacity and design of the RF unit, and the installation location.

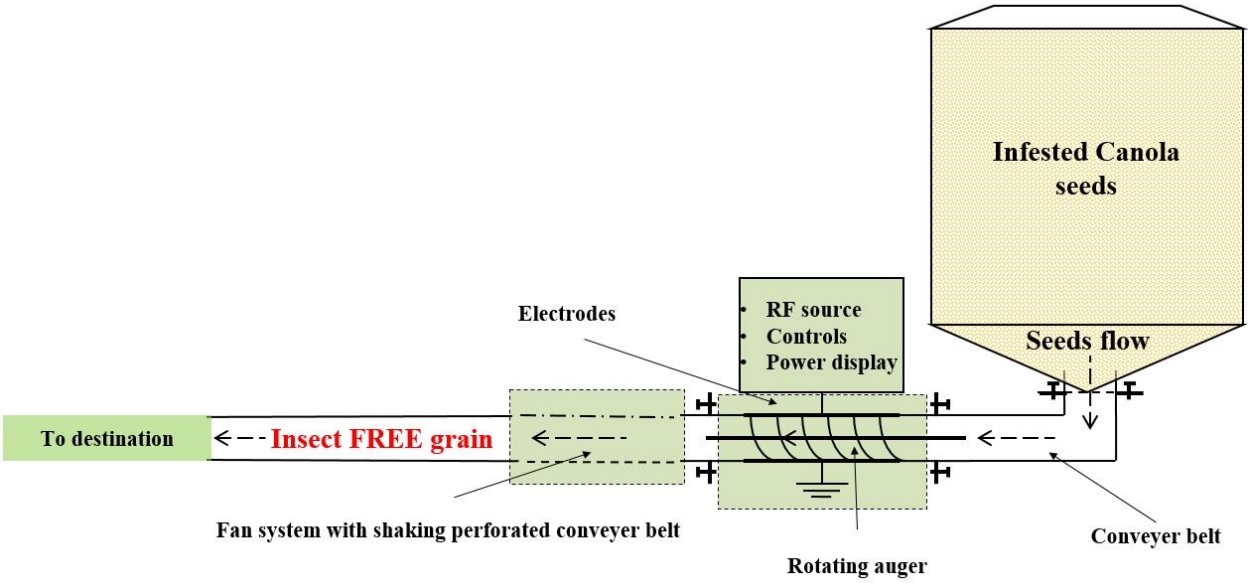

(a)

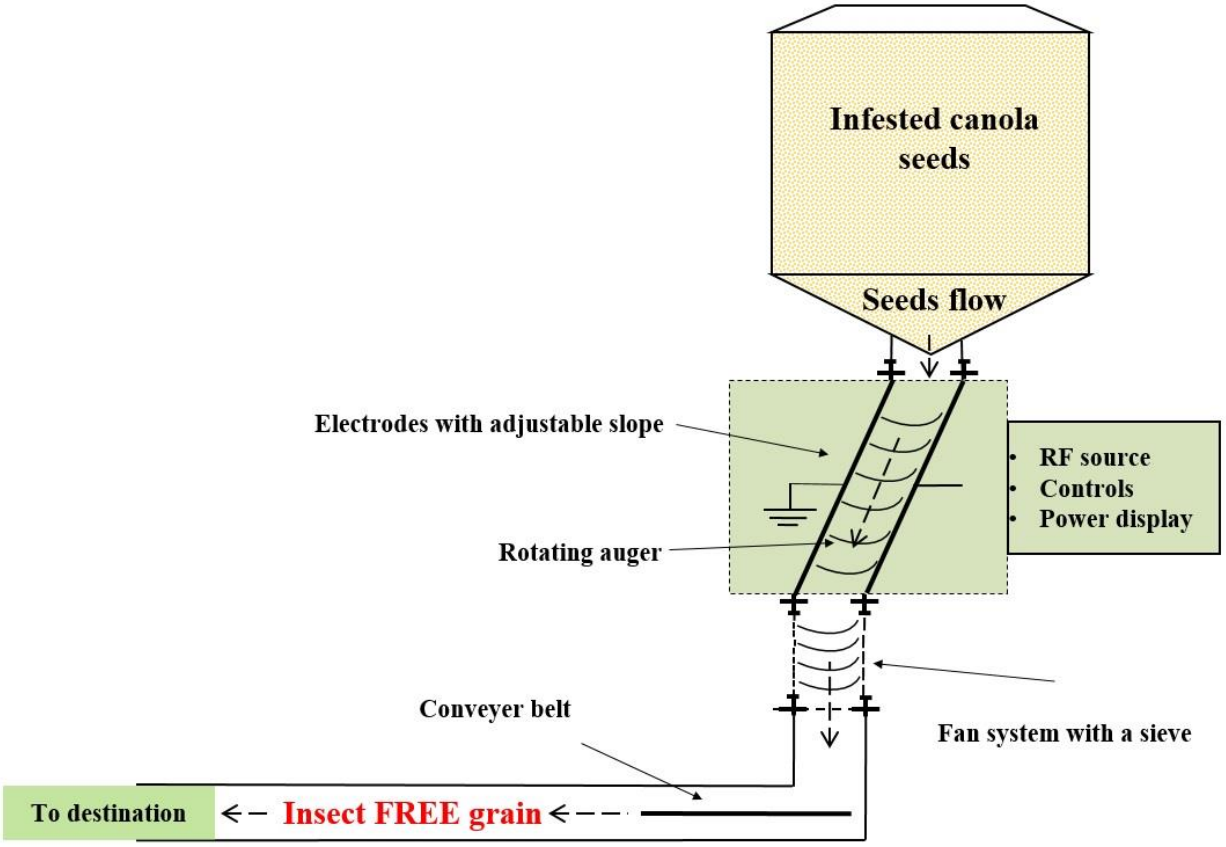

(b)

Figure 7. 5. Conceptual designs of the scaled-up RF disinfestation process combined with the rotating auger mixer, the hot air system, the shaking perforated conveyer belt, and the fan system (a) and with the gravity chute, the electrodes with adjustable slope, the rotating auger, the conveyer belt, and the fan system (b).

7.11 References

Bramson, M. A. 1968. Infrared radiation, Plenum press, N.Y.

Canadian Grain Commission. 2013. http://www.grainscanada.gc.ca/storage-entrepose/pip-irp/rfb-trf-eng.htm. (July. 15. 2016)

City of Saskatoon. 2016. https://www.saskatoon.ca/services-residents/power-water/saskatoon-light-power/electrical-rates. (effective September 1, 2015)

Gazor, H. R., and A. Mohsenimanesh. 2010. Modelling the drying kinetics of canola in fluidised bed dryer. *Czech Journal of Food Sciences* 28(6): 531-537.

Hallman, G. J., and D. L. Denlinger. 1998. Temperature sensitivity in insects and application in integrated pest management. Westview Press, Inc., pp. 7-53.

Hou, L., B. Ling, and S. Wang. 2014. Development of thermal treatment protocol for disinfesting chestnuts using radio frequency energy. *Postharvest Biology and Technology* 98: 65-71.

Koskiniemi, C. B., V. D. Truong, R. F. McFeeters, and J. Simunovic. 2013. Effects of Acid, Salt, and Soaking Time on the Dielectric Properties of Acidified Vegetables. *International Journal of Food Properties* 16(4): 917-927.

Mahroof, R., B. Subramanyam, and D. Eustace. 2003. Temperature and relative humidity profiles during heat treatment of mills and its efficacy against *Tribolium castaneum* (Herbst) life stages. *Journal of Stored Products Research* 39(5): 555-569.

Mills, R., and J. Pedersen. 1990. *A flour mill sanitation manual*. Eagan Press, ST. Paul, MN.

Nelson, S. O., and P. G. Bartley. 2002. Frequency and temperature dependence of the dielectric properties of food materials. *Transactions of the ASAE* 45(4): 1223-1227.

Nelson, S. O., P. G. Bartley, and K. C. Lawrence. 1998. RF and microwave dielectric properties of stored-grain insects and their implications for potential insect control. *Transactions of the ASAE* 41(3): 685.

Shrestha, B. L., and O. Baik. 2011. Permittivity of Mixtures of Saponaria vaccaria and Ethanol–Water Solution for RF Heating Assisted Extraction of Saponins. *Instrumentation and Measurement, IEEE Transactions on* 60(8): 2861-2871.

Shrestha, B., and O. Baik. 2013. Radio frequency selective heating of stored-grain insects at 27.12 MHz: A feasibility study. *Biosystems Engineering* 114(3): 195-204.

Sipahioglu, O., S. A. Barringer, I. Taub, and A. Prakash. 2003. Modeling the dielectric properties of ham as a function of temperature and composition. *Journal of Food Science* 68(3): 904-909.

Sweat, V. E. 1986. Thermal properties of foods. *Engineering properties of foods* 49.

Tang, J., H. Feng, and M. Lau. 2002. Microwave heating in food processing. *Advances in bioprocessing engineering* : 1-43.

Wang, S., M. Monzon, J. A. Johnson, E. J. Mitcham, and J. Tang. 2007. Industrial-scale radio frequency treatments for insect control in walnuts: I: Heating uniformity and energy efficiency. *Postharvest Biology and Technology* 45 (2): 240-246.

Wang, S., J. Tang, R. Cavalieri, and D. Davis. 2003. Differential heating of insects in dried nuts and fruits associated with radio frequency and microwave treatments. *Transactions-American Society of Agricultural Engineers* 46(4): 1175-1184.

Yin, X., S. Wang, J. Tang, J. D. Hansen, and S. Lurie. 2006. Thermal conditioning of fifth-instar Cydia pomonella (Lepidoptera: Tortricidae) affects HSP70 accumulation and insect mortality. *Physiological Entomology* 31(3): 241-247.

Yu, D. U., B. L. Shrestha, and O. D. Baik. 2015. Radio Frequency Dielectric Properties of Bulk Canola Seeds under Different Temperatures, Moisture Contents, and Frequencies for Feasibility of Radio Frequency Disinfestation. *International Journal of Food Properties* 18(12): 2746-2763.